

UNIVERSITÉ DE MONTRÉAL

FREEZE-DRIED CHITOSAN PLATELET-RICH PLASMA HYBRIDS FOR ROTATOR CUFF  
TEAR REPAIR

GABRIELLE DÉPRÉS TREMBLAY  
INSTITUT DE GÉNIE BIOMÉDICAL  
ÉCOLE POLYTECHNIQUE DE MONTRÉAL

THÈSE PRÉSENTÉE EN VUE DE L'OBTENTION  
DU DIPLÔME DE PHILOSOPHIAE DOCTOR  
(GÉNIE BIOMÉDICAL)

JUILLET 2017

UNIVERSITÉ DE MONTRÉAL

ÉCOLE POLYTECHNIQUE DE MONTRÉAL

Cette thèse intitulée:

FREEZE-DRIED CHITOSAN PLATELET-RICH PLASMA HYBRIDS FOR ROTATOR CUFF  
TEAR REPAIR

présentée par : DÉPRÉS TREMBLAY Gabrielle

en vue de l'obtention du diplôme de : Philosophiae Doctor

a été dûment acceptée par le jury d'examen constitué de :

Mme HOEMANN Caroline, Ph. D, présidente

M. BUSCHMANN Michael, Ph. D, membre et directeur de recherche

M. NAZHAT Showan, Ph. D, P. Eng, membre

Mme GALATZ Leesa M, MD, membre externe

**DEDICATION**

*TO MY BELOVED FAMILY*

## ACKNOWLEDGEMENTS

This is the end; the end of my Ph. D journey, but the beginning of a new journey. Although it seems short, it was the most stimulating and challenging experience yet. This thesis embraces time and work from many valuable people. First, I would like to thank my director Dr. Buschmann for this wonderful experience. He gave me the chance to work in his laboratory, to perform and also to work on the project I really wanted. Moreover, his directions and effective discussions helped me built strong analytical and problem-solving skills and also to develop deep interest in the research field. Without his illuminating instructions, this thesis could not have reached this present form. I need to thank him for his encouragement, guidance, coaching, and most of all, his patience with me. Thank you for the trust you had in me.

I would also like to express my profound gratitude to my amazing supervisor, Anik Chevrier. Anik has been wonderful to me; she helped me every time I needed it, she listened to me, she guided me, she always took time for me no matter what and she walked me through all of the stages of my project. I was lucky to work with her, if it would not been for her I would probably not have been here today and passionate about my project. I acknowledge your generosity and enthusiasm Anik. Thank you so much for the material, psychological and intellectual support you provided me over my Ph. D journey. Special thank you go to professors Caroline Hoemann and, Leesa Galatz, and Showan Nazhar for being members of my thesis committee. I'm really thankful for all your assistance.

During that time, I also had, the opportunity to make incredible and loyal friends and to cross paths with so many other colleagues with whom I had the chance to share theories, fears, joys, doubts, concerns and achievements; Thank you Karim, Mohamad-Gabriel, Colleen, Daniel, Rasheh, Leili, David, Ashkan, Genevieve, Ousama, Etienne, and Chi-Yuan. This laboratory taught me much more than I could have learned from any books. I also need to recognize the contributions of my colleagues, Julie Tremblay, Jun Sun, Genevieve Picard, Vincent Darras, Marc Lavertu, Nicolas Tran-Khanh, Monica Nelea and Chi-Yuan Chang.

This work would also have been impossible without the support of my beloved family. My parents, Monique and Sylvain, have always been the source of my inspiration. They are always there for me: to support me, to help me, to push me and of course to love me. They are the reason why I succeed. Thank you both for your unconditional faith and love in me. There is also

my little sister, Bianca, whom has been wonderful to me. She always tries to make me feel better when something is not right: you are amazing little sis. I would like to also thank, the love of my life, Jean-Sebastien. Thank you for always being there for me. Thank you for being so patient with me. I love you with all my heart and I want you to know that your love is everything to me. Also thank you to my best friends, Nimara, Ines and Roxanne. You were amazing to me and still are. A big thank you to those organizations that have provided funding for my studies and research: CRSNG and Ortho Regenerative Technologies Inc.

## RÉSUMÉ

Les déchirures de la coiffe du rotateur sont une des blessures musculo-squelettiques les plus répandues de l'épaule. Les techniques de réparation chirurgicales actuellement utilisées échouent dans environ 20 à 95% des cas dépendamment de l'âge, la taille, du tabagisme, du temps de guérison, de la qualité du tendon, de la qualité musculaire, de la réponse à la guérison et des traitements chirurgicaux. La majorité des déchirures chroniques des tendons surviennent principalement dans le supraspinatus, ce qui mène à des changements structurels tels que l'accumulation de gras, la perte de volume, le remodelage musculaire, la disparition de sarcomères et, parfois, une faiblesse musculaire profonde. Trouver un modèle animal similaire à l'humain est un défi de taille mais très utile pour améliorer notre compréhension des voies cellulaires et moléculaires impliquées dans la pathologie de la coiffe du rotateur. Les pathologies du tendon sont aggravées par son potentiel de guérison limité, attribué à la présence de changements dégénératifs et à une vascularité relativement faible. Le développement de nouvelles technologies pour traiter les déchirures de la coiffe du rotateur nécessite également des tests sur des modèles animaux afin d'évaluer l'innocuité et l'efficacité du traitement, avant d'effectuer des tests cliniques pour éventuellement améliorer les options de traitement thérapeutique. Il est donc important d'évaluer les modèles animaux utilisés pour la recherche des pathologies de la coiffe du rotateur; Idéalement, ceux-ci présenteraient une dégénérescence des tendons, une atrophie musculaire et une infiltration de gras similaire à celle de l'humain. Notre premier but était donc de recenser les traitements cliniques actuels utilisés pour guérir la coiffe du rotateur, de décrire les nouvelles stratégies en cours de développement clinique et préclinique.

Nos résultats ont démontré qu'aucun animal n'a une anatomie comparable à celle des humains. Bien que les dernières techniques de sutures semblent augmenter le taux de guérison des tendons, ceci n'a pas été traduit par une amélioration des résultats cliniques. Les patches de matrix extracellulaire n'ont pas démontrées de résultats prometteurs dans les essais cliniques randomisés. Il n'existe encore aucune étude sur la réparation de la coiffe du rotateur utilisant des facteurs de croissances chez l'humain. L'utilisation de PRP en orthopédie est encore controversée et malheureusement aucunes des stratégies actuellement utilisées améliore la réparation des déchirures de la coiffe du rotateur. Une solution possible pourrait être l'utilisation d'implants de

chitosan-PRP. En résumé, plusieurs stratégies de réparation sont disponibles, mais d'autres essais cliniques sont nécessaires pour trouver le traitement optimal pour la réparation de la coiffe du rotateur.

Les implants de chitosane (CS)-PRP ont démontrés qu'ils pouvaient améliorer la réparation du ménisque, de la coiffe du rotateur et la réparation du cartilage dans des modèles précliniques. Cela nous a conduits à étudier les mécanismes d'action *in vitro* et *in vivo* des implants CS-PRP. Des formulations lyophilisées contenant 1% (p / v) de chitosane (80% désacétylé et masse moléculaire moyenne de 38 kDa), 1% (p / v) de trehalose, un lyoprotectant, et 42,2 mM de chlorure de calcium, l'activateur de caillot, ont été solubilisés dans du PRP. L'objectif de cette étude était d'étudier les mécanismes possibles par lesquels le chitosan inhibe la rétraction des caillots hybrides CS-PRP *in vitro*, caractériser l'effet du chitosan, du tréhalose et une combinaison sur l'activation plaquettaire et la sécrétion granulaire *in vitro*, caractériser le profil de libération de PDGF-AB et EGF à partir de caillots hybrides CS-PRP *in vitro*, et d'évaluer histologiquement la résidence, la bioactivité et la biodégradabilité des implants CS-PRP *in vivo*. Nos hypothèses de départ étaient que (1) le chitosane se lierait aux plaquettes d'une manière non spécifique inhibant l'agrégation plaquettaire dans les caillots hybrides et la rétraction du caillot médiée par les plaquettes; (2) le chitosane activerait les plaquettes et induirait la sécrétion des granules; (3) la libération de facteurs de croissances à faible point isoélectrique (chargé négativement à pH neutre), comme EGF, serait plus soutenue par les implants de CS-PRP que la libération de facteurs de croissances avec des points isoélectriques élevés (chargés positivement à pH neutre), tel PDGF-AB, en raison d'interactions électrostatiques avec le chitosane cationique; (4) Les implants CS-PRP résideraient beaucoup plus longtemps que le PRP seul *in vivo*, où ils induiraient le recrutement cellulaire et l'angiogenèse, mais seraient également dégradés à l'intérieur de 6 semaines.

Nos images confocales, SEM et TEM soutiennent notre première hypothèse selon laquelle le chitosan recouvre physiquement les plaquettes et autres composants du caillot sanguin pour inhiber l'agrégation plaquettaire, nécessaire pour la rétraction du caillot. Dans les caillots hybrides, le chitosane interfère physiquement avec la capacité des plaquettes à adhérer l'une à l'autre ainsi qu'au réseau de fibrine, exerçant ainsi des forces mécaniques. Nos deuxième et troisième objectifs visaient à déterminer si les plaquettes étaient activées dans les caillots

hybrides CS-PRP et, dans l'affirmative, comment les facteurs de croissance dérivés des plaquettes sont libérés des caillots hybrides CS-PRP. Conformément à notre troisième hypothèse, nous avons constaté que le chitosane induisait l'activation des plaquettes et la sécrétion des granules dans les suspensions cellulaires, même plus que l'ADP, un agoniste plaquettaire connu. Fait intéressant, l'incubation de la suspension cellulaire avec tréhalose et chitosane a légèrement diminué l'expression de Pac-1 et de p-sélectine par rapport à l'incubation avec du chitosane seul.

Même si les conditions d'essai dans le dosage de cytométrie en flux sont différentes du caillot hybride, nous avons prévu que les plaquettes dans les caillots hybrides CS-PRP seraient activées et libèreraient leur granules, ce qui a été déterminé par des tests ELISA. Notre troisième hypothèse de départ, était que le point isoélectrique des facteurs de croissance dérivés des plaquettes déterminerait comment les facteurs de croissance seraient libérés des hybrides CS-PRP. Le point isoélectrique du PDGF est de 9,8 et dans des conditions physiologiques, nous nous attendions à une répulsion ionique entre le PDGF-AB chargé positivement et le chitosane cationique qui provoquerait une libération rapide et courte. Pendant ce temps, on s'attendait à ce qu'EGF, avec un point isoélectrique de 4,6, se lirait au chitosane dans des conditions physiologiques et serait libéré de manière plus continue. Contrairement à cela, nous avons constaté que les caillots hybrides CS-PRP ont soutenu et augmenté la libération de PDGF-AB et d'EGF pendant 1 semaine *in vitro*, ce qui suggère que d'autres facteurs supplémentaires contrôlent leur libération dans ce système *in vivo*. Nous avons aussi constaté que les niveaux cumulatifs de PDGF-AB et EGF libérés dans le milieu de culture étaient plus élevés dans les caillots CS-PRP par rapport aux caillots PRP. En ce qui concerne la libération des facteurs de croissance, il est important de considérer la contribution de chaque type de cellule présente dans la préparation PRP. Les plaquettes sont les principaux contributeurs à la libération de facteurs de croissance du PRP et des corrélations positives ont déjà été trouvées entre les doses de plaquettes et la quantité de facteurs de croissance libérés, y compris PDGF-AB, TGF- $\beta$ 1, VEGF et EGF. Notre quatrième objectif était d'étudier les implants *in vivo*, et nous avons démontré qu'ils présentaient une résidence plus longue et une bioactivité plus élevée que le PRP.

En résumé, le chitosan enrobe physiquement les plaquettes, les cellules sanguines et les brins de fibrine dans les implants CS-PRP, ce qui inhibe l'agrégation plaquettaire, nécessaire pour la rétraction du caillot. Les plaquettes sont activées, granules sécrétées et des niveaux plus élevés de



PDGF-AB et d'EGF sont libérés à partir de caillots CS-PRP par rapport aux caillots PRP *in vitro*. Enfin, les implants CS-PRP résident pendant au moins 6 semaines après implantation sous-cutanée et induisent le recrutement cellulaire et la synthèse de tissu de granulation, confirmant une résidence plus longue et une bioactivité plus élevée par rapport au PRP *in vivo*.

L'objectif de la troisième étude était d'évaluer si les implants CS-PRP étaient capables d'améliorer la réparation des déchirures de la coiffe du rotateur dans un modèle de lapin. Des déchirures complètes ont été créées bilatéralement dans le tendon supraspinatus (SSP) des lapins blancs de Nouvelle Zélande (n = 4 dans une étude de faisabilité pilote suivie de n = 13 dans une étude d'efficacité plus large), qui ont été réparés à l'aide de sutures transosseuses. Du côté traité, les implants CS-PRP ont été injectés dans les tunnels transosseux et dans le tendon lui-même, et la guérison a été évaluée histologiquement à des points temporels allant de 1 à 2 mois après la chirurgie. Nos hypothèses de départ étaient les suivantes: 1) Les implants CS-PRP induiraient le recrutement de cellules polymorphonucléaires (PMN) à des moments précoces après la chirurgie, 2) Les implants CS-PRP seraient dégradés 2 mois après la chirurgie et 3) Les implants CS-PRP amélioreraient la réparation des déchirures de la coiffe du rotateur grâce à une augmentation du recrutement cellulaire, de l'angiogenèse et du remodelage osseux.

L'un de nos objectifs était de déterminer la répartition de l'implant et d'évaluer la dégradation de l'implant au fil du temps. Un jour après la chirurgie, les implants CS-PRP résidaient à l'intérieur du creux osseux, dans les tunnels latéraux et également sur les surfaces du tendon. Les implants CS-PRP ont également inhibé l'ossification hétérotopique du tendon SSP à 2 mois tout en favorisant la fixation du tendon SSP à la tête humérale grâce à un remodelage osseux accru à la tubérosité supérieure.

Les implants CS-PRP ont induit le recrutement de PMNs à des moments précoces après la chirurgie, soutenant notre première hypothèse. Contrairement à la deuxième hypothèse, la dégradation des implants et les réactions inflammatoires associées étaient encore en cours dans 3 sur 9 épaules traitées à 2 mois. Les résultats ont partiellement soutenu notre troisième hypothèse selon laquelle CS-PRP améliorerait la réparation de la coiffe du rotateur, en améliorant la fixation du tendon SSP grâce à un remodelage osseux amélioré. De manière inattendue, de petites zones de tissu de granulation riche en neutrophiles entourant les tissus apoptotiques / nécrotiques étaient visibles dans 3 épaules traitées avec CS-PRP à 2 mois. La suppression de l'ossification

hétérotopique du tendon SSP (HO) par le traitement CS-PRP a été une découverte inattendue dans cette étude. Cette étude semble fournir des preuves que les implants CS-PRP sont sans danger et efficaces pour améliorer la réparation des déchirures de la coiffe du rotateur dans un petit modèle animal et que cela pourrait être traduit dans un contexte clinique.

L'objectif de la quatrième étude était d'étudier l'effet de l'utilisation d'implants de CS-PRP en conjonction avec des ancrages de suture dans des modèles de déchirure de la coiffe du rotateur ovins aigus et chroniques et voir si cela pouvait améliorer la réparation de la coiffe du rotateur. Dans deux études de faisabilité, des déchirures unilatérales de pleine épaisseur ont été créées dans le tendon de l'infraspinatus (ISP) de brebis. Dans le modèle chronique (n = 4 brebis), les tendons ont été recouverts d'une membrane de silicone permettant une dégénération chronique pendant 6 semaines, tandis que les tendons ont été réparés immédiatement dans le modèle aigu (n = 4 brebis). Les tendons ISP transectés ont été rattachés à des ancrages de suture et dans le cas des épaules traitées; Les implants composés de CS lyophilisé solubilisé dans du PRP autologue ont été appliqués en plus sur l'interface tendon-os et sur le site réparé.

Le modèle chronique a induit une dégénérescence et une rétraction importante du tendon et du muscle, ce qui a rendu la réparation beaucoup plus difficile que dans le modèle aigu. Le traitement par implants CS-PRP a induit le recrutement de cellules polymorphonucléaires à 2 semaines post-opératoires et a également amélioré l'organisation structurelle du tendon ISP à 3 mois. Le traitement a également augmenté le remodelage osseux et la croissance interne à l'interface tendon-os à 3 mois, ce qui suggère qu'une fixation plus robuste pourrait être obtenue en combinant les implants CS-PRP et les ancrages de suture. Ces études pilotes fournissent la première preuve que les implants CS-PRP peuvent améliorer la réparation des déchirures de la coiffe du rotateur dans de grands modèles animaux.

Notre hypothèse de départ a été partiellement soutenue par le fait que le traitement avec des sutures d'ancrage + CS-PRP a conduit à une amélioration de l'apparence structurelle du tendon, à un remodelage osseux et une croissance accrue à la jonction tendon-os. Nous avons constaté que recouvrir les tendons pendant 6 semaines avec des membranes de silicone de 5 cm empêchait probablement une diffusion adéquate d'éléments nutritifs et entraînait une mort cellulaire et une dégénérescence sévère du tendon lui-même, ce qui a rendu certains tendons non réparables. Bien que la dégénérescence n'ait pas été aussi marquée lorsque les tendons ont été

recouverts pendant 2 semaines avec une membrane de silicone de 5 mm, le rattachage à l'empreinte initiale aurait été difficile à atteindre puisque l'unité tendineuse avait considérablement rétracté. Nous avons constaté que les tissus cicatriciels abondants comblaient l'écart entre le tendon et la tubérosité après 2 et 6 semaines. À partir de maintenant, nous considérons que le modèle de réparation aiguë est plus cohérent et facilement reproductible que le modèle chronique.

Des cellules polymorphonucléaires (PMN) ont été observées dans le tissu de réparation du tendon de l'épaule traité avec des ancras + CS-PRP 2 semaines post-implantation. Le tendon traité avec des ancras a seulement montré de la chondrogénèse et l'expression de GAG dans le corps du tendon à 6 semaines, alors que ce n'était pas le cas avec le tendon traité avec les ancras + CS-PRP. De manière inattendue, la technique de réparation des ancras + CS-PRP a entraîné un meilleur résultat structurel du tendon que les ancras seules à 3 mois, probablement par une modulation du moment de la séquence de guérison ou par un remodelage des tissus de réparation accru. Il n'y avait aucun effet délétère spécifique au traitement dans l'articulation de l'épaule, ce qui suggère que les implants CS-PRP sont sécuritaires. Les anomalies structurelles étaient visibles dans la plupart des glénoïdes, ce qui suggère que des contraintes plus importantes sont appliquées sur cette surface par rapport à la tête humérale dans le modèle des brebis. L'infiltration de gras dans le muscle ISP a été induite dans les modèles à la fois chronique et aiguë, et aucun traitement n'a pu inverser cet effet. Une synovite transitoire légère était présente dans l'épaule traitée avec CS-PRP à 2 semaines, ce qui a été résolu à 6 semaines et 3 mois, une fois que le biomatériau a été dégradé.

En résumé, les techniques de développement pour augmenter la réparation de la coiffe du rotateur restent cliniquement pertinentes. Les défis techniques associés au modèle de réparation chronique chez les brebis rendent le modèle aigu plus préférable pour les études futures. Ces deux études pilotes fournissent la première preuve que les implants CS-PRP améliorent la réponse de guérison chez les grands modèles animaux de réparation de la coiffe du rotateur, en partie grâce à un remodelage osseux accru au tissu de réparation du tendon et à l'interface osseuse sous-jacente.

## ABSTRACT

Rotator cuff tears are the most common musculoskeletal injury occurring in the shoulder. Current surgical repair fails to heal in 20 to 95% of cases depending on age, size, smoking, time of repair, tendon quality, muscle quality, healing response, and surgical treatments. The majority of chronic tendon tears occurs mostly in the supraspinatus and ultimately leads to structural changes such as fatty accumulation, loss of volume, muscle remodeling, subtraction of sarcomeres, and sometimes, profound muscle weakness. Finding the right animal model is challenging but critically important to improve our understanding of the cellular and molecular pathways involved in rotator cuff pathology. These problems are worsened by the limited healing potential of injured tendons, attributed to the presence of degenerative changes and relatively poor vascularity of the cuff tendons. Development of new techniques to treat rotator cuff tears also requires testing in animal models to assess safety and efficacy prior to clinical testing to improve therapeutic treatment options. Hence it is important to evaluate appropriate animal models for rotator cuff research with degeneration of tendons, muscular atrophy and fatty infiltration similar to humans. Our first purpose was to review current clinical treatments and new repair strategies under development both clinically and pre-clinically.

Our findings showed that none of the animals have anatomy comparable to humans. Although the latest suture techniques seem to somewhat increase the rate of tendon healing, this has not been translated into improved clinical and functional outcomes. Extracellular matrix (ECM) patches have not shown promising results in randomized clinical trials and scaffolds still need clinical studies. Still no study exists on rotator cuff repair using growth factors in humans. Platelet-rich plasma (PRP) use in orthopedics is still controversial and none of these strategies enhance rotator cuff tear repair. One possible effective technique could be using chitosan-PRP implants. In summary, several repair strategies are available but further clinical trials are needed to find the optimal treatment for rotator cuff repair.

Chitosan (CS)-PRP implants have been shown to improve meniscus and cartilage repair in pre-clinical models. This has led us to investigate *in vitro* and *in vivo* mechanisms of action of CS-PRP implants. Our second purpose was to investigate possible mechanisms by which chitosan inhibits retraction of CS-PRP hybrid clots *in vitro*, characterize the effect of chitosan,

trehalose and a combination of both on platelet activation and granule secretion *in vitro*, characterize the release profile of PDGF-AB and EGF from CS-PRP hybrid clots *in vitro*, and histologically assess the residency, bioactivity and biodegradability of CS-PRP implants *in vivo*. Our starting hypotheses were that (1) chitosan would bind to platelets in a non-specific way inhibiting platelet aggregation in hybrid clots and platelet-mediated clot retraction; (2) chitosan would activate platelets and induce granule secretion; (3) the release of growth factors with low isoelectric point (negatively charged at neutral pH), such as EGF, would be more sustained from CS-PRP hybrids than the release of growth factors with high isoelectric points (positively charged at neutral pH), such as PDGF-AB, due to electrostatic interactions with cationic chitosan; (4) CS-PRP implants would reside longer than PRP *in vivo*, where they would induce cell recruitment and angiogenesis, but would be degraded within 6 weeks.

Confocal, SEM and TEM images supported our first hypothesis that chitosan physically coats platelets and other components of the blood clot to inhibit platelet aggregation, needed for clot retraction. In the hybrid clots, chitosan physically interferes with the ability of the platelets to adhere to each other and the fibrin network, hence exerting mechanical forces. Our second and third aims were to investigate whether platelets are activated in CS-PRP hybrid clots and, if so, how platelet-derived growth factors are released from CS-PRP hybrid clots. Consistent with our third hypothesis, we found that chitosan induces platelet activation and granule secretion in cell suspensions, even more so than ADP, a known platelet agonist. Interestingly, incubation of cell suspension with trehalose along with chitosan slightly decreased expression of Pac-1 and p-selectin compared to incubation with chitosan alone.

Even though test conditions in the flow cytometry assay are different than in the hybrid clot system, we expected platelets within the CS-PRP hybrid clots to be activated and release their granule content, and this was ascertained by ELISA assays. Our third starting hypothesis was that the isoelectric point of platelet-derived growth factors would determine how growth factors would be released from our CS-PRP hybrids. The isoelectric point of PDGF is 9.8 and, under physiological conditions, we expected ionic repulsion between positively charged PDGF-AB and cationic chitosan to result in burst release. Meanwhile, EGF, which has an isoelectric point of 4.6, would be expected to bind to chitosan under physiological conditions and be released in a more sustained manner. In contrast to this, we found that CS-PRP hybrid clots sustained and increased

release of both PDGF-AB and EGF for 1 week *in vitro*, which suggested that additional factors are controlling their release in this system. We found that cumulative levels of PDGF-AB and EGF released in the culture medium were higher in the case of CS-PRP clots compared to PRP clots. With regard to growth factor release, it is important to consider the contribution of each cell type present in the PRP preparation. Platelets are the main contributors to growth factor release from PRP and positive correlations were previously found between platelet doses and the amount of released growth factors including PDGF-AB, TGF- $\beta$ 1, VEGF and EGF. Our fourth aim was to investigate the implants *in vivo*, and they were shown to exhibit longer residency and higher bioactivity than PRP.

In summary, chitosan physically coats platelets, blood cells and fibrin strands in CS-PRP hybrid clots, thus inhibiting platelet aggregation, which is required for clot retraction. Platelets are activated; granules secreted and higher levels of PDGF-AB and EGF are released from CS-PRP hybrid clots compared to PRP clots *in vitro*. Finally, CS-PRP implants reside for at least 6 weeks post-implantation subcutaneously and induce cell recruitment and granulation tissue synthesis, confirming a longer residency and higher bioactivity compared to PRP *in vivo*.

Our third purpose was to assess whether CS-PRP implants were capable of improving rotator cuff tear repair in a rabbit model. Complete tears were created bilaterally in supraspinatus (SSP) tendons of New Zealand White rabbits (n=4 in a pilot feasibility study followed by n=13 in a larger efficacy study), which were repaired using transosseous suturing. On the treated side, CS-PRP implants were additionally injected into the transosseous tunnels and the tendon itself, and healing was assessed histologically at time points ranging from 1 day to 2 months post-surgery. Our starting hypotheses were that: 1) CS-PRP implants would induce recruitment of polymorphonuclear cells (PMN) at early time points post-surgery, 2) CS-PRP implants would be degraded by 2 months post-surgery, and 3) CS-PRP implants would improve transosseous rotator cuff repair through an increase in cell recruitment, angiogenesis and bone remodeling.

One of our objectives was to determine implant distribution and assess implant degradation over time. At 1 day post-surgery, CS-PRP implants were resident inside the bony trough, in the lateral tunnels and also adhered to tendon surfaces. CS-PRP implants inhibited

heterotopic ossification of the SSP tendon at 2 months while also favoring attachment of the SSP tendon to the humeral head through increased bone remodelling at the greater tuberosity.

CS-PRP implants induced PMN recruitment at early time points post-surgery, supporting our first hypothesis. In contrast to the second hypothesis, implant degradation and associated inflammatory reactions were still ongoing in 3 out of 9 treated shoulders at 2 months. Results partially supported our third hypothesis that CS-PRP would improve rotator cuff tear repair, since treatment improved SSP tendon attachment through increased bone remodeling. Unexpectedly, small areas of neutrophil-rich granulation tissue surrounding apoptotic/necrotic tissues were visible in 3 CS-PRP treated shoulders at 2 months. The suppression of SSP tendon heterotopic ossification (HO) by CS-PRP treatment was an unexpected finding in this study. The bony trough was incompletely healed in some rabbits at 2 months. This study seems to provide evidence that CS-PRP implants are safe and effective in improving rotator cuff tear repair in a small animal model, and that this could potentially be translated into clinical setting.

Our fourth purpose was to investigate the effect of using CS- PRP implants in conjunction with suture anchors in chronic and acute ovine rotator cuff tear models and see if it can improve rotator cuff repair. In two subsequent pilot feasibility studies, unilateral full-thickness tears were created in the infraspinatus (ISP) tendons of mature female Texel-Cross sheep. In the chronic model (n=4 sheep), the tendons were capped with silicone and allowed to degenerate to chronic stage for 6 weeks, while the tendons were immediately repaired in the acute model (n=4 sheep). Transected ISP tendons were reattached with suture anchors and, in the case of treated shoulders; implants composed of freeze-dried CS solubilized in autologous PRP were additionally applied to the tendon-bone interface and on top of the repaired site.

The chronic defect model induced significant tendon degeneration and retraction, which made repair more challenging than in the acute defect model. Treatment with CS-PRP implants induced recruitment of polymorphonuclear cells at 2 weeks post-operatively and improved ISP tendon structural organization at 3 months. Treatment also increased bone remodeling and ingrowth at the tendon-bone interface at 3 months, suggesting that a more robust attachment could be achieved by combining CS-PRP implants with suture anchors.

Our starting hypothesis was supported in that treatment with anchors + CS-PRP implants led to improved tendon structural appearance and increased bone remodeling and ingrowth at the tendon-bone junction. We found that capping the ISP tendons for 6 weeks with 5-cm silicone tubes likely prevented proper nutrient diffusion and led to cell death and severe tendon degeneration, which rendered some tendons unrepairable. Although degeneration was not as marked when the tendons were capped for 2 weeks with 5-mm silicone length, reattachment at the footprint would have been difficult to achieve since the tendon-muscle unit had significantly retracted. We found that abundant scar tissues were bridging the gap between the capped tendon and the tuberosity after 2 weeks and 6 weeks. As of now, we consider the acute repair model to be more consistent and easily reproducible.

Polymorphonuclear (PMN) cells were observed in the tendon repair tissue of the shoulder treated with anchors + CS-PRP for 2 weeks. The tendon treated with anchors only showed chondrogenesis and GAG expression within the tendon body at 6 weeks, while the tendon treated with anchors + CS-PRP did not. Unexpectedly, the anchors + CS-PRP repair technique resulted in better tendon structural outcome than anchors only at 3 months, possibly through a modulation of timing of the healing sequence or through increased repair tissue remodeling. There were no treatment-specific deleterious effects in the shoulder joints, suggesting that CS-PRP implants have high safety. Structural abnormalities were visible in most glenoids, suggesting that greater stresses are applied on that surface compared to the humeral head in sheep. Fatty infiltration of the ISP muscle was induced in both chronic and acute models, and no treatment was able to reverse that effect. Mild transient synovitis was present in the shoulder treated with CS-PRP at 2 weeks, and this was resolved at the later 6 weeks and 3 months time points, once the biomaterial was degraded.

In summary, developing techniques to augment of rotator cuff repair remains clinically relevant. The technical challenges associated with the chronic repair model in the sheep make the acute model more preferable for future studies. These pilot studies provide the first evidence that CS-PRP implants improve the healing response in large animal models of rotator cuff repair, partly through increased bone remodeling at the tendon repair tissue and underlying bone interface.



## TABLE OF CONTENTS

DEDICATION.....	III
ACKNOWLEDGEMENTS .....	IV
RÉSUMÉ.....	VI
ABSTRACT.....	XII
TABLE OF CONTENTS .....	XVII
LIST OF TABLES .....	XXII
LIST OF FIGURES.....	XXIII
LIST OF SYMBOLS AND ABBREVIATIONS.....	XXX
LIST OF APPENDICES .....	XXXVI
CHAPTER 1 INTRODUCTION .....	1
1.1 General objective.....	4
CHAPTER 2 LITERATURE REVIEW .....	7
2.1 Basic biology of tendons .....	7
2.2 Tendon and enthesis development .....	12
2.3 Tendon and enthesis healing .....	14
2.4 Rotator Cuff Anatomy and Pathology.....	16
2.5 Surgical Treatments of Rotator Cuff Tears .....	18
2.6 Animal Models of Rotator Cuff Repairs .....	22
2.6.1 Rat .....	22
2.6.2 Rabbit .....	24
2.6.3 Sheep.....	25
2.6.4 Dogs and non-human primates.....	26

2.7	Technologies under Development for Rotator Cuff Repair .....	28
2.7.1	Platelet-rich plasma .....	28
2.7.2	Tendon Patches & Grafts .....	31
2.7.3	Cells.....	33
2.7.4	Scaffolds, Cells and Combinations .....	35
2.7.5	Growth Factors & Cytokines.....	38
2.8	Chitosan.....	40
2.8.1	Chitosan/whole blood hybrids for cartilage repair .....	49
2.8.2	Rationale for using chitosan-PRP hybrids in rotator cuff repair .....	52
CHAPTER 3	ORGANIZATION OF ARTICLES .....	53
CHAPTER 4	ARTICLE 1: ROTATOR CUFF REPAIR: A REVIEW OF SURGICAL TECHNIQUES, ANIMAL MODELS, AND NEW TECHNOLOGIES UNDER DEVELOPMENT .....	55
4.1	Introduction .....	57
4.2	Rotator Cuff Anatomy and Pathology.....	58
4.3	Surgical Treatments of Rotator Cuff Tears .....	59
4.4	Animal Models of Rotator Cuff Repair.....	60
4.5	Technologies Under Development for Rotator Cuff Repair Augmentation .....	63
4.5.1	Extracellular Tendon Patches.....	63
4.5.2	Scaffolds.....	64
4.5.3	Stem Cells .....	65
4.5.4	Growth Factors & Cytokines.....	66
4.5.5	Platelet-rich plasma .....	67
4.5.6	Chitin and chitosan.....	69

4.6	Conclusions .....	70
CHAPTER 5 ARTICLE 2 :CHITOSAN INHIBITS PLATELET-MEDIATED CLOT RETRACTION, INCREASES PLATELET-DERIVED GROWTH FACTOR RELEASE, AND INCREASES RESIDENCE TIME AND BIOACTIVITY OF PLATELET-RICH PLASMA <i>IN VIVO</i> .....		
		91
5.1	Introduction .....	93
5.2	Materials and methods .....	95
5.2.1	Preparation of freeze-dried chitosan formulations .....	95
5.2.2	Preparation of platelet-rich plasma (PRP).....	96
5.2.3	Solubilization of freeze-dried chitosan formulations in platelet-rich plasma (PRP) .	96
5.2.4	Assessment of clot retraction .....	97
5.2.5	Confocal fluorescent and spinning disk microscopy imaging .....	97
5.2.6	Scanning electron microscopy (SEM) imaging .....	98
5.2.7	Transmission electron microscopy (TEM) imaging.....	98
5.2.8	Preparation of cell suspension and flow cytometry .....	99
5.2.9	Quantification of growth factors released from clots.....	99
5.2.10	Subcutaneous implantation .....	100
5.2.11	Statistical analysis .....	101
5.3	Results .....	102
5.3.1	Clot retraction and platelet aggregation are inhibited in chitosan-PRP hybrid clots	102
5.3.2	Chitosan coats clot components in chitosan-PRP hybrid clots .....	104
5.3.3	Chitosan induces platelet activation and granule secretion in cell suspension .....	106
5.3.4	Chitosan-PRP hybrids provide a greater and sustained release of PDGF-AB and EGF over time.....	107

5.3.5 Chitosan-PRP hybrids reside for at least 6 weeks in vivo and induce cell recruitment.....	108
5.4 Discussion .....	109
5.5 Summary .....	114
CHAPTER 6 ARTICLE 3: FREEZE-DRIED CHITOSAN-PRP IMPLANTS IMPROVE SUPRASPINATUS TENDON ATTACHMENT IN A TRANSOSSEOUS ROTATOR CUFF REPAIR MODEL IN THE RABBIT .....	123
6.1 Introduction .....	126
6.2 Materials and methods .....	128
6.2.1 Rotator cuff tear model, surgical repair and study design.....	128
6.2.2 Preparation of freeze-dried chitosan formulations .....	132
6.2.3 Preparation of platelet-rich plasma (PRP).....	132
6.2.4 Solubilization of freeze-dried chitosan formulations in PRP and injection of CS-PRP implants .....	132
6.2.5 Specimen collection and histological processing .....	133
6.2.6 Micro CT analysis .....	138
6.2.7 Statistical analysis .....	138
6.3 Results .....	139
6.3.1 CS-PRP implants adhered to SSP tendon tissue and were resident within the bony trough and lateral tunnels at 1 day post-surgery .....	139
6.3.2 CS-PRP implants induced recruitment of polymorphonuclear (PMN) cells from day 1 to day 14 post-surgery .....	141
6.3.3 CS-PRP implants inhibited heterotopic ossification of SSP tendon tissue at 2 months.....	142
6.3.4 CS-PRP implants significantly improved attachment of SSP tendon at 2 months ..	145

6.3.5	CS-PRP implants induced bone remodeling at the greater tuberosity at 2 months..	149
6.3.6	CS-PRP treatment was safe.....	151
6.4	Discussion .....	153
CHAPTER 7 ARTICLE 4: FREEZE-DRIED CHITOSAN-PLATELET-RICH PLASMA IMPLANTS FOR ROTATOR CUFF TEAR REPAIR: PILOT OVINE STUDIES .....		166
7.1	INTRODUCTION.....	168
7.2	MATERIALS AND METHODS .....	170
7.2.1	Preparation of freeze-dried chitosan formulations .....	170
7.2.2	Preparation of platelet-rich plasma (PRP).....	171
7.2.3	Experimental study design and surgical technique .....	171
7.2.4	Specimen collection and histological processing.....	175
7.3	RESULTS.....	176
7.3.1	The chronic repair model was more challenging than the acute repair model.....	176
7.3.2	CS-PRP implants induced recruitment of polymorphonuclear cells to the ISP tendon at 2 weeks and improved ISP tendon structural organization at 3 months .....	179
7.3.3	CS-PRP implants increased bone remodeling at the ISP tendon-bone junction.....	181
7.3.4	CS-PRP implants did not induce any treatment-specific deleterious effects in the shoulder joint.....	183
7.4	DISCUSSION .....	186
7.5	CONCLUSION .....	190
CHAPTER 8 GENERAL DISCUSSION .....		200
CHAPTER 9 CONCLUSION AND RECOMMENDATIONS.....		211
BIBLIOGRAPHY .....		217
APPENDICES .....		254

## LIST OF TABLES

Table 2-1: Zones of fibrocartilaginous entheses .....	12
Table 2-2: Advantages and disadvantages of different animal models for rotator cuff repair.....	27
Table 6-1: Design of Study 1-Pilot feasibility study.....	129
Table 6-2: Design of Study 2-Larger efficacy study.....	129
Table 6-3: Microscopic scoring of SSP tendon.....	134
Table 6-4: Microscopic scoring of SSP enthesis.....	136
Table 7-1: Design of the chronic repair study.....	173
Table 7-2: Design of the acute repair study. ....	174
Table 9-1: Clinical studies comparing arthroscopic versus open rotator cuff repair. ....	254
Table 9-2: Clinical studies comparing different suturing techniques. ....	261
Table 9-3: Rotator cuff rabbit repair models.....	269
Table 9-4: Rotator cuff sheep repair models.....	279
Table 9-5: Clinical studies comparing PRP study in Rotator cuff repair.....	287

## LIST OF FIGURES

Figure 2-1: Schematic drawing of a basic tendon structure (Docheva, Muller et al. 2015). .....	7
Figure 2-2: Anatomy of a normal tendon (Sharma and Maffulli 2005).....	8
Figure 2-3: Chemical structure of chitin .....	41
Figure 2-4: Chitin extracted from shellfish from which chitosan is made by N-deacetylation (Ahmadi, Oveisi et al. 2015). .....	43
Figure 2-5: Chitosan flow production (Ibrahim and Zairy 2015). .....	44
Figure 2-6: Schematic representation of chitosan structure (Dash, Chiellini et al. 2011). .....	45
Figure 2-7: Schematic illustration of chitosan's versatility: At low pH, chitosan's amine groups are protonated conferring polycationic behaviour to chitosan. At high pH, chitosan's amines are deprotonated and reactive (Dash, Chiellini et al. 2011). .....	46
Figure 5-1: After clotting for 1 hour at 37°C, clot retraction and serum expression (expressed as % clot mass lost) was greater from PRP clots compared to CS-PRP hybrid clots (a). Data are presented as mean (diamond) and median (line) of n=7 clots from 3 different donors; Box: 25 <sup>th</sup> and 75 <sup>th</sup> percentile; Whisker Box to the most extreme point within 1.5 interquartile range. The Mixed model task in SAS Enterprise Guide 7.1 and SAS 9.4 was used to compare the different groups using sample (CS-PRP vs PRP) as a fixed effect and donor as a random effect. * p < 0.05 compared to PRP. Platelet aggregates were smaller in CS-PRP hybrid clots (b, d & f) compared to PRP clots (c, e & g), as shown by spinning disk microscopy images (b & c), confocal microscopy images (d & e) and 3-D stacks of confocal microscopy images (f & g). An Alexa-647 fibrinogen tracer was added to allow imaging of fibrin-covered platelets and fibrin in white. A Rhodamine-chitosan tracer was added to allow imaging of chitosan in red in d) and orange in f). .....	103
Figure 5-2: Chitosan (CS) appeared to be coating cellular and fibrous elements in scanning electron microscopy (SEM) images of CS-PRP clots (a & b) while the fibrin (F) network was readily visible in PRP clots (c & d). Chitosan (CS) was found in the space between cellular elements and also at the surface of erythrocytes (E), platelet aggregates (P) and	

fibrin (F) in transmission electron microscopy (TEM) images of CS-PRP clots (e & f). Erythrocytes (E) were tightly packed and platelet aggregates (P) were large in TEM images of PRP clots (g & h). ..... 105

Figure 5-3: a) Flow cytometric analysis of PAC-1 (a) and p-selectin (b) staining of cell suspension (unactivated in red). As expected, incubation with ADP (20  $\mu$ m in green) and chitosan (in dark blue), both known platelet agonists, led to platelet activation (a) and granule secretion (b). In contrast, incubation with trehalose alone (in yellow) had no effect on platelet activation (a) or granule secretion (b). Interestingly, incubation with chitosan and trehalose simultaneously (in pale blue) decreased the intensity of both fluorescent signals compared to incubation with chitosan alone (in dark blue). ..... 106

Figure 5-4: PDGF-AB (a) and EGF (b) cumulative release in culture medium was greater for CS-PRP clots compared to PRP clots. Data are presented as mean (circle) and median (line) of n=13 clots from 6 different donors; Box: 25<sup>th</sup> and 75<sup>th</sup> percentile; Whisker: Box to the most extreme point within 1.5 interquartile range. The Mixed model task in SAS Enterprise Guide 7.1 and SAS 9.4 was used to compare the different groups with post-hoc analysis to look at pair-wise differences using sample and time as fixed effects and donor as a random effect. \* p < 0.05 compared to PRP. Insets show total amount of growth factors released. .... 108

Figure 5-5: Formulations containing 1% (w/v) chitosan (CS  $M_n$  38-43kDa and DDA 80-85%) with 1% (w/v) trehalose and 42.2 mM CaCl<sub>2</sub> were solubilized in autologous PRP and injected subcutaneously in rabbits, where they were found to be resident and induce cell recruitment at two weeks (a-c), four weeks (d-f), and six weeks (g-i) post-implantation. Invasion of the CS-PRP implants by host cells was accompanied by granulation tissue (GT) synthesis and formation of new blood vessels (BV). In contrast, recalcified PRP implants were completely degraded within a few days (not shown since the implant was absent). Outlines in a, d & g show where higher magnification images b, c, e, f, h & i were acquired. .... 109

Figure 6-1: a-d) Surgical procedure. A complete surgical tear was created in the supraspinatus (SSP) tendon of the rotator cuff, as close as possible to the insertion site (a). Two 3.0 prolene sutures were pre-placed through the bony trough, the lateral tunnels (b) and the



tendon itself in a modified Mason-Allen pattern. In the case of treated shoulders, the CS-PRP mixture (150  $\mu$ L) was injected into the bony trough prior to tightening the sutures (c), and it flowed out of all lateral tunnels. Sutures were tightened to attach the tendon to the humeral head (d). The CS-PRP mixture (150  $\mu$ L) was then injected at the repaired insertion site and into the tendon itself. e) Schematic representation of the surgical model. f) Area in red is the region of interest (ROI) that was set over the greater tuberosity and used for micro-CT analysis. .... 130

Figure 6-2: a to h) Safranin O/Fast Green-stained paraffin sections of shoulder treated with transosseous suturing + CS-PRP after 1 day. Polymorphonuclear cells (PMNs) were recruited to the bony trough (b), the lateral tunnels (c), to the endomyseal SSP muscle space (d) and to the SSP tendon (h). In some histological sections, needle tracks containing CS-PRP implant were visible within the SSP tendon (e & f). Note that stump of the tendon was not fully debrided in these samples (a and e). i to k) A rhodamine-chitosan tracer was used to image chitosan with epifluorescence in bright red. At one day post-surgery, chitosan-PRP hybrid implant was found adhering to the SSP tendon surface (i) and in the bony trough (j & k). .... 140

Figure 6-3: Safranin O/Fast Green-stained paraffin sections of shoulder treated with transosseous suturing + CS-PRP (a to d) or suturing only (e to h) after 7 days. Residual structurally normal SSP tendon tissue was apparent and gaps were present at the tear site in all samples (a, b, e & f). Polymorphonuclear (PMN) cells were abundant in the granulation tissue of the CS-PRP treated shoulder only (c vs g). New bone was forming at the lateral aspect of the cortical bone in both groups (example shown in d). Chondrogenesis was observed in the SSP tendon of the control sutured shoulder only (h). Outlines in a & e show where higher magnification images were acquired. .... 142

Figure 6-4: Safranin O/Fast Green-stained paraffin sections of intact shoulders (a to d), and test shoulders treated with transosseous suturing + CS-PRP (e to h) or suturing only (i to l) after 2 months, showing best and worst overall tendon scores for all groups. SSP tendon structure was altered in all surgically treated shoulders with several tendons displaying a highly cellular and vascular phenotype (e, f, i & j). Inflammatory PMN-rich tissue was present in 3 out of 9 shoulders treated with transosseous suturing + CS-PRP at 2 months (g & h).

Heterotopic ossification within the SSP tendon was observed in 5 out of 9 shoulders treated with transosseous suturing (k & l). Data in m are presented as mean (circle), median (line); Box: 25<sup>th</sup> and 75<sup>th</sup> percentile; Whisker: Box to the most extreme point within 1.5 interquartile range. \*  $p < 0.05$  compared to intact. #  $p < 0.05$  compared to sutures group. &  $p < 0.05$  compared to sutures + CS-PRP group. .... 145

Figure 6-5: Safranin O/Fast Green-stained paraffin sections of intact shoulders (a to d), and test shoulders treated with transosseous suturing + CS-PRP (e to h) or suturing only (i to l) after 2 months, showing best and worst overall enthesis scores for all groups. The original tendon stump was often observed in surgically treated shoulders (e, f, i & j). In the best repair cases, fibrocartilage formation and partial restoration of the tidemark were observed at the enthesis (f & j). In the worst repair cases, gaps were present at the tendon-bone interface (h & l), although treatment with transosseous suturing + CS-PRP decreased such instances (m). Data in m are presented as mean (circle), median (line); Box: 25<sup>th</sup> and 75<sup>th</sup> percentile; Whisker: Box to the most extreme point within 1.5 interquartile range. \*  $p < 0.05$  compared to intact. #  $p < 0.05$  compared to sutures group. .... 148

Figure 6-6: Polarized light microscopy images of SSP entheses. In the best cases, wave-like structures and alignment of the collagen fibres parallel to the long axis of the SSP tendon were visible (a, c & e). In the worst cases, very little collagen alignment was apparent in the fibrous tissue adjacent to the bone (b, d & f). .... 148

Figure 6-7: Micro-CT of intact (a) and surgically treated shoulder at 1 day (b), and test shoulders treated with transosseous suturing + CS-PRP (c to g) or suturing only (d to h) after 2 months. Incomplete repair of cortical bone at the lateral aspect of the humerus (c & d) and lateral bone formation (e & f) were present in all shoulders, regardless of treatment. Incomplete repair of the bone troughs was observed bilaterally in 5 rabbits (g & h). In half the treated shoulders, bone remodeling was highly stimulated by chitosan-PRP treatment (compare panel c to d), which led to increases in bone surface (j) and connectivity (k). Data in i, j & k are presented as mean (circle), median (line); Box: 25<sup>th</sup> and 75<sup>th</sup> percentile; Whisker: Box to the most extreme point within 1.5 interquartile range. \*  $p < 0.05$  compared to intact. #  $p < 0.05$  compared to sutures group. &  $p < 0.1$  compared to intact. .... 150

Figure 6-8: Safranin O/Fast Green-stained paraffin sections of intact shoulders (a to d), and test shoulders treated with transosseous suturing + CS-PRP (e to h) or suturing only (i to l) after 2 months, showing best and worst OOHAS scores for humeral head and glenoid articular surfaces (a to l). Some structural abnormalities such as GAG depletion, fissures, cell changes and thinning of the articular cartilage were occasionally observed in both humeral head (b, f & j) and glenoid (d, h & l) surfaces, although average histological scores were not significantly different from intact (m). Data in m are presented as mean (circle), median (line); Box: 25<sup>th</sup> and 75<sup>th</sup> percentile; Whisker: Box to the most extreme point within 1.5 interquartile range. .... 152

Figure 6-9: Safranin O/Fast Green-stained paraffin sections of SSP muscles from intact shoulders (a & b), and test shoulders treated with transosseous suturing + CS-PRP (c & d) or suturing only (e & f) after 2 months, showing best and worst scores for fatty infiltration. Surgical treatment induced fatty infiltration of SSP muscle after 2 months (g). Data in g are presented as mean (circle), median (line); Box: 25<sup>th</sup> and 75<sup>th</sup> percentile; Whisker: Box to the most extreme point within 1.5 interquartile range. \*  $p < 0.05$  compared to intact. .... 153

Figure 7-1: Chronic tear model and repair with CS-PRP. Full-thickness rotator cuff tears were created in the infraspinatus (ISP) tendon of the shoulder close to the enthesis (a, b) and capped with 5 cm length of silicon (c) in 4 sheep. At 6 weeks after surgery, the tendons were macroscopically abnormal (d) and 2 tendons were found to be irreparable. One tendon was repaired with 4 suture anchors in the suture bridge configuration. One tendon was repaired with one suture anchor + CS-PRP. The sutures were pre-placed in a Mason-Allen pattern and a first injection of 0.5 mL CS-PRP was applied at the debrided bone interface (e). The anchor was inserted to tighten the sutures and an additional 0.5 mL CS-PRP implant was applied on top of tendon at the repaired site and also under the tendon. Macroscopic appearance of an ISP tendon capped for 2 weeks with 5 mm length of silicon (f). .... 177

Figure 7-2: Acute tear model and repair with CS-PRP. Full-thickness rotator cuff tears were created in the infraspinatus (ISP) tendon of the shoulder close to the enthesis in 4 sheep (a, b). All tendons were immediately repaired with 4 suture anchors in a suture bridge configuration. In 2 out of 4 sheep, repair was augmented with CS-PRP. The first row of anchors were inserted and the sutures were passed (c) and a first injection of 0.5 mL CS-

PRP was applied at the debrided bone interface (d). The second row of anchors were inserted to tighten the sutures (e) and an additional 0.5 mL CS-PRP was applied on top of tendon at the repaired site and also under the tendon (f). ..... 178

Figure 7-3: Safranin O/Fast Green stained paraffin sections of the ISP tendons in the chronic repair model. Intact control tendons were organized in bundles, as expected (a to c). Bundle organization was still apparent in areas of untreated tendons at chronic stage, while other areas were disorganized, hypercellular and vascularized or hypocellular (d to i). The tendon of the shoulder treated for 2 weeks with suture anchors was mostly disorganized, hypercellular and vascularized, with a small hypocellular area (j to l). The tendon of the shoulder treated with suture anchors + CS-PRP was mostly disorganized, hypercellular and vascularized, with a small area organized in bundles and another area rich in polymorphonuclear cells (m to o) ..... 180

Figure 7-4: Safranin O/Fast Green-stained paraffin sections and polarized light microscopy (d, h, l, p & t) images of the ISP tendons in the acute repair model. Intact control tendons were organized in bundles, as expected (a to d). At 6 weeks post-surgery, the tendons were mostly composed of a disorganized and vascular fibrous repair tissue in both groups (e to l). Chondrogenesis and GAG expression were apparent in the anchors only group at 6 weeks (e&f). At 3 months post-surgery, the tendon in the anchors only group contained aligned tissue, expressed high levels of GAG, and had a small area organized in bundles (m to p). In contrast, the tendon in the anchors + CS-PRP group was mostly organized in bundles with a smaller area of tendon-like repair tissue (m to t). ..... 180

Figure 7-5: Safranin O/Fast Green stained paraffin sections of the ISP tendon entheses in the chronic repair model. Intact controls had normal entheses consisting of 1) unmineralized fibrocartilage, 2) tidemark, 3) mineralized fibrocartilage and 4) bone, as expected (a to c). The tidemark was still recognizable 2 weeks after defect creation (d), but not at longer time points or after repair (g, j & m). Scar tissue was growing above the entheses in the untreated chronic defects (d&g), suggesting that some spontaneous repair can occur even without any treatment in this model. Integration of the scar tissue with the underlying bone was achieved through bone remodeling and ingrowth into the scar tissue (f, i, l & o). Treatment with anchors + CS-PRP increased the area of remodeling bone (compare o to l). ..... 182

Figure 7-6: Safranin O/Fast Green stained paraffin sections of the ISP tendon entheses in the acute repair model. Intact controls had normal entheses consisting of 1) unmineralized fibrocartilage, 2) tidemark, 3) mineralized fibrocartilage and 4) bone, as expected (a to c). Scar tissue was growing superior to the entheses from 6 weeks (d to i) to 3 months (j to o) post-surgery. Integration of the scar tissue with the underlying bone was achieved through bone remodeling and ingrowth into the scar tissue (d to o). This was more apparent in the anchors + CS-PRP group (compare g&m to d&j). The site of anchor insertion was apparent in some sections (\* in panel j).....183

Figure 7-7: Safranin O/Fast Green stained sections of humeral head and glenoid articular surfaces from intact controls (a&b), from the chronic defect model (c to f) and from the acute defect model (g to j). The humeral articular surfaces were all structurally normal but showed signs of GAG depletion (a, c, e, g & i). Mild structural abnormalities were observed at the center of some glenoid articular surfaces, including GAG depletion, hypercellularity, cell cloning and fissures (k to m). These were apparent in all treatment groups as well as the intact controls.....184

Figure 7-8: Hematoxylin and Eosin (a, d & e) and Safranin O/Fast Green (b & c) stained paraffin sections of muscle biopsies from intact control (a), from the chronic defect model (b & c) and from the acute defect model (d & f). Fatty infiltration was not prevented by any treatment.....185

Figure 7-9: Hematoxylin and Eosin (a, d & e) and Safranin O/Fast Green (b & c) stained paraffin sections of synovial biopsies from intact control (a), from the chronic defect model (b & c) and from the acute defect model (d & f). There was mild synovitis and increased cell infiltration in the chronic model treated with anchors + CS-PRP for 2 weeks (c).....186

## LIST OF SYMBOLS AND ABBREVIATIONS

a-PRP	Activated Platelet-Rich Plasma
Ac	Acetyl
ADP	Adenosine Diphosphate
ADSC	Adipose Derived Stem Cell
AMSC	Adipocyte Mesenchymal Stem Cell
aP-PRP	Activated Pure Platelet-Rich Plasma
ASES	American Shoulder and Elbow Surgeons score
bFGF	Beta-Fibroblast Growth Factor
BM	Bone Marrow
BM-MSC	Bone Marrow Mesenchymal Stem cell
BMAC	Bone Marrow Aspirate Cells
BMP-13	Bone Morphogenic Protein
BMSC	Bone Marrow Stem Sell
BS	Bone Surface area
BSA	Bovine Serum Albumin
BV	Bone Volume
BV	Blood Vessels
CaCl <sub>2</sub>	Calcium Chloride
cAMP	Cyclic AMP
CH <sub>3</sub> COOH	Acetic Acid
Col	Collagen
Col-I	Type I collagen

Col-II	Type II collagen
Col-X	Type X collagen
CS	Chitosan
CS-GP	Chitosan-Glycerol Phosphate
CS-PRP	Chitosan-Platelet-Rich Plasma
CT	Computed Tomography
DDA	Degree of Deacetylation
DNA	Deoxyribonucleic acid
DR	Double-Row
ECM	Extracellular Matrix
EGF	Endothelial Growth Factor
ELISA	Enzyme-Linked Immunosorbent Assay
FC	Fibrocartilage
FD	Freeze-Dry
FG	Fast Green
FGF	Fibroblast Growth Factor
FITC	Fluorescein Isothio-Cyanate
g	Gram
GAGs	Glycosaminoglycans
GF	Growth factor
Glc	D-glucosamine
GlcN	D-glucosamine
GlcNAc	N-acetyl-D-glucosamine
GP	Glycerol Phosphate
GPIIb-IIIa	Glycoprotein 2 $\beta$ -3 $\alpha$

GT	Granulation Tissue
H&E	Hematoxylin and Eosin
H <sub>2</sub> O	Water
H <sub>2</sub> SO <sub>4</sub>	Sulfuric Acid
HA	Hyaluronic Acid
HA	Hyaluronic Acid
HCl	Hydrochloric Acid
HCL	Hydrochloric Acid
HCOOH	Formic Acid
HNO <sub>3</sub>	Nitric Acic
IGF	Insulin Growth Factor
Ihh	Indian Hedgehog
IL	Interleukin
ISP	Infraspinatus
JOA	Japanese Orthopaedic Association
KCL	Potassium Chloride
kDa	Kilodalton
kg	Kilogram
kV	Kilovolt
L-PRF	Leukocyte-Rich Platelet-Rich Fibrin
L-PRP	Leukocyte-Rich Platelet-Rich Plasma
M	Molar
MA	Masson-Allen
MgCl <sub>2</sub>	Magnesium Chloride



mL	Millilitre
mm	Millimeter
MMP	Matrix Metalloproteinase
MRI	Magnetic Resonance Imaging
MSC	Mesenchymal Stem Cell
MW	Molecular Weight
Na <sub>2</sub> HPO <sub>4</sub>	Sodium Phosphate Dibasic
NaCl	Sodium Chloride
NaHCO <sub>3</sub>	Sodium Carbonate
NBF	Normal Buffered Formalin
NZW	New Zealand White
P-PRF	Pure Platelet-Rich Fibrin
P-PRP	Pure platelet-rich plasma
PDGF	Platelet Derived Growth Factor
PGE <sub>2</sub>	Prostaglandin E2
PLGA	Polyglycolic acid
PLLA	Poly-L-Lactic acid
PMN	Polymononuclear cells
PRF	Platelet-Rich Fibrin
PRGF	Platelet Rich in Growth Factors
PRP	Platelet-Rich Plasma
PTH	Parathyroid Hormone
PTHrP	Parathyroid Hormone related Peptide
RBC	Red blood cell
RC	Rotator Cuff

RCT	Rotator Cuff Tear
rhPDGF	Human recombinant Platelet-Derived Growth Factor
Runx	Runt-related transcription factor
Saf-O	Safranin-O
SC	Stem Cells
SCP	Subscapularis
SCX	Scleraxis
SEM	Scanning Electron Microscopy
SIS	Small Intestine Submucosa
SPCHT	Porous Chitosan Sponges Scaffold
SR	Single-Row
SSP	Supraspinatus
TDSC	Tendon-Derived Stem Cells
TEM	Transmission electron microscopy
TGF	Transforming Growth Factor
TIMP	Tissue inhibitors of metalloproteinase
TM	Teres minor
TNF	Tumour Necrosis Factor
TOE	Transosseous-Equivalent
TP	Tricalcium Phosphate
TSPC	Tendon Stem Cell progenitor Cell
UCLA	University of California, Los Angeles score
v/v	volume/volume
VEGF	Vascular Endothelial Growth Factor

w/v      Weight by volume

$\alpha$       Alpha

$\beta$       Beta

$\mu$       Micro

$\mu\text{L}$       Microlitre

## LIST OF APPENDICES

APPENDIX A – CLINICAL STUDIES COMPARING ARTHROSCOPIC VERSUS OPEN ROTATOR CUFF REPAIR.....	254
APPENDIX B – CLINICAL STUDIES COMPARING DIFFERENT SUTURING TECHNIQUES.....	261
APPENDIX C – ROTATOR CUFF RABBIT REPAIR MODELS .....	269
APPENDIX D – ROTATOR CUFF SHEEP REPAIR MODELS .....	279
APPENDIX E- CLINICAL STUDIES COMPARING PRP STUDY IN ROTATOR CUFF REPAIR.....	287

## CHAPTER 1 INTRODUCTION

More than 28 million Americans are affected by musculoskeletal injuries, estimated to cost more than \$254 billion each year (Praemer, Furner et al. 1999). Rotator cuff tears are among the most common injuries occurring in the shoulder and are often seen in older athletes of overhead sports, like tennis or basketball (Yamamoto, Takagishi et al. 2010). It is a widespread crisis, causing high rate of morbidity and inability in workplaces and sports (Lehman, Cuomo et al. 1995, Yanke and Chubinskaya 2015). Rotator cuff tears are associated with structural and architectural alterations of the musculotendinous unit, such as tendon retraction, fatty infiltration and muscular atrophy (Antoniades, Scher et al. 1979, Borges, Borchard et al. 2007, Periyah, Halim et al. 2014).

Cuff tears result in shoulder pain, stiffness, weakness and loss of motion (Trent, Bailey et al. 2013). It usually starts as an acute tendinopathy with progressive degeneration leading to a partial thickness tear and eventually full rupture (Neer, Craig et al. 1983). The shoulder joint can still function with minimal pain in spite of a rotator cuff tear by using the deltoid and the scapular stabilizing muscles (Feeley, Gallo et al. 2009), however limited function of upper extremities will impair the ability to carry out basic activities (Nho, Brown et al. 2009, Yamamoto, Takagishi et al. 2010). Rotator cuff injury is the second most common musculoskeletal pathology after lower back pain (Picavet and Schouten 2003) and is the most common shoulder condition that patients seek therapy for (Gomoll, Katz et al. 2004, Riley 2004).

Cuff tears may cause irreversible changes in the structural and physiological properties of the shoulder, causing intolerable chronic pain (Funakoshi, Majima et al. 2006) and severe functional disability, as well as compromise joint mechanics leading to degenerative changes (Aurora, McCarron et al. 2007). Degenerative changes in the structure and composition of the tendons make healing very difficult. After surgical repair, failure rate ranges between 20 to 95% (Galatz, Ball et al. 2004) due to tendon degeneration, hypo vascularization (Cohen 1985, Jackson 2007, Gulotta, Kovacevic et al. 2009, Longo, Franceschi et al. 2009, Lui, Zhang et al. 2010, Longo, Forriol et al. 2011, Ahmad, Howard et al. 2012), muscle atrophy, fatty infiltration of tendon and muscle and a lack of tendon-to-bone integration (Gartsman 1997, Totani, Cumashi et al. 1998, 2005). Tendon vascularization is mostly compromised at the junction zones and sites of

torsion, friction or compression (Sharma and Maffulli 2006), which reduces the chances of adequate self-repair (Chahla, Dean et al. 2016).

Patients with re-tears usually experience some pain relief but continue to have lower functional outcomes (Heldin and Westermarck 1999, Galatz, Ball et al. 2004). Rotator cuff insertion site, also known as the enthesis, is never completely reformed after surgical reattachment (Gulotta and Rodeo 2009, Chung, Kim et al. 2014). The overall structure, composition, and organization of a normal insertion site do not regenerate, especially, the calcified cartilage zone (Gerber, Schneeberger et al. 1999). Instead, healing occurs through fibrovascular disorganized scar tissue formation (Pencev and Grotendorst 1988, Robertson, Maley et al. 1993), lacking strength, load-to-failure, and biomechanical tendon properties leading to increased risk of further damage and high re-tear rates (Galatz, Ball et al. 2004, Angeline and Rodeo 2012, Del Buono, Oliva et al. 2012) (Galatz, Ball et al. 2004, Boileau, Brassart et al. 2005, Galatz, Sandell et al. 2006, Angeline and Rodeo 2012, Del Buono, Oliva et al. 2012).

Current standard surgical treatment involves open or arthroscopic repair of torn tendons frequently using suture anchors in a variety of configurations (McElvany, McGoldrick et al. 2015). The goal of suturing repair is to increase initial fixation strength, mechanical stability and increase biological tendon-to-bone healing (Cole, ElAttrache et al. 2007), which most often fails. The current suturing techniques are thought to increase footprint contact area, which could improve the rate of healing but re-tear rates are still relatively high (Denard and Burkhart 2013). Considerable variation in surgical procedures exists, confirming the lack of a single reliable technique (McElvany, McGoldrick et al. 2015). It is recognized that current surgical treatments need improvement (Gerber, Fuchs et al. 2000, Galatz, Ball et al. 2004). Improving repair techniques could be achieved through biological or synthetic tendon grafts or through augmentation devices (Dwivedi, Chevrier et al. 2017, Ghazi zadeh, Chevrier et al. 2017), however success is limited. The current goal is to completely regenerate the fibrocartilaginous insertion zones through biological augmentation. A good cuff repair technique should decrease pain, increase strength as well as range of motion (Cole, ElAttrache et al. 2007). New techniques in tissue engineering have been postulated to increase rotator cuff tear repair, such as scaffolds, growth factors and cell seeding (Derwin, Badylak et al. 2010), but their uses are still preliminary.

Despite the advances in tissue engineering, rotator cuff tear repair still represents an enormous challenge.

Platelet-rich plasma (PRP) is a plasma fraction with a high platelet concentration (Deprés-Tremblay, Chevrier et al. 2017) that is obtained through whole blood centrifugation divided by weight particle. Activation of platelets in PRP releases several growth factors, such as PDGF, TGF- $\beta$ , IGF, VEGF, and EGF (Sheth, Simunovic et al. 2012). PRP has been suggested to stimulate revascularization and enhance growth factors that could potentially increase tendon healing (Barber, Hrnack et al. 2011). Growth factor release at the injury site could eventually lead to cell proliferation, cell differentiation and angiogenesis (Sheth, Simunovic et al. 2012). PRP has been used to treat several soft tissue pathologies, however the results have been inconsistent, possibly due to its short half-life and high diffusibility (Li, Xu et al. 2014). Routine use of PRP to treat rotator cuff tears is not supported by current clinical evidence (Castricini, Longo et al. 2011).

Chitosan (CS), a biodegradable and biocompatible natural polymer, is obtained through chitin deacetylation (Muzzarelli 2009, Krueger, Wenke et al. 2012). Once injected, chitosan is slowly hydrolyzes by lysozymes and produces chito-oligomers, which favours correct deposition, assembly and orientation of collagen fibrils in ECM reformation in tissues (Muzzarelli, Mattioli-Belmonte et al. 1999). In the context of cartilage repair, implants of CS-glycerol phosphate (GP)/blood have previously been shown by our research group to increase cell recruitment, vascularization and bone remodeling (Chevrier, Hoemann et al. 2007, Hoemann, Sun et al. 2007), activate a beneficial phenotype of pre-wound healing macrophages (Hoemann, Chen et al. 2010) and enhance tissue repair integration through osteoclast activity (Chen, Sun et al. 2011), all of which are expected to also be beneficial for rotator cuff repair. More recently, we have developed freeze-dried formulations of CS that can be solubilized in PRP to form injectable CS-PRP implants that coagulate *in situ*. We have shown that residency time and bioactivity of CS-PRP implants are superior to that of PRP alone *in vivo* (Chevrier, Hoemann et al. 2007). CS-PRP implants were tested in meniscus repair models and were shown to induce cell migration and repair tissue synthesis, while PRP alone or wrapping the meniscus with a collagen membrane did not (Chevrier, Deprés-Tremblay et al. 2016, Ghazi zadeh, Chevrier et al. 2017). CS-PRP were also tested in a chronic cartilage repair model and were

shown to improve repair tissue quality and induced bone remodeling, while treatment with PRP alone did not (Dwivedi, Chevrier et al. 2017). Hence, the starting hypothesis for this project was that the biological effects of CS-PRP hybrid implants would also be beneficial for rotator cuff tear repair.

## **1.1 General objective**

The aim of the current thesis was to make significant contributions to enhance current surgical rotator cuff tear repair strategies. The research presented here was carried out with an objective to improve current surgical procedures in rotator cuff tear repair by applying chitosan-PRP implants. In the first study, the mechanisms of action of chitosan-PRP implants were investigated *in vitro* and *in vivo*, focusing on the effect of chitosan on platelet-mediated clot retraction, on platelet activation and granule secretion, on the release of growth factors (PDGF-AB and EGF) from PRP and CS-PRP, on the induction of cellular recruitment by the implants, bioactivity and on their biodegradability. In the second study, pilot and pivotal studies in a small rabbit model investigated how chitosan-PRP implants improved transosseous rotator cuff tear repair. Finally, in the third study, the effect of using chitosan-PRP implants in conjunction with suture anchors was investigated in larger chronic and acute sheep models.

## **1.2 Study 1: Chitosan inhibits platelet-mediated clot retraction, increases platelet-derived growth factor release, and increases residence time and bioactivity of platelet-rich plasma *in vivo***

### **1.2.1 Hypotheses for Study 1**

Our starting hypotheses were that:

- Chitosan would bind to platelets in a non-specific fashion to inhibit platelet aggregation in hybrid clots and platelet-mediated clot retraction;
- Chitosan would activate platelets and induce granule secretion;



- The release of growth factors with low isoelectric point (negatively charged at neutral pH), such as EGF, would be more sustained from CS-PRP hybrids than the release of growth factors with high isoelectric points (positively charged at neutral pH), such as PDGF-AB, due to electrostatic interactions with cationic chitosan;
- CS-PRP implants would reside longer than PRP *in vivo*, where they would induce cell recruitment and angiogenesis, but be degraded within 6 weeks.

### **1.2.2 Methods and objectives for Study 1**

Gravimetric measurements, confocal and electronic microscopy were used to investigate possible mechanisms by which chitosan inhibits clot retraction in hybrid clots. Flow cytometry and ELISAs were used to characterize the effect of chitosan and lyoprotectant on platelet activation, granule secretion and growth factor release. Finally, subcutaneous implantation in rabbits was used to assess implant residency and biodegradability *in vivo*.

## **1.3 Study 2: Freeze-dried chitosan-PRP implants improve transosseous rotator cuff repair in a rabbit model**

The aim of this study was to assess whether chitosan-PRP implants are capable of improving transosseous rotator cuff repair in a rabbit model, focusing on implant distribution at early time points and the histological properties of the repaired site at later time points.

### **1.3.1 Hypotheses for Study 2**

Our starting hypotheses were that:

- CS-PRP implants would induce recruitment of polymorphonuclear cells (PMN) at early time points post-surgery;
- CS-PRP implants would be degraded by 2 months post-surgery;
- CS-PRP implants would improve transosseous rotator cuff repair through an increase in cell recruitment, angiogenesis and bone remodeling.

### **1.3.2 Methods and objectives for Study 2**

Complete bilateral surgical tears were created in the supraspinatus tendon of the rotator cuff of skeletally mature rabbits. The tears were immediately repaired with sutures via a transosseous repair technique. On the treated side, a hybrid mixture of freeze-dried chitosan reconstituted with autologous PRP was injected into the transosseous tunnels and the tendon itself. The objective of the pilot study was to determine feasibility of using CS-PRP implants to improve rotator cuff repair in a small number of rabbits. The objective of the larger efficacy study was to determine the histological properties of the repaired site at 8 weeks post-surgery.

## **1.4 Study 3: Freeze-dried chitosan-platelet-rich plasma implants for rotator cuff tear repair: Pilot ovine studies**

The aim of this study was to investigate the feasibility of using chitosan-PRP hybrids in large chronic and acute animal models of rotator cuff repair.

### **1.4.1 Hypotheses for Study 3**

Our starting hypothesis was that:

- CS-PRP implants would have positive effects on chronic and acute rotator cuff repair through increased cell recruitment, vascularization and bone remodeling.

### **1.4.2 Methods and objectives for Study 3**

A complete surgical tear in the infraspinatus tendon of the rotator cuff was induced unilaterally in the shoulder of sheep. In the chronic model, the end of the tendon was covered with a 5-cm-long silicon tube to prevent spontaneous healing. The tear was repaired with suture anchors six weeks after release. In the acute repair model, a complete surgical tear was also created in the infraspinatus, but the tear was immediately repaired with suture anchors. In both models, a hybrid mixture of freeze-dried chitosan reconstituted with autologous PRP was injected at the repaired site at the time of repair, and healing was assessed histologically.

## CHAPTER 2 LITERATURE REVIEW

### 2.1 Basic biology of tendons

Healthy tendons are white brilliant soft connective tissue structures (Sharma and Maffulli 2005), made up of tenoblasts and tenocytes that constitute about 90-95% of the cellular elements of tendons (Kannus and Jozsa 1991), with the remaining 5-10% consisting of chondrocytes at the tendon attachment site, synovial and vascular cells (Sharma and Maffulli 2005). Tenoblasts are immature spindle-shaped tendon cells with high metabolic activity. Once mature, they transform into tenocytes, which are characterized by a lower metabolic activity (Kannus and Jozsa 1991). Tenocytes are responsible for the production of extracellular matrix (ECM) including collagens, proteoglycans and other ECM proteins (Birk and Mayne 1997). Tendons are viscoelastic tissues that display stress relaxation and creep (Viidik 1973, Oxlund 1986) with high mechanical strength and good flexibility (O'Brien 1992, Kirkendall and Garrett 1997). Tendon tensile strength is proportional to the thickness of the tendon and collagen content. Approximately 20% to 30% of the dry weight of tendon is made up of proteoglycans, glycosaminoglycans, minor collagen (type-III, & type-XII), elastin and cell materials (Koob and Vogel 1987, Vogel, Sandy et al. 1994), while collagen type-I accounts for 65-80%.

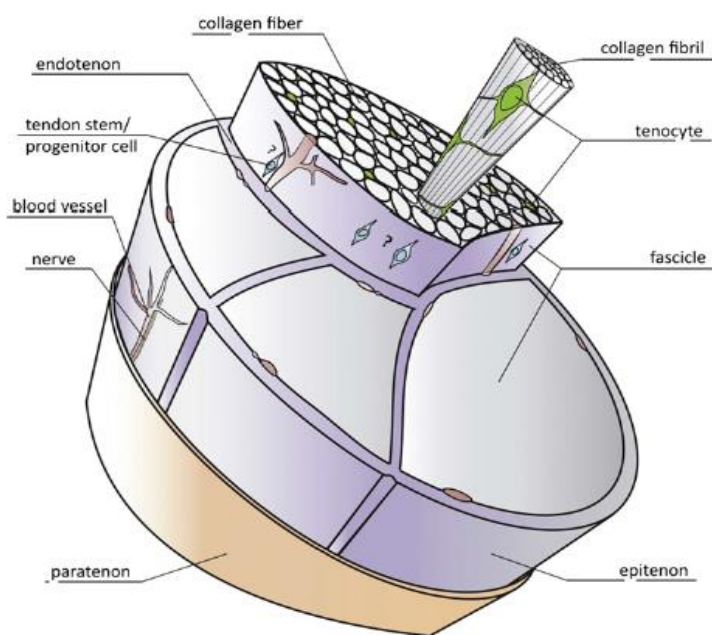


Figure 2-1: Schematic drawing of a basic tendon structure (Docheva, Muller et al. 2015).

Tendons not only transmit muscle forces to bones, but also act as buffers by absorbing external forces, limiting eventual muscle damage (Best and Garrett 1994). Thus they distribute loads applied to them in order to execute movements (Benjamin, Toumi et al. 2006).

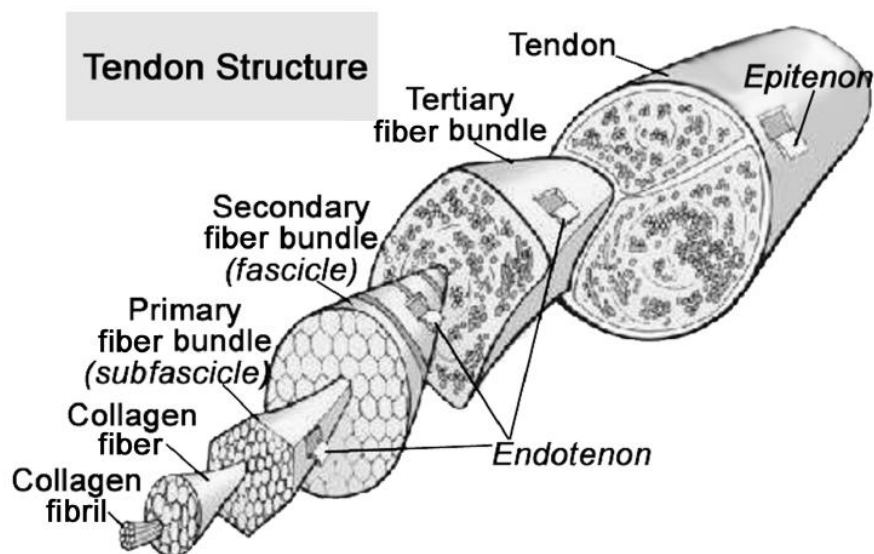


Figure 2-2: Anatomy of a normal tendon (Sharma and Maffulli 2005).

Tendon cellularity, vascularity and natural healing ability are extremely low (Benjamin and Ralphs 1997). Tendon vascularity is mostly compromised at junctional zones and point of torsion, friction or compression (Sharma 2006). Tendons receive their blood supply mainly via the epitendinous blood vessels, myotendinous and osteotendinous junctions and through the paratenon or the synovial sheath (Carr and Norris 1989, Kvist, Hurme et al. 1995). Few vessels perforate through the tendon body as they are obstructed by the calcified barrier (Doschak and Zernicke 2005). The circulus articuli vasculosus, a meshwork of vasculature around the joint, provides nutrient to the glenohumeral joint (Bray, Smith et al. 2001), which necessitates reapposition of these surrounding soft tissue and meshwork structures, once injured (Bunker, Ilie et al. 2014). Adhesion formation after intrasynovial tendon injury results in major clinical problems (Manske 2005). Disruption of the synovial sheath allows granulation tissue and exogenous tenocytes to invade the repair site. Surrounding cells predominate over endogenous tenocytes, allowing the surrounding tissue to attach to the repair site forming adhesions (Sharma and Maffulli 2005).

Tendons consume on average 7.5 times less oxygen than skeletal muscles using anaerobic energy production, leading to low metabolic energy requirements. Low metabolic energy demand is required to carry heavy loads and maintain tension over long periods of time (Williams 1993), thus reducing the risk of ischemia and necrosis, especially during tensional stresses. However, this results in slow healing and recovery once damaged (Williams 1993, Docheva, Muller et al. 2015). At low strain rates, tendons are able to absorb more mechanical energy but are a lot less efficient at carrying mechanical loads. At higher strain rates, tendons are stiffer but more efficient in transmitting larger loads from muscles to bones (Wang 2006). Excessive loading during physical exercises can also lead to tendon degeneration (Selvanetti, Cipolla et al.). Tendons respond to excessive loadings by inflammation or degeneration (Benazzo, Zanon et al. 2000), usually manifested by pain, formation of lipids, proteoglycans and eventual calcification in tendon lesions (Kannus and Jozsa 1991). This can lead to the release of various cytokines and changes in cellular activities (Leadbetter 1992). Ischemia of tendons will occur when tendons are under maximum load for a prolonged period of time and once reperfusion has occurred, free radicals will be released, causing damage to tendons (Goodship, Birch et al. 1994, Bestwick and Maffulli 2000), degeneration and even tenocytes death (Birch, Rutter et al. 1997). Excessive mechanical loading also induces prostaglandin E2, an inflammatory mediator capable of decreasing collagen production and proliferation (Langberg, Skovgaard et al. 1999, Cilli, Khan et al. 2004). Disproportionate loading also induces stretching in tenocytes activating protein kinases and biological responses (Arnoczky, Tian et al. 2002). Moreover, injured tendons cannot restore the native extracellular matrix, but instead change the biological and mechanical environments (Montgomery, Petrigliano et al. 2012), forming scar tissue and disorganized extracellular matrix (Katzel, Wolenski et al. 2011).

However, repetitive healthy loading can increase remodeling and functional improvements in tendons (Magnusson, Langberg et al. 2010). Remodeling is a healthy balance between synthesis and degradation of collagen, required during healing (Bishop, Klepps et al. 2006). Healthy mechanical loading might also improve healing of injured tendons (Groth 2004). Nevertheless immobilization or disuse can lead to stress deprivation, hence changing tendon cell shape, number, and collagen fiber alignment leading to degeneration (Hannafin, Arnoczky et al. 1995), however short-term immobilization can help recovery and healing of tendons in certain

scenarios (Ma, Shen et al. 2007, De Aguiar, Chait et al. 2009). Without significant amount of mechanical loading, atrophy, decreased in tensile strength and stiffness will eventually occur (Amiel, Woo et al. 1982), changing its organization and mechanical properties of the unloaded tendon (Uchida, Tohyama et al. 2005, Thomopoulos, Zampiakis et al. 2008, Galatz, Charlton et al. 2009).

Tendons are attached to bone through a specialized interface referred to as the insertion site, also known as the enthesis (Lu and Thomopoulos 2013), or osteotendinous junction (Benjamin, Toumi et al. 2006). The distinct organization of this tendon-to-bone insertion site is essential for proper function of the glenohumeral joint and accounts for the surgical challenges associated with reconstruction of damaged entheses (Apostolakos, Durant et al. 2014). The enthesis is defined as a specialized area where tendon meets bone (Benjamin and Ralphs 2001) and is critical as it allows for the transmission of forces, while dissipating forces away from the enthesis itself (Benjamin, Kumai et al. 2002, Angeline and Rodeo 2012, Lu and Thomopoulos 2013). Mineral content and collagen fiber orientation give the enthesis a unique transition with grading mechanical properties (Thomopoulos, Genin et al. 2010). Tendon-bone attachments are biomechanically, compositionally, and structurally complex. Their compositions vary dramatically along their length in collagen structure, ECM, mineral content, geometry, and viscoelasticity properties. This gradation in the composition and structure (Stouffer, Butler et al. 1985, Moffat, Sun et al. 2008, Genin, Kent et al. 2009, Liu, Birman et al. 2011) distributes forces from a flexible to a rigid material (Thomopoulos, Genin et al. 2010), by a shallow attachment angle (Liu, Birman et al. 2011, Picker 2011).

Two types of tendon attachment sites exist, according to the types of tissue present at the attachment, either dense fibrous connective tissue or fibrocartilage. They equate in indirect or direct attachments, respectively (Woo S 1988). Fibrous entheses attach directly to bone via fibrous tissue, similar in structure to the tendon body and are found in the deltoid attachment to humerus, adductor magnus to linea aspera of the femur, and pronator teres (Benjamin, Kumai et al. 2002, Lu and Thomopoulos 2013). Fibrocartilaginous entheses attach to bone through a layer of fibrocartilage at tendon-bone interface (Benjamin and Ralphs 2001, Benjamin, Kumai et al. 2002, Lu and Thomopoulos 2013) and are more prone to overuse injuries (Benjamin, Kumai et al. 2002, Lu and Thomopoulos 2013). Fibrocartilaginous entheses are found at the rotator cuff

and Achilles tendons (Lu and Thomopoulos 2013, Padulo, Oliva et al. 2013). A typical fibrocartilaginous enthesis has 4 distinct zones; pure dense fibrous connective tissue (tendon), uncalcified fibrocartilage, calcified fibrocartilage, and bone. Pure dense fibrous connective tissue is composed of pure tendon, populated by fibroblasts (Lu and Thomopoulos 2013), consisting mainly of linearly arranged collagen type-I and -III, elastin and proteoglycans (Laiho, Weis et al. 1990, Wrana, Attisano et al. 1994, Angeline and Rodeo 2012, Lu and Thomopoulos 2013). Uncalcified fibrocartilage is an avascular zone of uncalcified or unmineralized fibrocartilage populated by fibrochondrocytes and consists of the proteoglycan aggrecan and type-I, type-II and type-III collagens (Kim, Galatz et al. 2009, Angeline and Rodeo 2012, Lu and Thomopoulos 2013). The uncalcified fibrocartilage zone functions as a force damper to dissipate stress generated by collagen fibers bending (Benjamin and Ralphs 2001). Then the tidemark, a basophilic line separating the uncalcified and calcified fibrocartilage zones, is defined as a mechanical boundary between soft and hard tissue (Angeline and Rodeo 2012), decreasing the risk of damage during movement (Angeline and Rodeo 2012). Calcified fibrocartilage is an avascular zone of calcified or mineralized fibrocartilage populated by fibrochondrocytes, which consists predominantly of type-II collagen as well as aggrecan and type-I and -X collagens (Laiho, Weis et al. 1990, Wrana, Attisano et al. 1994, Benjamin and Ralphs 2001, Scott, Cook et al. 2007, Angeline and Rodeo 2012, Lu and Thomopoulos 2013, Padulo, Oliva et al. 2016). This zone represents the “true” junction of the tendon insertion, creating a boundary with the subchondral bone (Benjamin and Ralphs 2001). This junction is highly irregular and provides mechanical integrity to the enthesis (Benjamin and Ralphs 2001). Lastly, bone, which consists of osteoclasts, osteocytes, and osteoblasts residing in a matrix type-I collagen and carbonated apatite mineral (Angeline and Rodeo 2012, Lu and Thomopoulos 2013).

Table 2-1: Zones of fibrocartilaginous entheses

Zones	Composition
<i>Zone 1</i> <i>Pure dense fibrous connective tissue; Tendon</i>	Type-I collagen, tendon cells aligned. Ordered arrays oriented in direction of tensile force (Smith, Xia et al. 2012).
<i>Zone 2</i> <i>Uncalcified fibrocartilage</i>	Type-II collagen with high levels of pericellular Type-III collagen, small amount of type-I collagen, decorin, and aggrecan (Kumagai, Sarkar et al. 1994, Spiller, Wrona et al. 2016).
<i>Zone 3</i> <i>Calcified fibrocartilage</i>	Type-II, -I and -X collagen and aggrecan (Galatz, Rothermich et al. 2007). Fibril less aligned (Spiller, Wrona et al. 2016).
<i>Zone 4</i> <i>Bone</i>	Stiff carbonated hydroxyl apatite mineral within a scaffold of type-I collagen (Spiller, Wrona et al. 2016).

## 2.2 Tendon and enthesis development

Several critical factors influence the formation of the enthesis. Scleraxis (Scx) is a transcription factor associated with tendons and tenogenesis and is expressed in progenitors cells of all tendon tissues (Cserjesi, Brown et al. 1995, Schweitzer, Chyung et al. 2001, Brent, Schweitzer et al. 2003, Murchison, Price et al. 2007). SOX-9 is associated with chondrogenesis, expressed in proliferative chondrocytes, and responsible for chondrocyte differentiation (Huang, Chung et al. 2001, Asou, Nifuji et al. 2002, Akiyama 2008). Indian Hedgehog (Ihh) and parathyroid hormone related protein (PTHrP) drive chondrocyte proliferation and differentiation which form a feedback loop maintaining proliferative cells available for development at the growth plate (Thomopoulos, Genin et al. 2010). These factors, identified as having important roles in growth



plate development, may also play a role in the development of the enthesis. Fibrocartilaginous entheses are formed by endochondral ossification (Bunker, Ilie et al. 2014). Initially, mesenchymal stem cells (MSCs) differentiate into chondrocytes (Saha 1971) that deposit cartilaginous material, which becomes calcified (Benjamin and Ralphs 1998), then chondrocytes form the mineralized cartilage matrix (Blitz, Viukov et al. 2009). Finally chondrocytes align in rows and collagen fibers line up parallel to the long axis of the tendon (Clark and Harryman 1992, Rickert, Jung et al. 2001). During enthesis development, tendon first attached to the hyaline cartilage of the humeral head, which is not yet mineralized. Next the ossification occurs where the hyaline cartilage becomes eroded by osteoclasts and lamellar bone is deposited by osteoblasts remaining in matrix (Gao, Messner et al. 1996, Benjamin and McGonagle 2009). Finally, the hyaline cartilage rudimentary bone is resorbed and the fibrocartilage continues to form as a result of fibroblast metaplasia resulting in the formation of a graded enthesis (Gao, Messner et al. 1996, Benjamin and McGonagle 2009). In a mature enthesis, chondrocytes are well aligned in rows in the calcified and non-calcified fibrocartilages, which increase tensile strength and fibrocartilaginous matrix integrity (Rickert, Jung et al. 2001). Moreover, mature fibrocartilaginous enthesis shares many similarities to the growth plate structure development also formed through endochondral ossification of bone, which has characteristics of an arrested growth front (Watkins, Auer et al. 1985, Blitz, Viukov et al. 2009). The growth plate is divided into different zones according to the morphology of the cells as well as the state of calcification (Provot and Schipani 2005). These zones include the reserve zone, the proliferative zone, and the hypertrophic zone. It is likely that the transcription factors that modulate growth plate maturation play a role in enthesis maturation. Similar chondrocyte-like cells appear at the enthesis development and eventually mineralize to create the interface between the tendon and bone (Thomopoulos, Genin et al. 2010). Increasing tissue mineralization could increase tendon-bone healing (Rotini, Marinelli et al. 2011), since enthesis mineralization probably coincides with mineralization of the proximal epiphysis in the layer organization (Schwartz, Pasteris et al. 2012). Hence reinforcement of fibrocartilage could be achieved by increasing the number of collagen fibers and spatial organization (Coleman, Fealy et al. 2003, Snyder, Arnoczky et al. 2009, Longo, Lamberti et al. 2012, Tutwiler, Litvinov et al. 2016). It has been suggested that entheses can act as growth plates for apophyses at tendon attachment sites (Knese and Biermann

1958). The cartilage at the enthesis is initially derived from that of the embryonic bone rudiment. However, this hyaline cartilage is eroded during endochondral ossification and replaced by enthesis fibrocartilage that develops within the adjacent tendon by fibroblast metaplasia (Gao, Messner et al. 1996).

## **2.3 Tendon and enthesis healing**

Tendon healing depends on multiple cell sources, which include fibroblasts (Abrahamsson, Lundborg et al. 1989), inflammatory cells (Gelberman, Chu et al. 1992, Boyer, Watson et al. 2001), synovial cells (Ark, Gelberman et al. 1994, Abrahamsson, Gelberman et al. 1995, Amiel, Harwood et al. 1995) and mesenchymal stem cells (MSCs) (Yamamoto, Tokura et al. 2003). An injured or compromised tendon passes through 3 different main healing phases. The inflammatory phase begins with inflammatory cells migrating to the repair site guided by chemotactic factors, characterized by an influx of blood vessels and fibroblasts (Gulotta and Rodeo 2009) eventually forming a hematoma. Inflammatory cells such as neutrophils, monocytes and macrophages are attracted to the site by pro-inflammatory cytokines (Lin, Cardenas et al. 2004). Macrophages play essential roles in promoting and resolving inflammation and in facilitating tissue repair (Thomopoulos, Parks et al. 2015). Macrophages are classified into two groups, classically activated (M1) or alternatively activated (M2), both driven by specific conditions (Murray, Allen et al. 2014). In tendon injury, it is hypothesized that M1 macrophages promote repair by stimulating ECM production and that later on M2 macrophages resolve inflammation and clear excess ECM (Sugg, Lubardic et al. 2014). Disturbing this homeostasis between M1 and M2 macrophages may result in defective repair and impaired tissue function.

After few days the proliferation stage starts by synthesizing the ECM component, mostly collagen type-III and proteoglycans, in a random manner by the recruited fibroblasts, inducing cell proliferation and matrix deposition. An increased in cellularity and water absorption is observed. 6-8 weeks after injury, the remodeling stage takes place consisting of 2 sub-stages lasting around 1 or 2 years. The first sub-stage, the consolidation stage, involves a decreased in cellularity, matrix production, fibrous tissue, and collagen type-III is replaced by collagen type-I, through tissue remodeling due to ECM turnover mediated by matrix metalloproteinases (MMPs)

(Gulotta and Rodeo 2009). The collagen fibers start to organize, resulting in stiffness and strength. 10 weeks after injury, the maturation stage starts increasing collagen fibril crosslinking and tendinous tissue formation (Docheva, Muller et al. 2015).

While fibrocartilaginous transition zone forms during fetal development, scar tissue rich in type-III collagen (Hynes 1999, Awad, Boivin et al. 2003) and weaker mechanical strength (Patel, Gualtieri et al. 2016) forms between the interfaces in adult tendon-to-bone healing (St Pierre, Olson et al. 1995, Thomopoulos, Hattersley et al. 2002, Spiller, Nassiri et al. 2015, Spiller, Wrona et al. 2016). Healing following cuff repair depends on robust mechanical properties at the junction between bone and tendon (Lee, Lee et al. 2016), which could be influenced through modulation of cell signaling pathways. Tendon to bone healing represents an enormous clinical challenge due to the lack of regeneration of this specialized structure (St Pierre, Olson et al. 1995, Liu, Panossian et al. 1997, Fujioka, Thakur et al. 1998, Aoki, Oguma et al. 2001, Wong, Qin et al. 2009, Spiller, Wrona et al. 2016). All fibrocartilages associated with normal entheses are avascular and this also contributes to a poor healing response at and near attachment sites. The avascularity reflects the mechanical conditions to which the tissues are subject, notably compression (Benjamin, Toumi et al. 2006). Attachment of tendon to bone presents a great challenge during surgical repair because a soft compliant material attaches itself to a stiff material. Mineralized interface region exhibited significantly greater compressive mechanical properties than the non-mineralized region (Moffat, Sun et al. 2008). It is thus important to note that the restoration of a normal enthesis can be significantly enhanced by a variety of biological modulators (Benjamin, Toumi et al. 2006).

Whether entheses can reform after surgical reattachment are questions of considerable clinical importance. Surgical reattachment of rotator cuff tear with current repair techniques leads to a more abrupt interface and a disorganized scar tissue that is mechanically a lot weaker than a native interface (Thomopoulos, Hattersley et al. 2002, Tutwiler, Litvinov et al. 2016). This exposes the insertion to high stresses and an increased risk for failure (Smith, Xia et al. 2012). Enthesis healing appears to depend upon bone ingrowth into fibrovascular interface tissue. Therefore secure healing between tendon-bone, involves bone ingrowth into fibrocartilage and outer tendon (Gulotta and Rodeo 2009). Moreover, healing is often delayed in both animal models (Shea, Hallows et al. 2002) and in the clinical situation (Liu, Hang et al. 1996), how to

accelerate the healing process also becomes a focus of interest. A method that speeds tendon healing without causing muscle fiber atrophy and pennation angle change could be beneficial (Melamed, Beutel et al. 2015). Restoration of this footprint might increase the likelihood of a regenerated native-like enthesis with normal function.

## **2.4 Rotator Cuff Anatomy and Pathology**

The rotator cuff muscles are a group of muscles consisting of the subscapularis, supraspinatus, infraspinatus, and the teres minor (Di Giacomo 2008). The last three are inseparable, while the subscapularis is joined to the rest of the cuff via the rotator interval (Parsons, Apreleva et al. 2002). All of these muscles are attached to the head of the humerus via their specific tendons, which control rotation and position of the arm (Di Giacomo 2008). The rotator cuff muscles assist shoulder motion but primarily provide stability (Di Giacomo 2008) by keeping the head of the humerus in place, centred into the glenoid, through exertion of forces in the coronal and transverse planes (Parsons, Apreleva et al. 2002), allowing abduction or forward elevation of the arm (Basmajian and Bazant 1959, Saha 1971). This centering is achieved by matching forces around the glenohumeral joint (Pandey and Jaap Willems 2015). The supraspinatus and the infraspinatus have long sarcomere lengths, which contribute to glenohumeral stability in resting position while the subscapularis stabilizes the glenohumeral joint in the position of apprehension (Di Giacomo 2008). The subscapularis is the largest and most powerful tendon that arises from the anterior surface of the scapula. It intertwines with the supraspinatus tendon at the greater tuberosity of the humerus and acts as the main internal rotator (Parsons, Apreleva et al. 2002). It initiates abduction and acts throughout the range of abduction of the shoulder (Parsons, Apreleva et al. 2002). The infraspinatus is a thick triangular muscle, arising as fleshy fibers with tendinous fibers at the edges of its surface. The ISP tendon glides over the lateral border of the spine of the scapula, passes across the posterior part of the capsule and inserts into the greater tuberosity (Di Giacomo 2008). The teres minor is a fine, elongated muscle that starts from the dorsal face of the scapula. It inserts itself in the posterior part of the capsule (Di Giacomo 2008). The infraspinatus and the teres minor both lie below the scapular spine and act as external rotators. The infraspinatus primarily acts with the arm in neutral

position and the teres minor is active with external rotation in 90° of abduction (Parsons, Apreleva et al. 2002). The supraspinatus is a long, thin muscle with fibers arising from the medial portion and the base of the fossa of the scapula. The supraspinatus has the shortest fibers of the four rotator cuff muscles and operates over the greater sarcomere length range (Mathewson, Kwan et al. 2014). The SSP tendon portion converges with those of the subscapularis and the infraspinatus and acts as the superior stabilizer of the humeral head (Di Giacomo 2008). It inserts into the major tuberosity and a small portion inserts into the lesser tuberosity, which may serve more as an accessory attachment. The supraspinatus tendon is constrained on either side by other soft tissues and passes underneath the coracoacromial arch, making it prone to compression (Lake, Miller et al. 2010). Areas of tendons that are subjected to compression, like under the acromion, produced significant amounts of proteoglycans to resist deformation in the direction of compression (Klinger, Buchhorn et al. 2008, Seeherman, Archambault et al. 2008). The majority of tendon tears occur in the supraspinatus, more specifically in the “so-called” critical zone, about 1-cm proximal to the insertion of the central portion (Rudzki, Adler et al. 2008). The anterior portion transmits the majority of the contractile load, and since more stress is applied to the anterior section of the shoulder on a daily basis, leading to high risk for a tear.

Major conditions affecting tendons are tendinitis, characterized by inflammation and pain, and tendinosis, a tendinous degeneration (Maffulli, Khan et al. 1998). Many factors, either intrinsic or extrinsic, are involved in the onset and progression of tendinopathies, such as age, gender, anatomical variants, body weight, smoking, systemic disease, sporting activities, physical loading, occupation, and environmental conditions (Riley 2004, Rees, Wilson et al. 2006). Rotator cuff injuries are common and often require surgical repair to restore the tendon to its bone. Chronic rotator cuff tears are associated with structural changes such as fatty accumulation, loss of muscle volume, retraction, which all result in muscle remodeling, retraction of sarcomeres and profound muscle weakness (Williams and Rockwood 1996). The deltoid becomes the only shoulder elevator if the supraspinatus tendon is torn and dysfunctional (Parsons, Apreleva et al. 2002). However, if the sarcomeres of the muscles become overstretched so that the myofilaments overlap, the contractile function becomes compromised (Di Giacomo 2008). Progression of a tear will also lead to superior subluxation of the humeral head and

eventually, dysfunction of the shoulder. Pathology in rotator cuff tear is also influenced by the micro vascular supply of rotator cuff tendons (Parsons, Apreleva et al. 2002). A cuff tear is considered irreparable when closing results in poor footprint coverage or when the closure results in post-operative retear (Pandey and Jaap Willems 2015), hence reparability is dependent on size and shape of the tear. Cuff tears can be traumatic, due to significant trauma or degeneration, which are multifactorial in aetiology (Pandey and Jaap Willems 2015), and often involve one or more tendons (Smith, Xia et al. 2012).

## **2.5 Surgical Treatments of Rotator Cuff Tears**

The most common surgical interventions available to repair rotator cuff tears involve different suturing techniques. Open repair techniques were the first to be performed but mini-open or fully arthroscopic procedures are now the gold standard. The superiority of arthroscopy versus open or mini-open repair is still unproven and controversial at this point (Galatz, Ball et al. 2004) (**Appendix A**).

Ji et al. (Ji, Bi et al. 2015), Liem et al. (Liem, Bartl et al. 2007) and Kasten et al. (Kasten, Keil et al. 2011) found no significant difference between arthroscopy versus mini-open repair patients. Nho et al. (Nho, Shindle et al. 2007) and Van der Zwaal et al. (van der Zwaal, Thomassen et al. 2013) also observed no difference in functional outcomes, range of motion and complication rates between mini-open and arthroscopy. However, in another study, a greater re-tear rate was observed in patients who had undergone arthroscopy versus the ones whom had had mini-open surgery (Zhang, Gu et al. 2014). Mall et al. (Mall, Chahal et al. 2012) found no difference in arthroscopy versus open repair. However, although Bishop et al. (Bishop, Klepps et al. 2006) showed comparable results in arthroscopy versus open repair for tears smaller than 3 cm, the re-tear rate was doubled after arthroscopy with tears larger than 3 cm. Feeley et al. (Feeley, Gallo et al. 2009) showed that arthroscopy resulted in less soft-tissue trauma in elderly patients with low functional demands since it is a slightly invasive surgical intervention. However, arthroscopy requires high dexterity to be performed correctly (Baleani, Ohman et al. 2006) and can also lead to the resection of the corticoacromial ligament, which worsens rotator cuff tears. Moreover arthroscopic treatment can lead to greater failures compare to open surgical

suture repair (Koh, Kang et al. 2011). Some studies have shown that arthroscopic procedures can decrease postoperative pain, facilitate faster recovery and give better aesthetic results (Verma, Dunn et al. 2006, Kang, Henn et al. 2007). However, others (Shinoda, Shibata et al. 2009, Kim, Lee et al. 2013) have found no significant difference between open and arthroscopic procedures both of which significantly improve clinical outcomes and shoulder function. Lorbach et al. (Lorbach and Tompkins 2012) hypothesized that since arthroscopy results in less pain after surgery, patients may tend to exercises sooner.

Initially, transosseous tunnels were used to perform open rotator cuff repair. This technique uses sutures placed directly into transosseous tunnels inside the greater tuberosity for tendon fixation (Cole, ElAttrache et al. 2007), but is limited by bone quality (Denard and Burkhart 2013). Now, cuff repair is usually performed with suture anchors using different configurations: the single-row, the double-row, and the suture bridge repair technique, also called the transosseous-equivalent repair technique. The goal of using suture anchors is to restore the initial footprint and tendon alignment by suturing the tendon directly into the humeral head (Cole, ElAttrache et al. 2007). This technique increases footprint contact area, which is thought to improve the rate of healing but this requires a non-degenerated tendon with a good healing potential (Docheva, Muller et al. 2015) and re-tear rates are still fairly high (Denard and Burkhart 2013). The suture bridge, or the transosseous-equivalent technique (TOE), is an improvement of the double-row repair technique. This approach seems to provide a more uniform compression and a greater surface contact, which is expected to enhance the attachment and the pull-out strength (Cole, ElAttrache et al. 2007). This procedure is also assumed to restore normal anatomy and function of the shoulder (Di Giacomo 2008). Furthermore it may create excessive tension on the tendon leaving an avascular area at the repair site (Denard and Burkhart 2013). A common problem of early failure with suture anchors is the pull out of the suture through the tendon (Baleani, Ohman et al. 2006).

In controlled laboratory studies using cadaveric shoulders Kim et al. (Kim, Elattrache et al. 2006) compared double-row versus single-row repairs; DR had 42% less gap formation, 46% more stiffness and 48% more load at failure than SR repair. Mazzocca et al. (Mazzocca, Millett et al. 2005) found similar outcomes for both techniques, but DR had greater success at restoring the initial footprint of the tear. Apreleva et al. (Apreleva, Ozbaydar et al. 2002) compared

transosseous with single-row anchors; and the transosseous technique seemed to be best at restoring the anatomy of the supraspinatus tendon. (Park, Cadet et al. 2005) had comparable results, where transosseous repair resulted in greater ultimate load of failure and lower pressure on the repair site. Transosseous repair was also compared to double-row technique by Waltrip et al (Waltrip, Zheng et al. 2003) using cadaveric shoulders. Transosseous repair increased the number of cycles to failure. It was also shown that transosseous repair concentrated the stress at the attachment site; while DR and SR repair concentrated the stress on the bursal side of the tendon, which may explain the greater rate of re-tear in these techniques (Sano, Wakabayashi et al. 2006). Siskosky et al. (Siskosky MJ 2007) showed that transosseous-equivalent (TOE) had higher ultimate load of failure but no change in initial stiffness or gap formation compared to DR repair. TOE was also shown to be more resistant to rotational and shear stress and to reduce gap formation (Costic RS 2006, Cole, ElAttrache et al. 2007). Therefore, it seems like TOE is better in cadaveric studies, but that has not translated into superior clinical outcomes.

In clinical studies comparing different suturing techniques (**Appendix B**), Aydin et al. (Aydin, Kocaoglu et al. 2010), Grasso et al. (Grasso, Milano et al. 2009), Nho et al. (Nho, Slabaugh et al. 2009), Wall et al. (Wall, Keener et al. 2009), and Koh et al (Koh, Kang et al. 2011) found no significant difference in clinical outcomes between arthroscopic single-row (SR) repairs versus arthroscopic double-row (DR) repairs. Ying et al. (Ying, Lin et al. 2014) also found that both techniques improved clinical outcomes. The UCLA shoulder scoring test, incidence of recurrent defects, shoulder muscle strength, range of motion and patient satisfaction were similar in the two groups with tears smaller than 3 cm. However, double-row showed a greater rate of tendon healing, smaller rate of re-tear and greater muscle strength in patients with tears greater than 3cm (Ying, Lin et al. 2014). On the other hand, Ma et al (Ma, Chow et al. 2011), Mascarenhas et al. (Mascarenhas, Chalmers et al. 2014) and Trappey et al. (Trappey and Gartsman 2011) showed that DR repair provides better tendon strength compared to SR. Carbonel et al. (Carbonel, Antonio Martinez et al. 2012), Chen et al. (Chen, Xu et al. 2013), and Prasathaporn et al. (Prasathaporn, Kuptniratsaikul et al. 2011) demonstrated that DR repair group had higher rate of tendon healing compared to SR repair group. In addition, Millett et al. (Millett, Warth et al. 2014) found a higher re-tear rate with SR repair patients compared to DR. Gartsman et al. (Gartsman, Drake et al. 2013) compared TOE to SR and found a higher tendon healing rate



in TOE repair. Even if there is no consensus on which surgical technique to use, the suture bridge technique may seem to be more appropriate at repairing massive rotator cuff tear, since it provides a more uniform compression hence favoring healing rate.

A common surgical procedure performed on symptomatic patients with massive tear, muscle atrophy and fatty accumulation is arthroscopic debridement (Clement, Nie et al. 2012). This procedure involves irrigation and debridement of joint surfaces, thus removing enzymes and crystals to provide short-term pain relief, but long-term success is limited. Furthermore, more than a third of surgeries result in unsuccessful outcomes such as persistent pain and disabilities (Seitz, McClure et al. 2011). However, cuff repairs are prone to failure regardless of repair technique used (Heldin and Westermarck 1999, Galatz, Ball et al. 2004). The best rotator cuff tear surgical treatment is currently a topic of debate, since current repair strategies do not regenerate the functionally graded transitional tissue interface (Smith, Xia et al. 2012). A biological strategy improving patient's intrinsic healing potential is needed (Melamed, Beutel et al. 2015). When rotator cuff pathology is a result of mechanical impingement, reshaping the acromion by acromioplasty may be the favored surgical procedure. The acromioplasty is believed to relieve the pressure on the cuff, caused by impingement (Neer, Craig et al. 1983). However, reviews found no statistically significant difference in subjective outcome after arthroscopic rotator cuff repair with or without acromioplasty at intermediate follow-up with failure rates ranging from 15 to 20% (Chahal, Mall et al. 2012, Shi and Edwards 2012). In addition, acromioplasty with coracoacromial (CA) ligament release increases superior glenohumeral instability (Su, Budoff et al. 2009).

## **2.6 Animal Models of Rotator Cuff Repairs**

Animal models are practical means to understand molecular pathways and pathologies of rotator cuff tears and to develop new technologies to improve existing treatments (Liu, Manzano et al. 2011). Rotator cuff repair animal models should lack spontaneous tendon healing or scar tissue formation after tendon injury. Although no animal model is identical to human, the tendon size should also allow for suture repair techniques as used in humans. Ideally, irreversible muscular atrophy, stiffness and fatty accumulation should be present post-injury (Derwin, Baker et al. 2007). Quadrupeds use their supraspinatus to accelerate, while humans use it in arm raising. The supraspinatus muscle acts against gravity and under greater strain in humans compared to animals. Shoulder movement in quadrupeds is restricted to the sagittal plane, while bipeds rotate and move in the coronal plane, providing more mobility (Sonnabend and Young 2009). Quadrupeds use their forelimbs for weight bearing during locomotion and not for overhead activities, which differs greatly from humans (Grumet, Hadley et al. 2009) and makes it challenging to find a good animal model for shoulder injuries. Moreover a true rotator cuff is defined as the blending of individual flat tendons to form a single insertion. Rabbits, rats, dogs and sheep all have tendons that do not blend before inserting into humeral head; hence they all lack this aspect of the human rotator cuff anatomy (Sonnabend and Young 2009). An acute rotator cuff tear model is also inappropriate to study tendon degeneration, but useful to evaluate atrophy and fatty accumulation in rotator cuff muscles (Liu, Manzano et al. 2011). Chronic rotator cuff models have also been developed, mostly in the sheep (Coleman, Fealy et al. 2003, Gerber, Meyer et al. 2004).

### **2.6.1 Rat**

Rats have the greatest anatomic similarity to humans because of the presence of an acromial arch and the overhead reaching activities (Derwin, Baker et al. 2007). Only in rats is the acromion immediately adjacent and positioned over the supraspinatus tendon, similar to humans (Soslowky, Carpenter et al. 1996). The rat's forward arm elevation is similar to human arm abduction (Perry, Getz et al. 2009) and the range of motion decreases after rotator cuff tears in rats, which is consistent with alterations in shoulder function observed in humans (Perry, Getz et

al. 2009). Rotator cuff tears in rats will also result in cartilage degeneration in the humeral head and the glenoid (Kramer, Bodendorfer et al. 2013). However, the acromial arch structure is somewhat different in quadrupeds: the portion of the rat supraspinatus muscle that passes under acromial arch is muscular and not tendinous like in humans (Grumet, Hadley et al. 2009).

Although the rat is a reasonable model, it has a few major differences with respect to human. First, rotator cuff tears heal better in rats than in humans, due to the higher regenerative potential of their musculoskeletal system (Liu, Manzano et al. 2011). Rotator cuff tears undergo spontaneous healing in rats, which does not happen in human (Derwin, Baker et al. 2010). The supraspinatus provides less coverage in rat and most of the coverage is from the subscapularis instead (Liu, Manzano et al. 2011). In addition, the rat supraspinatus lacks the irreversible accumulation of muscular fat and postoperative re-tears making it less suitable to evaluate repair techniques (Derwin, Baker et al. 2010). In rats, the infraspinatus tendon may be a better model to represent the human supraspinatus, since it undergoes more fatty accumulation, muscular atrophy and more muscular retraction (Liu, Manzano et al. 2011). Re-tear has not been documented post-operatively in rat model, making it less suitable for translational studies (Galatz, Charlton et al. 2009). Even with these limitations, the rat is seen as an appropriate and cost-effective model to investigate initial safety, repair mechanisms and efficacy of treatments although its small size makes it challenging to perform surgical repairs (Derwin, Baker et al. 2007).

Rats are mostly used to investigate extrinsic and intrinsic factors that contribute to rotator cuff tears. In rats, most studies have been done using the transosseous tunnels repair technique with the SSP tendon (Galatz, Rothermich et al. 2005, Galatz, Sandell et al. 2006, Galatz, Charlton et al. 2009, Ide, Kikukawa et al. 2009, Bedi, Kovacevic et al. 2010, Liu, Manzano et al. 2011, Manning, Kim et al. 2011, Hettrich, Beamer et al. 2012, Buchmann, Sandmann et al. 2013, Oak, Gumucio et al. 2014, Zhao, Peng et al. 2014, Zhao, Zhao et al. 2014, Ross, Maerz et al. 2015, Zhao, Xie et al. 2015, Huegel, Kim et al. 2016, Peach, Ramos et al. 2017, Tucker, Gordon et al. 2017). Briefly, the supraspinatus is exposed by supination of the forearm, transected from its tendon insertion site. A drill hole is created transversely in a craniolecaudal orientation through the proximal humerus. Fibrocartilage is removed from the insertion site. The tendon is grasped using a double-armed 5-0 Prolene suture in a Mason-Allen method. The suture is then passed through the drill hole and tied the distal supraspinatus to its original footprint on the humeral

head (Galatz, Charlton et al. 2009). Only one study used the transosseous repair technique with the ISP tendon (Harada, Mifune et al. 2016). Two more recent studies used polyamide nonabsorbable sutures repair technique in a Mason-Allen configuration with the SSP tendon (Melamed, Beutel et al. 2015, Fabis, Danilewicz et al. 2016).

## 2.6.2 Rabbit

In rabbit rotator cuff tears, atrophy occurs at early time points and fatty accumulation occurs at later time points similar to humans (Liu, Manzano et al. 2011). The rotator cuff in rabbits also heals in a fashion that is similar to humans (Gupta and Lee 2007). The supraspinatus and infraspinatus tendons have both been used as repair models, but recent studies have shown that the subscapularis could be a better approximation of human conditions since it passes under an enclosed arch and that fatty accumulation is prominent (Edelstein, Thomas et al. 2011). The subscapularis tendon and the scapular channel are similar in human; both travel beneath the acromion and insert into the greater tuberosity of the humerus (Grumet, Hadley et al. 2009). In that respect, the rabbit's subscapularis may be more comparable to the human supraspinatus. The rabbit is also bigger than the rat therefore facilitating surgical models and many standard-of-care surgical techniques (Thomopoulos, Parks et al. 2015), as larger animals provide greater accuracy and reproducibility (Derwin, Baker et al. 2007).

The rabbit model is mostly used to study muscular changes associated with rotator cuff tears like muscle atrophy, twitch tension which is a single contraction in response to a brief threshold stimulation and fatigue index which determines energy depletion during exercise (Edelstein, Thomas et al. 2011). Most of the preclinical studies in rabbits have used the transosseous repair technique with the SSP tendon (**Appendix C**) (Uhthoff, Sano et al. 2000, Matsumoto, Uhthoff et al. 2002, Sano, Kumagai et al. 2002, Uhthoff, Seki et al. 2002, Uhthoff, Trudel et al. 2003, Uhthoff, Matsumoto et al. 2003a, Koike, Trudel et al. 2005, Kobayashi, Itoi et al. 2006, Koike, Trudel et al. 2006, Chang, Chen et al. 2009, Trudel, Ramachandran et al. 2010a, Trudel, Ryan et al. 2010b, Trudel, Ramachandran et al. 2012a, Trudel, Ryan et al. 2012b, Friel, Wang et al. 2013, Uhthoff, Coletta et al. 2014, Uhthoff, Coletta et al. 2014, Friel, McNickle et al. 2015, Gilotra, Nguyen et al. 2015, Kim, Kim et al. 2016, Cheon, Kim et al. 2017, Trudel, Melkus

et al. 2017). Briefly, a 3-cm longitudinal anterolateral skin incision is made, exposing the SSP tendon. A complete surgical tear is created, as close as possible to the insertion site. The remaining fibrocartilaginous stump is removed. A bony trough (2 mm diameter and 5-7 mm deep) is drilled in the cancellous bone of the greater tuberosity. Three small drill holes (1.4 mm diameter) are drilled from the lateral aspect of the humerus to connect to the bony trough. Two 3.0 prolene sutures are passed through the lateral holes, the bony trough and the tendon itself in a modified Mason-Allen configuration and tightened over the lateral aspect of the cortex, thus pulling the tendon over the bony trough.

Some studies used the transosseous repair technique with the ISP tendon (Funakoshi, Majima et al. 2006, Yokoya, Mochizuki et al. 2008, Itoigawa, Suzuki et al. 2015) Few studies used either the single-row (Nho, Cole et al. 2006, Quigley, Gupta et al. 2013, Oh, Kim et al. 2015, Kim, Kim et al. 2016) or the double-row (Quigley, Gupta et al. 2013, Oh, Chung et al. 2014) or the transosseous-equivalent repair technique (suture bridge) (Quigley, Gupta et al. 2013, Fei and Guo 2015, Kim, Kim et al. 2016). Only one study used polyamide non-absorbable sutures with the SSP tendon (Fabis, Danilewicz et al. 2016) and one used the transosseous mattress sutures repair technique with the ISP tendon (Inui, Kokubu et al. 2012).

### **2.6.3 Sheep**

Tendons in sheep heal spontaneously even without surgical intervention, unless healing is actively stopped (Gerber, Meyer et al. 2004). Since it is fairly easy to wrap the end of its tendons to prevent spontaneous healing, the sheep becomes an interesting choice for a chronic model (Coleman, Fealy et al. 2003). The sheep infraspinatus is similar in size to the human supraspinatus (Edelstein, Thomas et al. 2011). Although the sheep infraspinatus is not intraarticular, there is still a bursa under the tendon and repair has some contact with the synovial fluid that lubricates the bursa (Turner 2007). Availability, ease of handling and housing, low cost and acceptance to society as a research animal, makes ovine model useful to study rotator cuff tear repair (Turner 2007). Large animal models, like rabbit, sheep and canine have a high re-tear rates post-operative, making them suitable to test various repair techniques for human conditions (Derwin, Baker et al. 2007, Schlegel, Hawkins et al. 2007).

Most of the studies involving sheep models have either used the double suture anchors repair technique with the ISP tendon (**Appendix D**) (Lewis, Schlegel et al. 1999, Meyer, Hoppeler et al. 2004, Meyer, Lajtai et al. 2006, Kovacevic and Rodeo 2008, Zumstein, Rumian et al. 2014, Luan, Liu et al. 2015) or the transosseous bony trough technique with the ISP tendon (Gerber, Schneeberger et al. 1999, Lewis, Schlegel et al. 1999, Schlegel, Hawkins et al. 2006, Rodeo, Potter et al. 2007, Klinger, Buchhorn et al. 2008, Kovacevic and Rodeo 2008). Briefly, the double suture anchors involve two suture anchors that are deployed into the dense bone of the medial footprint of the proximal humerus, 1 cm apart and 2 mm to 4 mm deep to the cortex. Sutures are passed from inferior to superior through the infraspinatus tendon and tied in simple mattress fashion on the superior surface of the tendon (Luan, Liu et al. 2015). The transosseous repair technique briefly involves two or three modified Mason-Allen stitches that are placed into the tendon end and passed through a bony trough created at the site of the original insertion and tied over the greater tuberosity (Gerber, Schneeberger et al. 1999). Some studies used the Mason-Allen bone screws repair technique (Gerber, Meyer et al. 2004, Gerber, Meyer et al. 2009, Gerber, Meyer et al. 2015, Peterson, Ohashi et al. 2015, Wieser, Farshad et al. 2015), in which the rotator cuff is repaired by re-attaching the bone chip to its original site or as near to this site as possible with attachment of the remaining sutures to a 3.5-mm cortical bone screw with a washer (Wieser, Farshad et al. 2015). Few other studies used the TOE suture bridge repair technique (Lovric, Ledger et al. 2013), single row repair technique (Uggen, Dines et al. 2010), allograft bone-suture anchors in Mason-Allen pattern (Coleman, Fealy et al. 2003), and bioabsorbable suture anchors technique in Mason-Allen pattern (Klinger, Buchhorn et al. 2008, Baums, Spahn et al. 2012, Baums, Schminke et al. 2015).

#### **2.6.4 Dogs and non-human primates**

Although the above three mentioned species are the most commonly used, dogs are sometimes used as an animal model for rotator cuff repair since they tolerate casting, slinging, treadmill running, post-operative rehabilitation protocols, and are good chronic models (Derwin, Baker et al. 2007). Canine models also produce loads to the rotator cuff that are similar in magnitude to those experienced on a daily basis by humans (Edelstein, Thomas et al. 2011).

However, they are less accepted by the society as research animal. Non-human primates have very similar function and anatomy to humans, but are rarely used due to high cost and complexity of their housing and treatment (Edelstein, Thomas et al. 2011).

Table 2-2: Advantages and disadvantages of different animal models for rotator cuff repair.

Animal models	Advantages:	Disadvantages:
Rat	<ul style="list-style-type: none"> <li>• Acromial arch &amp; overhead activities</li> <li>• SSP below arch</li> <li>• Cost-effective</li> <li>• Similar forward arm elevation</li> </ul>	<ul style="list-style-type: none"> <li>• Scar tissue formation &amp; healing RC without treatment</li> <li>• No postoperative re-tears</li> <li>• Small size</li> <li>• SSP shorter</li> <li>• Fat infiltration in ISP only</li> <li>• RCT heals better</li> <li>• Less coverage from SSP</li> <li>• SSP that passes under arch is musculous and not tendinous</li> <li>• Weight-bearing joint</li> </ul>
Rabbit	<ul style="list-style-type: none"> <li>• Larger &amp; more accurate</li> <li>• Scapular bony tunnel</li> <li>• Similar muscle atrophy &amp; fatty infiltration</li> <li>• Similar healing properties</li> <li>• Good to study RCT &amp; nerve injury</li> <li>• Subscapularis similar to human SSP</li> <li>• Used for auto grafts &amp; dermal grafts</li> </ul>	<ul style="list-style-type: none"> <li>• Weight-bearing joint</li> <li>• Minimal or no overhead activities</li> <li>• ISP is muscular and not tendinous</li> <li>• Less effective at retaining sutures</li> <li>• More bony prominence</li> </ul>
Sheep	<ul style="list-style-type: none"> <li>• Larger &amp; more accurate</li> <li>• Ease of handling &amp; housing</li> <li>• Accurate to repeat surgeries</li> <li>• ISP similar size to human SSP</li> <li>• Availability</li> <li>• Good chronic model &amp; to test various suturing techniques</li> </ul>	<ul style="list-style-type: none"> <li>• Weight-bearing joint</li> <li>• Anatomy not comparable to human</li> <li>• Spontaneous healing</li> <li>• No overhead activities</li> </ul>
Dog	<ul style="list-style-type: none"> <li>• Produce loads to the rotator cuff that are similar to humans</li> <li>• Tolerate casting, slinging, treadmill running, and post-operative rehabilitation protocols.</li> <li>• Good chronic models</li> </ul>	<ul style="list-style-type: none"> <li>• Ethical challenges</li> </ul>

Non-human Primate	<ul style="list-style-type: none"> <li>• Most similar function and anatomy to humans</li> </ul>	<ul style="list-style-type: none"> <li>• High cost and complexity of their housing and treatment</li> <li>• Ethical challenges</li> </ul>
-------------------	---	---

## 2.7 Technologies under Development for Rotator Cuff Repair

### 2.7.1 Platelet-rich plasma

Platelet-rich plasma (PRP) has gained popularity in sports medicine and orthopaedics but its efficacy in rotator cuff tear repair is still unclear. To obtain PRP, small amount of the patient's own blood is spun through a centrifugation process to concentrate platelets. Several types of PRP have been used for clinical cuff repair augmentation (**Appendix E**). PRP can be applied as a liquid (with or without calcium-based activation prior to application) or can be implanted as a solid matrix, in which case it is called platelet-rich fibrin (PRF). In addition, the isolation process will determine whether the PRP or the PRF contains leukocytes or not. There are four distinct PRP formulations. First the leukocyte-reduced platelet-rich fibrin matrices (P-PRF), which are made from activating autogenous thrombin within the plasma to create fibrin clots and this formulation of sequestered platelets can be sutured between tendon-bone interface (Otarodifard, Bruce Canham et al.). Second, leukocyte-enriched platelet-rich fibrin matrices (L-PRF), which is obtained as a result of slow polymerization, in order to keep leukocytes. Leukocytes are white blood cells that release cytokines and growth factors and are hypothesized to aid in healing (Otarodifard, Bruce Canham et al. , Dohan Ehrenfest, Rasmusson et al. 2009). This L-PRF matrix is believed to hold many growth factors and cytokines, and can release them in the wound site for prolonged times (Kumar and Shubhashini 2013). The third formulation leukocyte-platelet-rich plasma (L-PRP) is prepared by retaining the leukocytes during the PRP process formulation. The fourth formulation, platelet rich in growth factors (P-PRP), a preparation of plasma with high concentrations of platelets and growth factors, in which leukocytes have been eliminated during the process (Patel, Gualtieri et al. 2016). There is also BMAC (bone marrow aspirate concentrate) that is obtained through centrifugation of iliac crest punctuation.



Platelets release growth factors from the  $\alpha$ -granules and the dense granules, which contain many different cytokines and bioactive factors, such as growth factors (Rodeo, Delos et al. 2012) that have chemotactic paracrine roles, which regulate inflammation, angiogenesis, synthesis and remodeling of tissues (Andia, Sanchez et al. 2010, Zhou, Estrera et al. 2013). The growth factors within these platelets, such as insulin-like growth factor-1 (IGF-1), platelet-derived growth factor (PDGF), vascular endothelial growth factor (VEGF), and transforming growth factor-B (TGF-B), have all been implicated in tendon healing (Otarodifard, Bruce Canham et al. , Lu, Vo et al. 2008).

Pre-clinical studies investigating PRP for rotator cuff repair are few. Most use the rat model (Beck, Evans et al. 2012, Hapa, Cakici et al. 2012, Cabitza, Banfi et al. 2014, Dolkart, Chechik et al. 2014, Ersen, Demirhan et al. 2014), with a few studies published in rabbits (Chung, Song et al. 2013, Wu, Dong et al. 2014). Some studies showed repair improvement with application PRP, while others did not. BMAC (bone marrow aspirate concentrate)-PRP has been shown to increase proliferation and migration of tendon-derived stem cells (TDSCs) and prevent the aberrant chondrogenic and osteogenic differentiation of TDSC (Kim, Song et al. 2017).

Clinical data of PRP for rotator cuff repair is more abundant (**Appendix E**). Leukocyte-rich PRF has been used as solid implants to attempt cuff repair augmentation by a few groups (Sanchez Marquez, Martínez Díez et al. 2011, Antuna, Barco et al. 2013, Zumstein, Rumian et al. 2014), but no improvement was reported. Pure-PRF devoid of leukocytes was used more often (Barber, Hrnack et al. 2011, Castricini, Longo et al. 2011, Bergeson, Tashjian et al. 2012, Rodeo, Delos et al. 2012, Weber, Kauffman et al. 2013), with two studies showing lower re-tear rates with P-PRF (Barber, Hrnack et al. 2011, Castricini, Longo et al. 2011), two studies showing more failures with P-PRF (Bergeson, Tashjian et al. 2012, Rodeo, Delos et al. 2012) and one study showing no difference between both groups (Weber, Kauffman et al. 2013). Leukocyte-rich PRP was used in a four Level I trials, where showed no clinical improvement but a lower re-tear rate compared to the control group (Randelli, Arrigoni et al. 2011), better repair integrity (Gumina, Campagna et al. 2012) and less post-operative pain (Holtby, Christakis et al. 2016). Charousset et al. (Charousset, Zaoui et al. 2014) compared massive rotator cuff tear repaired arthroscopically with or without L-PRP (Level III study) and found no difference in outcomes, either functionally or radiographically, however, retears tended to be lower in the L-PRP group (Charousset, Zaoui

et al. 2014). Studies using P-PRP devoid of leukocytes employed plateletpheresis systems (Jo, Kim et al. 2011, Jo, Shin et al. 2013, Malavolta, Conforto Gracitelli et al. 2014, Jo, Shin et al. 2015) or centrifugation methods (Ruiz-Moneo, Molano-Munoz et al. 2013, Flury, Rickenbacher et al. 2016, Gwinner, Gerhardt et al. 2016, Pandey, Bandi et al. 2016) to isolate the PRP. Five studies showed less re-tear or partial re-tears in the P-PRP-treated group (Jo, Kim et al. 2011, Jo, Shin et al. 2013, Malavolta, Conforto Gracitelli et al. 2014, Jo, Shin et al. 2015, Pandey, Bandi et al. 2016), while five studies showed no effect of P-PRP (Ruiz-Moneo, Molano-Munoz et al. 2013, Flury, Rickenbacher et al. 2016, Gwinner, Gerhardt et al. 2016).

The most effective platelet and leukocyte counts, as well as the ratio of plasma proteins, timing of delivery (Salamanna, Veronesi et al. 2015), remains unknown (Murray, LaPrade et al. 2016). The majority of PRP-augmented rotator cuff studies have used PRP at the time of surgery (Castricini, Longo et al. 2011, Rodeo, Delos et al. 2012). Once activated, platelets release growth factors almost immediately with total elution within one hour, and a half-life of few minutes (Mooren, Hendriks et al. 2010). A tendon healing study showed that the spike in cell proliferation, growth factors production, ECM production occurs within 7-14 days post-injury (Galatz, Sandell et al. 2006). Furthermore, each cytokine will contribute at different time points after repair (Murray, LaPrade et al. 2016). Thus, timing of delivery remains an important clinical question for optimizing tendon healing (Murray, LaPrade et al. 2016). It has been postulated that PRP will improve tendon healing by increasing the concentration of growth factors and by promoting revascularization of surrounding tissues (Barber, Hrnack et al. 2011), however, results have been inconsistent so far.

Taken together, these studies seem to reflect a lack of significant evidence or any strong benefit for the use of PRP-augmentation RC repair (Castricini, Longo et al. 2011, Randelli, Arrigoni et al. 2011, Theodoropoulos 2011, Jo, Shin et al. 2013). Different studies used different PRP preparations with different platelet concentration and different surgical approaches, which may explain the different outcomes. Lower re-tear rates may translate into improved clinical scores at longer time points, and in that respect, treatment with PRP might eventually improve cuff repair. The efficacy of PRP remains an open question in orthopedic rotator cuff repair. Moreover there is no evidence that delivery of GF alone induces tendon regeneration or scarless healing (Galatz, Gerstenfeld et al. 2015). Future research should use high or higher

concentrations, a more sustained delivery method (Lu, Vo et al. 2008), and maybe several administration dosages intraoperatively (Patel, Gualtieri et al. 2016).

## **2.7.2 Tendon Patches & Grafts**

Grafts are used as scaffolds for tissue ingrowth and as collagen substitutes; a perfect scaffold should increase load to failure and decrease stress, thus shielding injured tissue (Barber, Herbert et al. 2008). They require good strength and tissue compatibility and some are made up of polycarbonate polyurethane, polytetrafluoroethylene, and polyester. Concerns include persistent inflammation and loss of integrity over time, with fragmentations leading to mechanical failure (Murray, LaPrade et al. 2016). Biological patches are used as a vehicle and structural support in tissue engineering and cellular delivery (Denard, Jiwani et al. 2012). Natural biomaterials include, collagen, silk, fibrin, hyaluronic acid, elastin, alginate, chitosan, porcine small intestine submucosa (SIS), human, porcine, bovine dermis and decellularized tendon xenografts (Clark and Harryman 1992, Longo, Lamberti et al. 2010, Longo, Lamberti et al. 2012). Some patches are nondegradable and aim to provide permanent mechanical support to promote self-healing

The concept of ECM patches is to reinforce the strength of a repair by offloading the tendon repair. The patch could provide a scaffold for new growth and differentiation. They may also be used a delivery vehicle for cells and GFs (Galatz, Gerstenfeld et al. 2015). ECMs are derived from dermis, small intestine submucosa (SIS), fascia lata, and pericardium, obtained through decellularization treatment, chemical cross-linking, lamination of multiple layers, or lyophilisation (Aurora, McCarron et al. 2007). A porcine collagen dermal patch (Badhe, Lawrence et al. 2008) was used as a RC augmentation repair in a study of 10 patients, which showed significant functional improvement with 80% graft potency on MRI at 4.5 years. However, Soler et al (Soler, Gidwani et al. 2007) used a porcine dermal collagen as an augmentation material for massive RC tear repair, and all patients demonstrated signs and symptoms of a recurrent tear. Dopirak et al. (Bond, Dopirak et al. 2008) tested Graftjacket, an extracellular matrix (ECM) human cadaveric dermis scaffold, during arthroscopic total rotator cuff replacement in 16 patients. The overhead strength was improved but failure was reported in

3 patients (Bond, Dopirak et al. 2008). Positive outcomes after applying human dermis as an augmentation in large RC defects were documented in other studies (Snyder, Arnoczky et al. 2009, Rotini, Marinelli et al. 2011). Other studies showed improvement in maximum load but not in linear stiffness at the repair site (Omae, Steinmann et al. 2012). Burkhead et al. (Burkhead WZ 2007) showed an increase tissue ingrowth into the Graftjacket graft itself after two years. Patients with arthroscopic SR repair augmented with Graftjacket had higher ASES (American Shoulder and Elbow Surgeons) and constant shoulder scores after 24 months (Barber, Burns et al. 2012). The extracellular matrix grafts are still available and sometimes used in surgery as augmentation devices for soft tissue. ECM grafts showed benefits in some animal studies but not in recent randomized controlled clinical trials (Ahmad, Henson et al. 2013). Hence further investigations are needed to prove their efficacy. Futures controlled comparison studies are necessary to clearly define the advantages and limitation of each biomaterial. When using any ECM devices, it is important to note that a loss of mechanical and suture retention properties is expected (Aurora, McCarron et al. 2007). However, all of the processed ECM devices have similar hydroxyproline content as tendon, except GraftJacket (Aurora, McCarron et al. 2007).

Extracellular devices such as small intestine submucosa (SIS) have been used as scaffolds for the repair of full-thickness infraspinatus tear in a canine model. Six months after the surgery, the injured tendon was similar to native tendon (Adams, Zobitz et al. 2006). However, it was impossible to determine if the observed site was remodeled tissue or new tissue. SIS scaffold was also tested in supraspinatus tendon of rabbits. After only 8 weeks, 4 of 5 implants were replaced by dense collagen, but load to failure was inferior to control tendon (Aurora, McCarron et al. 2007). Metcalf et al. (Metcalf MH 2002) used Restore, a small intestine submucosa (SIS) scaffold deriving from a porcine source, in 12 patients during arthroscopic procedures. Two years post-surgery, MRI showed thickening and incorporation of cells but no improvement in shoulder function (Metcalf MH 2002). Moreover, Sclamberg et al. (Sclamberg, Tibone et al. 2004) used MRI to evaluate 11 patients 6 months post-implantation of Restore and revealed that 10 of 11 repairs had failed. Iannotti et al. (Iannotti, Codsi et al. 2006) also tested Restore in human cuff repair and found an increase in pain and inferior tendon healing. Barber et al. (Barber, Burns et al. 2012) tested Restore and 15 patients had poor quality tendon, 4 patients had postoperative inflammatory reactions and all had decreased tendon strength and adduction strength. SIS and

dermis devices may not be able to provide good mechanical reinforcement in rotator cuff tear repairs (Aurora, McCarron et al. 2007).

Hirooka et al. (Hirooka, Yoneda et al. 2002) tested a synthetic scaffold, made up of polytetrafluoroethylene for reconstructing rotator cuff tears in 27 patients. They obtained fairly good results; the JOA score (Shoulder surgery classification system issued by Japanese Orthopedic Association) was improved and so was the abduction strength. Unfortunately, there is still limited data on its effectiveness.

There is also the possibility of tendon transfer, when the rotator cuff tear is considered irreparable with tendon retraction and fatty infiltration (Thes, Hardy et al. 2015). They can be derived from autografts, allografts, or xenografts. However, musculotendinous transfer results in donor site morbidity (Funakoshi, Majima et al. 2005). The latissimus dorsi with or without the teres major transfer has been shown to increase mobility and function, as well as decrease pain (Namdari, Voleti et al. 2012, Grimberg and Kany 2014). However, it does not prevent humeral head migration or progression of osteoarthritis (Grimberg and Kany 2014). Only one animal study has used fresh autograft fascia lata scaffold in supraspinatus using a rabbit model (Sano, Kumagai et al. 2002). Two weeks post-implantation, collagen type-II and -III were increased as well as chondrocytes and cell density, similar to the natural healing process (Sano, Kumagai et al. 2002). In addition, rarely does the transferred tendon material match the tensile properties of the repaired tissue (Docheva, Muller et al. 2015). Moreover, patch grafts become mechanically weaker over time (Funakoshi, Majima et al. 2005). The ideal scaffold should be biocompatible, support cell attachment growth with high surface area, promote tenogenic differentiation pathway, and not inflammatory responses, and, when not biodegradable, be able to mimic native tendon architecture and mechanical properties (Docheva, Muller et al. 2015).

### **2.7.3 Cells**

Mesenchymal stem cells (MSCs) have been studied over the last two decades for the treatment of bone defects, cartilage and meniscal regeneration, tendinopathies and muscle lesions (Lendeckel, Jodicke et al. 2004), for their ability to differentiate into different mesodermal tissues

(Mora, Iban et al. 2015). MSCs may facilitate RC tear healing directly, by differentiating into tenocytes or osteoblasts, or by recruiting progenitor cells, and by reducing inflammation (Murray, LaPrade et al. 2016).

Kida et al. (Kida, Morihara et al. 2013) created a bone marrow chimeric (BMC) rat by bone transplantation. Four weeks after the transplantation, they transected the supraspinatus from its insertion site bilaterally. On the right shoulder an extra drilling procedure was made in the greater tuberosity of the humerus. A total of six holes were drilled to perform the transosseous repair technique, while no drilling was performed on the contra lateral shoulder (control group). At four weeks post-surgery, BM-MSCs infiltrated the repaired tendon and mechanical resistance was increased in the drilling group (Kida, Morihara et al. 2013). Gulotta et al (Gulotta, Kovacevic et al. 2009) have applied bone marrow-derived mesenchymal stem cells (BMSC) in a rotator cuff repair model in 80 rats. They observed no improvement in histological or biomechanical properties; hence they hypothesized that BMSC alone, may not be sufficient for rotator cuff tear repair improvement. Oh et al. (Oh, Chung et al. 2014) tested adipose tissue mesenchymal stem cells (AMSCs) in rotator cuff rabbit repair. The AMSC group showed better tendon healing and more regeneration compared to the non-AMSC group (Oh, Chung et al. 2014).

Only two clinical studies have studied the application of MSCs in rotator cuff surgery. One study harvested bone marrow mononuclear cells (BMMCs) from iliac crest of 14 patients during transosseous stitches repair. These patients had higher UCLA shoulder-scoring test compared to pre-operative and the MRIs showed better tendon integrity (Ellera Gomes, da Silva et al. 2012). However this study had no control group, rendering conclusions difficult. Hernigou et al. (Hernigou, Flouzat Lachaniette et al. 2014) observed significant improvement in healing outcomes in patients receiving MSCs with standard-of-care RC repair at 10 years follow up. MSCs as an enhancement therapy improved healing rate and quality of the repaired surface (Hernigou, Flouzat Lachaniette et al. 2014). Although two clinical studies have evaluated MSCs in the context of RC repair, no level I studies have yet been performed (Ellera Gomes, da Silva et al. 2012, Hernigou, Flouzat Lachaniette et al. 2014). A recent review (Beitzel, McCarthy et al. 2013) concluded that the use of MSCs augmentation in cuff repair should be considered an experimental technique demonstrating the need for further research (Apostolakos, Durant et al. 2014).

Yokoya et al. (Yokoya, Mochizuki et al. 2012) showed an improved mechanical strength and an increase in collagen type-I with a polylactic acid scaffold seeded with BMSCs in a rat model at 4 months. Kim et al. (Kim, Lee et al. 2013) compared the use of a tridimensional open-cell polylactic acid scaffold with and without BMSCs in RC repair. At 6 weeks, BMSCs augmentation showed greater amount of collagen type-I to controls. Allogeneic tendon stem/progenitor cells (TSPCs) were seeded on a silk-collagen scaffold that was implanted in a rabbit rotator cuff injury model. Results showed that TSPC-seeded silk-collagen scaffold increased collagen content and biological environment without any sign of inflammation (Shen, Chen et al. 2012).

Then in 2011, Gulotta et al. (Gulotta, Kovacevic et al. 2010) used allogeneic BM-MSCs transduced with membrane type-1 matrix metalloproteinase in supraspinatus acute repair. At four weeks, they observed an increase in fibrocartilage and biomechanical strength. A rat model was used to test allogeneic BM-MSCs transduced with human bone morphogenetic protein-13 (BMP-13) in acute supraspinatus tendon repair. No change in structure, composition or strength was observed at the repair site compared to untransduced MSCs-treated group (Gulotta, Kovacevic et al. 2011). Allogeneic BM-MSCs were then transduced with adenoviral-mediated scleraxis (Ad-Scx) in rat supraspinatus acute repair. An increased in fibrocartilage, mechanical resistance and stiffness was seen compared to the group treated with MSCs only (Gulotta, Kovacevic et al. 2011). When cells are to be used, it might be more appropriate to introduce them at the later stage when they can enhance endogenous healing process (Docheva, Muller et al. 2015). However, it is still unclear whether the phenotype remains stable when the cells are implanted into a tendon lesion (Docheva, Muller et al. 2015).

#### **2.7.4 Scaffolds, Cells and Combinations**

Scaffolds provide a temporary template during tissue regeneration, some even mimic the native ECM properties (Funakoshi, Majima et al. 2005). Ideally, they would promote cellular attachment, migration, proliferation, differentiation to the proper phenotype, allow vascularization and nutrient delivery, have good biodegradation rate and mechanical properties adequate to support new tissue formation (Chang, Kuo et al. 2009).

Funakoshi et al. (Funakoshi, Majima et al. 2006) used a nonwoven chitin fabric in the repair of infraspinatus tears in 21 rabbits; they observed an increase in cell number and collagen fiber alignment. Structural and biomechanical properties were also enhanced, however a few specimens had detached at the tendon-bone junction (Funakoshi, Majima et al. 2006). Poly (D, L-lactide-co-glycolide) (PLGA) scaffolds created by electro spinning were introduced in the infraspinatus of rabbits. An increase in bone formation at the scaffold-bone interface and an increase in type-II collagen and proteoglycan content were observed. However no significant difference was seen in ultimate failure load and stiffness, although the tendons were weaker than normal (Inui, Kokubu et al. 2012). Elderly rat models were used to study the efficacy of MSCs with a collagen membrane. A chronic defect was created, detaching the supraspinatus from its insertion site. One month post-injury, the tears were repaired with sutures only, Collagen-1 membrane (OrthoADAPT bioimplant, Penta Biomedical) or Collagen-1 membrane with MSCs implanted. The group with OrthoADAPT seeded with MSCs had significantly higher maximum load at 3 months (Tornero-Esteban, Hoyas et al. 2015). However the stiffness was not increased. The authors suggested that MSCs could potentially increase rotator cuff healing (Tornero-Esteban, Hoyas et al. 2015).

BMSCs harvested from iliac crest of two rabbits during arthroscopy were cultured and seeded on polylactic acid scaffold and the same scaffold without stem cells was used in contralateral shoulders. The scaffold seeded with stem cells showed an increase in collagen type-I (Kim, Lee et al. 2013). Yokoya et al. (Yokoya, Mochizuki et al. 2012) used polyglycolic acid sheet seeded with cultured autologous BMSCs in the repair of infraspinatus lesions in rabbits. After 16 weeks, collagen type-I and the mechanical strength were significantly increased. Moreover a knitted silk-collagen scaffold seeded with allogeneous stem cells harvested from Achilles tendons were used to augment rotator cuff repair in rabbits. Fibroblasts ingrowth in the scaffolds and a decrease in lymphocyte infiltration were observed (Shen, Chen et al. 2012).

Lu et al. (Lu and Thomopoulos 2013) developed a triphasic scaffold to mimic the graded transitional zones of the entheses. The 3-layered scaffold was produced using PLGA knitted sheets, PLGA micro spheres and PLGA/bioactive glass micro spheres to mimic the tendon, fibrocartilage, and bone regions, respectively. Fibroblasts were seeded onto the PLGA sheets, osteoblasts were seeded onto the bioactive glass, and although some migration was observed into



the central core no fibrocartilage-like region formation was observed in the central core of the scaffold. Moreover neither the tensile properties nor the attachment potential of the triphasic scaffold have been reported in this study (Paxton, Baar et al. 2012). Moffat et al. (Moffat KL 2011) used a biphasic-nanofiber scaffold containing mineralized and nonmineralized regions for RCT repair in rats. They showed viable chondrocytes with collagen-proteoglycan matrix in both regions of the scaffold with fibrocartilage-like transition zone.

Then a single pluripotent cell type design (Zuk, Zhu et al. 2002, Guilak, Awad et al. 2004, Kern, Eichler et al. 2006) was stimulated by gradations of different local stimuli to eventually be used in tendon-to-bone construct (Phillips, Burns et al. 2008, Wang, Wenk et al. 2009, Shi, Wang et al. 2010). The hypothesis was that stimuli would induce local cell differentiation, resulting in graded cells and tissue type (Zuk, Zhu et al. 2002, Guilak, Awad et al. 2004, Kern, Eichler et al. 2006). Ma et al. (Ma, Goble et al. 2009) proposed to culture tissue phases with MSCs separately and then allow them to self assemble (Ma, Goble et al. 2009). However, osteoblast-like and fibroblast-like cells interactions did not generate a fibrocartilage transition zone. Phillips et al. (Phillips, Burns et al. 2008) cultured fibroblasts on a construct that had been conjugated with a linearly graded increase in Runx2, an osteoblastic transcription factor. The osteoblastic transdifferentiation of the cells positively correlated to Runx2 concentration, indicating that a graded interface could be obtained (Phillips, Burns et al. 2008). MSCs were seeded on the surface of a silk construct adsorbed with BMP-2 and IGF-1 in osteochondral medium (Wang, Wenk et al. 2009). This construct resulted in graded increases in calcium, GAG deposition and collagen type-I, -II and -X gene transcriptions. The gradient achieved resembled the native transition from unmineralized to mineralized fibrocartilage to bone (Wang, Wenk et al. 2009). The stratified tissue construct poses practical challenges for use. Isolating fibroblasts, chondrocytes, and osteoblasts from three different sites would involve costs and high levels of pain (Smith, Xia et al. 2012).

Hence cells, scaffolds and combination can aid rotator cuff tendon regeneration, but further studies are still required. This preclinical evidence can be used as a step forward in clinical translation. However acceptable strategies for tendon pathology will require proper combination of cells and scaffolds to obtain successful outcomes (Montgomery, Petrigliano et al. 2011). Unfortunately no biological augmentations are perfectly suited for rotator cuff repairs yet.

### 2.7.5 Growth Factors & Cytokines

Growth factors can be applied by local injection or subcutaneous injection (Rickert, Jung et al. 2001, Hamada, Katoh et al. 2006, Uggen, Dines et al. 2010). GFs are rapidly cleared following injection, but this could be resolved by using scaffolds or coated suture material seeded with GFs. Growth factors are produced mostly by platelets and fibroblasts and are able to control growth and differentiation of different cells (Ahmad, Henson et al. 2013). Platelet-derived growth factor (PDGF) is known to increase collagen type-I and induce TGF- $\beta$ I (Wurgler-Hauri, Dourte et al. 2007). FGF-2 applied to repaired SSP tears in rat resulted in accelerated bone ingrowth thus improving biomechanical properties and histological scores at 2 weeks. However, no differences were seen at 4 and 6 weeks, suggesting that FGF-2 accelerated ingrowth but not the final outcome (Ide, Kikukawa et al. 2009). Human recombinant PDGF-BB implanted in collagen type-I graft for RC repair improved biomechanical strength and anatomic appearance of healing tendons in a sheep model (Hee, Dines et al. 2011). It was also tested in rat rotator cuff repair where the group treated with PDGF-BB had collagen-bundle alignment similar to controls (Wurgler-Hauri, Dourte et al. 2007). PDGF-BB was shown to increase DNA and collagen synthesis from tenocytes in vitro (Uggen, Dines et al. 2005). Uggen et al. (Uggen, Dines et al. 2010) tested PDGF-BB in the infraspinatus tendon repair in sheep. They used PDGF-BB-coated sutures to repair the tendon, which resulted in better histological properties after 6 weeks at the bone-to-tendon junction but did not change tendon strength. Subsequently rhPDGF-BB-coated sutures (human recombinant) were used in sheep and improved histological scores, but no change was observed in load-to-failure (Ide, Kikukawa et al. 2009). Another study in sheep used a type-1 collagen scaffold with rhPDGF-BB (human recombinant Platelet-derived growth factor) to augment infraspinatus repair (Hee, Dines et al. 2011). The anatomic appearance was significantly enhanced as well as the biomechanical strength.

Regenerative fetal wound healing is characterized by low expression of TGF- $\beta$ 1 and TGF- $\beta$ 2, with high levels of TGF- $\beta$ 3 and in contrast, adult scar-mediated wound healing was characterized by opposite expression. TGF- $\beta$ 3 is a cytokine that plays a role in cell proliferation, differentiation and matrix synthesis. Its expression is relatively high during fetal wound healing but decreases in post-natal stages. Hence it was hypothesized that exogenous injection of TGF- $\beta$ 3 could promote scarless healing (Huang, Wang et al. 2002). This hypothesis led to a study

assessing TGF- $\beta$  in a rat supraspinatus tear repair model. TGF- $\beta$ 1 group had an increase in type-III collagen and a scar-mediated repair with poorer mechanical properties. TGF- $\beta$ 1 group showed no difference histologically and biomechanically compared to controls (Kim and Lee 2011). A recent study by the same research group observed healing enhancement and an increase in strength of tendon-bone healing following sustained TGF-B3 injections (Manning, Kim et al. 2011). Kovacevic et al. (Kovacevic, Fox et al. 2011) tested the delivery of TGF-B3 in an injectable calcium-phosphate scaffold in repaired RC of rats. TGF-B3 improved the strength of the repair sites at 4 weeks significantly.

Healing of the insertion site is dependent on bone ingrowth into the repaired tendon (Rodeo, Potter et al. 2007). It was hypothesized that osteoinductive GFs would improve tendon-bone healing. BMPs belong to the TGF-B superfamily and stimulate bone formation, regulate fibrocartilage, neotendon, and ligament formation (Hoemann and Fong 2017). For these reasons, the ability of BMPs to improve RC healing is currently under investigation in preclinical studies. Local application of BMP-2 for enthesis formation in a rotator cuff rabbit model resulted in increased ultimate failure loads for BMP-2 (Hashimoto, Yoshida et al. 2007). Dines et al. (Dines, Weber et al. 2007) used recombinant BMP-14 coated sutures, which accelerated tendon healing and enhanced strength. However, no biomechanical or histologic difference was observed. Addition of BMP-13 on a collagen scaffold improved the loads to failure at 6 weeks (Murray, Kubiak et al. 2007). Rodeo et al. (Rodeo, Potter et al. 2007) used BMP-2, -3, -4, -5, -6 and BMP-7, TGF-B1, TGF-B3, and FGF within an osteoinductive bone protein extract placed on the tendon-bone interface and that resulted in no improvement. Addition of osteoinductive GFs and BMP-12 on tendon-to-bone healing in a sheep model showed increased formation of new bone, fibrocartilage and improved load-to-failure (Kovacevic and Rodeo 2008). RhBMP-2-coated human cadaveric dermal patch was inserted in a chronic rotator cuff rabbit injury, where it increased new bone formation and improved biomechanical properties such as ultimate tensile strength (Lee, Lee et al. 2016). All of these new technologies involving growth factors face important challenges. The amount of growth factor needed, the right combination of GFs or genetic modification, and if so, which GFs or genes to target, the incorporation of carriers for the GFs, and the timing of delivery still need to be clarified (Docheva, Muller et al. 2015).

Ultimately, this topic of orthopaedic medicine will need to be further studied, however the future of this field is promising (Apostolakos, Durant et al. 2014)

Metalloproteinase (MMP) inhibitors can also be used since MMPs synthesis is increased in the case of rotator cuff tears, which degrades the extracellular matrix (Del Buono, Oliva et al. 2012). A healthy balance between MMPs and MMP inhibitors is important in maintaining integrity of ECM tissue (Brew and Nagase 2010). Dysregulation, with elevated levels of MMPs is associated with tendon degeneration and rupture (Riley 2004). Inhibitors of MMP-13 were shown to enhance fibrocartilage formation, collagen organization plus the load to ultimate failure (Bedi, Fox et al. 2010, Del Buono, Oliva et al. 2012).

However there is still no study on rotator cuff repair using growth factors in humans (Randelli, Randelli et al. 2014). Growth factors can enhance repair and enable tissue regeneration, nevertheless clinical investigations are required to establish the proper timing, dosage and the delivery method (Ahmad, Henson et al. 2013) (Angeline and Rodeo 2012).

## 2.8 Chitosan

Chitin ( $\beta$  (1 $\rightarrow$ 4) N-acetyl-D-glucosamine) is a natural polysaccharide synthesized by many living organisms and made up of ordered crystalline microfibrils (Younes and Rinaudo 2015). Chitin occurs as two allomorphs,  $\alpha$  and  $\beta$ .  $\alpha$ -chitin isomorph is the most abundant one and is mostly found in fungal and yeast cell walls, krills, lobsters, crab tendons, shrimp shells, and insect cuticles (Younes and Rinaudo 2015).  $\alpha$ -chitin is formed by recrystallization (Persson, Domard et al. 1992, HELBERT and SUGIYAMA 1998), in vitro biosynthesis (Bartnicki-Garcia, Persson et al. 1994), or enzymatic polymerization (Sakamoto, Sugiyama et al. 2000).  $\beta$ -chitin isomorph is a lot less abundant and is only found in association with other proteins in squid pens (Rudall 1969, Rudall and Kenchington 1973) and tubes synthesized by pogonophoran and vestimetiferan worms (Blackwell 1965). The chains in these two allomorphs are organized in sheets and held by intra-sheet hydrogen-bonds, which control solubility, swelling and reactivity (Younes and Rinaudo 2015).

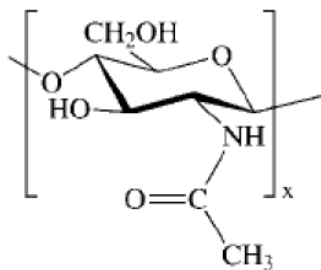


Figure 2-3: Chemical structure of chitin.

Chitin isolation from shellfish requires the removal of two main components, proteins by deproteination (DP) and inorganic calcium carbonate by demineralization (DM) processes. Several different procedures can be used to carry out deproteination and demineralization, like chemical or enzymatic treatments (Younes and Rinaudo 2015). Chemical deproteination is performed using chemicals that simultaneously depolymerize the biopolymer. Complete removal of proteins is extremely important, since a high proportion of the population is allergic to shellfish (Younes and Rinaudo 2015). Enzymatic DP can either be performed after or before DM using both purified and crude extracted proteases, but is, however, a lot less efficient than chemical methods (Younes and Rinaudo 2015). Chemical demineralization is useful in removal of minerals, primarily calcium carbonate and is performed by acid treatment with HCL, HNO<sub>3</sub>, H<sub>2</sub>SO<sub>4</sub>, CH<sub>2</sub>COOH, or HCOOH (Percot, Viton et al. 2003). Dimineralization treatments mostly change with the mineralization degree, extraction time, temperature, particle size, acid concentration and solute-solvent ratio (Younes and Rinaudo 2015). However, chemical treatments have some drawbacks; it harms the physico-chemical properties, affects waste H<sub>2</sub>O with contaminants, and increases the cost of chitin purification process. On the other hand, biological DM using microorganisms, increases reproductibility, decreases process time, is easier, involves less solvent consumption and decreases energy consumption. Deproteination and demineralization can be processed simultaneously by adding different strains of microorganisms (Younes and Rinaudo 2015). Moreover in some cases, an extra step is also added, decolorization, which removes residual chitin pigments.

Unfortunately, chitin is not readily used due to its high level of acetylated groups, rigid structure, and its poor solubility in aqueous solution (Ahmadi, Oveisi et al. 2015). Hence is

frequently modified to chitosan for biomedical applications, which involves 4 steps, demineralization (DM), deproteination (DP), decolorization (DC), and deacetylation (DA) of chitin. Chitosan is a linear semi-synthetically derived aminopolysaccharide copolymer of  $\beta$  (1 $\rightarrow$ 4) linked D-glucosamine (GlcN) and N-acetyl-glucosamine (GlcNAc): a polymer of N-acetyl-2-amino-2-deoxy-D-glucopyranose and 2-amino-2-deoxy-D-glucopyranose in the repeating glucosidic residue (Agrawal, Strijkers et al. 2010). Its backbone is similar to cellulose, in which the repeating units are linked through (1 $\rightarrow$ 4)  $\beta$ -glycosidic bonds with a modified degree of N-deacetylation, except that the acetyl amino group replaces the hydroxyl group on C2 position (Holland, Tessmar et al. 2004, Dash, Chiellini et al. 2011).

First the rigid crystalline structure of chitosan is obtained from arthropod exoskeleton by alkaline N-deacetylation of chitin (Roberts 1992) (Sun, Wang et al. 2009). Chitin deacetylation removes acetyl groups from the GlcNA monomeric units to generate D-glucosamine (Glc) (Baskar and Sampath Kumar 2009). The percentage of acetyl groups removed by the chemical deacetylation is termed the degree of deacetylation (DDA), which is equivalent to the ratio of glucosamine to the sum of glucosamine and N-acetyl-glucosamine units. Either acid or alkali can be used to chemically deacetylate chitin to obtain chitosan polymer. However, glycosidic bonds are more susceptible to acid, hence alkali deacetylation is used more often (No and Meyers 1995, Hajji, Younes et al. 2014). Chitin deacetylation can be done either heterogeneously (Chang, Tsai et al. 1997) or homogeneously (Sannan, Kurita et al. 1976). Heterogeneous deacetylation involves treating chitin with hot concentrated solution of NaOH during few hours, and chitosan is produced as an insoluble residue with 85-99% DDA (Younes and Rinaudo 2015). Homogeneous deacetylation involves dispersion of chitin in concentrated NaOH, followed by dissolution in crushed ice, and produces soluble chitosan with a DDA around 45 to 55% (Kurita, Sannan et al. 1977). The deacetylation conditions used will determine the polymer molar mass and DDA. Alternatively, naturally occurring chitin deacetylases found mostly in fungi and insects (Sundara 1982) can also catalyze the hydrolysis of the N-acetyl amino bonds in chitin (Araki and Ito 1974, Alfonso, Nuero et al. 1995, Gao, Katsumoto et al. 1995, Tsigos and Bouriotis 1995, Tokuyasu, Ohnishi-Kameyama et al. 1996). Then depolymerisation can be performed as a last step to break down the polymer into monomers or a mixture of monomers. Usually polymers are depolymerized at high temperatures, driven by an increase in entropy. Several techniques exist

for depolymerisation, such as ultrasound (Tang, Huang et al. 2003), heat (Jarry, Chaput et al. 2001), enzymatic hydrolysis (Howard, Ekborg et al. 2003), and chemical hydrolysis (Mao, Shuai et al. 2004). The favored technique is using nitrous acid since it is economical, rapid and can be controlled easily to produce desired sizes of chitosan monomers (Tommeraas, Varum et al. 2001).

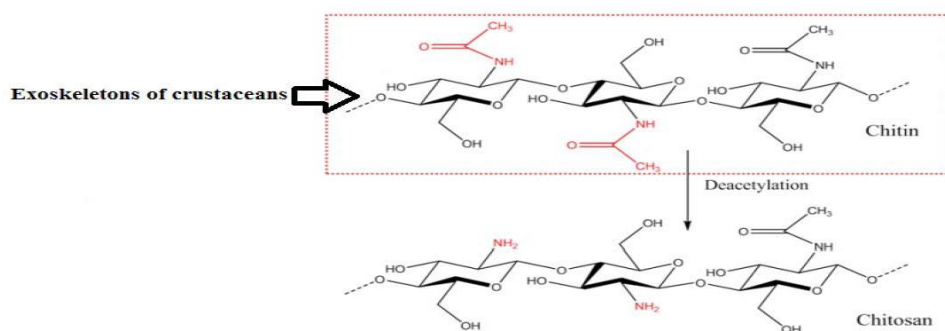


Figure 2-4: Chitin extracted from shellfish from which chitosan is made by N-deacetylation (Ahmadi, Oveisi et al. 2015).

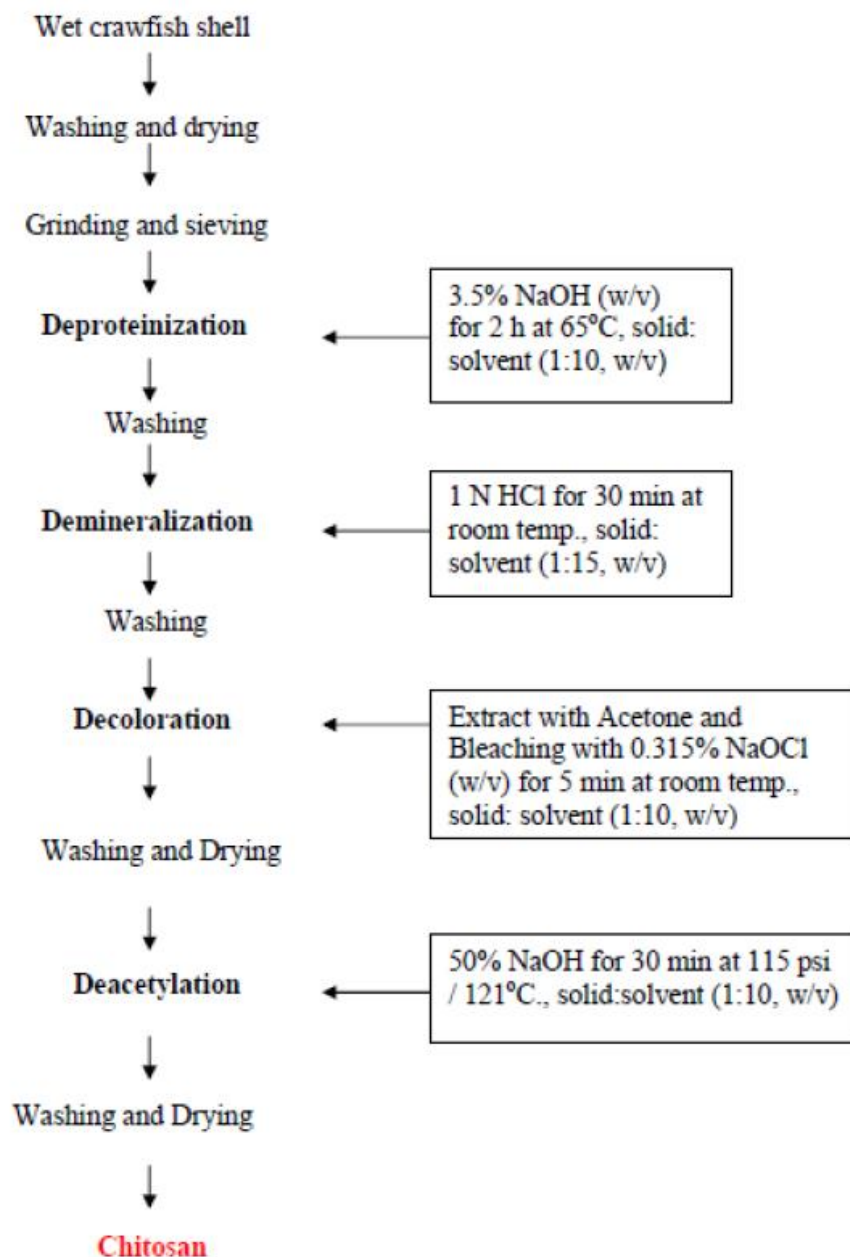


Figure 2-5: Chitosan flow production (Ibrahim and Zairy 2015).

Chitosan is used in various fields, such as drug delivery, gene therapy, vaccines and tissue engineering (Hoemann and Fong 2017), because of its polycationic, biocompatible, antibacterial, wound healing, mucoadhesive and biodegradable properties. N-acetyl moieties in chitosan are structurally related to various GAGs and HAs, thus making it suitable for tissue engineering



uses (Suh and Matthew 2000, Hoemann, Hurtig et al. 2005). It can also be processed into hydrogels (Roughley, Hoemann et al. 2006, Hastings, Kelly et al. 2012), nanofibers (Jayakumar, Prabakaran et al. 2010), beads (Jayakumar, Reis et al. 2007), microparticles (Prabakaran and Mano 2004), nanoparticles (MacLaughlin, Mumper et al. 1998, Koping-Hoggard, Varum et al. 2004), and porous scaffolds (Ma, Gao et al. 2003, Yan, Wang et al. 2010, Barroso, Viveiros et al. 2014).

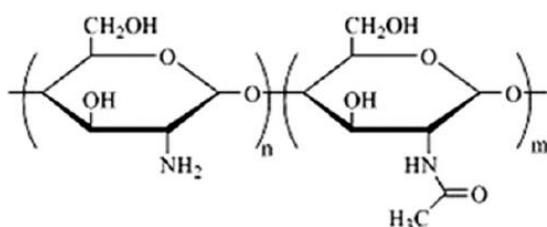


Figure 2-6: Schematic representation of chitosan structure (Dash, Chiellini et al. 2011).

Chitosan is insoluble at high pH, although this can be reversed by sulphating the amines, making the molecule anionic and H<sub>2</sub>O soluble (Suh and Matthew 2000). Chitosan is a very interesting molecule since it is fairly easy to modify its physicochemical properties. The relative ratio of N-acetyl-G-glucosamine and D-glucosamine residues determine the polymer's structure (Dash, Chiellini et al. 2011). At pH higher than 6.0, due to quaternisation of the amine group that have a pka of 6.3, the amines become deprotonated and the biopolymer loses its charge, thus becoming insoluble (Dash, Chiellini et al. 2011). At lower pH, the amine groups get protonated and become positively charged. As pka value depends on chitosan DDA, the solubility depends on DDA and the methods of deacetylation used (Cho, Jang et al. 2000). Both the molar mass and DDA affect its solubility, mechanical strength, and its degradation rate. Increasing DDA decreases the number of relative positions for hydrolysis degradation, which results in decreased degradation rate and greater crystallinity (Kurita, Sannan et al. 1977, Hirano, Tsuchida et al. 1989, SASHIWA, #160 et al. 1991).

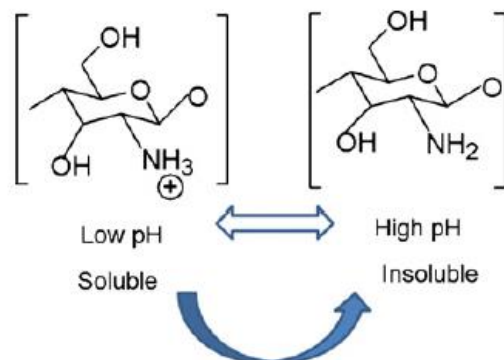


Figure 2-7: Schematic illustration of chitosan's versatility: At low pH, chitosan's amine groups are protonated conferring polycationic behaviour to chitosan. At high pH, chitosan's amines are deprotonated and reactive (Dash, Chiellini et al. 2011).

Chitosan biocompatibility refers to the ability to interact with living cells, tissues or organs without being toxic or triggering immunological reaction or rejections, hence tolerated and accepted by biological systems after being brought into direct contact with them (Halim, Keong et al. 2012). Once inside the body, chitosan can be degraded by chitinases, which are lysosomal enzymes that provide a first-line innate immune defense by damaging any chitin-containing pathogen cell walls or by lysozymes found in various cell types (Lee, Da Silva et al. 2011). Chitinases hydrolyze the 0-linkage between consecutive GlcNA residues in chitin-like molecules (Eide, Norberg et al. 2012). Therefore chitosan biodegradability refers to the breakdown of the polymer into smaller fractions of D-glucosamine and N-acetyl-glucosamine oligomers and monomers, catalyzed by either enzymes or chemicals (Halim, Keong et al. 2012).

Chitosan is also known to influence the migration behaviour of immunomodulatory cells, such as neutrophils and macrophages (Okamoto, Minami et al. 1993, Kosaka, Kaneko et al. 1996), and is considered a neutro-chemoattractive (Usami, Okamoto et al. 1994, Usami, Okamoto et al. 1994, Usami, Okamoto et al. 1998), which does not provoke chronic

inflammation (Hoemann and Fong 2017). Chitosan stimulatory effect on macrophages and neutrophils is due to its acetyl residues on its chain. Chitosan only transiently increases the immune system reaction, due to body reaction when impregnated with tissue fluids, which eventually becomes biotolerated and metabolized by degradation (Nishimura, Nishimura et al. 1986, Muzzarelli 1997, Ueno, Mori et al. 2001). Innate immune responses and clearance rates correlates with both physical form and chitosan chemical structure (Hoemann and Fong 2017).

Modifications, such as changes in DDA, cross-linking, polyethylene glycol (PEG) treatment, wheat germ agglutination treatment, rigorous heat treatment, and oxygen plasma treatment influence its biocompatibility and biodegradability (Halim, Keong et al. 2012). Higher DDA induces chitosan-cell interactions because of its free amino group (Dash, Chiellini et al. 2011), and induces inflammatory response due to a decrease in degradation rate (Kean and Thanou 2011). However, lower DDA chitosan degrades faster leading to the accumulation of many amino saccharides, resulting in acute inflammatory reaction (Dash, Chiellini et al. 2011). This can lead to negligible fibrous tissue encapsulation (Kim, Seo et al. 2008), by stimulating macrophages activity, increasing nitric oxide, reactive oxygen species, TNF- $\alpha$ , interferon, IL-1, TGF- $\beta$  and PDGF. Nevertheless, since proteins and lipids are lacking in its structure, it is impossible to develop specific antibodies against chitosan or its oligomers, unless coupled in subsystems with other substances, such as albumin (Rodriguez-Vazquez, Vega-Ruiz et al. 2015).

Chitosan has positive effects on wound healing such as hemostasis, tissue regeneration and fibroblast synthesis of collagen (Sun, Wang et al. 2009). It is used as a scaffold material for tissue regeneration, since it increases granulation tissue formation, cell adhesion, angiogenesis, proliferation, function and integration of repair tissue with host tissue (Hoemann, Hurtig et al. 2005) (Yao, Yang et al. 2012). Chitosan cationic scaffold has also a suitable microstructure, desired mechanical strength, ability to support cell residence and an appropriate degradation rate for tissue engineering. It also prevents scar tissue from re-modeling and supports tissue regeneration (Yao, Yang et al. 2012). CS increases wound healing, cellular organization (Okamoto Y 1992), inflammatory cells and fibroblasts recruitment via N-acetyl-B-D-glucosamine, which is released during its gradual degradation (Ueno, Yamada et al. 1999, Kojima, Okamoto et al. 2004, Dai, Tanaka et al. 2011, Jayakumar, Prabakaran et al. 2011c). CS produces less scarring (Ueno, Yamada et al. 1999, Ueno, Mori et al. 2001, Azad, Sermsintham et

al. 2004), induces vascularity and supplies chito-oligomers at the lesion site, resulting in better collagen fibril incorporation into ECM (Shigemasa and Minami 1996, Rao and Sharma 1997). High DDA CS increases fibroblast proliferation while low DDA decreases fibroblastic activity (Howling, Dettmar et al. 2001). Stimulation of fibroblastic proliferation requires the presence of serum, in which CS interacts with GFs present in the serum, hence potentiating their effects (Howling, Dettmar et al. 2001). Chitosan is also linked to scarless healing in soft tissue and adhesion formation during tendon healing after surgery (Wang, Mo et al. 2010). The lack of precipitation, coupled with the in situ gelling of chitosan permits it to adhere to the repair site long enough to modulate the healing sequence, thus increasing tissue regeneration (Cho, Kim et al. 2008, Melamed, Beutel et al. 2015). Functional and performance properties are associated with chitosan DDA and molar mass. Furthermore, biological properties, such as wound healing and osteogenesis enhancement as well as degradation by lysosomes in subsystems (Gerentes, Vachoud et al. 2002) are affected by viscosity. Viscosity is proportionally correlated with chitosan concentration and molar mass and is inversely correlated with temperature and chain length. Deacetylation conditions also change viscosity by changing inter- and intra-molecular repulsion forces within the copolymer (Dash, Chiellini et al. 2011). It also decreases with increased acetic acid concentration, due to increased protonation and solubilisation. Acetic acid can increase solubility and decrease the pH of the solution (Agnihotri, Kulkarni et al. 2006).

Moreover, because of its cationic hemostatic properties, chitosan activates platelets (Chou, Fu et al. 2003), while inhibiting clot retraction mechanisms. With its high positive charge density, chitosan adheres to negatively charged biological tissues and displays good cell adhesive properties. Chitosan is capable of promoting wound healing through modulation of inflammatory and other cell functions, such as PMNs, macrophages and fibroblasts (Ueno, Mori et al. 2001). It also increases granulation tissue formation and thickness of wound tissues (Ueno, Yamada et al. 1999, Ueno, Mori et al. 2001). However if CS resists degradation, a fibrous encapsulation will be formed around the implant and the tissue adjacent will be scarce of macrophages and populated with fibroblasts (Azab, Doviner et al. 2007).

To our knowledge, there have been only a small number of publications using chitosan in rotator cuff repair. Melamed et al. (Melamed, Beutel et al. 2015) found that rotator cuff tear repair augmented with chitosan gel matrix enhanced healing of soft tissues, as well as fibrous

tissue, fibroblastic response and cell migration (Melamed, Beutel et al. 2015). However, the regenerated tendon-bone insertion site was not similar to native with neither a tidemark present nor an increase in collagen type-II. Chitosan was also shown to increase rotator cuff repair in rats by decreasing muscle fiber fibrosis and by preventing muscle atrophy (Robinson, Pachornik et al. 2010). Moreover, a nonwoven chitin fabric used as a matrix in cuff repair increased biological as well as mechanical regeneration of rotator cuff in rabbits (Funakoshi, Majima et al. 2006).

### **2.8.1 Chitosan/whole blood hybrids for cartilage repair**

Cartilage repair by current surgical methods is challenging, due to its avascular structure, its lack of significant progenitor cells, and its poor regenerative ability (Martins, Michelacci et al. 2014). Strategies for cell implantation within joints poses huge challenges, since joint is a fluid environment, that bears strong shear forces, mechanical loads, and is stiff (Martins, Michelacci et al. 2014). Cartilage scaffolds require a structure that induces growth of new tissue, mechanical characteristics similar to native, thus increasing chances that the reparative strategy will be compatible with host's tissue cells (Athanasίου, Shah et al. 2001, Sittinger, Hutmacher et al. 2004). Chitosan structure resembles GAGs closely, which seems to be appropriate for cartilage regeneration, since GAGs are a major component of the cartilage ECM (Majima, Irie et al. 2007), and chitosan is also known to have very good wound healing properties (Sivashankari and Prabakaran 2016).

Marrow-stimulation alone for cartilage repair does not produce hyaline-like repair cartilage, partly because the blood clot in the lesion retracts to a smaller percentage of its original volume via platelet-mediated clot retraction mechanisms (Morgenstern, Ruf et al. 1990, White 2000). Our laboratory had the idea several years ago that stabilizing the blood clot formed in the cartilage lesion could potentially improve cartilage repair by providing a suitable environment for migration of progenitor cells and formation of new repair tissue. This gave rise to the concept of mixing solubilized CS, which is thrombogenic and has wound healing properties, with autologous blood to produce injectable implants. Incorporation of chitosan stabilizes blood clots by creating an adherent clot capable of resisting clot retraction mechanisms (Chevrier, Hoemann et al. 2007, Hoemann, Sun et al. 2007, Marchand, Rivard et al. 2009). Near-neutral solutions of

chitosan-GP (Chenite, Chaput et al. 2000) can be mixed with whole blood and injected over surgically prepared cartilage defects where they solidify *in situ* (Hoemann, Hurtig et al. 2005, Hoemann, Sun et al. 2007). Blood clots release various chemotactic factors, clots contain fibrin which permits integrin-based cell attachment and migration, and erythrocytes hemolyze after 3 days (Chevrier, Hoemann et al. 2007), leaving porous channels that allow cellular migration (Hoemann and Fong 2017). CS-GP/blood implants induced several significant modifications in the healing sequence at early time points in microdrilled cartilage defects of skeletally mature NZW rabbits. Mingling of CS particles with blood clot in CS-GP/blood implants promoted neutrophil and mesenchymal stem cell recruitment and transient vascularity, and increased remodeling of the subchondral bone, leading to better repair tissue integration (Chevrier, Hoemann et al. 2007, Hoemann, Sun et al. 2007, Chen, Sun et al. 2011). The hyaline quality of the repair tissue, as well as the integration of repair cartilage was improved within the lesion (Chevrier, Hoemann et al. 2007, Hoemann, Sun et al. 2007). CS-GP/blood implants also promoted macrophage polarization towards a pro-wound healing alternatively activated phenotype, labeled M2 (Hoemann, Chen et al. 2010, Chen, Sun et al. 2011). Macrophages have a phenotypic plasticity, which is also called macrophage polarization; in which they adopt different phenotypes either M1 or M2 (Mosser and Edwards 2008). M1 macrophages produce reactive oxygen species and secrete pro-inflammatory factors. M2 macrophages secrete high levels of anti-inflammatory factors and express low levels of pro-inflammatory mediators. Chitosan-GP/blood implants were also tested in sheep with microfractured condylar and trochlear defects, where the implants were shown to increase volume of repair tissues and increase hyaline character, GAG and collagen content, while decreasing the incidence of cyst formation (Hoemann, Hurtig et al. 2005).

In follow-up studies, thrombin was added to CS-GP/blood implants to accelerate solidification *in situ* (Marchand, Rivard et al. 2009, Marchand, Chen et al. 2011). Treatment with the implants improved structural integrity and integration of the repair tissue at 6 months and led to a higher hyaline quality of the repair tissue (Marchand, Chen et al. 2011). CS-GP/blood implants used in conjunction with coagulation factors also promoted large blood vessel formation in healing microdrill holes, particularly after residual CS particles were cleared (Mathieu, Chevrier et al. 2013).

Finally, in the latest studies, isotonic solutions of chitosan were mixed with whole blood and allowed to solidify prior to implantation into microdrill holes (Lafantaisie-Favreau, Guzman-Morales et al. 2013, Guzman-Morales, Lafantaisie-Favreau et al. 2014). Pre-solidified implants attracted neutrophils, osteoclasts and abundant bone marrow-derived stromal cells, which stimulated bone resorption followed by new woven bone repair and remodeling and promoted repair tissue-bone integration. Chitosan molar mass was found to affect healing. Implants containing CS of 150kDa degraded less quickly and induced more apoptotic neutrophils and bone resorption than other CS implants with lower molar mass (40 kDa or 10 kDa).

Chitosan-GP/blood implants were also tested in a randomized controlled trial of 80 patients with focal lesions on femoral condyles. Treatment was either microfracture augmented with chitosan-GP/blood implants (BST-CarGel, now from Smith and Nephew) or microfracture alone (Stanish, McCormack et al. 2013). At twelve months, tissue repair quantity and quality was superior for patients treated with BST-CarGel. The group showed significantly greater lesion filling and a more hyaline-like cartilage (Stanish, McCormack et al. 2013). At an average of 13 months, 21 out of 41 BST-CarGel treated patients and 17 of the 39 microfracture patients underwent elective second look arthroscopies during which osteochondral biopsies were collected. BST-CarGel group had better international cartilage repair society macroscopic score, the light microscopy showed better filling, integration, and tissue appearance. BST-CarGel group had significantly better structural parameters, surface architecture and better organization of the repair tissue, with collagen stratification similar to hyaline cartilage (Méthot, Changoor et al. 2015). The same randomized controlled trial was extended to 5 years. Patients were clinically assessed with MRI to quantify the degree of lesion filling, T2 relaxation time and with the Western Ontario and McMaster Universities Osteoarthritis index subscale. Patients treated with BST-CarGel showed greater lesion filling, greater repair tissue T2 relaxation time and superior tissue quantity and quality over 5 years compared to microfracture alone. Using chitosan-GP with uncoagulated whole blood reinforces blood clot, inhibits retraction, increases cell adhesion and prolongs residency of tissue repair factors found in the blood (Shive, Stanish et al. 2015 ). BST-CarGel is currently commercialized in several countries.

## 2.8.2 Rationale for using chitosan-PRP hybrids in rotator cuff repair

Our laboratory has recently implemented the use of PRP combined with freeze-dried chitosan formulations to form injectable implants for tissue repair applications (Chevrier, Darras et al. 2017). One drawback of the original BST-CarGel technology is that chitosan hydrolyzes over time, which leads to a loss of product viscosity (Varum, Ottoy et al. 2001). In addition, the chitosan and glycerolphosphate solutions must be stored in separate containers to prevent a solution to gel transition that occurs over time (Lavertu, Filion et al. 2008). One way to overcome these limitations is to lyophilize or freeze-dry the chitosan formulation. The use of platelet-rich plasma (PRP) instead of whole blood would be expected to enhance the implants' bioactivity due to the presence of high levels of platelet-derived growth factors. PRP releases growth factors that are important for tissue repair, regeneration and play vital roles as essential signalling molecules to initiate specific cell response in biological environment (Lee, Silva et al. 2011). PRP increases endothelial, epithelial, epidermal regeneration, collagen, soft tissue healing, hemostatic reponse to injury, and decreases dermal scarring (Mohammadi, Mehrtash et al. 2016). However, PRP diffuses very rapidly while quickly releasing its GFs (Busilacchi, Gigante et al. 2013), mitigating its effects and efficacy. Chitosan can be used as a stimulant for platelet activation with PRP treatment, since platelets are activated by physical or chemical stimuli, like CS (Zucker and Nachmias 1985, Kroll, Hellums et al. 1996, Li, Delaney et al. 2010, Brown, Narayanan et al. 2013) (Hattori and Ishihara 2016). Therefore CS could increase PRP treatment efficacy (Oktay, Demiralp et al. 2010, Busilacchi, Gigante et al. 2013, Kutlu, Aydin et al. 2013).

Initially, we systematically modified the chitosan molar mass and concentration, as well as lyoprotectant concentration in order to identify compositions that would rapidly (<1 minute) and completely solubilize in PRP, have paste-like handling properties upon solubilization and coagulate rapidly (<5 minutes) to form solid chitosan-PRP hybrid implants that are stable and homogenous (Chevrier, Darras et al. 2017). Chitosan-PRP implants were also shown to reside for at least 14 days *in vivo* and enhance cell recruitment to surrounding tissues compared to PRP alone (Chevrier, Darras et al. 2017). These chitosan-PRP implants were tested in a meniscus repair model where they were found to increase cell recruitment, vascularisation, remodeling and repair tissue integration compared to injection of PRP alone or wrapping with a collagen membrane (Chevrier, Deprés-Tremblay et al. 2015, Ghazi zadeh, Chevrier et al. 2017). Chitosan-



PRP implants were also used in a chronic cartilage repair model in the rabbit where they were shown to improve the quality of the repair tissue and induce bone remodeling (Dwivedi, Chevrier et al. 2017). All of the above would also be expected to have positive effects on rotator cuff tear repair, which triggered the initiation of the current project.

### CHAPTER 3 ORGANIZATION OF ARTICLES

The scientific contribution made by this thesis is presented here. The first scientific contribution was a literature review on rotator cuff repair. The purpose of the first paper was to review current clinical treatments and pre-clinical approaches for rotator cuff tear repair. The review focused on current clinical surgical treatments, new repair strategies under development both clinically and pre-clinically, and also described different animal models available for rotator cuff research. These findings were then further discussed as well as future directions for rotator cuff tear repair. The paper is entitled “Rotator cuff repair: A review of surgical techniques, animal models and new technologies under development”. Although previous manuscripts have reviewed accepted clinical treatments and pre-clinical models, to our knowledge, this is the first existing manuscript that combines both as well as technologies under development. The paper has been published in “Journal of Shoulder and Elbow Surgery”.

The purpose of the second study was to investigate possible mechanisms by which chitosan inhibits retraction of CS-PRP hybrid clots *in vitro*, characterize the effect of chitosan, trehalose and a combination of both on platelet activation and granule secretion *in vitro*, characterize the release profile of PDGF-AB and EGF from CS-PRP hybrid clots *in vitro*, and histologically assess the residency, bioactivity and biodegradability of CS-PRP implants *in vivo*. The results are presented in the article titled “Chitosan inhibits platelet-mediated clot retraction, increases platelet-derived growth factor release, and increases residence time and bioactivity of platelet-rich plasma *in vivo*”. This study explored the cellular and molecular mechanisms of chitosan-PRP implants both *in vitro* and *in vivo*; focusing on clot retraction, platelet activation and growth factor secretion, the induction of cellular recruitment, vascularization and

biodegradability of the implants. This paper has been submitted to the journal “Biomedical Materials”.

In the third study, chitosan-PRP hybrids were used in conjunction with surgical repair by suturing in a rabbit rotator cuff repair model. The objective was to assess implant retention at early time points post-operative and the histological properties of the repaired cuff at 2 months post-operative. The results are presented in the article titled “Freeze-dried chitosan-PRP implants improve supraspinatus tendon attachment in a transosseous rotator cuff repair in the rabbit”. This paper has been submitted to the “Journal of Orthopaedic Research”.

The purpose of the fourth study was to test whether chitosan-PRP hybrid are capable of improving rotator cuff healing after surgical repair in large animal models. The histological properties and repair responses at the attachment site of the infraspinatus tendon were investigated in delayed and acute repair sheep models. The results are presented in the article titled “Freeze-dried chitosan platelet-rich plasma implants for rotator cuff tear repair: Pilot ovine studies”. This paper has been submitted to the journal “ACS Biomaterials Science and Engineering”, for publication in a special issue entitled “Biomaterials in Canada”.

**CHAPTER 4      ARTICLE 1: ROTATOR CUFF REPAIR: A REVIEW OF  
SURGICAL TECHNIQUES, ANIMAL MODELS AND NEW  
TECHNOLOGIES UNDER DEVELOPMENT**

Journal of Shoulder and Elbow Surgery

Rotator cuff repair: A review of surgical techniques, animal models and new technologies under development

Gabrielle Deprés-Tremblay BSc <sup>1</sup>, Anik Chevrier PhD <sup>2</sup>, Martyn Snow MD <sup>3</sup>, Mark B Hurtig DVM <sup>4</sup>, Scott Rodeo MD <sup>5</sup> and Michael D Buschmann PhD <sup>1,2</sup>

<sup>1</sup>Biomedical Engineering Institute, Polytechnique Montreal, Montreal, QC, Canada, <sup>2</sup>Chemical Engineering Department, Polytechnique Montreal, Montreal, QC, Canada, <sup>3</sup>The Royal Orthopaedic Hospital, Birmingham, UK, <sup>4</sup>Department of Clinical Studies, University of Guelph, and <sup>5</sup>Sports Medicine and Shoulder Service, The Hospital for Special Surgery, New York, NY, USA

**Corresponding author:** Prof Michael D. Buschmann, Department of Chemical Engineering, Polytechnique Montreal, PO Box 6079 Succ Centre-Ville, Montreal, Quebec, Canada, H3C 3A7, Fax: 514 340 2980 Tel: 514 340 4711 ext. 4931, E-mail: michael.buschmann@polymtl.ca

Disclaimer: None.

**Acknowledgements:** This work was supported by the following funding sources: CIHR Operating Grant (MOP 115186) ; Ortho Regenerative Technologies Inc Research Contract.

**Abstract**

Rotator cuff tears are the most common musculoskeletal injury occurring in the shoulder. Current surgical repair fails to heal in 20 to 95% of cases depending on age, size, smoking, time of repair, tendon quality, muscle quality, healing response, and surgical treatments. These problems are worsened by the limited healing potential of injured tendons, attributed to the presence of degenerative changes and relatively poor vascularity of the cuff tendons. Development of new techniques to treat rotator cuff tears also requires testing in animal models to assess safety and efficacy prior to clinical testing. Hence it is important to evaluate appropriate animal models for rotator cuff research with degeneration of tendons, muscular atrophy and fatty infiltration similar to humans. The purpose of this paper is to review current clinical treatments and pre-clinical approaches for rotator cuff tear repair. The review will focus on current clinical surgical treatments, new repair strategies under development both clinically and pre-clinically, and will also describe different animal models available for rotator cuff research. These findings will then be discussed as well as future directions for rotator cuff tear repair.

**Keywords:** Rotator cuff repair, Animal models, Technologies under development

**Level of evidence:** Review article

## 4.1 Introduction

More than 28 million Americans are affected by musculoskeletal injuries, costing more than \$254 billion each year <sup>94</sup>. Rotator cuff injury is the second most common musculoskeletal pathology after lower back pain <sup>93</sup> and the most common shoulder condition for which patients seek therapy <sup>33</sup>. In the United Kingdom, the prevalence of shoulder problems based on consultations in primary care is estimated to be 2.4% <sup>71</sup>. Between 30% and 70% of such shoulder pain is due to disorders of the rotator cuff <sup>84</sup>. More than 17 million Americans may be susceptible for shoulder impairment due to rotator cuff tendon deterioration and eventual tearing <sup>68</sup>.

Cuff tears usually result in shoulder pain, stiffness, weakness and loss of motion. The shoulder joint can still function with minimal pain despite a rotator cuff tear; however, limited function of the upper extremities often impairs the ability to carry out basic activities. Rotator cuff disease may start as an acute tendinopathy with progressive degeneration leading to a partial thickness tear and eventually a complete tear <sup>85</sup>. Large tears result in disuse muscle atrophy with fatty accumulation within muscles, which may irreversibly decrease muscle function <sup>67</sup>. Following rotator cuff repair, failure to heal occurs in 20-95% of cases and has been shown to correlate with tear size, time from injury, tendon quality, fatty atrophy, and surgical repair technique. Degenerative changes in the structure and composition of the tendons make healing very difficult.

The aim of the current review is to describe the current clinical surgical treatments for rotator cuff tears, review the different animal models available for rotator cuff research and summarize new repair approaches that are under development both clinically and in pre-clinical studies. Although previous manuscripts have reviewed accepted clinical treatments and pre-

clinical models, to our knowledge, there is no existing manuscript that combines both as well as technologies under development.

## **4.2 Rotator Cuff Anatomy and Pathology**

The rotator cuff muscles are a group of muscles consisting of the subscapularis, supraspinatus, infraspinatus, and the teres minor<sup>32</sup>. All of these muscles are attached to the head of the humerus via their specific tendons, and control the rotation and position of the arm<sup>32</sup>. The rotator cuff muscles assist shoulder motion but primarily provide stability by centering and pressing the humeral head on the glenoid<sup>32</sup>, through exertion of forces in the coronal and transverse planes<sup>89</sup>. The supraspinatus and the infraspinatus contribute to glenohumeral stability in the resting position while the subscapularis stabilizes the glenohumeral joint in the position of apprehension<sup>32</sup>. Rotator cuff tendons respond to excessive loading by inflammation or degeneration<sup>5</sup>. This is usually manifested by pain, formation of lipids, proteoglycans and sometimes calcified tissues in the tendon lesions, which can lead to the release of various cytokines and adverse changes in cellular activities<sup>69</sup>. Rotator cuff tendon pathology is also influenced by the microvascular supply of rotator cuff tendons<sup>90</sup>.

Traditionally, degenerative rotator cuff tears were thought to begin at the anterior part of the supraspinatus tendon, adjacent to the biceps tendon. The anterior portion was believed to transmit the majority of the contractile load, and since more stress would be applied on a daily basis, this tendon would be at high risk for a tear<sup>83</sup>. However, recent studies suggest that degenerative tears occur about 15 mm posterior to the biceps within the crescent at the junction of supraspinatus and infraspinatus, hence a more posterior location<sup>56</sup>. These tears then propagate

in both anterior and posterior directions <sup>53</sup>. Chronic rotator cuff tears are associated with structural changes such as loss of muscle volume, fatty accumulation, retraction, which all result in muscle remodeling, subtraction of sarcomeres and profound muscle weakness <sup>115</sup>. Progression of a tear may also lead to superior subluxation of the humeral head and eventually, dysfunction of the shoulder. Pathology in rotator cuff tear is also influenced by the microvascular supply of rotator cuff tendons <sup>90</sup>. Rotator cuff tears can also result from an acute trauma, most frequently a fall onto an outstretched arm. Supraspinatus is again the most commonly involved tendon; however, there is a high association with subscapularis tears <sup>76</sup>.

### **4.3 Surgical Treatments of Rotator Cuff Tears**

Non-operative treatments can be used to manage the majority of rotator cuff tears, especially in patients with lower demands. However, rotator cuff tendons do not heal spontaneously and surgical treatments is often required in patients who have persistent symptoms and functional impairment post conservative treatment. Operative treatment of both traumatic and non-traumatic tears can be successful, with some authors reporting better results in younger patients with traumatic tears compared to degenerative tears <sup>9</sup>. Successful results were initially reported with both open repair techniques using deltoid detachment and then subsequently through a “mini-open” deltoid split. Currently, fully arthroscopic procedures are generally considered to be standard of care for the majority of tears. The superiority of arthroscopy versus open or mini-open repair is still unproven and controversial at this point (**Table 1**). Overall, functional outcomes, clinical scores and re-tear rates are similar between arthroscopy versus mini-open repair patients. However, mini-open repair seems to be associated with more post-

operative complications whereas decreased short-term pain is seen with arthroscopic repair. Faster recovery, a quicker return to exercise and better aesthetic results are other potential advantages of arthroscopic repair.

Initially, transosseous tunnels were used to perform open rotator cuff repair. This technique uses sutures placed directly into bone tunnels extending from the rotator cuff footprint, exiting laterally on the tuberosity where they are tied. A limitation of this technique can be bone quality and now, cuff repair is usually performed with suture anchors using different configurations: the single-row, the double-row, and the suture bridge repair, sometimes called the transosseous-equivalent (TOE) repair technique. The goal of using suture anchors is to restore the tendon footprint by suturing the tendon directly onto the tuberosity of the humerus. In controlled laboratory studies using cadaveric shoulders, the superior biomechanical performance of the transosseous-equivalent technique (TOE) over the double row technique and of the double row technique over the single row technique seems clear <sup>21, 55, 77, 105</sup>, but this has not been translated into better clinical or functional outcomes (**Table 2**). The double row repair technique does seem to improve the rate of tendon healing and to decrease re-tear rates over single row, and this could prove to be beneficial in the long-term.

#### **4.4 Animal Models of Rotator Cuff Repair**

Animal models are practical means to understand cellular and molecular pathways and pathology of rotator cuff tears and to develop new technologies to improve existing treatments. Rotator cuff repair animal models should lack spontaneous tendon healing after tendon injury. The tendon size should also allow for suture repair techniques similar to those used in humans.



Ideally, irreversible muscular atrophy, stiffness, and fatty accumulation should be present post-injury<sup>23</sup>. No animal model is identical to human, and each model has its advantages and disadvantages (**Table 3**). A true rotator cuff is defined as the blending of individual flat tendons to form a single insertion. Rabbits, rats, dogs and sheep all have tendons that do not blend before inserting into humeral head; hence they all lack this aspect of the human rotator cuff anatomy<sup>106</sup>.

Rats have the greatest anatomic similarity to humans because of the presence of an acromial arch<sup>23</sup>. However, the acromial arch structure is somewhat different in quadrupeds: the portion of the rat supraspinatus muscle that passes under acromial arch is muscular and not tendinous like in humans<sup>35</sup>. The rat's forward arm elevation is similar to human arm abduction and the range of motion decreases after rotator cuff tears both in rats and in humans<sup>91</sup>. Rotator cuff tears in rats will also result in cartilage degeneration on the humeral head and the glenoid<sup>64</sup>. Although the rat is a reasonable model, it has a few major differences with respect to human. First, rotator cuff tendon heals better in rats than in humans<sup>24,72</sup>. The supraspinatus provides less coverage in rat versus human and most of the coverage is from the subscapularis instead<sup>72</sup>. In addition, the rat supraspinatus lacks the irreversible accumulation of muscular fat and rates of failure of healing ("re-tears") seen in humans, making it less suitable to evaluate repair techniques<sup>24</sup>. In rats, the infraspinatus tendon may be a better model to represent the human supraspinatus, since it undergoes more fat accumulation, muscular atrophy and more muscular retraction<sup>72</sup>. Even with these limitations, the rat is seen as an appropriate and cost-effective model to investigate initial safety, repair mechanisms and efficacy of treatments although its small size makes it challenging to perform surgical repairs<sup>23</sup>.

The rabbit model is mostly used to study muscular changes associated with rotator cuff tears such as muscle atrophy, twitch tension (which is a single contraction in response to a brief threshold stimulation), and fatigue index (which determines energy depletion during exercise) <sup>26</sup>. In rabbit rotator cuff tears, atrophy occurs at early time points and fatty accumulation occurs at later time points as in human <sup>72</sup>. The rotator cuff in rabbits heals in a fashion that is similar to that of humans <sup>41</sup>. The supraspinatus and infraspinatus tendons have both been used as repair models in the rabbit, but recent studies have shown the subscapularis may be a better approximation of human pathology since it passes under an enclosed arch and fatty accumulation is prominent <sup>26</sup>. The subscapularis tendon and the scapular channel are similar in human; both travel beneath the acromion and insert into the greater tuberosity of the humerus <sup>35</sup>. In that aspect, the rabbit's subscapularis may be more comparable to the human supraspinatus. The rabbit is also bigger than the rat, therefore facilitating surgical models and techniques, as larger animals provide greater accuracy and reproducibility <sup>23</sup>.

The sheep infraspinatus is similar in size to the human supraspinatus <sup>26</sup>. Although the sheep infraspinatus is not intra-articular, there is still a bursa under the tendon and repair has some contact with the synovial fluid that lubricates the bursa <sup>108</sup>. Availability, ease of handling and housing, low cost and acceptance to society as a research animal, makes ovine models useful to study rotator cuff repair <sup>108</sup>. Transecting the infraspinatus tendon in sheep and performing an immediate repair does not mimic the human condition; However, acute studies are suitable to assess different repair techniques or biological augmentations <sup>92, 108</sup>. Animals are different than human due to their ability to heal through tissue ingrowth and neovascularisation <sup>108</sup>. In the sheep, once the infraspinatus tendon is cut from its insertion site, scar tissue can bridge the space between the tendon stump and the footprint <sup>108</sup>, although gaps at the tendon-bone interface are

often seen <sup>63, 92</sup>, and the resulting enthesis is usually reported as inferior to normal both histologically and biochemically <sup>73</sup>. In 2003, Coleman et al <sup>20</sup> developed a chronic model by covering the transected tendon end with Gore-Tex, which allowed for nutrient diffusion, to actively stop scar tissue formation around the stump while improving discrimination between tendon and scar tissue <sup>20</sup>. However, in chronic delayed repair, massive tendon retraction can prevent direct reattachment <sup>20</sup>. Turner et al <sup>108</sup> recommended to not exceed a timeframe of 4 weeks for a delayed repair. A different ovine chronic model involves releasing the infraspinatus by osteotomy and covering the bone fragment with a silicon tube <sup>31</sup>. This technique has been used to study muscle atrophy, fatty infiltration and retraction of the musculotendinous unit <sup>80</sup>, but does not approximate the human condition.

## **4.5 Technologies Under Development for Rotator Cuff Repair Augmentation**

### **4.5.1 Extracellular Tendon Patches**

Tendon patches are used as scaffolds for tissue ingrowth and as collagen substitutes, which should increase load to failure and decrease stress shielding compared to injured tissue (**Table 4**). Metcalf et al <sup>79</sup> used Restore, a small intestine submucosa (SIS) scaffold deriving from a porcine source, in 12 patients during arthroscopic procedures. Two years post-surgery, MRI showed thickening and incorporation of the material but shoulder function did not improve <sup>79</sup>. Sclamberg et al <sup>101</sup> used MRI to evaluate 11 patients 6 months post-implantation of Restore and revealed that 10 of 11 repairs had failed. Iannotti et al <sup>45</sup> also tested Restore in human cuff repair and found an increase in pain and inferior tendon healing. Bond et al <sup>8</sup> tested Graftjacket, an

extracellular matrix (ECM) human cadaveric dermis scaffold, during arthroscopic rotator cuff repair in 16 patients. The overhead strength was improved but failure was reported in 3 patients <sup>8</sup>. Burkhead et al <sup>10</sup> showed an increase tissue ingrowth into the Graftjacket patch after two years. Patients with arthroscopic SR repair augmented with Graftjacket had higher ASES (American Shoulder and Elbow Surgeons) and Constant shoulder scores after 24 months <sup>3</sup>. The extracellular matrix patches are used in surgery as augmentation devices but have not shown any benefit in recent randomized controlled clinical trials. Hence, further investigations are needed to prove their efficacy.

#### **4.5.2 Scaffolds**

Poly (D,L-lactide-co-glycolide) (PLGA) scaffolds created by electrospinning were introduced in the infraspinatus of rabbits, after surgically inducing a rotator cuff tear. An increase in bone formation at the scaffold-bone interface and an increase in type II collagen and proteoglycan content were observed. However, no significant difference was seen in ultimate failure load and stiffness between treated and untreated repairs <sup>48</sup>. BMSCs harvested from iliac crest of two rabbits during arthroscopic infraspinatus tear repair were cultured and seeded on poly-L-lactic acid scaffold and the same scaffold without stem cells was used in contralateral shoulders. The scaffold seeded with stem cells showed an increase in collagen type-1 <sup>60</sup>. Yokoya et al <sup>118</sup> used a polyglycolic acid sheet seeded with cultured autologous BMSCs in the repair of infraspinatus lesions in rabbits. After 16 weeks, collagen type-I and the mechanical strength were significantly increased. Silk-collagen scaffolds seeded with tendon stem/progenitor cells (TSPCs) increased collagen content without inducing inflammation in a rabbit rotator cuff injury model

<sup>103</sup>. This preclinical evidence can be used as a step forward in clinical translation. However, acceptable strategies for tendon pathology will require “the ideal” combination of cells and scaffolds to obtain successful outcomes. Currently the best cell/scaffold combination is unknown and concerns exist over future availability due to regulatory constraint and cost considerations.

### 4.5.3 Stem Cells

Bone marrow-derived mesenchymal stem cells (BMSC) failed to improve healing in a rat rotator cuff repair model <sup>36</sup>; however, adenoviral-mediated transduction of syngeneic BM-MSCs with the gene for membrane type-1 matrix metalloproteinase <sup>37</sup> or scleraxis (Ad-Scx) <sup>38</sup> was shown to increase fibrocartilage repair and tendon biomechanical strength. Conversely, transduction with human bone morphogenetic protein-13 (BMP-13) had no effect <sup>39</sup>. Drilling in the greater tuberosity while performing transosseous repair for the supraspinatus led to infiltration of the repaired tendon by BM-MSCs and increased mechanical resistance in a bone marrow chimeric (BMC) rat <sup>54</sup>. Adipose tissue mesenchymal stem cells (AMSC) improved tendon healing in a rotator cuff rabbit repair model <sup>86</sup>. One clinical study harvested bone marrow mononuclear cells (BMMCs) from the iliac crest of 14 patients during transosseous suture repair. These patients had higher UCLA shoulder scores compared to pre-operative and the MRIs showed better tendon integrity <sup>27</sup>, but this study had no control group, rendering conclusions difficult.

Few studies have used bone marrow aspirate concentrate (BMAC), which is usually taken from the iliac crest to augment rotator cuff repair. BMAC is prepared by centrifuging bone marrow aspirate to concentrate the mesenchymal stem cells. Hernigou et al <sup>43</sup> injected iliac crest

bone marrow-derived stem cells aspirated during arthroscopic single-row rotator cuff repair in 45 patients, while another 45 patients underwent arthroscopic SR repair without augmentation. At 6 months, 100% of the augmented-group had healed compared to 67% of the patients without BMAC. MRIs confirmed an increased healing rate and quality of the repaired surface with BMAC injection <sup>43</sup>. Centeno et al reported improved function and pain scores in a multi-site registry study of 102 patients, a subset of which had isolated rotator cuff tears that were treated with injections of bone marrow concentrate also containing platelet-rich plasma and platelet lysate <sup>14</sup>.

Another surgical approach to draw stem cells to the repair tissue is the “crimson duvet” technique. The crimson duvet is a clot issued from bone marrow vents, which are punctured in the greater tuberosity during rotator cuff repair. The perforation has to reach the cancellous bone, letting the bone marrow flow out. Microfracture of the greater tuberosity was used in two clinical trials <sup>82, 87</sup>, with one reporting greater healing in a subset of patients with larger tears <sup>82</sup>. Uthoff et al <sup>110</sup> argued that releasing BMSC from the greater tuberosity might enhance healing due to the influx of fibroblasts and vessels increasing the healing response.

#### **4.5.4 Growth Factors & Cytokines**

Growth factors can enhance repair and enable tissue regeneration; nevertheless, further clinical investigations are required to establish the proper timing, dosage and the delivery method. PDGF-BB was tested in rat rotator repair cuff model, where the treatment group was found to have collagen-bundle alignment similar to controls <sup>117</sup>. Uggen et al <sup>109</sup> used PDGF-BB-coated sutures to repair sheep infraspinatus tendon, which resulted in improved histological

properties after 6 weeks at the bone-to-tendon repair, but did not change tendon strength. An infraspinatus sheep repair model showed enhanced anatomical appearance and biomechanical strength with a type-1 collagen scaffold loaded with rhPDGF-BB<sup>42</sup>. TGF- $\beta$ 1 and TGF- $\beta$ 3 were used in rat supraspinatus tear repair. The TGF- $\beta$ 1 group had an increase in type III collagen and a scar-mediated repair with poorer mechanical properties. However, the TGF- $\beta$ 3 group showed no difference histologically and biomechanically compared to controls<sup>57</sup>. As of now, there is still no study on rotator cuff repair using growth factors in human.

#### **4.5.5 Platelet-rich plasma**

Platelet-rich plasma (PRP) has gained popularity in sports medicine and orthopaedics but its efficacy in rotator cuff tear repair is still unclear. To obtain PRP, a small amount of the patient's own blood is spun through a centrifugation process to concentrate the platelets. Several different types of PRP have been used in an attempt to augment repair. PRP can be applied as a liquid (with or without calcium-based activation prior to application) or can be implanted as a solid matrix, in which case it is called platelet-rich fibrin (PRF). PRF differs from PRP, where blood is collected without the use of any anticoagulant and is immediately centrifuged. In addition, the method of isolation will determine whether the PRP or the PRF contains leukocytes or not (leukocyte-PRP/PRF or pure-PRP/PRF), the benefits of which are currently unknown. Platelets release growth factors from the  $\alpha$ -granules and the dense granules, which contain many different cytokines and bioactive factors that have a chemotactic paracrine role, which regulates inflammation, angiogenesis, matrix synthesis, and remodeling of tissues. It has been postulated that PRP will improve tendon healing by increasing the concentration of growth factors and by

promoting revascularization of surrounding tissues; however, results have been inconsistent in clinical trials so far.

Pre-clinical studies investigating PRP for rotator cuff repair are few. Most use the rat model <sup>25, 65</sup>, with a few studies published in rabbits <sup>18, 116</sup>. Some studies showed repair improvement with application of PRP, while others did not.

Clinical data on PRP for rotator cuff repair is more abundant (**Table 5**). Leukocyte-rich PRF has been used as solid implants to attempt cuff repair augmentation by a few groups <sup>1, 121</sup>, but no improvement was reported. Pure-PRF devoid of leukocytes has been used more commonly, with two studies showing lower re-tear rates with P-PRF <sup>4, 13</sup>, one study showing no difference between both groups <sup>114</sup> and conversely, two studies showing more failures with P-PRF <sup>6, 97</sup>. Leukocyte-rich PRP was used in two Level I trials, where it showed no clinical improvement but a lower re-tear rate <sup>95</sup> and better repair integrity <sup>40</sup> compared to the control group. Studies using pure-PRP devoid of leukocytes employed plateletpheresis systems <sup>49-51, 75</sup> or centrifugation methods <sup>98</sup> to isolate the PRP. Four studies showed lower re-tear or partial re-tears in the pure PRP-treated group <sup>49-51, 75</sup>, while one study showed no effect of pure-PRP <sup>98</sup>. Lower re-tear rates may translate into improved clinical scores at longer time points, and in that respect, treatment with PRP might eventually improve cuff repair. It is particularly difficult to assess the efficacy of PRP from the different published studies, since they all vary in platelet count, single-versus double-spin cycles, methods of application, growth factor concentration, leukocyte concentration, platelet activation, surgical repair, and postoperative rehabilitation. The efficacy of PRP remains an open question in orthopedic rotator cuff repair.



#### 4.5.6 Chitin and chitosan

Chitosan is a linear copolymer of  $\beta$  (1 $\rightarrow$ 4) linked D-glucosamine (GlcN) and N-acetylglucosamine (GlcNAc) obtained from crustaceous exoskeleton by alkaline N-deacetylation of chitin. To our knowledge, there have been only a small number of publications using chitin and chitosan in rotator cuff repair. Funakoshi et al used a nonwoven chitin fabric in the infraspinatus of 21 rabbits where they observed an increase in cell number and collagen fiber alignment and enhanced structural and biomechanical properties <sup>29</sup>. Melamed et al <sup>78</sup> found that rotator cuff tear repair augmented with chitosan gel enhanced healing of soft tissues. Chitosan was also shown to improve rotator cuff repair in rats by decreasing muscle fiber fibrosis and by preventing muscle atrophy <sup>96</sup>.

Our laboratory has worked extensively with chitosan-glycerol phosphate (GP)/blood implants for cartilage repair applications. Near neutral solutions of chitosan-GP can be mixed with whole blood and injected over surgically prepared cartilage defects where they solidify in situ and improve marrow-stimulated cartilage repair <sup>44</sup>. We have recently implemented the use of PRP combined with freeze-dried chitosan to form injectable implants for tissue repair applications. Chitosan-PRP implants were shown to reside for at least 14 days *in vivo* and enhance cell recruitment to surrounding tissues compared to PRP alone. These chitosan-PRP implants were tested in a meniscus repair model where they were found to increase cell recruitment, vascularisation, remodeling and repair tissue integration compared to injection of PRP alone <sup>16</sup>. We are currently assessing whether these mechanisms will have similar beneficial effects in the context of rotator cuff repair.

## 4.6 Conclusions

The majority of chronic tendon tears occurs in the supraspinatus and ultimately leads to structural change such as fatty accumulation, loss of volume, muscle remodeling, subtraction of sarcomeres, and sometimes profound muscle weakness. Finding the right animal model is challenging but critically important to improve our understanding of the cellular and molecular pathways involved in rotator cuff pathology. Ultimately, such information is required to improve therapeutic treatment options. However, none of the animals have anatomy comparable to humans. Open versus mini-open or arthroscopy does not seem to have a significant impact on clinical outcomes. Latest generation techniques involve the use of different configuration of sutures. Double-row configuration seems to increase the rate of tendon healing but this has generally not translated into improved clinical and functional outcomes. ECM patches have shown some promising findings in some animal studies, but not in randomized clinical trials. Scaffolds and cells are becoming more popular in tissue engineering as a structural support and a cellular delivery aid but further clinical studies are still needed. Growth factors have been shown to improve healing but there is still no study on rotator cuff repair using growth factors in humans. One strategy would require using the ideal combination of growth factors and scaffold together to complement each other. PRP use in orthopedics is still controversial and under investigation for now, and there is still limited data on its effectiveness. None of these strategies are perfectly suited for rotator cuff tear repair. One possible effective technique could be using chitosan-PRP implants. In summary, several repair strategies are available but further clinical trials are needed to find the optimal treatment for rotator cuff repair.

## Acknowledgements

This work was supported by the following funding sources: CIHR Operating Grant (MOP 115186); Ortho Regenerative Technologies Inc Research Contract.

## References:

- 1 Antuna S, Barco R, Martinez Diez JM, Sanchez Marquez JM. Platelet-rich fibrin in arthroscopic repair of massive rotator cuff tears : A prospective randomized pilot clinical trial. *Acta Orthopaedica Belgica* 2013;79:25-30.
- 2 Aydin N, Kocaoglu B, Guven O. Single-row versus double-row arthroscopic rotator cuff repair in small- to medium-sized tears. *Journal of Shoulder and Elbow Surgery* 2010;19:722-725. 10.1016/j.jse.2009.11.053
- 3 Barber FA, Burns JP, Deutsch A, Labbe MR, Litchfield RB. A prospective, randomized evaluation of acellular human dermal matrix augmentation for arthroscopic rotator cuff repair. *Arthroscopy* 2012;28:8-15. 10.1016/j.arthro.2011.06.038
- 4 Barber FA, Hrnack SA, Snyder SJ, Hapa O. Rotator cuff repair healing influenced by platelet-rich plasma construct augmentation. *Arthroscopy* 2011;27:1029-1035. 10.1016/j.arthro.2011.06.010
- 5 Benazzo F, Zanon G, Maffulli N. An Operative Approach to Achilles Tendinopathy. *Sports Medicine and Arthroscopy Review* 2000;8:96-101.

- 6 Bergeson AG, Tashjian RZ, Greis PE, Crim J, Stoddard GJ, Burks RT. Effects of platelet-rich fibrin matrix on repair integrity of at-risk rotator cuff tears. *The American Journal of Sports Medicine* 2012;40:286-293. 10.1177/0363546511424402
- 7 Bishop J, Klepps S, Lo IK, Bird J, Gladstone JN, Flatow EL. Cuff integrity after arthroscopic versus open rotator cuff repair: A prospective study. *Journal of Shoulder and Elbow Surgery* 2006;15:290-299. 10.1016/j.jse.2005.09.017
- 8 Bond JL, Dopirak RM, Higgins J, Burns J, Snyder SJ. Arthroscopic replacement of massive, irreparable rotator cuff tears using a GraftJacket allograft: technique and preliminary results. *Arthroscopy* 2008;24:403-409.e401. 10.1016/j.arthro.2007.07.033
- 9 Braune C, von Eisenhart-Rothe R, Welsch F, Teufel M, Jaeger A. Mid-term results and quantitative comparison of postoperative shoulder function in traumatic and non-traumatic rotator cuff tears. *Archives of Orthopaedic and Trauma Surgery* 2003;123:419-424. 10.1007/s00402-003-0548-2
- 10 Burkhead Jr WZ, Schiffen SC, Krishnan SG. Use of graft jacket as an augmentation for massive rotator cuff tears. *Semin Arthroplasty* 2007;18:11-18.
- 11 Burks RT, Crim J, Brown N, Fink B, Greis PE. A prospective randomized clinical trial comparing arthroscopic single- and double-row rotator cuff repair: magnetic resonance imaging and early clinical evaluation. *The American Journal of Sports Medicine* 2009;37:674-682. 10.1177/0363546508328115
- 12 Carbonel I, Martinez AA, Calvo A, Ripalda J, Herrera A. Single-row versus double-row arthroscopic repair in the treatment of rotator cuff tears: a prospective randomized clinical study. *International Orthopaedics* 2012;36:1877-1883. 10.1007/s00264-012-1559-9

- 13 Castricini R, Longo UG, De Benedetto M, Panfoli N, Pirani P, Zini R et al. Platelet-Rich Plasma Augmentation for Arthroscopic Rotator Cuff Repair A Randomized Controlled Trial. *The American Journal of Sports Medicine* 2011;39:258-265. 10.1177/0363546510390780
- 14 Centeno CJ, Al-Sayegh H, Bashir J, Goodyear S, Freeman MD. A prospective multi-site registry study of a specific protocol of autologous bone marrow concentrate for the treatment of shoulder rotator cuff tears and osteoarthritis. *Journal of Pain Research* 2015;8:269-276. 10.2147/jpr.s80872
- 15 Charousset C, Grimberg J, Duranthon LD, Bellaiche L, Petrover D. Can a double-row anchorage technique improve tendon healing in arthroscopic rotator cuff repair?: A prospective, nonrandomized, comparative study of double-row and single-row anchorage techniques with computed tomographic arthrography tendon healing assessment. *The American Journal of Sports Medicine* 2007;35:1247-1253. 10.1177/0363546507301661
- 16 Chevrier A, Déprés-Tremblay G, Nelea M, Hurtig MB, Buschmann MD. Chitosan-platelet-rich plasma implants have in situ tissue building capacity and can be injected into meniscus defects to improve repair. *Transactions International Cartilage Repair Society* 2015;Chicago, USA.
- 17 Cho CH, Song KS, Jung GH, Lee YK, Shin HK. Early postoperative outcomes between arthroscopic and mini-open repair for rotator cuff tears. *Orthopedics* 2012;35:e1347-e1352. 10.3928/01477447-20120822-20

- 18 Chung SW, Song BW, Kim YH, Park KU, Oh JH. Effect of platelet-rich plasma and porcine dermal collagen graft augmentation for rotator cuff healing in a rabbit model. *The American Journal of Sports Medicine* 2013;41:2909-2918. 10.1177/0363546513503810
- 19 Colegate-Stone T, Allom R, Tavakkolizadeh A, Sinha J. An analysis of outcome of arthroscopic versus mini-open rotator cuff repair using subjective and objective scoring tools. *Knee Surgery, Sports Traumatology, Arthroscopy* 2009;17:691-694. 10.1007/s00167-008-0661-4
- 20 Coleman SH, Fealy S, Ehteshami JR, MacGillivray JD, Altchek DW, Warren RF et al. Chronic rotator cuff injury and repair model in sheep. *Journal of Bone and Joint Surgery-American Volume* 2003;85A:2391-2402.
- 21 Costic RS BP, Smolinski PJ, Gilbertson LG, Rodosky MW. Arthroscopic double row anchor repair of full thickness rotator cuff tear: Footprint restoration and biomechanical properties. *Transactions Orthopaedic Research Society, Chicago, IL* 2006.
- 22 Denard PJ, Jiwani AZ, Laedermann A, Burkhart SS. Long-Term Outcome of Arthroscopic Massive Rotator Cuff Repair: The Importance of Double-Row Fixation. *Arthroscopy* 2012;28:909-915. 10.1016/j.arthro.2011.12.007
- 23 Derwin KA, Baker AR, Codsì MJ, Iannotti JP. Assessment of the canine model of rotator cuff injury and repair. *Journal of Shoulder and Elbow Surgery* 2007;16:140S-148S. 10.1016/j.ise.2007.04.002
- 24 Derwin KA, Baker AR, Iannotti JP, McCarron JA. Preclinical Models for Translating Regenerative Medicine Therapies for Rotator Cuff Repair. *Tissue Engineering Part B-Reviews* 2010;16:21-30. 10.1089/ten.teb.2009.0209

- 25 Dolkart O, Chechik O, Zarfati Y, Brosh T, Alhajajra F, Maman E. A single dose of platelet-rich plasma improves the organization and strength of a surgically repaired rotator cuff tendon in rats. *Archives of Orthopaedic and Trauma Surgery* 2014;134:1271-1277. 10.1007/s00402-014-2026-4
- 26 Edelstein L, Thomas SJ, Soslowsky LJ. Rotator Cuff Tears: What have we learned from animal models? *Journal of Musculoskeletal & Neuronal Interactions* 2011;11:150-162.
- 27 Ellera Gomes JL, da Silva RC, Silla LM, Abreu MR, Pellanda R. Conventional rotator cuff repair complemented by the aid of mononuclear autologous stem cells. *Knee Surgery, Sports Traumatology, Arthroscopy* 2012;20:373-377. 10.1007/s00167-011-1607-9
- 28 Franceschi F, Ruzzini L, Longo UG, Martina FM, Zobel BB, Maffulli N et al. Equivalent clinical results of arthroscopic single-row and double-row suture anchor repair for rotator cuff tears: a randomized controlled trial. *The American Journal of Sports Medicine* 2007;35:1254-1260. 10.1177/0363546507302218
- 29 Funakoshi T, Majima T, Suenaga N, Iwasaki N, Yamane S, Minami A. Rotator cuff regeneration using chitin fabric as an acellular matrix. *Journal of Shoulder and Elbow Surgery* 2006;15:112-118. 10.1016/j.jse.2005.05.012
- 30 Gartsman GM, Drake G, Edwards TB, Elkousy HA, Hammerman SM, O'Connor DP et al. Ultrasound evaluation of arthroscopic full-thickness supraspinatus rotator cuff repair: single-row versus double-row suture bridge (transosseous equivalent) fixation. Results of a prospective, randomized study. *Journal of Shoulder and Elbow Surgery* 2013;22:1480-1487. 10.1016/j.jse.2013.06.020

- 31 Gerber C, Meyer DC, Schneeberger AG, Hoppeler H, Von Rechenberg B. Effect of tendon release and delayed repair on the structure of the muscles of the rotator cuff: An experimental study in sheep. *Journal of Bone and Joint Surgery-American Volume* 2004;86A:1973-1982.
- 32 Giovanni Di Giacomo NP, Alberto Costantini , Andrea De Vita. *Atlas of Functional Shoulder Anatomy*. Rome, Italy: Springer; 2008. (ISBN No. 978-88-470-0758-1)
- 33 Gomoll AH, Katz JN, Warner JJ, Millett PJ. Rotator cuff disorders: recognition and management among patients with shoulder pain. *Arthritis and Rheumatism* 2004;50:3751-3761. 10.1002/art.20668
- 34 Grasso A, Milano G, Salvatore M, Falcone G, Deriu L, Fabbriani C. Single-Row Versus Double-Row Arthroscopic Rotator Cuff Repair: A Prospective Randomized Clinical Study. *Arthroscopy* 2009;25:4-12. 10.1016/j.arthro.2008.09.018
- 35 Grumet RC, Hadley S, Diltz MV, Lee TQ, Gupta R. Development of a new model for rotator cuff pathology: the rabbit subscapularis muscle. *Acta Orthopaedica* 2009;80:97-103. 10.1080/17453670902807425
- 36 Gulotta LV, Kovacevic D, Ehteshami JR, Dagher E, Packer JD, Rodeo SA. Application of bone marrow-derived mesenchymal stem cells in a rotator cuff repair model. *The American Journal of Sports Medicine* 2009;37:2126-2133. 10.1177/0363546509339582
- 37 Gulotta LV, Kovacevic D, Montgomery S, Ehteshami JR, Packer JD, Rodeo SA. Stem cells genetically modified with the developmental gene MT1-MMP improve regeneration of the supraspinatus tendon-to-bone insertion site. *The American Journal of Sports Medicine* 2010;38:1429-1437. 10.1177/0363546510361235



- 38 Gulotta LV, Kovacevic D, Packer JD, Deng XH, Rodeo SA. Bone marrow-derived mesenchymal stem cells transduced with scleraxis improve rotator cuff healing in a rat model. *The American Journal of Sports Medicine* 2011;39:1282-1289. 10.1177/0363546510395485
- 39 Gulotta LV, Kovacevic D, Packer JD, Ehteshami JR, Rodeo SA. Adenoviral-mediated gene transfer of human bone morphogenetic protein-13 does not improve rotator cuff healing in a rat model. *The American Journal of Sports Medicine* 2011;39:180-187. 10.1177/0363546510379339
- 40 Gumina S, Campagna V, Ferrazza G, Giannicola G, Fratalocchi F, Milani A et al. Use of platelet-leukocyte membrane in arthroscopic repair of large rotator cuff tears: a prospective randomized study. *The Journal of Bone and Joint Surgery-American volume* 2012;94:1345-1352. 10.2106/jbjs.k.00394
- 41 Gupta R, Lee TQ. Contributions of the different rabbit models to our understanding of rotator cuff pathology. *Journal of Shoulder and Elbow Surgery* 2007;16:149S-157S. 10.1016/j.jse.2007.05.002
- 42 Hee CK, Dines JS, Dines DM, Roden CM, Wisner-Lynch LA, Turner AS et al. Augmentation of a rotator cuff suture repair using rhPDGF-BB and a type I bovine collagen matrix in an ovine model. *The American Journal of Sports Medicine* 2011;39:1630-1639. 10.1177/0363546511404942
- 43 Hernigou P, Flouzat Lachaniette CH, Delambre J, Zilber S, Duffiet P, Chevallier N et al. Biologic augmentation of rotator cuff repair with mesenchymal stem cells during

- arthroscopy improves healing and prevents further tears: a case-controlled study. *International Orthopaedics* 2014;38:1811-1818. 10.1007/s00264-014-2391-1
- 44 Hoemann CD, Hurtig M, Rossomacha E, Sun J, Chevrier A, Shive M et al. Chitosan-glycerol phosphate/blood implants improve hyaline cartilage repair in ovine microfracture defects. *Journal of Bone and Joint Surgery-American Volume* 2005;87A:2671-2686. 10.2106/JBJS.D.02536
- 45 Iannotti JP, Codsi MJ, Kwon YW, Derwin K, Ciccone J, Brems JJ. Porcine small intestine submucosa augmentation of surgical repair of chronic two-tendon rotator cuff tears. A randomized, controlled trial. *The Journal of Bone and Joint Surgery-American Volume* 2006;88:1238-1244. 10.2106/jbjs.e.00524
- 46 Ide J, Karasugi T, Okamoto N, Taniwaki T, Oka K, Mizuta H. Functional and structural comparisons of the arthroscopic knotless double-row suture bridge and single-row repair for anterosuperior rotator cuff tears. *Journal of Shoulder and Elbow Surgery* 2015;24:1544-1554. 10.1016/j.jse.2015.03.015
- 47 Ide J, Maeda S, Takagi K. A comparison of arthroscopic and open rotator cuff repair. *Arthroscopy* 2005;21:1090-1098. 10.1016/j.arthro.2005.05.010
- 48 Inui A, Kokubu T, Mifune Y, Sakata R, Nishimoto H, Nishida K et al. Regeneration of rotator cuff tear using electrospun poly(d,l-Lactide-Co-Glycolide) scaffolds in a rabbit model. *Arthroscopy* 2012;28:1790-1799. 10.1016/j.arthro.2012.05.887
- 49 Jo CH, Kim JE, Yoon KS, Lee JH, Kang SB, Lee JH et al. Does Platelet-Rich Plasma Accelerate Recovery After Rotator Cuff Repair? A Prospective Cohort Study. *The American Journal of Sports Medicine* 2011;39:2082-2090. 10.1177/0363546511413454

- 50 Jo CH, Shin JS, Lee YG, Shin WH, Kim H, Lee SY et al. Platelet-Rich Plasma for Arthroscopic Repair of Large to Massive Rotator Cuff Tears A Randomized, Single-Blind, Parallel-Group Trial. *The American Journal of Sports Medicine* 2013;41:2240-2248. 10.1177/0363546513497925
- 51 Jo CH, Shin JS, Shin WH, Lee SY, Yoon KS, Shin S. Platelet-Rich Plasma for Arthroscopic Repair of Medium to Large Rotator Cuff Tears: A Randomized Controlled Trial. *The American Journal of Sports Medicine* 2015;43:2102--2110. 10.1177/0363546515587081
- 52 Kasten P, Keil C, Grieser T, Raiss P, Streich N, Loew M. Prospective randomised comparison of arthroscopic versus mini-open rotator cuff repair of the supraspinatus tendon. *International Orthopaedics* 2011;35:1663-1670. 10.1007/s00264-011-1262-2
- 53 Keener JD, Galatz LM, Teefey SA, Middleton WD, Steger-May K, Stobbs-Cucchi G et al. A Prospective Evaluation of Survivorship of Asymptomatic Degenerative Rotator Cuff Tears. *Journal of Bone and Joint Surgery-American Volume* 2015b;97A:89-98. 10.2106/jbjs.n.00099
- 54 Kida Y, Morihara T, Matsuda K, Kajikawa Y, Tachiiri H, Iwata Y et al. Bone marrow-derived cells from the footprint infiltrate into the repaired rotator cuff. *Journal of Shoulder and Elbow Surgery* 2013;22:197-205. 10.1016/j.jse.2012.02.007
- 55 Kim DH, Elattrache NS, Tibone JE, Jun BJ, DeLaMora SN, Kvitne RS et al. Biomechanical comparison of a single-row versus double-row suture anchor technique for rotator cuff repair. *The American Journal of Sports Medicine* 2006;34:407-414. 10.1177/0363546505281238

- 56 Kim HM, Dahiya N, Teefey SA, Middleton WD, Stobbs G, Steger-May K et al. Location and initiation of degenerative rotator cuff tears: an analysis of three hundred and sixty shoulders. *The Journal of Bone and Joint Surgery-American Volume* 2010;92:1088-1096. 10.2106/jbjs.i.00686
- 57 Kim HM, Galatz LM, Das R, Havlioglu N, Rothermich SY, Thomopoulos S. The role of transforming growth factor beta isoforms in tendon-to-bone healing. *Connective Tissue Research* 2011;52:87-98. 10.3109/03008207.2010.483026
- 58 Kim KC, Shin HD, Lee WY, Han SC. Repair Integrity and Functional Outcome After Arthroscopic Rotator Cuff Repair Double-Row Versus Suture-Bridge Technique. *The American Journal of Sports Medicine* 2012;40:294-299. 10.1177/0363546511425657
- 59 Kim SH, Ha KI, Park JH, Kang JS, Oh SK, Oh I. Arthroscopic versus mini-open salvage repair of the rotator cuff tear: Outcome analysis at 2 to 6 years' follow-up. *Arthroscopy* 2003;19:746-754. 10.1016/s0749-8063(03)00395-5
- 60 Kim YS, Lee HJ, Ok JH, Park JS, Kim DW. Survivorship of implanted bone marrow-derived mesenchymal stem cells in acute rotator cuff tear. *Journal of Shoulder and Elbow Surgery* 2013;22:1037-1045. 10.1016/j.jse.2012.11.005
- 61 Koh KH, Kang KC, Lim TK, Shon MS, Yoo JC. Prospective Randomized Clinical Trial of Single-Versus Double-Row Suture Anchor Repair in 2-to 4-cm Rotator Cuff Tears: Clinical and Magnetic Resonance Imaging Results. *Arthroscopy* 2011;27:453-462. 10.1016/j.arthro.2010.11.059

- 62 Kose KC, Tezen E, Cebesoy O, Karadeniz E, Guner D, Adiyaman S et al. Mini-open versus all-arthroscopic rotator cuff repair: comparison of the operative costs and the clinical outcomes. *Advances in Therapy* 2008;25:249-259. 10.1007/s12325-008-0031-0
- 63 Kovacevic D, Rodeo SA. Biological augmentation of rotator cuff tendon repair. *Clinical Orthopaedics and Related Research* 2008;466:622-633. 10.1007/s11999-007-0112-4
- 64 Kramer EJ, Bodendorfer BM, Laron D, Wong J, Kim HT, Liu X et al. Evaluation of cartilage degeneration in a rat model of rotator cuff tear arthropathy. *Journal of Shoulder and Elbow Surgery* 2013;22:1702-1709. 10.1016/j.jse.2013.03.014
- 65 Lamplot JD, Angeline M, Angeles J, Beederman M, Wagner E, Rastegar F et al. Distinct effects of platelet-rich plasma and BMP13 on rotator cuff tendon injury healing in a rat model. *The American Journal of Sports Medicine* 2014;42:2877-2887. 10.1177/0363546514547171
- 66 Lapner PL, Sabri E, Rakhra K, McRae S, Leiter J, Bell K et al. A multicenter randomized controlled trial comparing single-row with double-row fixation in arthroscopic rotator cuff repair. *The Journal of Bone and Joint Surgery-American Volume* 2012;94:1249-1257. 10.2106/jbjs.k.00999
- 67 Laron D, Samagh SP, Liu X, Kim HT, Feeley BT. Muscle degeneration in rotator cuff tears. *Journal of Shoulder and Elbow Surgery* 2012;21:164-174. 10.1016/j.jse.2011.09.027
- 68 Lashgari CJ, Yamaguchi K. Natural history and nonsurgical treatment of rotator cuff disorders. In: Norris TR, editor. *Orthopaedic knowledge update 2: shoulder and elbow*. Rosemont, IL, USA: AAOS; 2002. p. 155-162.

- 69 Leadbetter WB. Cell-matrix response in tendon injury. *Clinics in Sports Medicine* 1992;11:533-578.
- 70 Liem D, Bartl C, Lichtenberg S, Magosch P, Habermeyer P. Clinical outcome and tendon integrity of arthroscopic versus mini-open supraspinatus tendon repair: A magnetic resonance imaging-controlled matched-pair analysis. *Arthroscopy* 2007;23:514-521. 10.1016/j.arthro.2006.12.028
- 71 Linsell L, Dawson J, Zondervan K, Rose P, Randall T, Fitzpatrick R et al. Prevalence and incidence of adults consulting for shoulder conditions in UK primary care; patterns of diagnosis and referral. *Rheumatology (Oxford, England)* 2006;45:215-221. 10.1093/rheumatology/kei139
- 72 Liu X, Manzano G, Kim HT, Feeley BT. A Rat Model of Massive Rotator Cuff Tears. *Journal of Orthopaedic Research* 2011;29:588-595. 10.1002/jor.21266
- 73 Luan T, Liu X, Easley JT, Ravishankar B, Puttlitz C, Feeley BT. Muscle atrophy and fatty infiltration after an acute rotator cuff repair in a sheep model. *Muscles, Ligaments and Tendons Journal* 2015;5:106-112.
- 74 Ma H-L, Chiang E-R, Wu H-TH, Hung S-C, Wang S-T, Liu C-L et al. Clinical Outcome and Imaging of Arthroscopic Single-Row and Double-Row Rotator Cuff Repair: A Prospective Randomized Trial. *Arthroscopy* 2012;28:16-24. 10.1016/j.arthro.2011.07.003
- 75 Malavolta EA, Conforto Gracitelli ME, Ferreira Neto AA, Henrique Assuncao J, Bordalo-Rodrigues M, de Camargo OP. Platelet-Rich Plasma in Rotator Cuff Repair A Prospective Randomized Study. *The American Journal of Sports Medicine* 2014;42:2446-2454. 10.1177/0363546514541777

- 76 Mall NA, Lee AS, Chahal J, Sherman SL, Romeo AA, Verma NN et al. An Evidenced-Based Examination of the Epidemiology and Outcomes of Traumatic Rotator Cuff Tears. *Arthroscopy* 2013;29:366-376. 10.1016/j.arthro.2012.06.024
- 77 Mazzocca AD, Millett PJ, Guanche CA, Santangelo SA, Arciero RA. Arthroscopic single-row versus double-row suture anchor rotator cuff repair. *The American Journal of Sports Medicine* 2005;33:1861-1868. 10.1177/0363546505279575
- 78 Melamed E, Beutel BG, Robinson D. Enhancement of acute tendon repair using chitosan matrix. *American Journal of Orthopedics (Belle Mead, NJ)* 2015;44:212-216.
- 79 Metcalf MH SF, III, Kelluzrm B. Surgical technique for xenograft (SIS) augmentation of rotator-cuff repairs. *Oper Tech Orthop* 2002:204–208.
- 80 Meyer DC, Hoppeler H, von Rechenberg B, Gerber C. A pathomechanical concept explains muscle loss and fatty muscular changes following surgical tendon release. *Journal of Orthopaedic Research* 2004;22:1004-1007. 10.1016/j.orthres.2004.02.009
- 81 Mihata T, Watanabe C, Fukunishi K, Ohue M, Tsujimura T, Fujiwara K et al. Functional and structural outcomes of single-row versus double-row versus combined double-row and suture-bridge repair for rotator cuff tears. *The American Journal of Sports Medicine* 2011;39:2091-2098. 10.1177/0363546511415660
- 82 Milano G, Saccomanno MF, Careri S, Taccardo G, De Vitis R, Fabbriciani C. Efficacy of marrow-stimulating technique in arthroscopic rotator cuff repair: a prospective randomized study. *Arthroscopy* 2013;29:802-810. 10.1016/j.arthro.2013.01.019

- 83 Minagawa H, Itoi E, Sato T, Konno N, Hongo M, Sato K. Morphology of the transitional zone of intramuscular to extramuscular tendons of the rotator cuff. *Journal of Shoulder and Elbow Surgery* 1996;5:S127. 10.1016/S1058-2746(96)80529-5
- 84 Mitchell C, Adebajo A, Hay E, Carr A. Shoulder pain: diagnosis and management in primary care. *BMJ (Clinical research ed)* 2005;331:1124-1128. 10.1136/bmj.331.7525.1124
- 85 Neer CS, 2nd, Craig EV, Fukuda H. Cuff-tear arthropathy. *The Journal of Bone and Joint Surgery-American Volume* 1983;65:1232-1244.
- 86 Oh JH, Chung SW, Kim SH, Chung JY, Kim JY. 2013 Neer Award: Effect of the adipose-derived stem cell for the improvement of fatty degeneration and rotator cuff healing in rabbit model. *Journal of Shoulder and Elbow Surgery* 2014;23:445-455. 10.1016/j.jse.2013.07.054
- 87 Osti L, Del Buono A, Maffulli N. Microfractures at the rotator cuff footprint: a randomised controlled study. *International Orthopaedics* 2013;37:2165-2171. 10.1007/s00264-013-1952-z
- 88 Park JY, Lhee SH, Choi JH, Park HK, Yu JW, Seo JB. Comparison of the clinical outcomes of single- and double-row repairs in rotator cuff tears. *The American Journal of Sports Medicine* 2008;36:1310-1316. 10.1177/0363546508315039
- 89 Parsons IM, Apreleva M, Fu FH, Woo SL. The effect of rotator cuff tears on reaction forces at the glenohumeral joint. *Journal of Orthopaedic Research* 2002;20:439-446. 10.1016/s0736-0266(01)00137-1



- 90 Parsons IMI, Apreleva M, Fu FH, Woo SLY. The effect of rotator cuff tears on reaction forces at the glenohumeral joint. *Journal of Orthopaedic Research* 2002;20:439.
- 91 Perry SM, Getz CL, Soslowky LJ. Alterations in function after rotator cuff tears in an animal model. *Journal of Shoulder and Elbow Surgery* 2009;18:296-304. 10.1016/j.jse.2008.10.008
- 92 Peterson DR, Ohashi KL, Aberman HM, Piza PA, Crockett HC, Fernandez JI et al. Evaluation of a collagen-coated, resorbable fiber scaffold loaded with a peptide basic fibroblast growth factor mimetic in a sheep model of rotator cuff repair. *Journal of Shoulder and Elbow Surgery* 2015;24:1764-1773. 10.1016/j.jse.2015.06.009
- 93 Picavet HS, Schouten JS. Musculoskeletal pain in the Netherlands: prevalences, consequences and risk groups, the DMC(3)-study. *Pain* 2003;102:167-178.
- 94 Praemer A, Furner S, Rice DP. *Musculoskeletal conditions in the United States; 1999.* (ISBN No. 0892032340)
- 95 Randelli P, Arrigoni P, Ragone V, Aliprandi A, Cabitza P. Platelet rich plasma in arthroscopic rotator cuff repair: a prospective RCT study, 2-year follow-up. *Journal of Shoulder and Elbow Surgery* 2011;20:518-528. 10.1016/j.jse.2011.02.008
- 96 Robinson D, Pachornik S, Shalom NB, Sagiv S, Melamed E, Nevo Z. The Use of a Chitosan-Based Hyaluronate Gel in Musculoskeletal Afflictions. In. *Advanced Technologies for Enhancing Quality of Life (AT-EQUAL)*, 2010; 2010, p. 75-78.
- 97 Rodeo SA, Delos D, Williams RJ, Adler RS, Pearle A, Warren RF. The effect of platelet-rich fibrin matrix on rotator cuff tendon healing: a prospective, randomized clinical study.

- The American Journal of Sports Medicine 2012;40:1234-1241.  
10.1177/0363546512442924
- 98 Ruiz-Moneo P, Molano-Munoz J, Prieto E, Algorta J. Plasma Rich in Growth Factors in Arthroscopic Rotator Cuff Repair: A Randomized, Double-Blind, Controlled Clinical Trial. *Arthroscopy* 2013;29:2-9. 10.1016/j.arthro.2012.08.014
- 99 Sanchez Marquez JM, Martínez Díez JM, Barco R, Antuña S. Functional results after arthroscopic repair of massive rotator cuff tears: Influence of the application platelet-rich plasma combined with fibrin. *Rev Esp Cir Ortop Traumatol* 2011;55:282-287.
- 100 Sauerbrey AM, Getz CL, Piancastelli M, Iannotti JP, Ramsey ML, Williams GR, Jr. Arthroscopic versus mini-open rotator cuff repair: a comparison of clinical outcome. *Arthroscopy* 2005;21:1415-1420. 10.1016/j.arthro.2005.09.008
- 101 Sclamberg SG, Tibone JE, Itamura JM, Kasraeian S. Six-month magnetic resonance imaging follow-up of large and massive rotator cuff repairs reinforced with porcine small intestinal submucosa. *Journal of Shoulder and Elbow Surgery* 2004;13:538-541. 10.1016/s1058274604001193
- 102 Severud EL, Ruotolo C, Abbott DD, Nottage WM. All-arthroscopic versus mini-open rotator cuff repair: A long-term retrospective outcome comparison. *Arthroscopy* 2003;19:234-238. 10.1053/jars.2003.50036
- 103 Shen W, Chen J, Yin Z, Chen X, Liu H, Heng BC et al. Allogeneous tendon stem/progenitor cells in silk scaffold for functional shoulder repair. *Cell Transplantation* 2012;21:943-958. 10.3727/096368911x627453

- 104 Shinoda T, Shibata Y, Izaki T, Shitama T, Naito M. A comparative study of surgical invasion in arthroscopic and open rotator cuff repair. *Journal of Shoulder and Elbow Surgery* 2009;18:596-599. 10.1016/j.jse.2008.12.005
- 105 Siskosky MJ EN, Chu E, Tibone JE, Lee TQ. Biomechanical evaluation of the “transosseous equivalent” rotator cuff repair technique using the PushLock for lateral fixation compared to the double-row technique. *Transactions American Academy of Orthopaedic Surgeons, San Diego, CA* 2007.
- 106 Sonnabend DH, Young AA. Comparative anatomy of the rotator cuff. *The Journal of Bone and Joint Surgery-British Volume* 2009;91:1632-1637. 10.1302/0301-620x.91b12.22370
- 107 Sugaya H, Maeda K, Matsuki K, Moriishi J. Functional and structural outcome after arthroscopic full-thickness rotator cuff repair: single-row versus dual-row fixation. *Arthroscopy* 2005;21:1307-1316. 10.1016/j.arthro.2005.08.011
- 108 Turner AS. Experiences with sheep surgery: Strengths and as an animal model for shoulder shortcomings. *Journal of Shoulder and Elbow Surgery* 2007;16:158S-163S. 10.1016/j.jse.2007.03.002
- 109 Uggen C, Dines J, McGarry M, Grande D, Lee T, Limpisvasti O. The effect of recombinant human platelet-derived growth factor BB-coated sutures on rotator cuff healing in a sheep model. *Arthroscopy* 2010;26:1456-1462. 10.1016/j.arthro.2010.02.025
- 110 Uthoff HK, Trudel G, Himori K. Relevance of pathology and basic research to the surgeon treating rotator cuff disease. *Journal of Orthopaedic Science* 2003;8:449-456. 10.1007/s10776-002-0624-5

- 111 van der Zwaal P, Thomassen BJW, Nieuwenhuijse MJ, Lindenburg R, Swen J-WA, van Arkel ERA. Clinical Outcome in All-Arthroscopic Versus Mini-Open Rotator Cuff Repair in Small to Medium-Sized Tears: A Randomized Controlled Trial in 100 Patients With 1-Year Follow-up. *Arthroscopy* 2013;29:266-273. 10.1016/j.arthro.2012.08.022
- 112 Verma NN, Dunn W, Adler RS, Cordasco FA, Allen A, MacGillivray J et al. All-arthroscopic versus mini-open rotator cuff repair: a retrospective review with minimum 2-year follow-up. *Arthroscopy* 2006;22:587-594. 10.1016/j.arthro.2006.01.019
- 113 Warner JJ, Tetreault P, Lehtinen J, Zurakowski D. Arthroscopic versus mini-open rotator cuff repair: a cohort comparison study. *Arthroscopy* 2005;21:328-332. 10.1016/j.arthro.2004.11.006
- 114 Weber SC, Kauffman JI, Parise C, Weber SJ, Katz SD. Platelet-rich fibrin matrix in the management of arthroscopic repair of the rotator cuff: a prospective, randomized, double-blinded study. *The American Journal of Sports Medicine* 2013;41:263-270. 10.1177/0363546512467621
- 115 Williams GR, Jr., Rockwood CA, Jr. Hemiarthroplasty in rotator cuff-deficient shoulders. *Journal of Shoulder and Elbow Surgery* 1996;5:362-367.
- 116 Wu Y, Dong Y, Chen S, Li Y. Effect of platelet-rich plasma and bioactive glass powder for the improvement of rotator cuff tendon-to-bone healing in a rabbit model. *International Journal of Molecular Sciences* 2014;15:21980-21991. 10.3390/ijms151221980

- 117 Wurgler-Hauri CC, Dourte LM, Baradet TC, Williams GR, Soslowsky LJ. Temporal expression of 8 growth factors in tendon-to-bone healing in a rat supraspinatus model. *Journal of Shoulder and Elbow Surgery* 2007;16:S198-203. 10.1016/j.jse.2007.04.003
- 118 Yokoya S, Mochizuki Y, Natsu K, Omae H, Nagata Y, Ochi M. Rotator cuff regeneration using a bioabsorbable material with bone marrow-derived mesenchymal stem cells in a rabbit model. *The American Journal of Sports Medicine* 2012;40:1259-1268. 10.1177/0363546512442343
- 119 Youm T, Murray DH, Kubiak EN, Rokito AS, Zuckerman JD. Arthroscopic versus mini-open rotator cuff repair: a comparison of clinical outcomes and patient satisfaction. *Journal of Shoulder and Elbow Surgery* 2005;14:455-459. 10.1016/j.jse.2005.02.002
- 120 Zhang Z, Gu B, Zhu W, Zhu L, Li Q. Arthroscopic versus mini-open rotator cuff repair: a prospective, randomized study with 24-month follow-up. *European Journal of Orthopaedic Surgery & Traumatology : Orthopedie Traumatologie* 2014;24:845-850. 10.1007/s00590-013-1263-5
- 121 Zumstein MA, Bielecki T, Ehrenfest DMD. The Future of Platelet Concentrates in Sports Medicine: Platelet-Rich Plasma, Platelet-Rich Fibrin, and the Impact of Scaffolds and Cells on the Long-term Delivery of Growth Factors. *Operative Techniques in Sports Medicine* 2011;19:190-197. 10.1053/j.otsm.2011.01.001
- 122 Zumstein MA, Rumian A, Lesbats V, Schaer M, Boileau P. Increased vascularization during early healing after biologic augmentation in repair of chronic rotator cuff tears using autologous leukocyte- and platelet-rich fibrin (L-PRF): a prospective randomized

controlled pilot trial. *Journal of Shoulder and Elbow Surgery* 2014;23:3-12.

10.1016/j.jse.2013.08.017

**CHAPTER 5      ARTICLE 2: CHITOSAN INHIBITS PLATELET-MEDIATED CLOT RETRACTION, INCREASES PLATELET-DERIVED GROWTH FACTOR RELEASE, AND INCREASES RESIDENCE TIME AND BIOACTIVITY OF PLATELET-RICH PLASMA *IN VIVO***

Biomedical Materials

Gabrielle Deprés-Tremblay <sup>1</sup>, Anik Chevrier <sup>2</sup>, Nicolas Tran-Khanh <sup>2</sup>, Monica Nelea <sup>2</sup> and Michael D Buschmann <sup>1,2</sup>

<sup>1</sup> Biomedical Engineering Institute and <sup>2</sup> Chemical Engineering Department, Polytechnique Montreal, Montreal, QC, Canada

**Running title:** Chitosan-PRP implants for tissue repair

**Corresponding author:** Prof Michael D. Buschmann, Department of Chemical Engineering, Polytechnique Montreal, PO Box 6079 Succ Centre-Ville, Montreal, Quebec, Canada, H3C 3A7, Fax: 514 340 2980 Tel: 514 340 4711 ext. 4931, E-mail: michael.buschmann@polymtl.ca

## **Abstract**

Platelet-rich plasma (PRP) has been used to treat different orthopaedic conditions, however, the clinical benefits of using PRP remain uncertain. Chitosan (CS)-PRP implants have been shown to improve meniscus, rotator cuff and cartilage repair in pre-clinical models. The purpose of this current study was to investigate *in vitro* and *in vivo* mechanisms of action of CS-PRP implants. Freeze-dried formulations containing 1% (w/v) chitosan (80% degree of deacetylation and number average molar mass 38 kDa), 1% (w/v) trehalose as lyoprotectant and 42.2 mM calcium chloride as clot activator were solubilized in PRP. Gravimetric measurements and molecular/cellular imaging studies revealed that clot retraction is inhibited in CS-PRP hybrid clots through physical coating of platelets, blood cells and fibrin strands by chitosan, which interferes with platelet aggregation and platelet-mediated clot retraction. Flow cytometry and ELISA assays revealed that platelets are activated and granules secreted in CS-PRP hybrid clots and that cumulative release of PDGF-AB and EGF is higher from CS-PRP hybrid clots compared to PRP clots *in vitro*. Finally, CS-PRP implants resided for up to 6 weeks in a subcutaneous implantation model and induced cell recruitment and granulation tissue synthesis, confirming greater residency and bioactivity compared to PRP *in vivo*.

## **Keywords**

Chitosan, platelet-rich plasma, clot retraction, platelet activation, implant residency



## 5.1 Introduction

Platelets are blood cell components that have recently been implicated in regulation of immune responses, cancer metastasis, vascular development, and angiogenesis, but are primarily responsible for haemostasis in the wound response, while simultaneously playing an essential role in healing by initiating specific cell responses through the release of several growth factors (1). Platelet-derived growth factors have received attention for tissue engineering and regeneration purposes in orthopedics and in other regenerative medicine fields. Unfortunately, growth factors are costly to produce and often inefficient in delivery to specific tissues (2). A more direct approach to produce and deliver growth factors is through injection of platelet-rich plasma (PRP). PRP is an autologous blood-derived product that has an increased concentration of platelets compared to physiological levels. Once the platelets in PRP are activated they release their alpha-granules containing multiple growth factors, among them PDGF, TGF- $\beta$ , VEGF, EGF and IGF-1. PRP has been used clinically to treat different orthopaedic conditions (3), since it is believed to enhance not only cell proliferation, but also extracellular matrix deposition, remodeling, angiogenesis, and collagen synthesis. However, delivery of PRP to specific sites is problematic since its physical stability is low resulting in rapid dispersion and low residence time (4). In addition, growth factors have a very short half-life and are released rapidly from PRP. Currently, the clinical benefits of using PRP to improve tissue repair and regeneration remain uncertain (3).

Chitosan, a polysaccharide obtained by chitin deacetylation, has been used in several tissue engineering and regenerative medicine applications (5). Chitosan is known to promote wound healing by enhancing migration of inflammatory cells, cell proliferation and matrix formation. This polysaccharide is non toxic, biocompatible and biodegradable, making it suitable for pre-clinical and clinical use. We have worked extensively with chitosan for several years, beginning with the initial discovery that chitosan can be mixed with glycerol phosphate (GP) and still remain soluble in near-

neutral conditions of pH and osmolality (6). Chitosan-GP solutions were mixed with whole blood to form voluminous stable clots that are applied to cartilage defects in order to improve repair induced by marrow stimulation procedures such as microfracture (7-10). We subsequently developed a method to produce lyophilized formulations of chitosan (CS), trehalose (as lyoprotectant) and calcium chloride (as clot activator) that are soluble in PRP and form injectable CS-PRP implants that coagulate rapidly *in situ* (4). We identified some formulation properties that control implant performance and showed that CS-PRP implants have the potential to improve meniscus, rotator cuff and cartilage repair (11-13). Combinations of chitosan and PRP have been used in other pre-clinical injury models as well, however, studies are scarce and report varying levels of success. Chitosan films (DDA 85% and 400 kDa) were used in conjunction with PRP in a rat excision model, and found to improve wound healing when compared to sham control, PRP or chitosan film alone (14). In a rabbit cranial defect model, an 86% DDA chitosan sponge used alone or in combination with PRP failed to improve repair compared to recalcified PRP alone (15). A composite of chitosan (DDA 94% and 680 kDa) and tricalcium phosphate (TP) was mixed with PRP and injected into osseous defects in the goat, where it improved repair compared to chitosan-TP by itself or untreated controls (16).

The purpose of the current study was to (1) investigate possible mechanisms by which chitosan inhibits retraction of CS-PRP hybrid clots *in vitro*, (2) characterize the effect of chitosan, trehalose and a combination of both on platelet activation and granule secretion *in vitro*, (3) characterize the release profile of PDGF-AB and EGF from CS-PRP hybrid clots *in vitro*, and (4) histologically assess the residency, bioactivity and biodegradability of CS-PRP implants *in vivo*. Our starting hypotheses were that (1) chitosan would bind to platelets in a non-specific fashion to inhibit platelet aggregation in hybrid clots and platelet-mediated clot retraction; (2) chitosan would activate platelets and induce granule secretion; (3) the release of growth factors with low isoelectric point (negatively charged at neutral pH), such as EGF, would be more sustained from CS-PRP hybrids than the release of growth factors with high isoelectric points (positively charged at neutral pH), such as PDGF-AB, due to

electrostatic interactions with cationic chitosan; (4) CS-PRP implants would reside longer than PRP *in vivo*, where they would induce cell recruitment and angiogenesis, but be degraded within 6 weeks.

## 5.2 Materials and methods

### 5.2.1 Preparation of freeze-dried chitosan formulations

Raw chitosans were purchased from Marinard, processed in-house and characterized by NMR spectroscopy (17) for degree of deacetylation (DDA) and size-exclusion chromatography/multi-angle laser light scattering (18) for number average molar mass ( $M_n$ ). Chitosan (80% DDA;  $M_n$  38 kDa) was dissolved in deionized water and 28 mM hydrochloric acid (Sigma-Aldrich) for 16 hours on a rotator at room temperature. Filter-sterilized  $\text{CaCl}_2$  (270 mM) and trehalose (15% w/v) solutions (both from Sigma-Aldrich) were then added to reach final concentrations of 1% (w/v) chitosan, 42.2 mM  $\text{CaCl}_2$  and 1% (w/v) trehalose prior to filtration through 0.2  $\mu\text{m}$  filters (Millipore). The solution was dispensed in 1-mL aliquots in 3-mL glass vials for freeze-drying with the following cycle: 1) Ramped freezing to  $-40^\circ\text{C}$  in 1 hour then isothermal 2 hours at  $-40^\circ\text{C}$ , 2)  $-40^\circ\text{C}$  for 48 hours at 100 millitorrs and 3) Ramped heating to  $30^\circ\text{C}$  in 12 hours then isothermal 6 hours at  $30^\circ\text{C}$ , at 100 millitorrs. 10 $\mu\text{L}$  Rhodamine-chitosan tracer (19) of corresponding DDA and  $M_n$  was added to the vials that were subsequently used for fluorescent microscopy.

### **5.2.2 Preparation of platelet-rich plasma (PRP)**

The Polytechnique Montreal institutional ethics committee approved the project and all subjects enrolled in this research (n=3 males and n=3 females, with some donors sampled more than once) responded positively to an Informed Consent Form. For each donor, blood was extracted and anti-coagulated with 12.9 mM sodium citrate. The blood was then centrifuged using an ACE E-Z PRP™ centrifuge at 160 g for 10 minutes at room temperature. The supernatant and first 1-2 mm of erythrocyte sediment was removed and then centrifuged again at 400 g for 10 minutes at room temperature. Only the bottom ~1.5 mL of each tube was retained and resuspended to make PRP. This isolation method yields a leukocyte-rich PRP (L-PRP) which typically contains ~3X more platelets than blood along with a leukocyte fraction (~0.8X that of blood) and a small erythrocyte fraction (~0.2X that of blood). Alexa-647 fibrinogen (Invitrogen) was prepared as a stock solution at 1.5 mg/mL in 0.1 M sodium bicarbonate (pH 8.3), and added to the PRP that was subsequently used for fluorescent microscopy (0.5mL of Alexa-647 fibrinogen added to 4.5mL of PRP).

### **5.2.3 Solubilization of freeze-dried chitosan formulations in platelet-rich plasma (PRP)**

Each freeze-dried cake (1mL freeze-dried formulation in each vial) was solubilized with 1mL of PRP and mixed vigorously for 10 seconds. The solubilized formulations were dispensed either into glass tubes to assess clot retraction and for imaging or into 48-well culture plates for characterization of release profiles.

## 5.2.4 Assessment of clot retraction

Chitosan-PRP formulations (~250  $\mu\text{L}$ ) were dispensed in glass tubes placed on a heat block at 37°C and allowed to clot for 1 hour. Serum was removed and % clot mass lost was quantified by gravimetric measurements. Clots were fixed with 0.5% (v/v) glutaraldehyde (EMS)/0.3% (w/v) paraformaldehyde (Sigma-Aldrich)/0.3% (v/v) Triton X-100 (Sigma-Aldrich). Controls were PRP recalcified with 42.2 mM  $\text{CaCl}_2$ . Duplicate clots were prepared for each donor, except for one donor, where one clot was prepared.

## 5.2.5 Confocal fluorescent and spinning disk microscopy imaging

Fixed clots were sectioned with a razor blade at ~ 1mm thickness and mounted with Mowiol 4-88 (Fluka)/glycerol (Sigma-Aldrich)/n-propyl gallate (Sigma-Aldrich) mounting medium (prepared in-house) on MatTek glass bottom dishes (Cedarlane). High resolution 2D and 3D images were captured with an Olympus FV1000 spectral confocal laser scanning microscope (Olympus Canada), using a PLAPON Apochromat oil objective (60X, NA 1.42). The excitation/emission wavelengths were 635/644-755 nm for the fibrin network (Alexa-647 fibrinogen tracer), and 543/555-625 nm for the chitosan (rhodamine tracer). Erythrocytes were also imaged for some samples (autofluorescence using 488/500-540 nm). The acquisition parameters were adjusted to avoid signal saturation. 3D images were reconstructed with Imaris software (Bitplane). The confocal microscope is also adapted for a Yokogawa spinning disk module (Quorum), controlled with the MetaMorph software (Molecular Devices). Given the high dynamic range of the EM-CCD digital camera (Hamamatsu), the spinning disk module was used to capture images with fixed acquisition settings for all the samples without reaching any signal saturation. Only the fibrin network was imaged with this module, using a UPLSAPO Super Apochromat objective (40X, NA 0.95) and excitation/emission wavelengths of 642/662-738 nm.

### **5.2.6 Scanning electron microscopy (SEM) imaging**

Fixed clots were embedded in paraffin (Fisher), sectioned at 3  $\mu\text{m}$  thickness with a Leica RM2155 microtome and collected on SuperFrost Plus glass slides (Fisher). The sections were then deparaffinized, post-fixed in 2% (v/v) glutaraldehyde (EMS)/0.1 M sodium cacodylate (Sigma) pH 7.2 and washed in water. The post-fixed sections were removed from slides using a super fine point tweezers and placed onto a conductive carbon adhesive tape (EMS). The sections were immobilized by blowing compressed air and then gold sputter coated for 25 seconds using an Agar manual gold sputter-coater (Marivac Inc).

SEM images were acquired with a Quanta FEG 200 ESEM (FEI Company) in high vacuum mode with working distance 5.6 to 5.7 mm and accelerating voltage 20kV.

### **5.2.7 Transmission electron microscopy (TEM) imaging**

Fixed clots were post-fixed in 1% (v/v) osmium tetroxide (Sigma-Aldrich), washed in deionized water, incubated with 2% (v/v) uranyl acetate (EMS) for 1 hour, washed, dehydrated in a graded ethanol series, cleared in xylene and embedded in Embed-812 (EMS) medium at 60°C. 100 nm sections were collected using a diamond blade and an RMC MT-7 ultramicrotome and mounted on copper grids. The images were acquired with a JEM 2000FXII transmission electron microscope (JEOL; Tokyo, Japan) operated at 80 kV.

### 5.2.8 Preparation of cell suspension and flow cytometry

Whole blood was anticoagulated with 10.9 mM sodium citrate, centrifuged at 190 g for 15 minutes and the supernatant collected. Supernatant was centrifuged at 2,500 g for 5 minutes to pellet the cells. Cell pellet was resuspended in HEPES/Tyrode's buffer (10 mM HEPES, 137 mM NaCl, 2.8 mM KCl, 1 mM MgCl<sub>2</sub>, 12 mM NaHCO<sub>3</sub>, 0.4 mM Na<sub>2</sub>HPO<sub>4</sub>, 5.5 mM glucose) with 1.35% (w/v) BSA (all from Sigma-Aldrich) and left to incubate for 1 hour. The cell suspension was then mixed with, either ADP (Sigma, final concentration 20 μM), solubilized chitosan 80% DDA *M<sub>n</sub>* 38 kDa (final concentration 1% w/v), trehalose (final concentration 1% w/v) or 1% (w/v) chitosan and (1% w/v) trehalose simultaneously. Fluorescein isothiocyanate (FITCs) labeled anti-Pac-1 and anti-CD62P antibodies (Biolegend), which recognize activated platelet GPIIb/IIIa complex and granule membrane protein P-selectin, respectively, were added to the tubes as per manufacturer's instructions and the tubes were incubated at room temperature for 20 minutes. The cells were fixed with 1% (w/v) paraformaldehyde/10 mM HEPES/0.15 mM NaCl pH 7.4 for 15 minutes at room temperature. The samples were then kept on ice until analysis. The fluorescence intensity of 10, 000 events per sample were analyzed using a flow Moflo cytometer (Beckman Coulter Life Sciences).

### 5.2.9 Quantification of growth factors released from clots

Freeze-dried chitosan cakes were solubilized in PRP as described above and 250 μL of the solubilized mixture was dispensed into each well of a 48-well plate culture plate and allowed to clot for 1 hour in air atmosphere at 37°C with 5%CO<sub>2</sub>. Wells were washed with 500 μL α-MEM cell culture medium (Invitrogen), the culture medium was immediately removed and replaced

with fresh  $\alpha$ -MEM cell culture medium. The cell culture medium were then removed and replenished at day 1, 3, 5 and 7. Culture medium was centrifuged at 400 g for 10 minutes and frozen at  $-80^{\circ}\text{C}$  prior to ELISA quantification using platelet-derived growth factor (PDGF-AB) or epidermal growth factor (EGF) Quantikine kits (Product N<sup>o</sup> DHD00C and DEG00 from RandD systems). Controls were PRP recalcified with 42.2 mM  $\text{CaCl}_2$ . Duplicate clots were prepared for each donor, except for one donor, where one clot was prepared.

### **5.2.10 Subcutaneous implantation**

The protocol for this study was approved by the University of Montreal ethics committee and was consistent with the Canadian Council on Animal Care guidelines for the care and use of laboratory animals. Five New Zealand White (NZW) male rabbits ( $> 2.5$  kg) were used for the study. Rabbits were anesthetized with ketamine/xylazine cocktail. From each animal, 18mL blood was collected from the ear artery and anticoagulated with sodium citrate (final citrate concentration 12.9 mM). Blood was centrifuged in an ACE EZ-PRP<sup>TM</sup> centrifuge for 10 min at 160 g and then for 10 min at 400 g to extract PRP, as described above. The back of the rabbit was shaved and the skin disinfected with 3 passages of Baxedin, then with 3 alternating passages of proviodine and isopropanol 70%. Freeze-dried chitosan formulations (300  $\mu\text{L}$ ) containing 1% (w/v) chitosan (80%-85% DDA and  $M_n$  36-43 kDa), 1% (w/v) trehalose and 42.2 mM  $\text{CaCl}_2$  were solubilised with 300  $\mu\text{L}$  of PRP and shaken vigorously for 10 seconds. A 1-cc syringe equipped with a 26 gauge needle was used to deliver 150  $\mu\text{L}$  of each implant under the skin of the back of the rabbits (n=4 CS-PRP implants injected in each rabbit). Controls consisted of 150  $\mu\text{L}$  PRP recalcified with 42.2 mM  $\text{CaCl}_2$  prior to injection (n=2 control PRP implants injected in



each rabbit). Animals were sacrificed at 2 weeks (n=2), 4 weeks (n=2) or 6 weeks (n=1) post-implantation. At the time of sacrifice, rabbits were anesthetized with ketamine/xylazine cocktail and euthanized with an overdose of sodium pentobarbital. The skin with attached implants was carefully removed and fixed in 10% neutral buffered formalin (NBF) (Fisher) for 3 days. Each implant was excised using razor blades and a horizontal band was collected from the central area for paraffin embedding. Paraffin sections (5  $\mu$ m) were collected and stained with Fast Green/Iron Hematoxylin (both from Sigma-Aldrich). The stained sections were then scanned for histological evaluation using a Nanozoomer RS system and images exported using NDPView software (both from Hamamatsu).

### **5.2.11 Statistical analysis**

All statistical analyses were performed with SAS Enterprise Guide 7.1 and SAS 9.4. Data in the text are presented as mean  $\pm$  SD. Data in the Figures are presented as median (line); Box: 25<sup>th</sup> and 75<sup>th</sup> percentile; Whisker: Box to the most extreme point within 1.5 interquartile range. The Mixed model task in SAS Enterprise Guide was used to compare the different groups with post-hoc analysis to look at pair-wise differences. Fixed effects were type of sample (CS-PRP vs PRP control) and time, while donor was a random effect, as some donors were sampled more than once.

## 5.3 Results

### 5.3.1 Clot retraction and platelet aggregation are inhibited in chitosan-PRP hybrid clots

Gravimetric measurements showed that PRP clots lost  $78\pm 4\%$  of their initial mass after clotting for 1 hour at  $37^{\circ}\text{C}$  (**Fig 5.1a**). Although there was some variability between donors, % mass loss was significantly less for chitosan-PRP hybrid clots at average  $21\pm 18\%$  (**Fig 5.1a**). Spinning disk microscopy and confocal microscopy images of clots fixed after clotting for 1 hour showed that platelet aggregates were smaller in chitosan-PRP hybrid clots (**Fig 5.1b, d & f**) compared to PRP clots (**Fig 5.1c, e & g**).

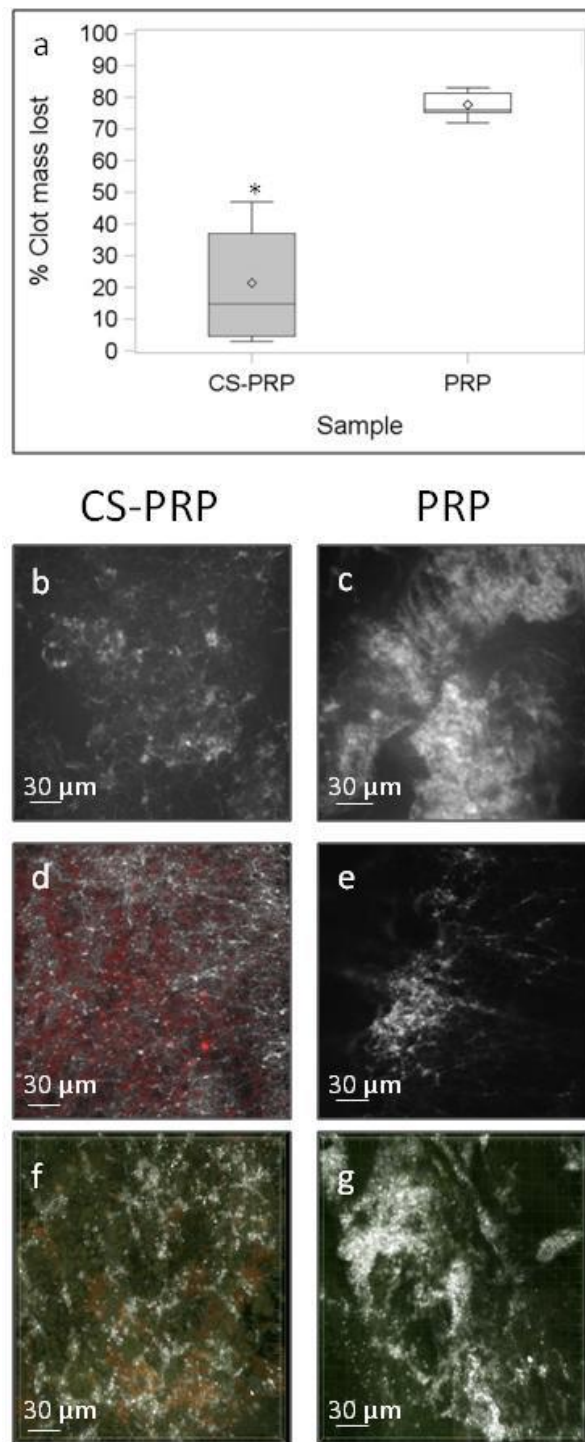


Figure 5-1 After clotting for 1 hour at 37°C, clot retraction and serum expression (expressed as % clot mass lost) was greater from PRP clots compared to CS-PRP hybrid clots (a). Data are presented as mean (diamond) and median (line) of n=7 clots from 3 different donors; Box: 25<sup>th</sup>

and 75<sup>th</sup> percentile; Whisker Box to the most extreme point within 1.5 interquartile range. The Mixed model task in SAS Enterprise Guide 7.1 and SAS 9.4 was used to compare the different groups using sample (CS-PRP vs PRP) as a fixed effect and donor as a random effect. \*  $p < 0.05$  compared to PRP. Platelet aggregates were smaller in CS-PRP hybrid clots (b, d & f) compared to PRP clots (c, e & g), as shown by spinning disk microscopy images (b & c), confocal microscopy images (d & e) and 3-D stacks of confocal microscopy images (f & g). An Alexa-647 fibrinogen tracer was added to allow imaging of fibrin-covered platelets and fibrin in white. A Rhodamine-chitosan tracer was added to allow imaging of chitosan in red in d) and orange in f).

### **5.3.2 Chitosan coats clot components in chitosan-PRP hybrid clots**

Scanning electron microscopy (SEM) images demonstrated that blood components were coated with chitosan in chitosan-PRP hybrid clots (**Fig 5.2a & b**). Both cells and fibers were covered by a coating of what is presumed to be chitosan (**Fig 5.2a & b**). In contrast, the fibrin network was readily visible in PRP clots (**Fig 5.2c & d**). In transmission electron (TEM) images of chitosan-PRP hybrid clots, chitosan was observed in the space between cellular elements, and also at the surface of fibrin strands, erythrocytes and platelets (**Fig 5.2e & f**). Erythrocytes were closely packed and platelet aggregates were large in PRP clots (**Fig 5.2g & h**).

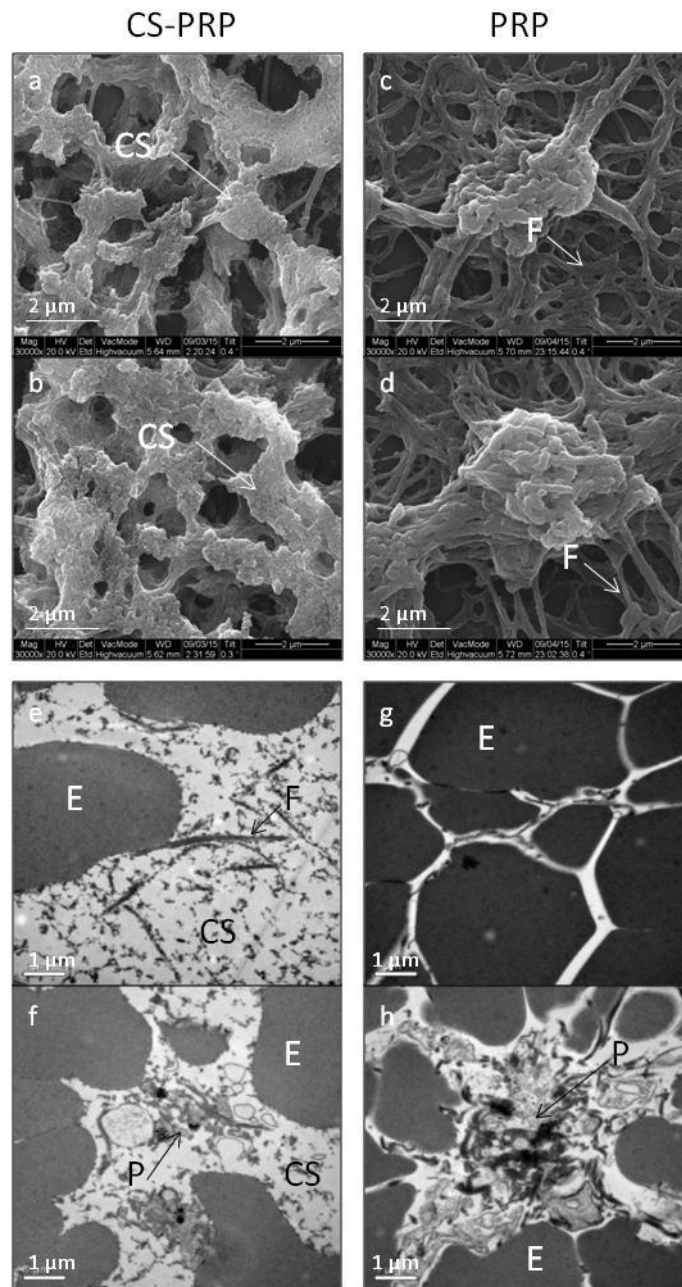


Figure 5-2 Chitosan (CS) appeared to be coating cellular and fibrous elements in scanning electron microscopy (SEM) images of CS-PRP clots (a & b) while the fibrin (F) network was readily visible in PRP clots (c & d). Chitosan (CS) was found in the space between cellular elements and also at the surface of erythrocytes (E), platelet aggregates (P) and fibrin (F) in transmission electron microscopy (TEM) images of CS-PRP clots (e & f). Erythrocytes (E) were tightly packed and platelet aggregates (P) were large in TEM images of PRP clots (g & h).

### 5.3.3 Chitosan induces platelet activation and granule secretion in cell suspension

As expected, incubation with ADP (in green), a known platelet agonist, caused increased Pac-1 and p-selectin expression in a cell suspension (unactivated cells in red) (**Fig 5.3**). Incubation with 1% (w/v) chitosan (in dark blue) also led to platelet activation (**Fig 5.3a**) and granule secretion (**Fig 5.3b**). In contrast, incubation with 1% (w/v) trehalose alone (in yellow) did not induce platelet activation and granule secretion (**Fig 5.3**). Finally, incubating the cell suspension with 1% (w/v) chitosan simultaneously with 1% (w/v) trehalose (in pale blue) induced platelet activation and granule secretion, albeit less than incubation with 1% (w/v) chitosan by itself (**Fig 5.3**).

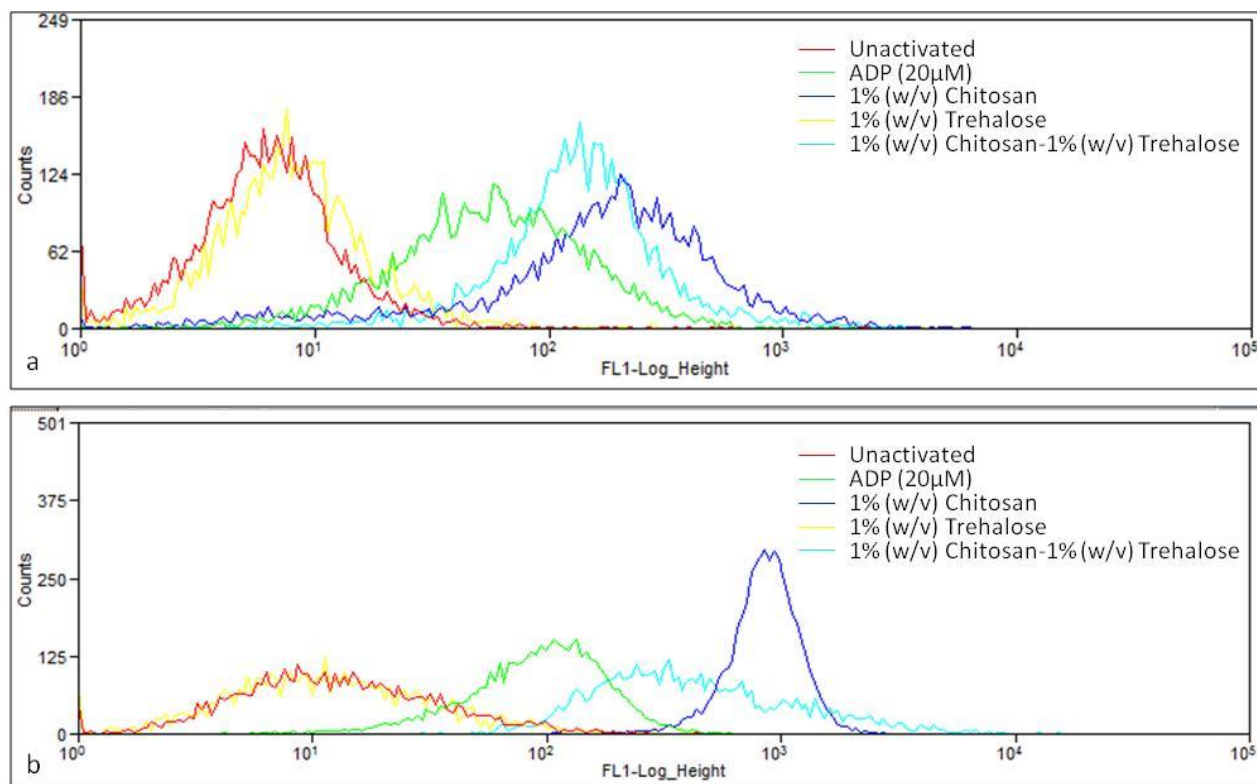


Figure 5-3 a) Flow cytometric analysis of PAC-1 (a) and p-selectin (b) staining of cell suspension (unactivated in red). As expected, incubation with ADP (20 µm in green) and chitosan (in dark

blue), both known platelet agonists, led to platelet activation (a) and granule secretion (b). In contrast, incubation with trehalose alone (in yellow) had no effect on platelet activation (a) or granule secretion (b). Interestingly, incubation with chitosan and trehalose simultaneously (in pale blue) decreased the intensity of both fluorescent signals compared to incubation with chitosan alone (in dark blue).

### **5.3.4 Chitosan-PRP hybrids provide a greater and sustained release of PDGF-AB and EGF over time**

PDGF-AB release into culture medium was ~100 times greater than that of EGF for both chitosan-PRP hybrid clots and PRP clots (**Fig 5.4**). For both growth factors, a phase of fast release was observed in the first 24 hours, followed by a more controlled release from day 1 to day 7 (**Fig 5.4**). In addition, for both growth factors, release was still ongoing at day 7 and no plateau had been reached (**Fig 5.4**). Both time ( $p < 0.0001$  and  $p < 0.0001$ ) and sample type ( $p < 0.0001$  and  $p = 0.0003$ ) had an effect on the release of PDGF-AB and EGF, respectively (**Fig 5.4**). The cumulative release of PDGF-AB from chitosan-PRP hybrid clots was significantly greater than the cumulative release from PRP clots from day 1 to day 7 (**Fig 5.4a**). Similarly, the cumulative release of EGF was significantly greater from chitosan-PRP hybrid clots than from PRP clots from day 3 to day 7 (**Fig 5.4b**).

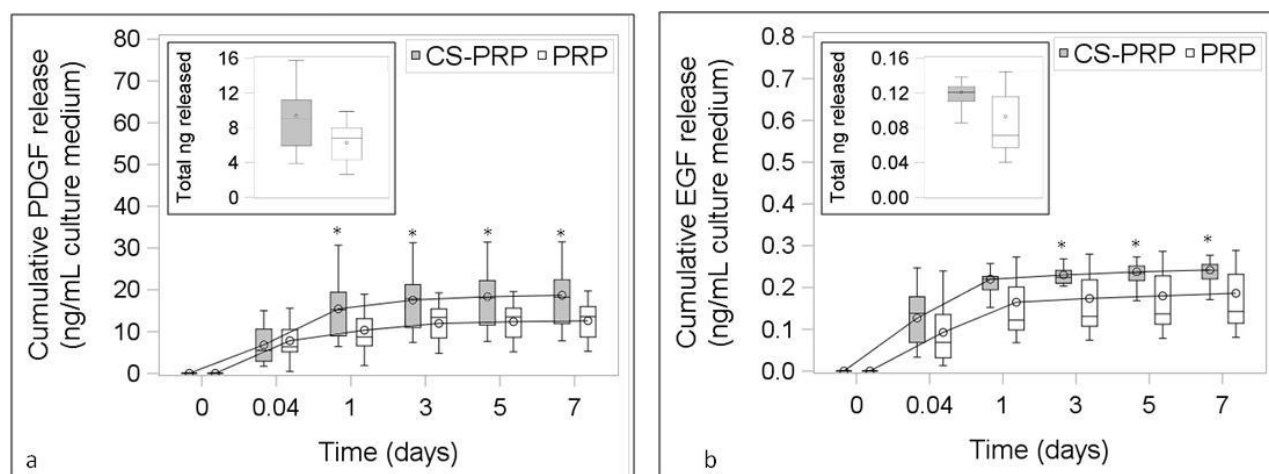


Figure 5-4 PDGF-AB (a) and EGF (b) cumulative release in culture medium was greater for CS-PRP clots compared to PRP clots. Data are presented as mean (circle) and median (line) of n=13 clots from 6 different donors; Box: 25<sup>th</sup> and 75<sup>th</sup> percentile; Whisker: Box to the most extreme point within 1.5 interquartile range. The Mixed model task in SAS Enterprise Guide 7.1 and SAS 9.4 was used to compare the different groups with post-hoc analysis to look at pair-wise differences using sample and time as fixed effects and donor as a random effect. \* p < 0.05 compared to PRP. Insets show total amount of growth factors released.

### 5.3.5 Chitosan-PRP hybrids reside for at least 6 weeks in vivo and induce cell recruitment

No PRP implants could be recovered for histology at any time point tested. In contrast, chitosan-PRP implants were resident for up to 6 weeks post-implantation (**Fig 5.5**). Host-derived cells were recruited to the implants and were observed invading the implants from 2 weeks on, along with granulation tissue synthesis and new blood vessel formation (**Fig 5.5**). None of the chitosan implants induced deleterious effects in rabbits. No sign of infection or rejection were noted macroscopically or histologically. Blood work was normal and rabbits did not develop anorexia post-surgery



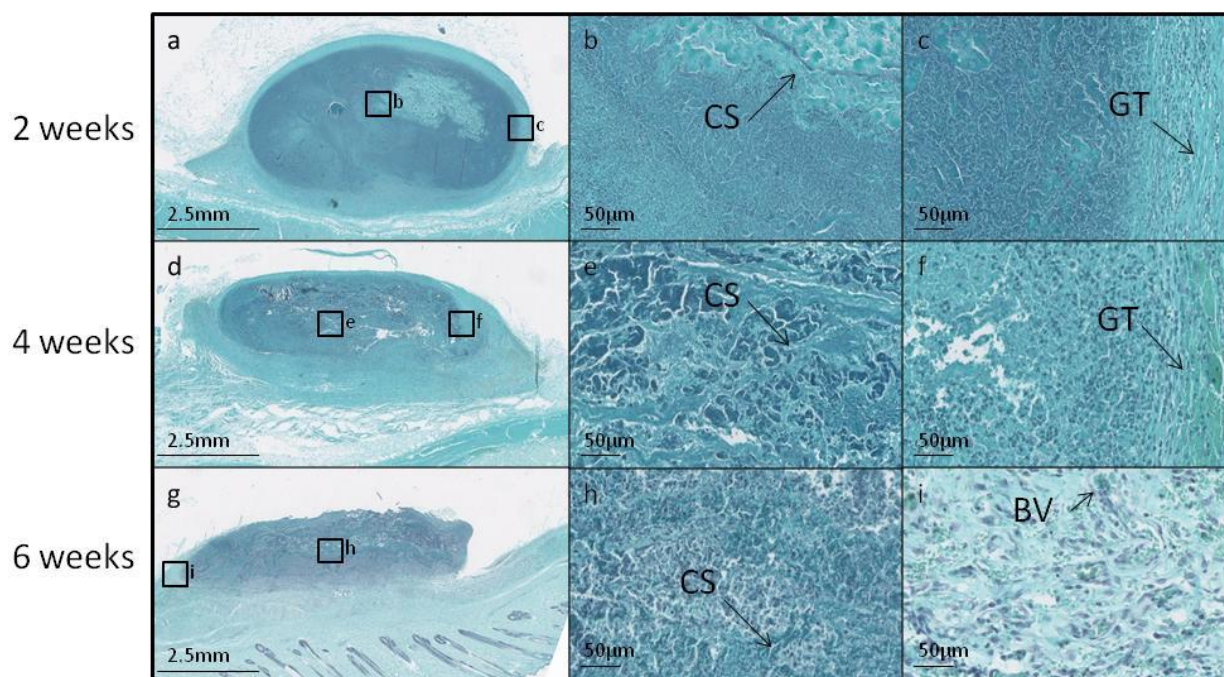


Figure 5-5 Formulations containing 1% (w/v) chitosan (CS  $M_n$  38-43kDa and DDA 80-85%) with 1% (w/v) trehalose and 42.2 mM  $\text{CaCl}_2$  were solubilized in autologous PRP and injected subcutaneously in rabbits, where they were found to be resident and induce cell recruitment at two weeks (a-c), four weeks (d-f), and six weeks (g-i) post-implantation. Invasion of the CS-PRP implants by host cells was accompanied by granulation tissue (GT) synthesis and formation of new blood vessels (BV). In contrast, recalcified PRP implants were completely degraded within a few days (not shown since the implant was absent). Outlines in a, d & g show where higher magnification images b, c, e, f, h & i were acquired.

## 5.4 Discussion

One objective of this study was to investigate the mechanisms by which chitosan inhibits platelet-mediated clot retraction and liquid expression in CS-PRP hybrids, as shown in **Figure 5.1a**. Under static or low shear stress a condition, which is the case here in our *in vitro* assay, platelet aggregation is mainly mediated by the interactions of GPIIb/IIIa on platelet surface with

fibrinogen (20). Stimulation of platelets with agonists induces cytoskeletal rearrangement, shape change, protein synthesis, granule secretion and increases the affinity of the GPIIb-IIIa platelet receptor for fibrinogen (21). Platelet aggregation results from binding of multiple platelets to the same fibrinogen molecule (1). Clot retraction, mediated by the platelet actin and myosin contractile system then follows, as long as platelet stimulation, comprising shape change and primary aggregation, are maintained (22, 23). In the absence or non-functioning GPIIb/IIIa, clot retraction does not occur. Confocal, SEM and TEM images (**Figures 5.1&2**) support our first hypothesis that chitosan physically coats platelets and other components of the blood clot to inhibit platelet aggregation, which is needed for clot retraction. In CS-PRP hybrids, chitosan physically interferes with the ability of the platelets to adhere to each other and the fibrin network and exert mechanical forces.

Our second and third aims were to investigate whether platelets are activated in CS-PRP hybrid clots and, if so, how platelet-derived growth factors are released from CS-PRP hybrid clots. Chitosan (DDA > 90% and 50 kDa) was previously shown to be a platelet agonist and stimulate platelet activation and GPIIb/IIIa expression *in vitro* (24). In another study, stimulation of platelet suspensions with chitosan (DDA 84%) induced p-selectin and GPIIb/IIIa expression, in a process that was shown to be modulated by plasma and extracellular matrix proteins (25). Consistent with these previously published data and our third hypothesis, we found that chitosan induces platelet activation and granule secretion in cell suspensions (**Figure 5.3**), even more so than ADP (20  $\mu$ m), a known platelet agonist. Interestingly, incubation of cell suspension with trehalose along with chitosan slightly decreased expression of Pac-1 and p-selectin compared to incubation with chitosan alone. This is consistent with published reports that lyoprotectants impede haemostatic mechanisms (26, 27).

Even though test conditions in the flow cytometry assay are different than in the hybrid clot system, we expected platelets within the CS-PRP hybrid clots to be activated and release their granule content, and this was ascertained by ELISA assays. In the case of physical adsorption of growth factors to chitosan, release is believed to be controlled by the electrostatic interactions that exist between the growth factors and the chitosan (28). Therefore, our third starting hypothesis was that the isoelectric point of platelet-derived growth factors would determine how growth factors would be released from our CS-PRP hybrids. The isoelectric point of PDGF is 9.8 (29) and, under physiological conditions, we expected ionic repulsion between positively charged PDGF-AB and cationic chitosan to result in burst release. Meanwhile, EGF, which has an isoelectric point of 4.6 (30) would be expected to bind to chitosan under physiological conditions and be released in a more sustained manner. In contrast to this, we found that CS-PRP hybrid clots sustained and increased release of both PDGF-AB and EGF for 1 week *in vitro*, which suggests that additional factors are controlling their release in this system (**Figure 5.4**).

We found that the cumulative levels of PDGF-AB and EGF released in the culture medium were higher in the case of CS-PRP clots compared to PRP clots (**Figure 5.4**). These results were not completely unexpected. Kutlu et al (31) previously prepared CS-PRP scaffolds by either adding PRP to a chitosan gel before freeze-drying or by delivering PRP to a lyophilized chitosan sponge. Sustained release of PDGF-BB was achieved in the first group, similarly to what we observed here, while a sharp burst release was observed in the second group. Interestingly, both of their CS-PRP scaffolds secreted higher cumulative levels of PDGF-BB when compared to unactivated PRP or PRP activated with type I collagen, similarly to what was found here for PDGF-AB. Hattori et al (32) showed that platelets in whole blood are activated when mixed with solutions of chitosan with different DDA and  $M_w$ . Of particular relevance to our study, the

amount of PDGF-AB released was the highest when chitosans of DDA 75-85% and  $M_w$  50-190 kDa were used in conjunction with calcium chloride than when calcium chloride was used by itself. Shen et al (33) showed that stimulation with chitosan of DDA > 90% and 450 kDa induced release of PDGF-AB and EGF from PRP for up to 60 minutes. Shimojo et al (34) prepared lyophilized scaffolds containing different concentrations of chitosan (DDA 83% and  $M_w$  400 kDa), loaded the scaffolds with PRP activated with autologous serum and calcium chloride and showed that PDGF-AB cumulative release was higher from the scaffolds compared to activated PRP alone, provided that the scaffolds be lyophilized at low temperatures. In a subsequent study, Shimojo et al (35) showed that stabilizing the chitosan scaffolds by treating them with NaOH prior to loading them with PRP was another way to increase cumulative PDGF-AB release from scaffolds lyophilized at  $-20^{\circ}\text{C}$ .

With regard to growth factor release, it is important to consider the contribution of each cell type present in the PRP preparation. Platelets are the main contributors to growth factor release from PRP and positive correlations were previously found between platelet doses and the amount of released growth factors including PDGF-AB, TGF- $\beta$ 1, VEGF and EGF (36, 37). While it appears that the inclusion of leukocytes in PRP increases the content of some pro-inflammatory cytokines (38-41), the effect of leukocytes on growth factor content and release is still not fully understood. Previous studies found that leukocyte-rich PRP contained higher concentrations of growth factors compared to leukocyte-poor PRP, but that may be due to the fact that systems that include the buffy coat layer are usually more efficient at capturing platelets (39, 42-46). However, positive correlations and close associations were also found between PRP leukocyte counts and levels of PDGF-AB, VEGF and EGF (36, 37) [ENREF 11](#), which suggests that leukocytes contribute to the release of growth factors from PRP. Here, we found increased

cumulative PDGF-AB and EGF release from CS-PRP clots compared to PRP clots (**Figure 5.4**). One possible reason for this is that chitosan used in conjunction with calcium chloride stimulates platelet activation and granule secretion more than calcium chloride by itself. Another possibility would be that leukocytes, especially monocytes, present in CS-PRP hybrids are secreting higher amounts of growth factors than in PRP without chitosan. While it has been reported that M0 and polarized M2a macrophages secrete PDGF-BB (47, 48), and that biodegradable chitosan particles (DDA 81.5% and  $M_n$  132 kDa) enhance release of PDGF-BB from M0 and M2a macrophages (49), we believe that the main contributors to growth factor release in the CS-PRP hybrid system are platelets and not monocytes, for the following reasons: 1) Monocytes typically require specific stimulatory signals to become macrophages, 2) There is a low number of monocytes present in each CS-PRP clot, compared to the number of platelets (on average ~ 2500X more platelets than monocytes); 3) In light of previous reports on the amount of growth factors released by M0 and M2a macrophages, it seems unlikely that such a limited number of monocytes could secrete the amount of PDGF-AB and EGF that was measured here in the culture medium.

Our fourth aim was to investigate the implants *in vivo*, and, as previously shown (4), CS-PRP hybrids exhibited longer residency and higher bioactivity than PRP (**Figure 5.5**). In a subcutaneous implantation model in the mouse, porous chitosan scaffolds were found to elicit neutrophil migration into the implantation area along with angiogenic activity, as was shown here as well (50). It is of interest to mention that the site of implantation along with implant volume influences biodegradability. We have previously shown that CS-PRP implants are degraded within 3 weeks in meniscus tears in the sheep (13), and between 2-8 weeks in rotator cuff tears (11) and cartilage lesions in the rabbit (12) compared to more than 6 weeks in the current study.

One limitation of this study is the low number of animals used for the *in vivo* subcutaneous implants study. Another limitation is the limited number of growth factors studied for the release profiles. We chose both EGF and PDGF-AB, since they are frequently assessed in the literature, and they have widely different isoelectric points. Nevertheless, future studies should involve a greater number of platelet-derived growth factors. It is also important to mention that *in vitro* release profiles cannot be extrapolated to the *in vivo* situation; however, these data improve our understanding of the CS-PRP technology.

## 5.5 Summary

Chitosan physically coats platelets, blood cells and fibrin strands in CS-PRP hybrid clots, thus inhibiting platelet aggregation, which is required for clot retraction. Platelets are activated, granules secreted and higher levels of PDGF-AB and EGF are released from CS-PRP hybrid clots compared to PRP clots *in vitro*. Finally, CS-PRP implants reside for at least 6 weeks post-implantation subcutaneously and induce cell recruitment and granulation tissue synthesis, confirming a longer residency and higher bioactivity compared to PRP *in vivo*.

## Acknowledgments

We acknowledge the technical contributions of Geneviève Picard and the funding sources (Canadian Institutes of Health Research, Canada Foundation for Innovation, Groupe de Recherche en Sciences et Technologies Biomédicales, Natural Sciences and Engineering Research Council of Canada, Ortho Regenerative Technologies Inc).

### **Competing interests**

AC and MDB hold shares and MDB is a Director of Ortho Regenerative Technologies Inc.

### **References**

1. Jurk K, Kehrel BE. Platelets: physiology and biochemistry. *Seminars in thrombosis and hemostasis*. 2005;31(4):381-92.
2. Lee K, Silva EA, Mooney DJ. Growth factor delivery-based tissue engineering: general approaches and a review of recent developments. *J R Soc Interface*. 2011;8(55):153-70.
3. Sheth U, Simunovic N, Klein G, Fu F, Einhorn TA, Schemitsch E, et al. Efficacy of autologous platelet-rich plasma use for orthopaedic indications: a meta-analysis. *The Journal of bone and joint surgery American volume*. 2012;94(4):298-307.
4. Chevrier A, Darras V, Picard G, Nelea M, Veilleux D, Lavertu M, et al. Injectable chitosan-platelet-rich plasma (PRP) implants to promote tissue regeneration: In vitro properties, in vivo residence, degradation, cell recruitment and vascularization. *Journal of tissue engineering and regenerative medicine*. 2017. In press.
5. Muzzarelli RAA. Chitins and chitosans for the repair of wounded skin, nerve, cartilage and bone. *Carbohydrate Polymers*. 2009;76(2):167-82.

6. Chenite A, Chaput C, Wang D, Combes C, Buschmann MD, Hoemann CD, et al. Novel injectable neutral solutions of chitosan form biodegradable gels in situ. *Biomaterials*. 2000;21(21):2155-61.
7. Hoemann CD, Hurtig M, Rossomacha E, Sun J, Chevrier A, Shive MS, et al. Chitosan-glycerol phosphate/blood implants improve hyaline cartilage repair in ovine microfracture defects. *Journal of Bone and Joint Surgery-American Volume*. 2005;87A(12):2671-86.
8. Stanish WD, McCormack RG, Forriol F, Mohtadi N, Pelet S, Desnoyers J, et al. Novel Scaffold-Based BST-CarGel Treatment Results in Superior Cartilage Repair Compared with Microfracture in a Randomized Controlled Trial. *Journal of Bone and Joint Surgery-American Volume*. 2013;95A(18):1640-50.
9. Shive MS, Stanish WD, McCormack RG, Forriol F, Mohtadi N, Pelet S, et al. BST-CarGel® Treatment Maintains Cartilage Repair Superiority over Microfracture at 5 Years in a Multicenter Randomized Controlled Trial. *Cartilage*. 2015 6(2):62-72.
10. Méthot S, Changoor A, Tran-Khanh N, Hoemann CD, Stanish WD, Restrepo A, et al. Osteochondral Biopsy Analysis Demonstrates That BST-CarGel Treatment Improves Structural and Cellular Characteristics of Cartilage Repair Tissue Compared With Microfracture. *Cartilage*. 2015.
11. Déprés-Tremblay G, Chevrier A, Buschmann MD, editors. Freeze-dried chitosan-PRP in a rabbit model of rotator cuff repair. *Transactions Orthopaedic Research Society*; 2017 San Diego, CA, USA.



12. Dwivedi G, Chevrier A, Hoemann CD, Buschmann MD. Freeze dried chitosan/platelet-rich-plasma implants improve marrow stimulated cartilage repair in rabbit chronic defect model. Transactions Orthopaedic Research Society; 2017 San Diego, CA, USA.
13. Ghazi zadeh L, Chevrier A, Hurtig MB, Farr J, Rodeo S, Hoemann CD, et al., editors. Freeze-dried chitosan-PRP injectable surgical implants for meniscus repair: results from pilot ovine studies. Transactions Orthopaedic Research Society; 2017 San Diego, CA, USA.
14. Mohammadi R, Mehrtash M, Hassani N, Hassanpour A. Effect of Platelet Rich Plasma Combined with Chitosan Biodegradable Film on Full-Thickness Wound Healing in Rat Model. Bulletin of emergency and trauma. 2016;4(1):29-37.
15. Oktay EO, Demiralp B, Senel S, Cevdet Akman A, Eratalay K, Akincibay H. Effects of platelet-rich plasma and chitosan combination on bone regeneration in experimental rabbit cranial defects. The Journal of oral implantology. 2010;36(3):175-84.
16. Bi L, Cheng W, Fan H, Pei G. Reconstruction of goat tibial defects using an injectable tricalcium phosphate/chitosan in combination with autologous platelet-rich plasma. Biomaterials. 2010;31(12):3201-11.
17. Lavertu M, Xia Z, Serreqi AN, Berrada M, Rodrigues A, Wang D, et al. A validated <sup>1</sup>H NMR method for the determination of the degree of deacetylation of chitosan. J Pharm Biomed Anal. 2003;32(6):1149-58.
18. Nguyen S, Winnik FM, Buschmann MD. Improved reproducibility in the determination of the molecular weight of chitosan by analytical size exclusion chromatography. Carbohydrate Polymers. 2009;75(3):528-33.

19. Ma O, Lavertu M, Sun J, Nguyen S, Buschmann MD, Winnik FM, et al. Precise derivatization of structurally distinct chitosans with rhodamine B isothiocyanate. *Carbohydrate Polymers*. 2008;72(4):616-24.
20. Jackson SP. The growing complexity of platelet aggregation. *Blood*. 2007;109(12):5087-95.
21. Platelet function : assessment, diagnosis, and treatment Quinn M, Fitzgerald D, editors. Totowa, NJ, USA: Humana Press; 2005.
22. Cohen I, Gerrard JM, White JG. Ultrastructure of clots during isometric contraction. *The Journal of cell biology*. 1982;93(3):775-87.
23. Cohen I. The mechanism of clot retraction. Platelet membrane glycoproteins. New York, NY, USA: Springer US; 1985. p. 299-323.
24. Chou TC, Fu E, Wu CJ, Yeh JH. Chitosan enhances platelet adhesion and aggregation. *Biochemical and biophysical research communications*. 2003;302(3):480-3.
25. Lord MS, Cheng B, McCarthy SJ, Jung M, Whitelock JM. The modulation of platelet adhesion and activation by chitosan through plasma and extracellular matrix proteins. *Biomaterials*. 2011;32(28):6655-62.
26. Bakaltcheva I, Reid T. Effects of blood product storage protectants on blood coagulation. *Transfusion medicine reviews*. 2003;17(4):263-71.
27. Luostarinen T, Niiya T, Schramko A, Rosenberg P, Niemi T. Comparison of Hypertonic Saline and Mannitol on Whole Blood Coagulation In Vitro Assessed by Thromboelastometry. *Neurocritical care*. 2011;14(2):238-43.

28. Yao K, Li J, Yao F, Yin Y. Chitosan-Based Hydrogels: Functions and Applications. Boca Raton, FL, USA: Taylor and Francis Group LLC CRC Press; 2012.
29. Antoniades HN, Scher CD, Stiles CD. Purification of human platelet-derived growth factor. Proceedings of the National Academy of Sciences of the United States of America. 1979;76(4):1809-13.
30. Taylor JM, Mitchell WM, Cohen S. Epidermal growth factor. Physical and chemical properties. The Journal of biological chemistry. 1972;247(18):5928-34.
31. Kutlu B, Aydin RST, Akman AC, Gumusderelioglu M, Nohutcu RM. Platelet-rich plasma-loaded chitosan scaffolds: Preparation and growth factor release kinetics. Journal of Biomedical Materials Research Part B-Applied Biomaterials. 2013;101B(1):28-35.
32. Hattori H, Ishihara M. Feasibility of improving platelet-rich plasma therapy by using chitosan with high platelet activation ability. Experimental and Therapeutic Medicine. 2016;DOI: 10.3892/etm.2017.4041.
33. Shen EC, Chou TC, Gau CH, Tu HP, Chen YT, Fu E. Releasing growth factors from activated human platelets after chitosan stimulation: a possible bio-material for platelet-rich plasma preparation. Clin Oral Impl Res. 2006;17( ):572-8.
34. Shimojo AA, Perez AG, Galdames SE, Brissac IC, Santana MH. Performance of PRP associated with porous chitosan as a composite scaffold for regenerative medicine. TheScientificWorldJournal. 2015;2015:396131.
35. Shimojo AA, Perez AG, Galdames SE, Brissac IC, Santana MH. Stabilization of porous chitosan improves the performance of its association with platelet-rich plasma as a composite

scaffold. *Materials science & engineering C, Materials for biological applications*. 2016;60:538-46.

36. Magalon J, Bausset O, Serratrice N, Giraud L, Aboudou H, Veran J, et al. Characterization and comparison of 5 platelet-rich plasma preparations in a single-donor model. *Arthroscopy : the journal of arthroscopic & related surgery : official publication of the Arthroscopy Association of North America and the International Arthroscopy Association*. 2014;30(5):629-38.

37. Weibrich G, Kleis WK, Streckbein P, Moergel M, Hitzler WE, Hafner G. Comparison of point-of-care methods for preparation of platelet concentrate (platelet-rich plasma). *Int J Oral Maxillofac Implants*. 2012;27(4):762-9.

38. Anitua E, Zalduendo MM, Prado R, Alkhraisat MH, Orive G. Morphogen and proinflammatory cytokine release kinetics from PRGF-Endoret fibrin scaffolds: Evaluation of the effect of leukocyte inclusion. *Journal of biomedical materials research Part A*. 2014.

39. Cavallo C, Filardo G, Mariani E, Kon E, Marcacci M, Pereira Ruiz MT, et al. Comparison of platelet-rich plasma formulations for cartilage healing: an in vitro study. *The Journal of bone and joint surgery American volume*. 2014;96(5):423-9.

40. Sundman EA, Cole BJ, Fortier LA. Growth Factor and Catabolic Cytokine Concentrations Are Influenced by the Cellular Composition of Platelet-Rich Plasma. *American Journal of Sports Medicine*. 2011;39(10):2135-40.

41. Pochini AC, Antonioli E, Bucci DZ, Sardinha LR, Andreoli CV, Ferretti M, et al. Analysis of cytokine profile and growth factors in platelet-rich plasma obtained by open systems and commercial columns. *Einstein (Sao Paulo, Brazil)*. 2016;14(3):391-7.

42. Castillo TN, Pouliot MA, Kim HJ, Dragoo JL. Comparison of Growth Factor and Platelet Concentration From Commercial Platelet-Rich Plasma Separation Systems. *American Journal of Sports Medicine*. 2011;39(2):266-71.
43. Leitner GC, Gruber R, Neumuller J, Wagner A, Kloimstein P, Hocker P, et al. Platelet content and growth factor release in platelet-rich plasma: a comparison of four different systems. *Vox Sanguinis*. 2006;91(2):135-9.
44. Masuki H, Okudera T, Watanebe T, Suzuki M, Nishiyama K, Okudera H, et al. Growth factor and pro-inflammatory cytokine contents in platelet-rich plasma (PRP), plasma rich in growth factors (PRGF), advanced platelet-rich fibrin (A-PRF), and concentrated growth factors (CGF). 2016;2(1):19.
45. Fitzpatrick J, Bulsara MK, McCrory PR, Richardson MD, Zheng MH. Analysis of Platelet-Rich Plasma Extraction. Variations in Platelet and Blood Components Between 4 Common Commercial Kits. *The Orthopaedic Journal of Sports Medicine*. 2017;5(1):2325967116675272.
46. Parrish WR, Roides B, Hwang J, Mafilios M, Story B, Bhattacharyya S. Normal platelet function in platelet concentrates requires non-platelet cells: a comparative in vitro evaluation of leucocyte-rich (type 1a) and leucocyte-poor (type 3b) platelet concentrates. *BMJ Open Sport & Exercise Medicine*. 2016;2(1).
47. Spiller KL, Anfang RR, Spiller KJ, Ng J, Nakazawa KR, Daulton JW, et al. The role of macrophage phenotype in vascularization of tissue engineering scaffolds. *Biomaterials*. 2014;35(15):4477-88.

48. Spiller KL, Nassiri S, Witherel CE, Anfang RR, Ng J, Nakazawa KR, et al. Sequential delivery of immunomodulatory cytokines to facilitate the M1-to-M2 transition of macrophages and enhance vascularization of bone scaffolds. *Biomaterials*. 2015;37:194-207.
49. Fong D, Ariganello MB, Girard-Lauziere J, Hoemann CD. Biodegradable chitosan microparticles induce delayed STAT-1 activation and lead to distinct cytokine responses in differentially polarized human macrophages in vitro. *Acta biomaterialia*. 2015;12:183-94.
50. VandeVord PJ, Matthew HWT, DeSilva SP, Mayton L, Wu B, Wooley PH. Evaluation of the biocompatibility of a chitosan scaffold in mice. *Journal of biomedical materials research*. 2002;59(3):585-90.

**CHAPTER 6      ARTICLE 3: FREEZE-DRIED CHITOSAN-PRP  
IMPLANTS IMPROVE SUPRASPINATUS TENDON ATTACHMENT  
IN A TRANSOSSEOUS ROTATOR CUFF REPAIR MODEL IN THE  
RABBIT**

Journal of Orthopaedic Research

Deprés-Tremblay G<sup>1</sup>, Chevrier A<sup>2</sup>, Snow M<sup>3</sup>, Rodeo S<sup>4</sup> and Buschmann MD<sup>1,2</sup>

<sup>1</sup>Biomedical Engineering Institute and <sup>2</sup>Chemical Engineering Department, Polytechnique, Montreal, QC, Canada, <sup>3</sup>The Royal Orthopaedic Hospital, Birmingham, UK, <sup>4</sup>Sports Medicine and Shoulder Service, The Hospital for Special Surgery, New York, NY, USA

Corresponding author: Prof Michael D. Buschmann, Department of Chemical Engineering, Ecole Polytechnique, PO Box 6079 Succ Centre-Ville, Montreal, Quebec, Canada, H3C 3A7, Fax: 514 340 2980 Tel: 514 340 4711 ext. 4931, E-mail: michael.buschmann@polymtl.ca

Running title: Chitosan-PRP for rotator cuff repair

Author contributions statement: All authors made substantial contributions to research design (GDT, AC, MS, SR, MDB), acquisition, analysis and interpretation of data (GDT, AC, MS, SR, MDB), drafting and revision of the paper (GDT, AC, MS, SR, MDB). All authors have read and approved the final submitted manuscript.



**Abstract**

Rotator cuff tears result in shoulder pain, stiffness, weakness and loss of motion. After surgical repair, failure rate ranges between 20 to 95% and it is recognized that current surgical treatments need improvement. The aim of the study was to assess whether implants composed of freeze-dried chitosan (CS) solubilized in autologous platelet-rich plasma (PRP) can improve rotator cuff repair in a rabbit model. Complete tears were created bilaterally in the supraspinatus (SSP) tendon of New Zealand White rabbits (n=4 in a pilot feasibility study followed by n=13 in a larger efficacy study), which were repaired using transosseous suturing. On the treated side, in addition to sutures, CS-PRP implants were injected into the transosseous tunnels and the tendon itself, and healing was assessed histologically at time points ranging from 1 day to 2 months post-surgery. CS-PRP implants were resident within transosseous tunnels and adhered to tendon surfaces at one day post-surgery and induced recruitment of polymorphonuclear cells from 1 to 14 days. CS-PRP implants improved attachment of the SSP tendon to the humeral head through increased bone remodeling at the greater tuberosity and also inhibited heterotopic ossification of the SSP tendon at 2 months. Using CS-PRP implants in conjunction with transosseous suturing improved attachment of the SSP tendon versus suturing alone, which would be expected to correlate with superior mechanical performance. This preliminary study provides evidence that CS-PRP implants are effective in improving rotator cuff tendon attachment in a small animal model, and could potentially be translated to a clinical setting.

**Keywords:** Rotator cuff repair, chitosan, platelet-rich plasma, injectable implants, rabbit model

## 6.1 Introduction

Rotator cuff tears are one of the most common shoulder pathologies <sup>1</sup> and are associated with structural and architectural alterations of the musculotendinous unit, such as tendon retraction, muscular atrophy and fatty infiltration. Rotator cuff tears may cause chronic pain and severe functional disability, as well as compromise joint mechanics leading to degenerative joint changes. Rotator cuff tears may require surgical repair, which attempts to reattach the tendon to bone through different suturing techniques. Repair success is affected by numerous factors, including patient age, number of tendons involved, and size of the tear <sup>2</sup>. Failure rates range between 20 to 95% <sup>3</sup> and tendon degeneration, hypovascularization, muscle atrophy, and lack of tendon-to-bone integration are some of the reasons proposed for failures.

The rotator cuff insertion site, also known as the enthesis, is never completely reformed after surgical reattachment <sup>4; 5</sup>. Instead, healing occurs through synthesis of a fibrovascular disorganized scar tissue composed largely of type III collagen, which lacks strength and proper biomechanical properties leading to high re-tear rates. Patients with re-tears can experience pain relief but usually continue to have compromised function. There have been attempts to improve rotator cuff repair with biological or synthetic tendon grafts or with augmentation techniques <sup>6</sup>; however, consistent healing of the rotator cuff following repair still remains an enormous clinical challenge.

Platelet-rich plasma (PRP) is a plasma fraction with a high platelet concentration that is obtained through centrifugation of whole blood. Activation of platelets within PRP can be

achieved by treatment with calcium chloride, thrombin, or contact with collagen, and leads to the release of several growth platelet-derived factors. The use of PRP to improve rotator cuff repair has been evaluated in both animal models and clinical studies since it is believed that growth factor release at the injury site could lead to cell proliferation, cell differentiation, and angiogenesis. However, the ability of PRP to improve rotator cuff repair is not supported by current clinical evidence <sup>7-10</sup>. Results have been inconsistent, possibly due to the lack of standardization of platelet separation techniques, variability in formulations of PRP used, as well as the short half-life, high diffusibility, and poor stability of PRP *in vivo*.

Chitosan (CS) is a biodegradable and biocompatible natural polymer obtained through chitin deacetylation <sup>11; 12</sup>. In the context of cartilage repair, implants of CS-glycerol phosphate (GP)/blood have previously been shown by our research group to increase cell recruitment, vascularization and bone remodeling <sup>13; 14</sup>, activate a beneficial phenotype of pre-wound healing macrophages <sup>15</sup> and enhance tissue repair integration through osteoclast activity <sup>16</sup>, all of which are expected to be beneficial for rotator cuff repair. More recently, we have developed freeze-dried formulations of CS that can be solubilized in PRP to form injectable CS-PRP implants that coagulate *in situ* <sup>17</sup>. We have shown that chitosan inhibits platelet-mediated clot retraction and increases platelet-derived growth factor release from PRP *in vitro* <sup>18</sup>. The residency time and bioactivity of CS-PRP implants have also been shown *in vivo* to be superior to that of PRP alone <sup>17; 18</sup>. Finally, CS-PRP implants were successfully used to augment cartilage and meniscus repair in small and large animal models <sup>19-21</sup>.

The aim of the current study was to assess whether CS-PRP implants can improve rotator cuff repair in a rabbit model. Surgical tears were created bilaterally in the supraspinatus (SSP)

tendon of the rotator cuff of New Zealand White (NZW) rabbits, which were immediately repaired with transosseous suturing. On the treated side, CS-PRP implants were additionally injected into the transosseous tunnels and the tendon itself. Healing was assessed histologically at time points ranging from 1 day to 2 months post-surgery. Our starting hypotheses were that: 1) CS-PRP implants would induce recruitment of polymorphonuclear cells (PMN) at early time points post-surgery, 2) CS-PRP implants would be degraded by 2 months post-surgery, and 3) CS-PRP implants would improve tendon healing through an increase in cell recruitment, angiogenesis, and bone remodeling.

## **6.2 Materials and methods**

### **6.2.1 Rotator cuff tear model, surgical repair and study design**

The protocol for this study was approved by the University of Montreal institutional committee (initial date of approval September 3<sup>rd</sup> 2015) and was consistent with the Canadian Council on Animal Care guidelines for the care and use of laboratory animals. The bilateral rotator cuff tear model was first validated in a pilot feasibility study in 4 retired breeder female NZW rabbits (**Table 1**). Then, a larger efficacy study was performed using 13 skeletally mature female NZW rabbits aged 9 months (**Table 2**). The SSP tendon was exposed and a complete tear was created with a scalpel blade, as close as possible to the insertion site (**Figure 1a**). The remaining stump was debrided, exposing the greater tuberosity. The tear was immediately repaired with a transosseous suturing technique described previously<sup>22-28</sup>. Briefly, a ~ 5 mm bony trough was drilled in the cancellous bone of the greater tuberosity using a high-speed

microdrill (Ideal model, Geneq Scientific Instruments Inc) fitted with a 2.1 mm diameter drill bit (Fine Science Tools). Three 1.4 mm diameter drill holes were then drilled from the lateral aspect of the humerus to connect to the bony trough (**Figure 1b**). Cold irrigation with Ringer's lactate was used throughout drilling. Two 3.0 prolene sutures were passed through the lateral holes, the bony trough and the tendon itself in a modified Mason-Allen pattern. In treated shoulders, in addition to sutures, CS-PRP implants were applied as described below (**Figure 1c**). Sutures were tightened over the lateral aspect of the humerus, thus pulling the tendon towards the greater tuberosity (**Figure 1d**). The animals were allowed ad libitum cage activity postoperatively. Pain control was achieved with transdermal fentanyl patches for 4 days and two rabbits had rymadyl injections for 3 consecutive days for additional pain relief.

Table 6-1. Design of Study 1-Pilot feasibility study.

<b>Group</b>	<b>Treatment shoulder 1</b>	<b>Treatment shoulder 2</b>	<b># Animals / timepoints</b>
1	Intact	Intact	n = 1 at day 0
2	Suturing + CS-PRP	Suturing + CS-PRP	n = 1 at day 1
3	Suturing + CS-PRP	Suturing	n = 1 at day 14 n = 1 at 2 months

Table 6-2. Design of Study 2-Larger efficacy study.

Group	Treatment shoulder 1	Treatment shoulder 2	# Animals / time points
1	Intact	Intact	n = 2 at day 0
2	Suturing + CS-PRP <sup>1</sup>	Suturing + CS-PRP <sup>1</sup>	n = 2 at day 1
3	Suturing + CS-PRP	Suturing only	n = 1 at day 7
4	Suturing + CS-PRP	Suturing only	n = 8 at 2 months

<sup>1</sup> A Rhodamine-chitosan tracer was used in these animals for imaging purposes.

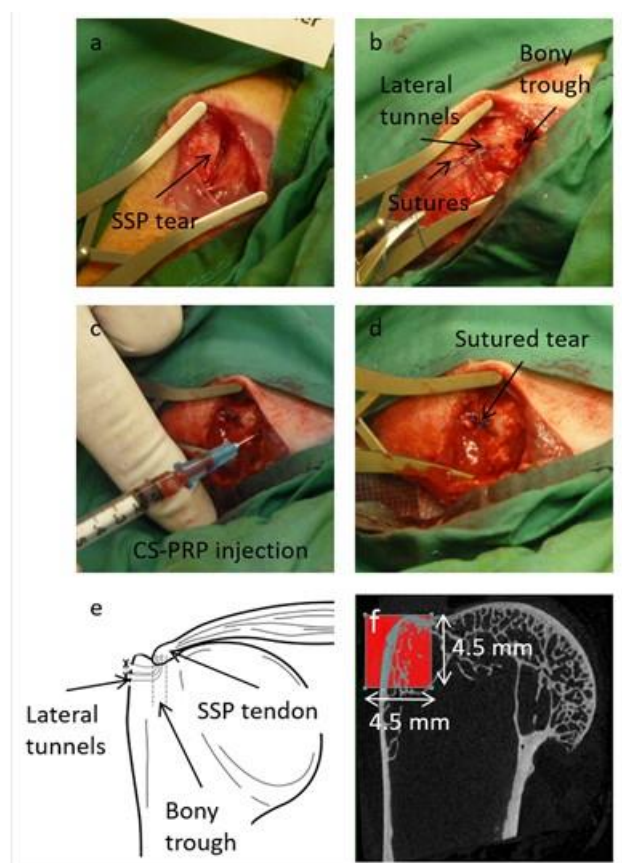


Figure 6-1. a-d) Surgical procedure. A complete surgical tear was created in the supraspinatus (SSP) tendon of the rotator cuff, as close as possible to the insertion site (a). Two 3.0 prolene sutures were pre-placed through the bony trough, the lateral tunnels (b) and the tendon itself in a

modified Mason-Allen pattern. In the case of treated shoulders, the CS-PRP mixture (150  $\mu$ L) was injected into the bony trough prior to tightening the sutures (c), and it flowed out of all lateral tunnels. Sutures were tightened to attach the tendon to the humeral head (d). The CS-PRP mixture (150  $\mu$ L) was then injected at the repaired insertion site and into the tendon itself. e) Schematic representation of the surgical model. f) Area in red is the region of interest (ROI) that was set over the greater tuberosity and used for micro-CT analysis.

### **6.2.2 Preparation of freeze-dried chitosan formulations**

Chitosan with 80.2% degree of deacetylation (DDA) and 36 kDa number average molar mass ( $M_n$ ) was used to prepare formulations containing 1 % (w/v) chitosan, 28mM HCl, 1% (w/v) trehalose as a lyoprotecting agent and 42.2 mM  $\text{CaCl}_2$  as a PRP activator. This chitosan solution was filter-sterilized and 300  $\mu\text{L}$  aliquots were distributed into sterile, de-pyrogenized 2cc glass vials and freeze-dried in 3 phases: 1) ramped freezing to  $-40^\circ\text{C}$  in 1 hour, isothermal 2 hours at  $-40^\circ\text{C}$ , 2)  $-40^\circ\text{C}$  for 48 hours, 3) ramped heating to  $30^\circ\text{C}$  in 12 hours, isothermal 6 hours at  $30^\circ\text{C}$ , at 100 millitorrs. Filter-sterile rhodamine-chitosan tracer <sup>29</sup> of corresponding  $M_n$  and DDA was added to 8 of the vials for imaging purposes.

### **6.2.3 Preparation of platelet-rich plasma (PRP)**

Prior to surgery, 9 mL of blood was drawn from the rabbit ear artery and anti-coagulated with 1 mL 3.8% (w/v) sodium citrate (final citrate concentration 12.9 mM). Blood was centrifuged for 10 min at 1300 rpm and then for 10 min at 2000 rpm using the ACE EZ-PRP<sup>TM</sup> centrifuge to extract ~ 1.5 mL PRP per rabbit. On average, the leukocyte-rich PRP contained  $838 \times 10^9/\text{L}$  platelets,  $6.0 \times 10^9/\text{L}$  leukocytes and  $1.7 \times 10^{12}/\text{L}$  erythrocytes.

### **6.2.4 Solubilization of freeze-dried chitosan formulations in PRP and injection of CS-PRP implants**

Freeze-dried chitosan cakes (300  $\mu\text{L}$ ) were solubilized with autologous PRP (300  $\mu\text{L}$ ) and injected using a 1-cc syringe equipped with a 25-gauge needle in 2 phases: 1) 150  $\mu\text{L}$  injected



prior to suturing the tendon, into the bony trough until it flowed out of the lateral tunnels and 2) 150  $\mu$ L injected following suturing, within the SSP tendon itself at the reattached insertion site. The rabbits were randomly divided into 3 groups (**Tables 1 & 2**): 1) Intact controls (n=3 rabbits; 1 rabbit in Study 1 and 2 rabbits in Study 2); 2) Animals treated bilaterally with suturing + CS-PRP and sacrificed at 1 day post-operative to assess implant distribution (n=3 rabbits; 1 rabbit in Study 1 and 2 rabbits in Study 2); 3) Animals treated with suturing + CS-PRP on one side and suturing only on the contralateral side and sacrificed at day 7 (n=1 rabbit in Study 2), day 14 (n=1 rabbit in Study 1) and at 2 months (n=9 rabbits; 1 rabbit in Study 1 and 8 rabbits in Study 2).

### **6.2.5 Specimen collection and histological processing**

Both shoulders were dissected carefully to remove the SSP muscle, its tendon, and the proximal part of the humerus in one piece and the glenoid articular surface. SSP tendon attachment was scored macroscopically as intact/native (0), completely attached with tissue different from native (1), partially attached with tissue different from native (2) or detached (3). The SSP muscle-tendon-humeral head complex and the glenoid surfaces were fixed with 10% neutral buffered formalin and trimmed for further processing. The calcified tissues were decalcified with 0.1N HCl with trace glutaraldehyde. All samples were dehydrated in graded alcohol solutions and cleared in xylene for paraffin processing. Sections (5 $\mu$ m thickness) were stained with Safranin O/Fast Green and scanned with a Nanozoomer RS (Hamamatsu) for histological evaluation by two blinded observers (GDT and AC). Histological scoring of the SSP tendon (**Table 3**) and SSP tendon enthesis (**Table 4**) was based on systems reported previously<sup>30</sup>:

<sup>31</sup>. Briefly, the SSP tendon was scored for cellularity, presence of tenocytes or inflammatory cells, vascularity, tissue organization, and heterotopic bone formation, with ranges between 0 (best score) to 3 (worst score). Inter-reader ICC for the tendon scoring system was excellent for 5 out of 6 categories (ICC > 0.90), and good for the heterotopic bone formation category (ICC = 0.68). The enthesis was scored for tendon attachment, attachment at anatomically correct location, presence of GAGs at the insertion site, and structural appearance of the enthesis, ranging between 0 (best score) to 2 (worst score) for the first three categories, and from 0 (best score) to 5 (worst score) for the last category. Inter-reader ICC was good for tendon attachment (ICC = 0.70) and excellent for attachment at anatomically correct location (ICC = 0.79), presence of GAGs at the insertion site (ICC = 0.80) and structural appearance of the enthesis (ICC = 0.95). Humeral head and glenoid articular surfaces were scored with the OARSI osteoarthritis cartilage histopathology assessment system <sup>32</sup>. Fatty infiltration in SSP muscle was scored as minimal (0), mild (1), moderate (2) or marked (3). A synovial fluid smear was stained with May-Grünwald-Giemsa staining for cell counting (% leukocyte differential).

Table 6-3 Microscopic scoring of SSP tendon.

Category to score		Score
I	Cellularity	
	Minimal	0
	Mild	1
	Moderate	2

	Marked	3
II	Tenocytes	
	Minimal	0
	Mild	1
	Moderate	2
	Marked	3
III	Inflammatory cells	
	None	0
	Mild	1
	Moderate	2
	Marked	3
IV	Vascularity	
	Minimal	0
	Mild	1
	Moderate	2
	Marked	3
	Tissue organization	

V	Native tendon	<b>0</b>
	Repair tissue mostly tendon-like	<b>1</b>
	Repair tissue a mixture of tendon-like tissue and highly cellular and vascular tissue	<b>2</b>
	Repair tissue highly cellular and vascular tissue	<b>3</b>
VI	Heterotopic bone formation within tendon, far from insertion site	
	None	0
	Slight	1
	Moderate	2
	Marked	3

Table 6-4 Microscopic scoring of SSP entheses.

Category to score		Score
I	Tendon attachment	
	Complete	0
	Partial	1
	Gap	2
	Attachment at anatomically normal site	

II	Yes	0
	Partially	1
	No	2
III	Structural appearance of the enthesis	
	Native insertion with tidemark throughout	0
	Insertion has continuity with bone ingrowth and fibrocartilage and tidemark partially present	1
	Insertion has continuity with bone ingrowth and fibrocartilage cells but no tidemark	2
	Insertion has continuity with fibrous tissue	3
	Insertion has continuity with fat	4
	No continuity	5
IV	Glycosaminoglycans at insertion site	
	Normal	0
	Slight	1
	None	2

### **6.2.6 Micro CT analysis**

Prior to decalcification, the SSP tendon-humeral head complex was scanned using the Skyscan x-ray microtomography 1172 (Kontich, Belgium) with an aluminium filter at 14.1  $\mu\text{M}$  pixel size resolutions and an X-ray source voltage of 56 kV, 1180 msec exposure, 0.45 rotation steps and 3 averaging frames. Images were reconstructed with NRecon software 1.6.1.5 (Kontich, Belgium), using the following parameters: Smoothing of 2, ring artifact reduction of 10, beam-hardening correction of 40%. Datasets were repositioned with DataViewer software 1.4.3 (Kontich, Belgium). The region of interest (4.5 mm in the x axis X 4.5 mm in the y axis X 3 mm in the z axis) was positioned on the edge of the greater tuberosity (**Figure 1f**) and 3D micro CT analysis was performed by using the global thresholding procedure in CTAn software 1.9.3.0 (Kontich, Belgium).

### **6.2.7 Statistical analysis**

Statistical analyses were performed using SAS Enterprise Guide 7.1 and SAS 9.4 (Toronto, ON, Canada). Sections were systematically collected at three sites from each shoulder and scores from the 2 readers were averaged for each section. The mixed model task was used for statistical analysis, where the fixed effect was treatment (Intact vs Sutures + CS-PRP vs Sutures), the random effect was the rabbit number and the repeated effect was the section number. Data in figures are presented as mean (circle); median (line); Box: 25th and 75th percentile; Whiskers:

Box to the most extreme point within 1.5 interquartile range.  $p < 0.05$  was considered statistically significant.

## **6.3 Results**

### **6.3.1 CS-PRP implants adhered to SSP tendon tissue and were resident within the bony trough and lateral tunnels at 1 day post-surgery**

At 1 day post-surgery, the attachment site of the SSP tendon was characterized by gap formation in all of the shoulders (**Figure 2a&e**). Despite our efforts, the stump of the SSP tendon was incompletely debrided in most cases (**Figure 2a&e**). The SSP tendons had areas that were structurally normal, and areas that had altered disorganized structure. Needle tracks containing CS-PRP implant were apparent in some cases (**Figure 2f**). In addition, CS-PRP implants were resident within the bony trough, the lateral tunnels and adhered to the tendon surface, as revealed by epifluorescent imaging (**Figure 2g, i, j &k**).

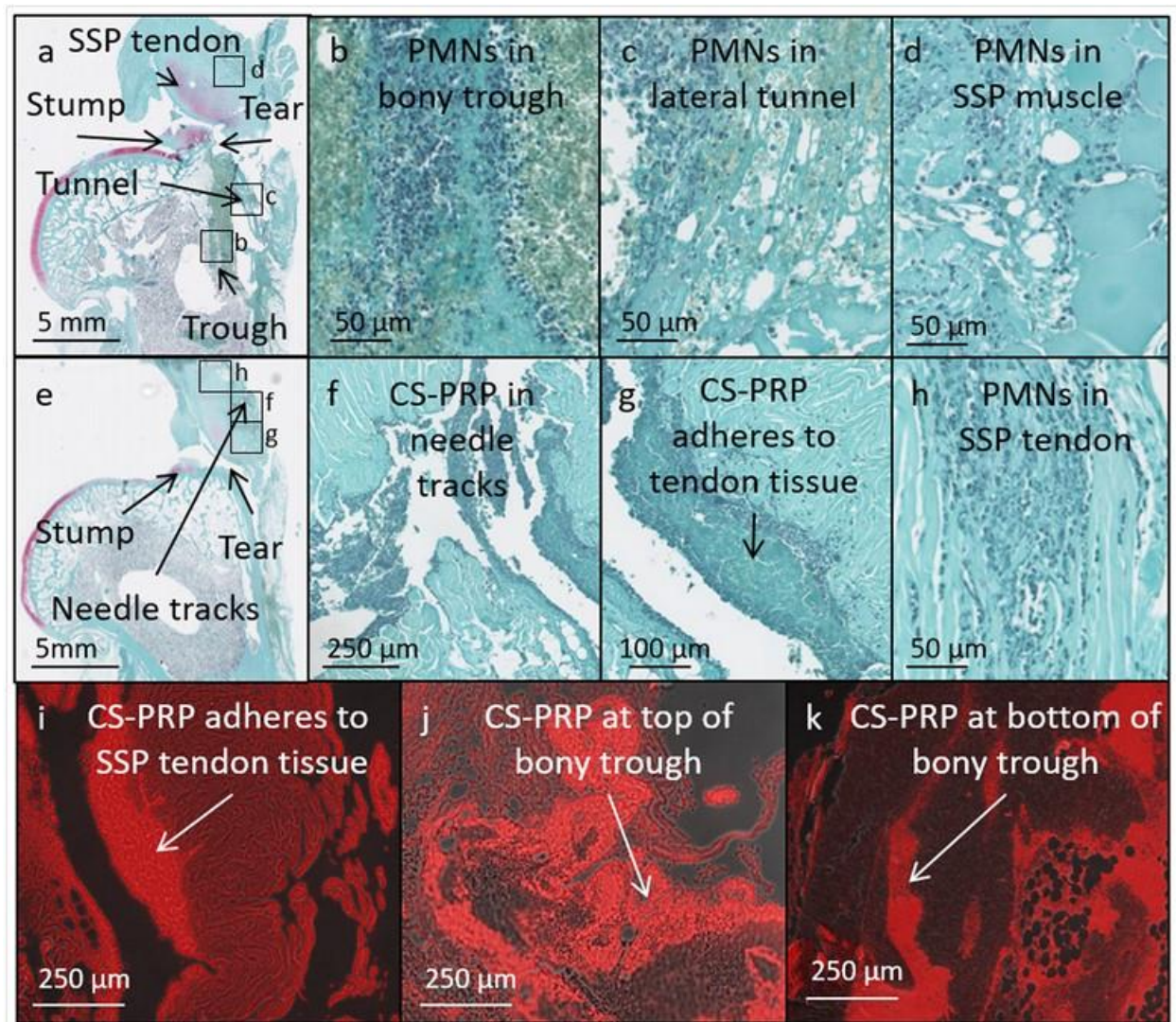


Figure 6-2. a to h) Safranin O/Fast Green-stained paraffin sections of shoulder treated with transosseous suturing + CS-PRP after 1 day. Polymorphonuclear cells (PMNs) were recruited to the bony trough (b), the lateral tunnels (c), to the endomyseal SSP muscle space (d) and to the SSP tendon (h). In some histological sections, needle tracks containing CS-PRP implant were visible within the SSP tendon (e & f). Note that stump of the tendon was not fully debrided in these samples (a and e). i to k) A rhodamine-chitosan tracer was used to image chitosan with epifluorescence in bright red. At one day post-surgery, chitosan-PRP hybrid implant was found adhering to the SSP tendon surface (i) and in the bony trough (j & k).



### **6.3.2 CS-PRP implants induced recruitment of polymorphonuclear (PMN) cells from day 1 to day 14 post-surgery**

In CS-PRP treated shoulders, PMN cells were recruited to the bony trough, the lateral tunnels, the SSP tendon and the endomysial space between SSP muscle fibers at day 1 (**Figure 2**), day 7 (**Figure 3**) and day 14. Tears were still evident at the insertion site, for both groups, with CS-PRP and without CS-PRP, at day 7 post-surgery (**Figure 3b&f**), but not by day 14, where granulation tissue had filled the space. The structure of the SSP tendons was altered in all cases at days 7 and 14, where residual native-appearing tendon tissue was surrounded by highly cellular and vascularized granulation tissue (**Figure 3**). New bone was forming at the lateral aspect of the humerus by day 7 in both groups, without and with CS-PRP (See example in **Figure 3d**). Chondrogenesis was visible within the SSP tendon body at 7 days, far from the insertion site, in the control sutured shoulder only (**Figure 3h**), but not in the case of CS-PRP treatment.

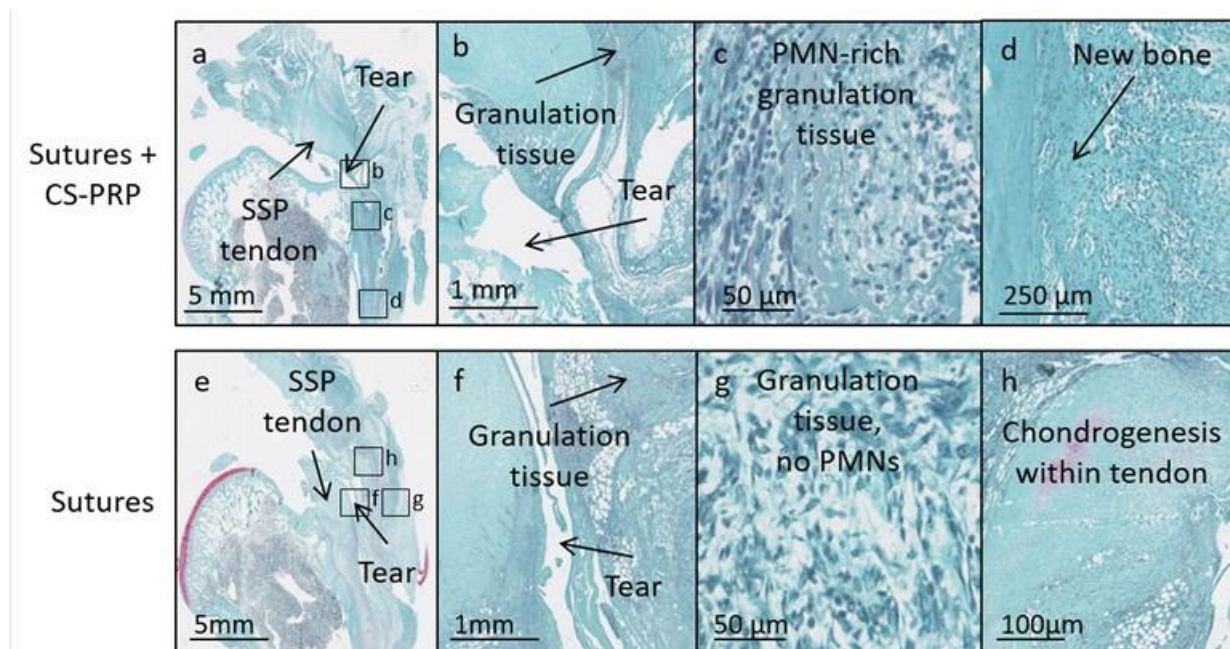


Figure 6-3. Safranin O/Fast Green-stained paraffin sections of shoulder treated with transosseous suturing + CS-PRP (a to d) or suturing only (e to h) after 7 days. Residual structurally normal SSP tendon tissue was apparent and gaps were present at the tear site in all samples (a, b, e & f). Polymorphonuclear (PMN) cells were abundant in the granulation tissue of the CS-PRP treated shoulder only (c vs g). New bone was forming at the lateral aspect of the cortical bone in both groups (example shown in d). Chondrogenesis was observed in the SSP tendon of the control sutured shoulder only (h). Outlines in a & e show where higher magnification images were acquired.

### 6.3.3 CS-PRP implants inhibited heterotopic ossification of SSP tendon tissue at 2 months

By 2 months post-surgery, significant remodeling of the SSP tendon structure had occurred in all shoulders, regardless of treatment (**Figure 4e to l**). SSP tendons were highly cellular and vascular compared to native intact tissues (**Figure 4**). Heterotopic bone formation

was observed in 5 out of 9 SSP tendons of control sutured shoulders and less frequently in the case of CS-PRP treatment ( $p=0.007$  comparing suturing only to suturing+CS-PRP; **Figure 4k, l & m**). In 6 out of 9 shoulders treated with CS-PRP, PMNs were no longer visible at 2 months. However, in the remaining 3 shoulders, neutrophil-rich granulation tissue and areas of apoptotic or necrotic tissue was still apparent ( $p<0.0001$  comparing suturing+CS-PRP to suturing only; **Figure 4g, h & m**). In contrast, there were no PMNs in any of the 9 control sutured shoulders.

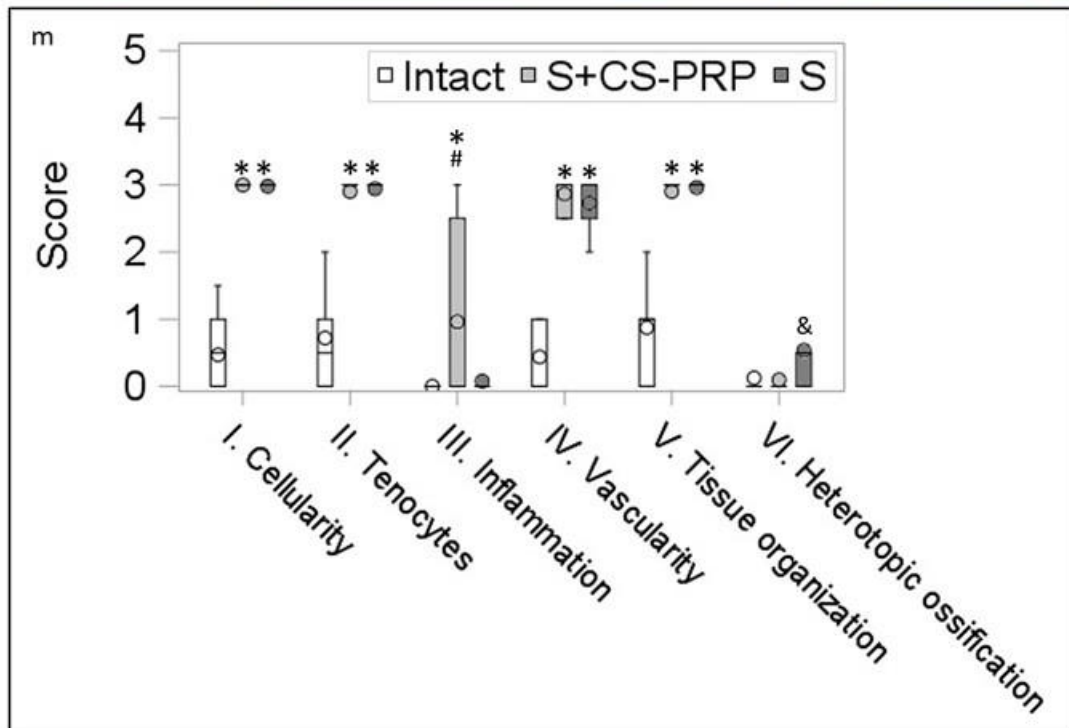
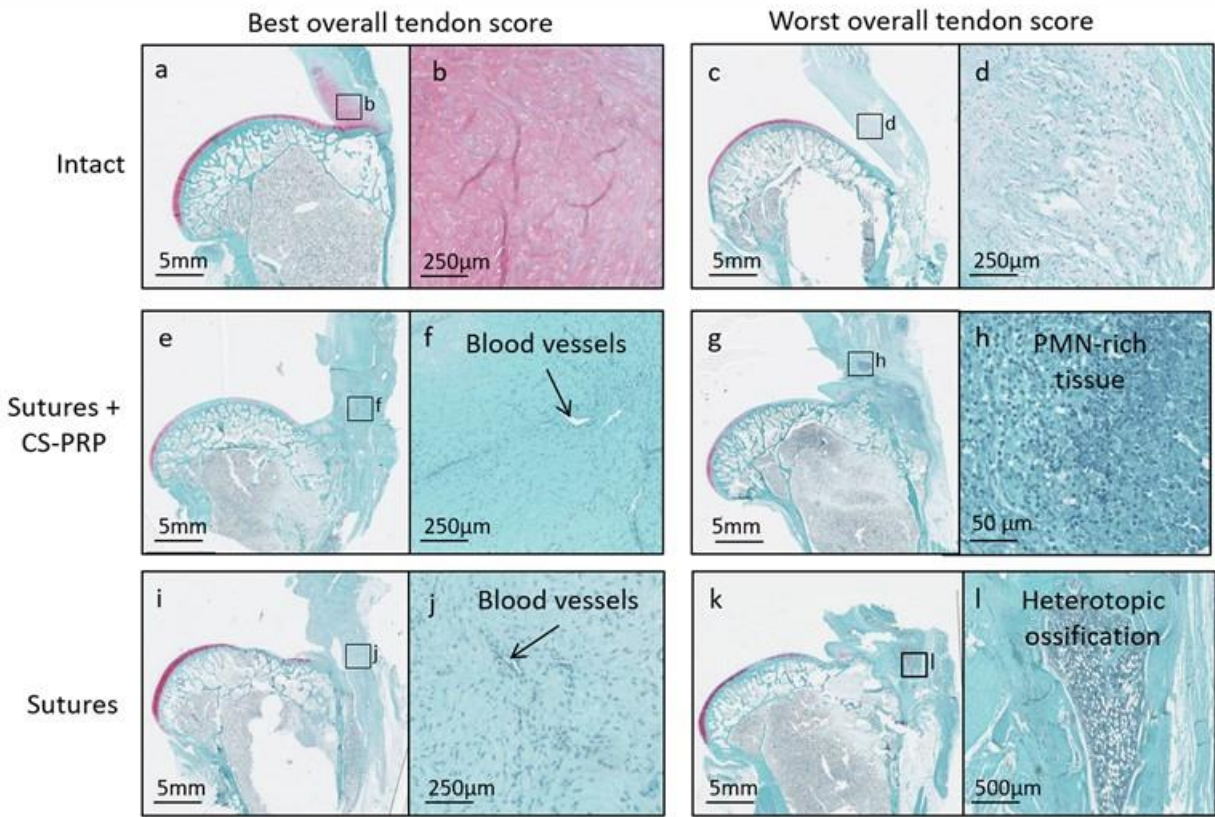


Figure 6-4. Safranin O/Fast Green-stained paraffin sections of intact shoulders (a to d), and test shoulders treated with transosseous suturing + CS-PRP (e to h) or suturing only (i to l) after 2 months, showing best and worst overall tendon scores for all groups. SSP tendon structure was altered in all surgically treated shoulders with several tendons displaying a highly cellular and vascular phenotype (e, f, i & j). Inflammatory PMN-rich tissue was present in 3 out of 9 shoulders treated with transosseous suturing + CS-PRP at 2 months (g & h). Heterotopic ossification within the SSP tendon was observed in 5 out of 9 shoulders treated with transosseous suturing (k & l). Data in m are presented as mean (circle), median (line); Box: 25<sup>th</sup> and 75<sup>th</sup> percentile; Whisker: Box to the most extreme point within 1.5 interquartile range. \*  $p < 0.05$  compared to intact. #  $p < 0.05$  compared to sutures group. &  $p < 0.05$  compared to sutures + CS-PRP group.

### **6.3.4 CS-PRP implants significantly improved attachment of SSP tendon at 2 months**

The macroscopic attachment score (ranging from 0 for intact/native to 3 for detached) was better for shoulders treated with suturing + CS-PRP (average score of 1) compared to shoulders treated with suturing only (average score of 2). CS-PRP treated shoulders also showed better microscopic SSP tendon attachment at the greater tuberosity ( $p=0.0333$  compared to suturing only) at 2 months (**Figure 5m**). In the best cases (**Figure 5f&j**), the enthesis had reformed with a partially calcified interface (in 14 out of 26 histological sections in the CS-PRP treated shoulders and in 7 out of 26 histological sections in the suturing only group). Polarized light microscopy (PLM) showed that collagen fibers were aligned parallel to the long axis of the SSP tendon in those cases, similar to the native intact enthesis (**Figure 6a, c & e**). In the worst cases (**Figure 5h&l**), there were gaps between the humeral head and the repair tissue (in 1 out of 26 histological

sections in the CS-PRP treated shoulders and in 2 out of 26 histological sections in the suturing only group).

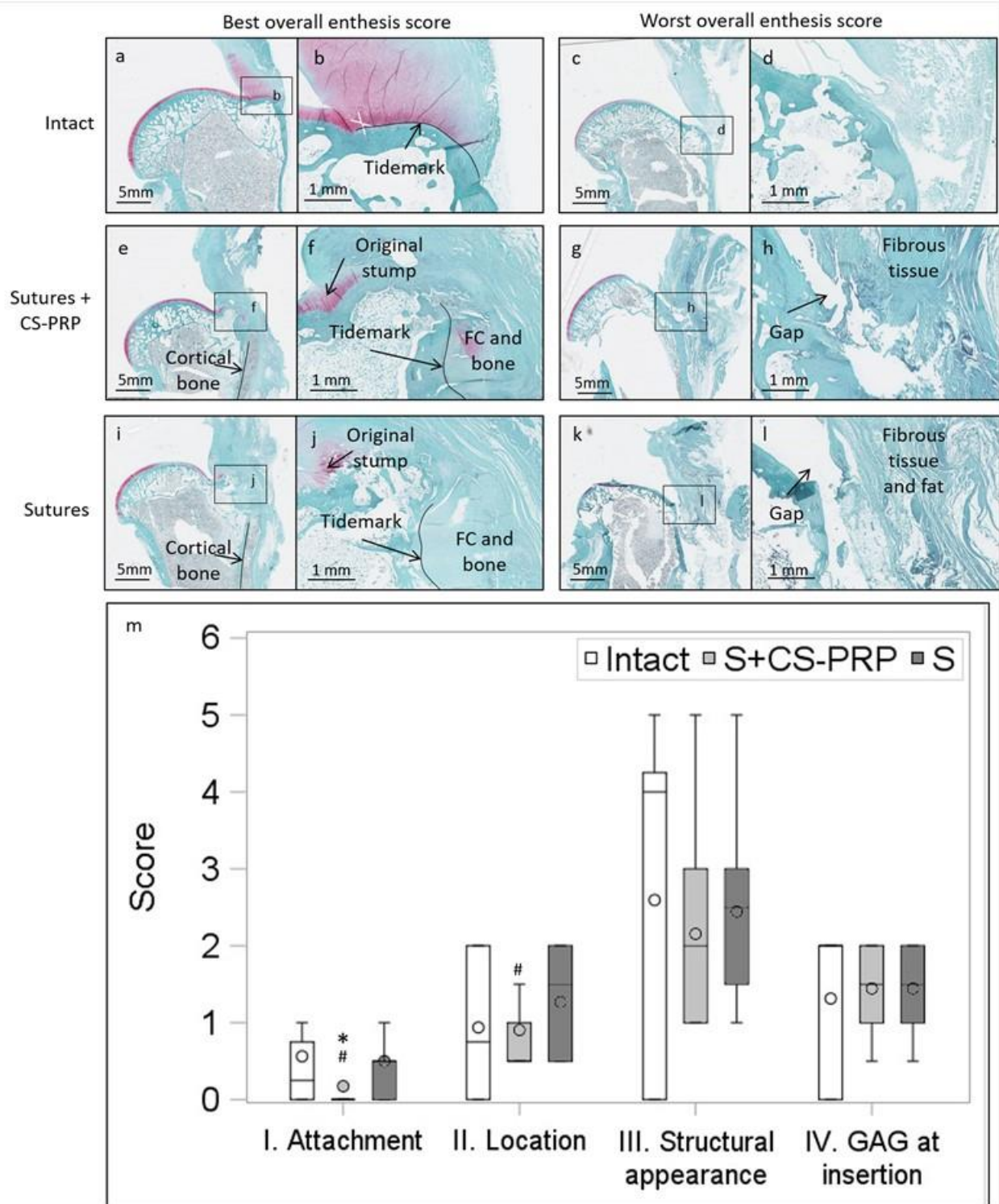


Figure 6-5. Safranin O/Fast Green-stained paraffin sections of intact shoulders (a to d), and test shoulders treated with transosseous suturing + CS-PRP (e to h) or suturing only (i to l) after 2 months, showing best and worst overall enthesis scores for all groups. The original tendon stump was often observed in surgically treated shoulders (e, f, i & j). In the best repair cases, fibrocartilage formation and partial restoration of the tidemark were observed at the enthesis (f & j). In the worst repair cases, gaps were present at the tendon-bone interface (h & l), although treatment with transosseous suturing + CS-PRP decreased such instances (m). Data in m are presented as mean (circle), median (line); Box: 25<sup>th</sup> and 75<sup>th</sup> percentile; Whisker: Box to the most extreme point within 1.5 interquartile range. \*  $p < 0.05$  compared to intact. #  $p < 0.05$  compared to sutures group.

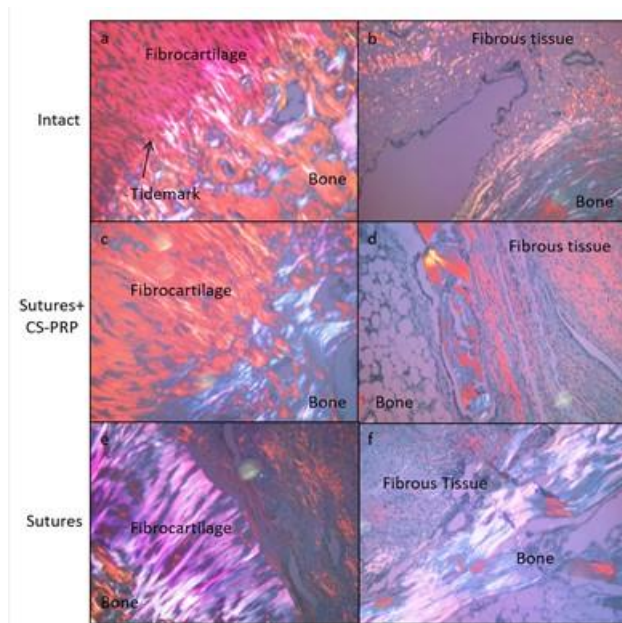


Figure 6-6. Polarized light microscopy images of SSP entheses. In the best cases, wave-like structures and alignment of the collagen fibres parallel to the long axis of the SSP tendon were visible (a, c & e). In the worst cases, very little collagen alignment was apparent in the fibrous tissue adjacent to the bone (b, d & f).



### **6.3.5 CS-PRP implants induced bone remodeling at the greater tuberosity at 2 months**

Micro-CT images showed that incomplete cortical bone repair at the lateral aspect of the humerus (**Figure 7c&d**) and lateral outgrowths of bone (Figure 7e&f) were present in all shoulders, regardless of treatment. Incomplete repair of the bony troughs was observed bilaterally in 5 out of 8 rabbits (**Figure 7g&h**), demonstrating variability in inherent capacity for bone repair between animals. In half the treated shoulders (4 out of 8), bone remodeling was highly stimulated by CS-PRP treatment (**Figure 7, compare panel c to d**), which led to increases in bone surface (**Figure 7j**) and connectivity (**Figure 7h**). In addition, connectivity density and Euler number were also significantly increased by CS-PRP treatment, while there was no significant difference between the two groups for the other 3D bone morphometric parameters assessed (bone volume, trabecular thickness, trabecular separation, trabecular number, trabecular pattern factor, structural model index, fractal dimension and degree of anisotropy).

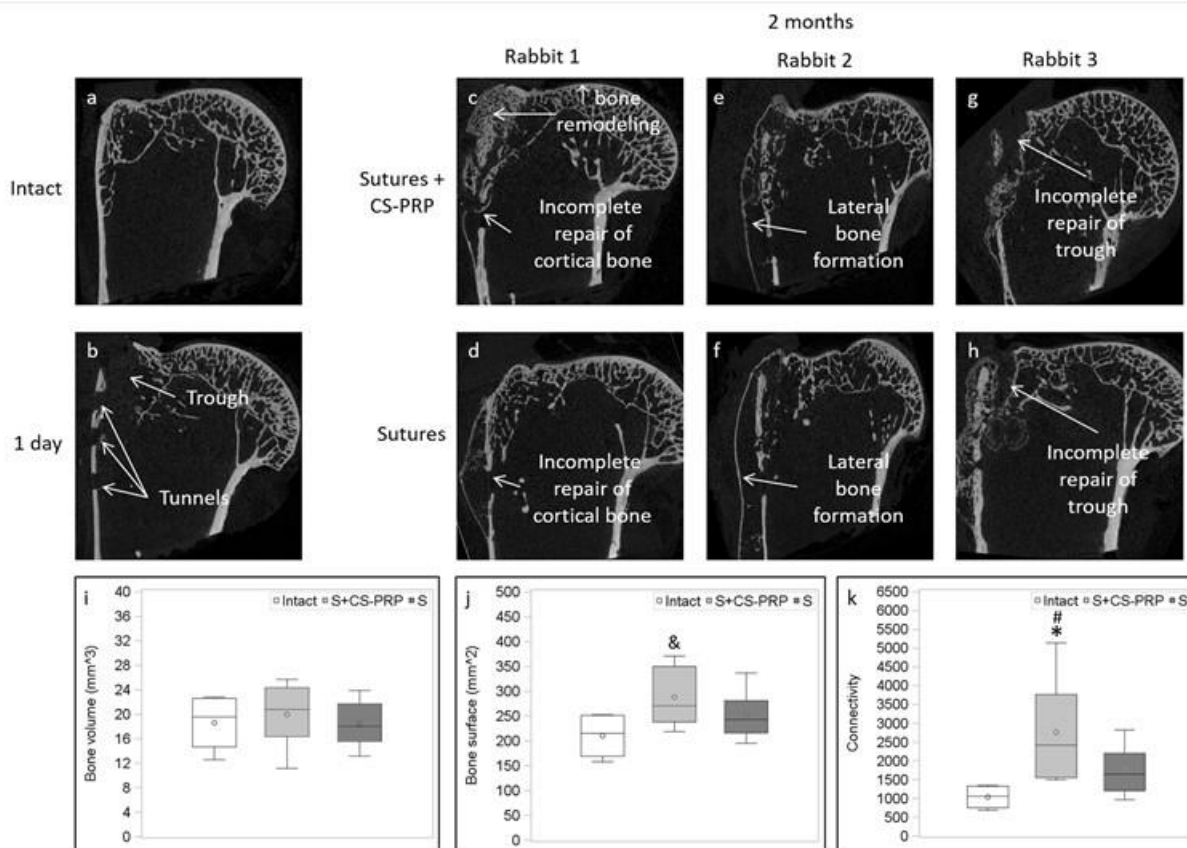


Figure 6-7. Micro-CT of intact (a) and surgically treated shoulder at 1 day (b), and test shoulders treated with transosseous suturing + CS-PRP (c to g) or suturing only (d to h) after 2 months. Incomplete repair of cortical bone at the lateral aspect of the humerus (c & d) and lateral bone formation (e & f) were present in all shoulders, regardless of treatment. Incomplete repair of the bone troughs was observed bilaterally in 5 rabbits (g & h). In half the treated shoulders, bone remodeling was highly stimulated by chitosan-PRP treatment (compare panel c to d), which led to increases in bone surface (j) and connectivity (k). Data in i, j & k are presented as mean (circle), median (line); Box: 25<sup>th</sup> and 75<sup>th</sup> percentile; Whisker: Box to the most extreme point within 1.5 interquartile range. \*  $p < 0.05$  compared to intact. #  $p < 0.05$  compared to sutures group. &  $p < 0.1$  compared to intact.

### 6.3.6 CS-PRP treatment was safe

Clinical and macroscopic observations showed that the CS-PRP formulation did not induce any adverse event in any of the rabbits. No infection, contracture, mobility disability, or excessive inflammatory reaction was observed. Body weights were stable throughout the study, and the surgical sites healed well with no sign of significant effusion. Some humeral head and glenoid articular surfaces showed mild degenerative changes, such as GAG depletion (**Figure 8f, j h & l**), hypocellularity and fissures (**Figure 8f & j**), hypercellularity (**Figure 8h**) and thinning (**Figure 8l**), although average histological scores were not significantly different than those of intact tissues (**Figure 8m**). Surgical detachment and reattachment of the SSP tendon induced mild fatty infiltration of the SSP muscles compared to intact tissues (**Figure 9**). Finally, % leukocyte differential within the synovial fluid was similar for both groups, with and without CS-PRP treatment at 2 months.

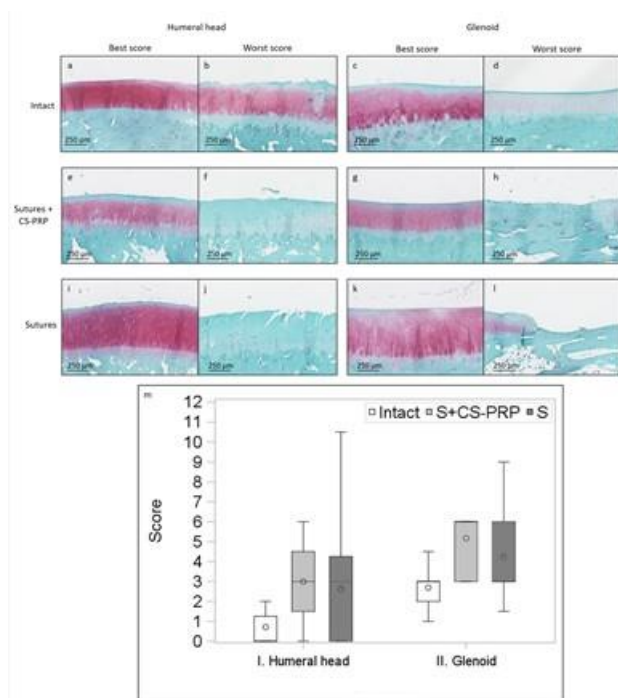


Figure 6-8. Safranin O/Fast Green-stained paraffin sections of intact shoulders (a to d), and test shoulders treated with transosseous suturing + CS-PRP (e to h) or suturing only (i to l) after 2 months, showing best and worst OCHAS scores for humeral head and glenoid articular surfaces (a to l). Some structural abnormalities such as GAG depletion, fissures, cell changes and thinning of the articular cartilage were occasionally observed in both humeral head (b, f & j) and glenoid (d, h & l) surfaces, although average histological scores were not significantly different from intact (m). Data in m are presented as mean (circle), median (line); Box: 25<sup>th</sup> and 75<sup>th</sup> percentile; Whisker: Box to the most extreme point within 1.5 interquartile range.

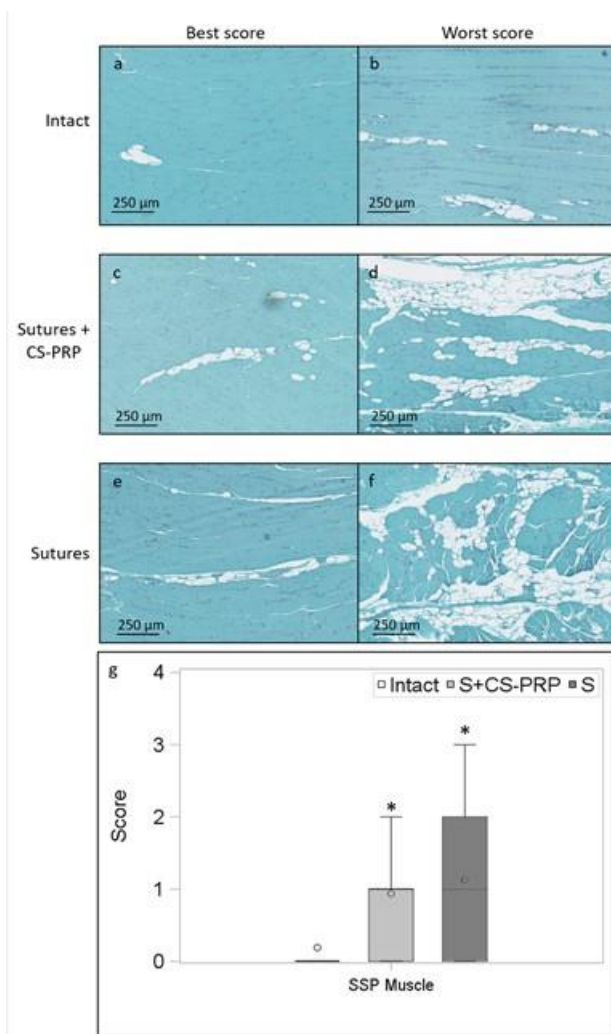


Figure 6-9. Safranin O/Fast Green-stained paraffin sections of SSP muscles from intact shoulders (a & b), and test shoulders treated with transosseous suturing + CS-PRP (c & d) or suturing only (e & f) after 2 months, showing best and worst scores for fatty infiltration. Surgical treatment induced fatty infiltration of SSP muscle after 2 months (g). Data in g are presented as mean (circle), median (line); Box: 25<sup>th</sup> and 75<sup>th</sup> percentile; Whisker: Box to the most extreme point within 1.5 interquartile range. \*  $p < 0.05$  compared to intact.

## 6.4 Discussion

The aim of the current study was to histologically assess whether CS-PRP implants are capable of improving rotator cuff surgical repair. A transosseous repair model in the rabbit was chosen (**Figure 1**) since it has been well described in the literature <sup>22-28</sup>. CS-PRP implants induced PMN recruitment at early time points post-surgery, supporting our first hypothesis. In contrast to the second hypothesis, implant degradation and associated inflammatory reactions were still ongoing in 3 out of 9 treated shoulders at 2 months. Results also supported our third hypothesis that CS-PRP would improve rotator cuff repair, since treatment improved SSP tendon attachment through increased bone remodeling.

One of our objectives was to determine implant distribution and assess implant degradation over time. At 1 day post-surgery, CS-PRP implants were resident inside the bony trough and lateral tunnels and also adhered to tendon surfaces (**Figure 2**), the latter probably due to the mucoadhesive properties of chitosan <sup>33</sup>. Similarly to CS-GP/blood implants <sup>13</sup>, CS-PRP implants stimulated the innate immune response and induced recruitment of PMN cells (**Figures 2&3**), which contributed to implant degradation. It is well known that chitosans with higher

degrees of deacetylation (DDA) and molar mass ( $M_n$ ) will have lower degradation rates, but the site of implantation will also have a significant impact on implant degradation rate. We have previously shown that CS-PRP implants containing chitosan of similar DDA and  $M_n$  as that used in the current study were degraded after 3 weeks in sheep meniscus tears<sup>19; 20</sup>, between 3 to 8 weeks in rabbit cartilage lesions<sup>21</sup>, but that they persisted for at least 6 weeks in a rabbit subcutaneous implantation model<sup>17; 18</sup>. Unexpectedly, small areas of neutrophil-rich granulation tissue surrounding apoptotic/necrotic tissues were visible in 3 out of 9 CS-PRP treated shoulders at 2 months (**Figure 4**). This suggests that implant degradation was not complete in these animals, as residual apoptotic/necrotic granulation tissues were previously shown to correlate with resident chitosan oligomer particles in a rabbit cartilage repair model<sup>34</sup>. Alternatively, it is also possible that PMNs could persist for some time after complete chitosan degradation. A leukocyte-rich PRP was used to prepare the implants in the current study, which would be expected to have an impact on the cytokine profile that is released upon activation. Previous *in vitro* studies have suggested that matrix metalloproteinases (MMP) and cytokines released from leukocyte-rich PRP could have deleterious effects on tendon healing<sup>35; 36</sup>. However, MMPs are believed to be essential for tissue remodeling during rotator cuff tear repair *in vivo*<sup>4; 37</sup> and clinical data regarding using leukocyte-rich versus leukocyte-poor PRP for rotator cuff repair is still inconclusive.

The suppression of SSP tendon heterotopic ossification (HO) by CS-PRP treatment was an unexpected finding in this study (**Figure 4**). HO is an abnormal formation of mature, lamellar bone in soft tissues where bone normally doesn't exist<sup>38</sup>. HO is a well known complication following surgical procedures or traumatic injuries<sup>39; 40</sup>. Osteoinductive factors are released as a

consequence of soft tissue trauma thus inducing formation of heterotopic bone <sup>41-43</sup>. The pathogenesis is unclear, but it may involve inappropriate differentiation of pluripotent mesenchymal stem cells (MSCs) into bone forming cells under growth factor influence <sup>44</sup>. HO occurs through endochondral ossification <sup>38</sup>, the first step of which is differentiation of MSCs into chondrocytes, an event we observed here in the control sutured shoulder at 7 days (**Figure 3**), but not in the shoulder treated with CS-PRP. Interestingly, CS-GP/blood implants were also previously shown to modulate the timing and spatial development of chondrogenesis and endochondral ossification in a rabbit cartilage repair model <sup>45</sup>.

The bone surrounding the bony trough is a probable source of repair cells in this model, as are bursa or synovial-derived cells <sup>22</sup>. The tendon stump appeared to contribute little to healing, and was integrated within the new repair tissue at 2 months in most cases (**Figure 5**). Improving tendon-bone healing is a common clinical challenge in rotator cuff repair. Development of bone-tendon junction occurs through chondrogenesis and tenogenesis, followed by mineralization <sup>46-50</sup>, while tendon-bone repair appears to depend upon bone ingrowth into fibrovascular interface tissue. Surgical reattachment of rotator cuff tendon with current repair techniques leads to a more abrupt interface and a disorganized scar tissue that is mechanically inferior to the native interface <sup>51; 52</sup>, and augmentation techniques still need to be developed to overcome this limitation. As reported previously <sup>22</sup>, enthesis regeneration was not achieved in the transosseous repair model used here; however, partial restoration of the calcified interface was more common with CS-PRP treatment (**Figures 5&6**). Growth factors synthesized and secreted by cells involved in tissue repair, such as platelets, inflammatory cells, fibroblasts, epithelial cells, and vascular endothelial cells <sup>53</sup>, all regulate tendon-bone repair, and it is likely that treatment with CS-PRP modulates

such signals. Gap formation is thought to be associated with impaired rotator cuff healing<sup>54</sup>, preventing enthesis reformation<sup>27</sup>. CS-PRP treatment promoted attachment of the SSP tendon, possibly through an increase in bone remodeling at the greater tuberosity (**Figure 7**). Previous cartilage repair studies in the rabbit also showed that both CS-GP/blood implants and CS-PRP implants promote bone remodeling and tissue integration<sup>13; 14; 16; 21</sup>. The bony trough was incompletely healed in some rabbits, consistent with previously published data showing that complete recovery of the bony trough only occurs after 12 weeks post-surgery in this model<sup>23</sup>.

No treatment-specific adverse events occurred during the study, which suggests high safety. Surgical detachment and immediate reattachment of the SSP tendon was sufficient to cause fatty infiltration of the SSP muscle but did not induce degeneration of the humeral head and glenoid articular surfaces (**Figures 8&9**), while treatment with CS-PRP did not alter the cell distribution within the synovial fluid of the shoulder.

This study had several limitations. No animal model fully reproduces human injury condition. The shoulder joints are weight-bearing in rabbits and acute tears do not represent human chronic tears. However, we chose this model since the rotator cuff in rabbits heals in a fashion that is similar to that of humans<sup>55</sup>. Additionally, the rabbit model allowed us to collect enough blood to extract the required PRP volume to solubilize the freeze-dried chitosan. Another limitation is that the transosseous repair technique used here differs from suture anchors which are more commonly used in humans. However, use of suture anchors would be difficult due to the small size of the glenohumeral joint in rabbits. The inability to limit weight bearing and activity post-operatively may contribute to sutures pulling out of the rabbit tendon. We did not include a suturing+PRP group here as an additional control since it is well established in the



current literature that PRP alone does not improve rotator cuff repair. However, it will be imperative to conduct a comparative study with a control group receiving treatment with suturing+PRP alone in order to distinguish between the effects arising from chitosan and from PRP. Moreover, our small sample size at early time points does not allow us to elaborate on the mechanisms involved in the repair process. Finally, although a histological improvement in SSP tendon attachment would be expected to translate into superior attachment strength, no biomechanical testing was performed.

Rotator cuff repair remains a pressing clinical challenge. Despite our study's limitations, our preliminary study showed that using CS-PRP implants in conjunction with transosseous suturing improves attachment of the SSP tendon to the humeral head compared to suturing alone. This study provides evidence that CS-PRP implants are safe and possibly effective in improving rotator cuff tear repair in a small animal model, and that this could potentially be translated to a clinical setting. Future work should involve a larger number of animals, a longer duration of follow-up, additional control groups, biomechanical testing, and assessment of efficacy in a larger animal model of rotator cuff repair.

### **Acknowledgements**

We acknowledge the technical contributions of Jun Sun and Geneviève Picard and the funding sources (Canadian Institutes of Health Research, Canada Foundation for Innovation, Groupe de Recherche en Sciences et Technologies Biomédicales, Natural Sciences and Engineering Research Council of Canada and Ortho Regenerative Technologies Inc.). AC and

MDB hold shares, MDB is a Director and MS and SR are clinical advisors of Ortho Regenerative Technologies Inc.

## References

1. Lehman C, Cuomo F, Kummer FJ, et al. 1995. The incidence of full thickness rotator cuff tears in a large cadaveric population. *Bull Hosp Joint Dis* 54:30-31.
2. Barber FA, Hrnack SA, Snyder SJ, et al. 2011. Rotator cuff repair healing influenced by platelet-rich plasma construct augmentation. *Arthroscopy* 27:1029-1035.
3. Galatz LM, Ball CM, Teefey SA, et al. 2004. The outcome and repair integrity of completely arthroscopically repaired large and massive rotator cuff tears. *J Bone Joint Surg-Am* 86A:219-224.
4. Gulotta LV, Rodeo SA. 2009. Growth factors for rotator cuff repair. *Clin Sports Med* 28:13-23.
5. Chung SW, Kim SH, Oh JH. 2014. Animal Experiments Using Rotator Cuff. *Clinics in Shoulder & Elbow* 17:84-90.
6. Deprés-Tremblay G, Chevrier A, Snow M, et al. 2016. Rotator cuff repair: a review of surgical techniques, animal models, and new technologies under development. *J Shoulder Elbow Surg* 25:2078-2085.

7. Vavken P, Sadoghi P, Palmer M, et al. 2015. Platelet-Rich Plasma Reduces Retear Rates After Arthroscopic Repair of Small- and Medium-Sized Rotator Cuff Tears but Is Not Cost-Effective. *Am J Sports Med* 43: 3070-6.
8. Li X, Xu C-P, Hou Y-L, et al. 2014. Are Platelet Concentrates an Ideal Biomaterial for Arthroscopic Rotator Cuff Repair? A Meta-analysis of Randomized Controlled Trials. *Arthroscopy* 30:1483-1490.
9. Zhao J-G, Zhao L, Jiang Y-X, et al. 2015. Platelet-Rich Plasma in Arthroscopic Rotator Cuff Repair: A Meta-analysis of Randomized Controlled Trials. *Arthroscopy* 31:125-135.
10. Warth RJ, Dornan GJ, James EW, et al. 2015. Clinical and Structural Outcomes After Arthroscopic Repair of Full-Thickness Rotator Cuff Tears With and Without Platelet-Rich Product Supplementation: A Meta-analysis and Meta-regression. *Arthroscopy* 31:306-320.
11. Krueger CA, Wenke JC, Masini BD, et al. 2012. Characteristics and impact of animal models used for sports medicine research. *Orthopedics* 35:e1410-1415.
12. Muzzarelli RAA. 2009. Chitins and chitosans for the repair of wounded skin, nerve, cartilage and bone. *Carb Polym* 76:167-182.
13. Chevrier A, Hoemann CD, Sun J, et al. 2007. Chitosan-glycerol phosphate/blood implants increase cell recruitment, transient vascularization and subchondral bone remodeling in drilled cartilage defects. *Osteoarthr Cart* 15:316-327.

14. Hoemann CD, Sun J, McKee MD, et al. 2007. Chitosan-glycerol phosphate/blood implants elicit hyaline cartilage repair integrated with porous subchondral bone in microdrilled rabbit defects. *Osteoarthr Cart* 15:78-89.
15. Hoemann CD, Chen GP, Marchand C, et al. 2010. Scaffold-Guided Subchondral Bone Repair Implication of Neutrophils and Alternatively Activated Arginase-1+Macrophages. *Am J Sports Med* 38:1845-1856.
16. Chen G, Sun J, Lascau-Coman V, et al. 2011. Acute Osteoclast Activity following Subchondral Drilling Is Promoted by Chitosan and Associated with Improved Cartilage Repair Tissue Integration. *Cartilage* 2:173-185.
17. Chevrier A, Darras V, Picard G, et al. 2017. Injectable chitosan-platelet-rich plasma (PRP) implants to promote tissue regeneration: In vitro properties, in vivo residence, degradation, cell recruitment and vascularization. *J Tiss Eng Reg Med* In Press.
18. Deprés-Tremblay G, Chevrier A, Tran-Khanh N, et al. 2016. Chitosan-platelet-rich plasma implants for tissue repair - in vitro and in vivo characteristics. *World Biomaterials Congress*. Montreal, QC, Canada.
19. Chevrier A, Deprés-Tremblay G, Hurtig MB, et al. 2016. Chitosan-platelet-rich plasma implants can be injected into meniscus defects to improve repair. *Transactions Orthopaedic Research Society*. Orlando, FL, USA.
20. Ghazi zadeh L, Chevrier A, Hurtig MB, et al. 2017. Freeze-dried chitosan-PRP injectable surgical implants for meniscus repair: results from pilot ovine studies. *Transactions Orthopaedic Research Society*. San Diego, CA, USA.

21. Dwivedi G, Chevrier A, Hoemann CD, et al. 2017. Freeze dried chitosan/platelet-rich-plasma implants improve marrow stimulated cartilage repair in rabbit chronic defect model Transactions Orthopaedic Research Society. San Diego, CA, USA.
22. Uthoff HK, Sano H, Trudel G, et al. 2000. Early reactions after reimplantation of the tendon of supraspinatus into bone. A study in rabbits. *J Bone Joint Surg-Br* 82:1072-1076.
23. Uthoff HK, Seki M, Backman DS, et al. 2002. Tensile strength of the supraspinatus after reimplantation into a bony trough: an experimental study in rabbits. *J Shoulder Elbow Surg* 11:504-509.
24. Uthoff HK, Matsumoto F, Trudel G, et al. 2003a. Early reattachment does not reverse atrophy and fat accumulation of the supraspinatus--an experimental study in rabbits. *J Orthop Res* 21:386-392.
25. Koike Y, Trudel G, Uthoff HK. 2005. Formation of a new enthesis after attachment of the supraspinatus tendon: A quantitative histologic study in rabbits. *J Orthop Res* 23:1433-1440.
26. Koike Y, Trudel G, Curran D, et al. 2006. Delay of supraspinatus repair by up to 12 weeks does not impair enthesis formation: a quantitative histologic study in rabbits. *J Orthop Res* 24:202-210.
27. Trudel G, Ramachandran N, Ryan SE, et al. 2012a. Improved strength of early versus late supraspinatus tendon repair: a study in the rabbit. *J Shoulder Elbow Surg* 21:828-834.

28. Trudel G, Ryan SE, Rakhra K, et al. 2012b. Muscle tissue atrophy, extramuscular and intramuscular fat accumulation, and fat gradient after delayed repair of the supraspinatus tendon: A comparative study in the rabbit. *J Orthop Res* 30:781-786.
29. Ma O, Lavertu M, Sun J, et al. 2008. Precise derivatization of structurally distinct chitosans with rhodamine B isothiocyanate. *Carb Polym* 72:616-624.
30. Watkins JP, Auer JA, Gay S, et al. 1985. Healing of surgically created defects in the equine superficial digital flexor tendon: collagen-type transformation and tissue morphologic reorganization. *Am J Vet Res* 46:2091-2096.
31. Ide J, Kikukawa K, Hirose J, et al. 2009. The effects of fibroblast growth factor-2 on rotator cuff reconstruction with acellular dermal matrix grafts. *Arthroscopy* 25:608-616.
32. Pritzker KP, Gay S, Jimenez SA, et al. 2006. Osteoarthritis cartilage histopathology: grading and staging. *Osteoarthr Cart* 14:13-29.
33. Henriksen I, Green KL, Smart JD, et al. 1996. Bioadhesion of hydrated chitosans: An in vitro and in vivo study. *Int J Pharms* 145:231-240.
34. Lafantaisie-Favreau CH, Guzman-Morales J, Sun J, et al. 2013. Subchondral pre-solidified chitosan/blood implants elicit reproducible early osteochondral wound-repair responses including neutrophil and stromal cell chemotaxis, bone resorption and repair, enhanced repair tissue integration and delayed matrix deposition. *BMC Musculosk Dis* 14:1-16.

35. Dragoo JL, Braun HJ, Durham JL, et al. 2012. Comparison of the acute inflammatory response of two commercial platelet-rich plasma systems in healthy rabbit tendons. *Am J Sports Med* 40:1274-1281.
36. McCarrel TM, Minas T, Fortier LA. 2012. Optimization of leukocyte concentration in platelet-rich plasma for the treatment of tendinopathy. *J Bone Joint Surg-Am* 94: 141-148.
37. Fabis J, Kordek P, Bogucki A, et al. 1998. Function of the rabbit supraspinatus muscle after detachment of its tendon from the greater tubercle - Observations up to 6 months. *Acta Orthop Scand* 69:570-574.
38. Zhang J, Zhao Y, Hou X, et al. 2014. The inhibition effects of insulin on BMP2-induced muscle heterotopic ossification. *Biomaterials* 35:9322-9331.
39. Barfield WR, Holmes RE, Hartsock LA. 2017. Heterotopic Ossification in Trauma. *Orthop Clin North Am* 48:35-46.
40. Balboni TA, Gobezie R, Mamon HJ. 2006. Heterotopic ossification: Pathophysiology, clinical features, and the role of radiotherapy for prophylaxis. *Int J Rad Onc Biol Phys* 65:1289-1299.
41. Sneath RJ, Bindi FD, Davies J, et al. 2001. The effect of pulsed irrigation on the incidence of heterotopic ossification after total hip arthroplasty. *J Arthroplasty* 16:547-551.
42. Nilsson OS, Persson PE. 1999. Heterotopic bone formation after joint replacement. *Curr Op Rheumatol* 11:127-131.

43. Chalmers J, Gray DH, Rush J. 1975. Observations on the induction of bone in soft tissues. *J Bone Joint Surg-Br* 57:36-45.
44. Lewallen DG. 1995. Heterotopic ossification following total hip arthroplasty. *Instr Course Lect* 44:287-292.
45. Chevrier A, Hoemann CD, Sun J, et al. 2011. Temporal and spatial modulation of chondrogenic foci in subchondral microdrill holes by chitosan-glycerol phosphate/blood implants. *Osteoarthr Cart* 19:136-144.
46. Rees JD, Wilson AM, Wolman RL. 2006. Current concepts in the management of tendon disorders. *Rheumatology (Oxford, England)* 45:508-521.
47. Lin TW, Cardenas L, Soslowsky LJ. 2004. Biomechanics of tendon injury and repair. *J Biomec* 37:865-877.
48. Hamada Y, Katoh S, Hibino N, et al. 2006. Effects of monofilament nylon coated with basic fibroblast growth factor on endogenous intrasynovial flexor tendon healing. *J Hand Surg* 31:530-540.
49. Lu HH, Thomopoulos S. 2013. Functional attachment of soft tissues to bone: development, healing, and tissue engineering. *Ann Rev Biomed Eng* 15:201-226.
50. Thomopoulos S, Genin GM, Galatz LM. 2010. The development and morphogenesis of the tendon-to-bone insertion - What development can teach us about healing. *J Musculoskel Neur Int* 10:35-45.



51. Thomopoulos S, Hattersley G, Rosen V, et al. 2002. The localized expression of extracellular matrix components in healing tendon insertion sites: an in situ hybridization study. *J Orthop Res* 20:454-463.
52. Thomopoulos S, Williams GR, Soslowky LJ. 2003. Tendon to bone healing: differences in biomechanical, structural, and compositional properties due to a range of activity levels. *J Biomech Eng* 125:106-113.
53. Kobayashi M, Itoi E, Minagawa H, et al. 2006. Expression of growth factors in the early phase of supraspinatus tendon healing in rabbits. *J Shoulder Elbow Surg* 15:371-377.
54. Omi R, Gingery A, Steinmann SP, et al. 2016. Rotator cuff repair augmentation in a rat model that combines a multilayer xenograft tendon scaffold with bone marrow stromal cells. *J Shoulder Elbow Surg* 25:469-477.
55. Gupta R, Lee TQ. 2007. Contributions of the different rabbit models to our understanding of rotator cuff pathology. *J Shoulder Elbow Surg* 16:149S-157S.

**CHAPTER 7      ARTICLE 4: FREEZE-DRIED CHITOSAN-PLATELET-  
RICH PLASMA IMPLANTS FOR ROTATOR CUFF TEAR REPAIR:  
PILOT OVINE STUDIES**

ACS Biomaterials Science and Engineering

*Gabrielle Deprés-Tremblay<sup>1</sup>, Anik Chevrier<sup>2</sup>, Mark B Hurtig<sup>3</sup>, Martyn Snow<sup>4</sup>, Scott Rodeo<sup>5</sup> and*

*\*Michael D Buschmann<sup>1,2</sup>*

<sup>1</sup>Biomedical Engineering Institute and <sup>2</sup>Chemical Engineering Department, Polytechnique, Montreal, QC, Canada, <sup>3</sup>Department of Clinical Studies, University of Guelph, Guelph, ON, Canada, <sup>4</sup>The Royal Orthopaedic Hospital, Birmingham, UK, <sup>5</sup>Sports Medicine and Shoulder Service, The Hospital for Special Surgery, New York, NY, USA

KEYWORDS Rotator cuff tear, chitosan, platelet-rich plasma, chronic repair, acute repair, ovine models.

## ABSTRACT

### Abstract

Rotator cuff tear is a very common shoulder pathology. Different suturing techniques have been used for surgical cuff repair, but failure of healing remains a significant clinical challenge. The objective of this study was to investigate the effect of using chitosan (CS)-platelet-rich plasma (PRP) implants in conjunction with suture anchors in chronic and acute ovine rotator cuff tear models. In two subsequent pilot feasibility studies, unilateral full-thickness tears were created in the infraspinatus (ISP) tendon of mature female Texel-cross sheep. In the chronic model (n=4 sheep), the tendons were capped with silicon and allowed to retract for 6 weeks, leading to degenerative changes, while the tendons were immediately repaired in the acute model (n=4 sheep). Transected ISP tendons were reattached with suture anchors and, in the case of treated shoulders, implants composed of freeze-dried CS solubilized in autologous PRP were additionally applied to the tendon-bone interface and on top of the repaired site. The chronic defect model induced significant tendon degeneration and retraction, which made repair more challenging than in the acute defect model. Half the tendons in the chronic repair model were found to be irreparable at 6 weeks. In the other half, the tendons could not be reattached to the footprint due to significant retraction, which made this a model of tissue formation in a gap. In contrast, the acute tendon repair model was executed easily. Treatment with CS-PRP implants

induced recruitment of polymorphonuclear cells at 2 weeks post-operative and improved ISP tendon structural organization at 3 months. Treatment also increased bone remodeling and ingrowth at the tendon-bone interface at 3 months, suggesting that a more robust attachment could be achieved by combining CS-PRP implants with suture anchors. These very preliminary studies provide the first evidence that CS-PRP implants can improve rotator cuff repair in large animal models.

## 7.1 INTRODUCTION

Rotator cuff tears are a common cause of morbidity in adults and one of the most common shoulder pathologies<sup>1-2</sup>. Cuff tears are associated with fatty infiltration, muscle atrophy, tendon retraction, and structural and architectural alterations of the musculotendinous unit<sup>3-5</sup>. Ruptures of rotator cuff tendons may eventually lead to irreversible changes in the shoulder, causing chronic pain and severe functional disability. Persistent tendon defects with constant exposure of the intra-articular joint surface and fluid will occur if a rotator cuff tear is not repaired within a certain time-frame after injury<sup>6</sup>. It is believed that there may be a “point of no return” in rotator cuff injury, with formation of scar tissue and infiltration of fat, after which the elasticity of the muscle-tendon unit can no longer return to normal<sup>7</sup>.

The goal of rotator cuff repair is to restore the footprint by suturing the tendon directly to the tuberosity using sutures anchors and varying suture configurations with the aim of increasing initial fixation strength, and mechanical stability under cyclic loading<sup>8</sup>. These procedures are assumed to increase footprint contact area, and restore normal structure and function of the shoulder<sup>9</sup>, while improving the rate of healing<sup>10</sup>. However, patients often experience failed

healing or re-tears <sup>11-12</sup>. Failure to heal occurs in 20 to 95% of cases at 2-years following surgical repair <sup>11, 13</sup>, depending on surgical treatment used <sup>14-15</sup>, time from injury <sup>16</sup>, tendon quality <sup>17</sup>, muscle quality <sup>18</sup>, biological healing response <sup>19</sup>, patient age, number of tendons involved, and tear size <sup>20</sup>. One limitation of current surgical procedures is that regeneration of the structure and composition of the native enthesis is not achieved following surgical fixation, biological augmentation is one possible approach to overcome this limitation <sup>21</sup>.

Growth factors are known to be important in cell chemotaxis, proliferation, matrix synthesis and cell differentiation <sup>22</sup>, and platelet-rich plasma (PRP) is a readily available source of autologous growth factors. PRP injections have been used clinically to treat rotator cuff tears, since it is believed that increased concentration of platelet-derived growth factors will stimulate revascularization of soft tissue and enhance tendon healing <sup>20</sup>. However, current clinical evidence does not support the routine use of PRP injections to treat rotator cuff tears <sup>23-27</sup> and PRP injections are still very controversial in the orthopaedic field. Variability in the isolation protocols and resulting preparations and the poor stability of PRP *in vivo* are two possible reasons why results have been inconsistent to date.

Chitosan (CS) is a biodegradable polymer that has been used for several tissue repair and regeneration applications. Our laboratory has implemented the use of PRP combined with freeze-dried CS to form injectable implants that coagulates *in situ* <sup>28</sup>. *In vitro* release of platelet-derived growth factors is increased and platelet-mediated clot retraction is inhibited by mixing PRP with chitosan <sup>29</sup>. CS-PRP implants were shown to reside for at least 6 weeks subcutaneously *in vivo* and enhance cell recruitment to surrounding tissues compared to PRP alone <sup>28-29</sup>. CS-PRP

implants were tested in ovine meniscus repair models where they increased cell recruitment, vascularization, remodeling and repair tissue integration compared to injection of PRP alone or wrapping the meniscus with a collagen membrane<sup>30-31</sup>. Finally, CS-PRP implants improved marrow-stimulated cartilage repair and induced bone remodeling in a chronic rabbit defect model<sup>32</sup>. We hypothesized that all of the above would also be beneficial to rotator cuff repair, and we subsequently showed in a small rabbit model that CS-PRP implants improve transosseous rotator cuff repair, by favoring tendon attachment through increased bone remodeling<sup>33</sup>.

The two pilot feasibility studies presented here investigated whether CS-PRP implants can also improve rotator cuff repair in larger sheep models. The first study used a chronic repair model, where tendons were allowed to degenerate to a chronic stage prior to repair, while an acute model with immediate repair was used in the second study. In both repair models, the infraspinatus (ISP) tendons were surgically transected and repaired using suture anchors with or without additional application of CS-PRP implants and healing was assessed histologically. Our starting hypothesis was that CS-PRP implants would have positive effects on chronic and acute rotator cuff repair through increased cell recruitment, vascularization and bone remodeling

## **7.2 MATERIALS AND METHODS**

### **7.2.1 Preparation of freeze-dried chitosan formulations**

Chitosan (degree of deacetylation 80.2%, number average molar mass  $M_n$  36,000 g/mol, weight average molar mass  $M_w$  65,000 g/mol, polydispersity index 1.8) was used to prepare

formulations containing 1% (w/v) chitosan, 28 mM HCl, 1% (w/v) trehalose as a lyoprotecting agent (Life Science) and 42.2 mM CaCl<sub>2</sub> as a PRP activator (Sigma-Aldrich). Formulations were filter-sterilized and distributed in 1 mL aliquots into sterile, de-pyrogenized 3cc glass vials for lyophilization using the following steps: 1) ramped freezing to -40°C in 1 hour, isothermal 2 hours at -40°C, 2) -40°C for 48 hours, 3) ramped heating to 30°C in 12 hours, isothermal 6 hours at 30°C, at 100 millitorrs.

### **7.2.2 Preparation of platelet-rich plasma (PRP)**

Blood was drawn from the sheep jugular vein immediately prior to surgery. One small tube of blood was drawn for complete blood count and platelet analysis. Then, two 9ml tubes of blood were collected per sheep and anti-coagulated with 1 mL 3.8% (w/v) sodium citrate each (final citrate concentration 12.9 mM). Blood was centrifuged for 10 min at 1300 rpm and then for 10 min at 2000 rpm using the ACE EZ-PRP centrifuge to extract ~ 3 mL PRP per sheep. The isolated leukocyte-rich PRP contained an average of 409 X 10E9/L platelets (2X that of whole blood), 6.2 X 10E9/L leukocytes (1X that of whole blood) and 2.4 X 10E12/L erythrocytes (0.2X that of whole blood).

### **7.2.3 Experimental study design and surgical technique**

The protocol for this study was approved by the University of Montreal committee “Comité de déontologie de l’expérimentation sur les animaux” (initial date of approval March 10<sup>th</sup> 2016) and was consistent with the Canadian Council on Animal Care guidelines for the care and use of laboratory animals. Eight adult Texel-cross female sheep (age ranging from 2-6 years;

weight ranging from 55-70kg) were divided into a chronic repair model group (**Table 1**) and an acute repair model group (**Table 2**). In both groups, the surgical method included unilateral exposure of the infraspinatus tendons (ISP) through a muscle separating approach to the lateral aspect of the shoulder using general anesthesia and aseptic technique. The ISP tendon was transected from its original footprint on the humerus, creating a full-thickness rotator cuff tear. The humeral head was debrided with a surgical scalpel removing any tendinous tissue still attached. In both the chronic and acute repair models, the surface of the tuberosity was roughened with use of a curette and the tendon surface slightly abraded prior to anchor insertion.

In the chronic repair model (n = 4 sheep; **Table 1 & Figure 1**), the tendons were capped with a 5-cm silicon tube (3/4" wide Penrose drain) to prevent spontaneous re-attachment and to allow the tear to degenerate to a chronic stage for 6 weeks. The capped tendons were engulfed in scar tissue after 6 weeks, at the time of the second surgery. After freeing the tendons from scar tissue and removing the silicon tubes, we found that the muscle-tendon unit had significantly retracted, leaving a gap of several centimeters between the end of the tendon and the tuberosity. In two sheep, the ISP tendons were torn as soon as they were pulled to close the gap to the tuberosity, and were found to be irreparable. Therefore, in those 2 sheep, a defect was created in the contralateral shoulders, but this time the ISP tendon was capped with a shorter 5-mm silicon tube and allowed to degenerate to a chronic stage for 2 weeks, without any further attempt to repair. In the third sheep, the 6-week chronic defect was repaired with suture anchors and sutured in a suture bridge configuration using four 4.65 mm PEEK Swivelock anchors and 2 mm FiberTape sutures (Arthrex, Product N° AR2324-PSLC and AR-7237). In the fourth sheep, the 6-week chronic defect was repaired with one suture anchor with the ISP tendon sutured using a



Masson-Allen configuration and the CS-PRP implant was additionally applied in a 2-part manner. Freeze-dried chitosan (1mL cake) was solubilized with 1 mL autologous PRP and 0.5 mL CS-PRP injected at the footprint prior to anchor insertion and then 0.5 mL CS-PRP was injected on top and under the tendon after reattachment. In both of the above repairable cases, the tendons were too retracted to be reattached at the footprint, hence a gap remained between the tendon and tuberosity after repair, making this a model of tissue formation in a gap. In the 2 sheep where the degenerated tendons were re-attached, the contralateral shoulders were left intact. The animals were allowed to walk ad libitum postoperatively and necropsy was 2 weeks after second surgery (n=4 sheep).

Table 7-1. Design of the chronic repair study.

Sheep #	Treatment Right shoulder	Treatment Left shoulder	Necropsy
1	ISP tendon initially left intact. 6 weeks later, tendon transected and capped with <u>5 mm</u> silicon	ISP tendon transected and capped with <u>5 cm</u> silicon 6 weeks later, tendon was found to be irreparable	6 week chronicity + 2 weeks
2	ISP tendon initially left intact. 6 weeks later, tendon transected and capped with <u>5 mm</u> silicon	ISP tendon transected and capped with <u>5 cm</u> silicon 6 weeks later, tendon was found to be irreparable	6 week chronicity + 2 weeks
3	ISP tendon transected and capped with <u>5 cm</u> silicon. 6 weeks later, tendon repaired with 4 suture anchors	Intact control	6 week chronicity + 2 weeks
4	ISP tendon transected and capped with <u>5 cm</u> silicon.	Intact control	6 week chronicity

	6 weeks later, tendon repaired with 1 suture anchor + CS-PRP		+ 2 weeks
--	--	--	-----------

In the acute repair model (n = 4 sheep; **Table 2 & Figure 2**), the tendons were transected and immediately repaired with suture anchors and sutured in a suture bridge configuration using four 4.65 mm PEEK Swivelock anchors and 2 mm FiberTape sutures (Arthrex, Product N° AR2324-PSLC and AR-7237). In 2 out of 4 sheep, CS-PRP implants were additionally applied in a 2-part manner. The first proximal row of anchors was securely inserted and the sutures were passed through the ISP tendon. Freeze-dried chitosan (1mL cake) was solubilized with 1 mL autologous PRP and 0.5 mL CS-PRP was injected at the footprint. The sutures were tightened and the second (distal) row of anchors was inserted. Then, 0.5 mL CS-PRP was injected on top of the repaired site and under the tendon. The animals were allowed to walk ad libitum postoperatively and necropsy was 6 weeks (n=2 sheep) and 3 months (n=2 sheep) after repair.

Table 7-2. Design of the acute repair study.

Sheep #	Treatment Right shoulder	Treatment Left shoulder	Necropsy
1	Tendon transected and immediately repaired with 4 suture anchors	Intact control	6 weeks
2	Intact control	Tendon transected and immediately repaired with 4	3 months

		suture anchors	
3	Tendon transected and immediately repaired with 4 suture anchors + CS-PRP	Intact control	6 weeks
4	Intact control	Tendon transected and immediately repaired with 4 suture anchors + CS-PRP	3 months

#### **7.2.4 Specimen collection and histological processing**

Animals were euthanized by sedation followed by captive bolt pistol. The shoulders were dissected and the humeral head-ISP-tendon unit complex was harvested en bloc from just proximal to the musculotendinous junction. Glenoid surfaces, muscle biopsies and synovial membrane biopsies were collected. All samples were fixed for several days in 10% neutral buffered formalin and trimmed for further processing. The ISP insertion sites, humeral head and glenoid surfaces were decalcified with HCl with trace glutaraldehyde. All samples were dehydrated in graded ethanol series, cleared with xylene and embedded in paraffin. Sections (5 $\mu$ m thickness) were stained with Safranin O/Fast Green or Hematoxylin and Eosin, scanned with a Nanozoomer RS (Hamamatsu) and images exported using NDP View software (Hamamatsu) for qualitative histological assessment. In addition, polarized microscopy images of the ISP tendons were obtained with an Axiolab (Zeiss) microscope equipped with a CCD camera (Hitachi HV-F22 Progressive Scan Colour 3-CCD).

## 7.3 RESULTS

### 7.3.1 The chronic repair model was more challenging than the acute repair model

After 6 weeks of chronic degeneration, ISP tendons capped with 5-cm silicon tubes became macroscopically abnormal throughout and were red, spongy (**Figure 1d**), biomechanically weak, and easily torn. Two of the four tendons were irreparable. Significant retraction had occurred to the extent that the tendons could not be reattached at the anatomic footprint. In the two cases where the tendons were found to be irreparable, a decision was made to operate on the contralateral shoulders, cap the ISP tendons with smaller 5-mm silicon tubes and allow the tears to degenerate to a chronic stage for 2 weeks. Significant retraction and structural abnormalities of the ISP tendon under the capped end were apparent after 2 weeks (**Figure 1f**), although changes were less severe than in the 6-week chronic model. In both the 6-week capped and the 2-week capped unrepaired defects, abundant scar tissue surrounded the capped ISP tendons and bridged the gap to the tuberosity, which suggests that a robust repair response occurs in this model, even in the presence of a silicon barrier. In contrast to the chronic model, the acute tear model was easily executed and the transected ISP tendons could be reattached at the footprint (**Figure 2**).

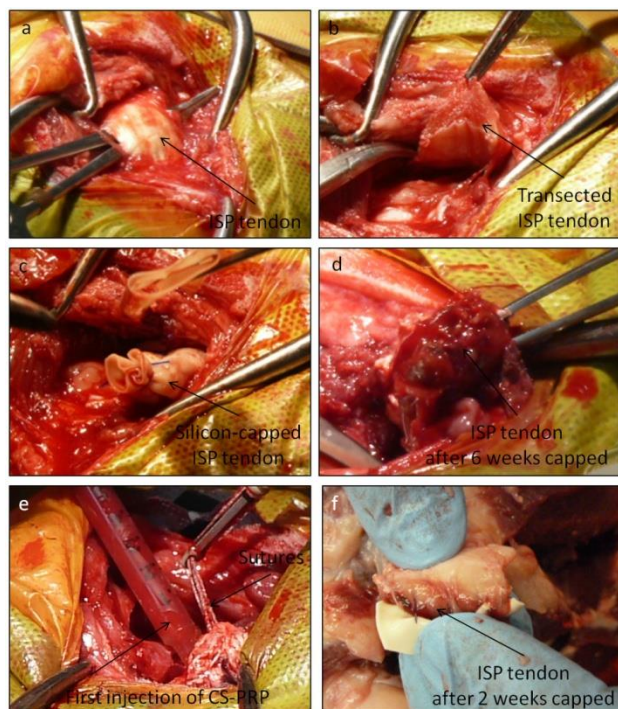


Figure 7-1. Chronic tear model and repair with CS-PRP. Full-thickness rotator cuff tears were created in the infraspinatus (ISP) tendon of the shoulder close to the enthesis (a, b) and capped with 5 cm length of silicone (c) in 4 sheep. At 6 weeks after surgery, the tendons were macroscopically abnormal (d) and 2 tendons were found to be irreparable. One tendon was repaired with 4 suture anchors in the suture bridge configuration. One tendon was repaired with one suture anchor + CS-PRP. The sutures were pre-placed in a Mason-Allen pattern and a first injection of 0.5 mL CS-PRP was applied at the debrided bone interface (e). The anchor was inserted to tighten the sutures and an additional 0.5 mL CS-PRP implant was applied on top of tendon at the repaired site and also under the tendon. Macroscopic appearance of an ISP tendon capped for 2 weeks with 5 mm length of silicone (f).

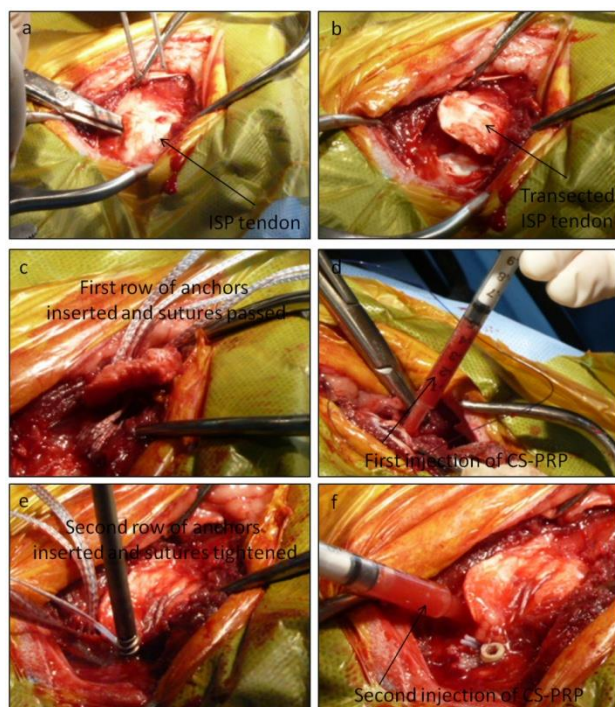


Figure 7-2. Acute tear model and repair with CS-PRP. Full-thickness rotator cuff tears were created in the infraspinatus (ISP) tendon of the shoulder close to the enthesis in 4 sheep (a, b). All tendons were immediately repaired with 4 suture anchors in a suture bridge configuration. In 2 out of 4 sheep, repair was augmented with CS-PRP. The first row of anchors were inserted and the sutures were passed (c) and a first injection of 0.5 mL CS-PRP was applied at the debrided bone interface (d). The second row of anchors were inserted to tighten the sutures (e) and an additional 0.5 mL CS-PRP was applied on top of tendon at the repaired site and also under the tendon (f).

### **7.3.2 CS-PRP implants induced recruitment of polymorphonuclear cells to the ISP tendon at 2 weeks and improved ISP tendon structural organization at 3 months**

As expected, intact ISP tendons consisted of fibrocartilaginous tissue organized in bundles with sparse cells and a small amount of glycosaminoglycans (GAG) (**Figure 3a-c & Figure 4a-d**). Histologically, none of the test tendons were structurally similar to intact (**Figures 3 & 4**). Acellular areas were observed in ISP tendons of the chronic defect model, for both the 2-week capped and the 6-week capped, (**Figure 3**), but not in tendons of the acute model (**Figure 4**). The 6-week chronic defect repaired with anchors + CS-PRP at 2 weeks had a portion of tendon repair tissue that was rich in polymorphonuclear cells (**Figure 3o**). In the acute model of tendon repair without augmentation, there was evidence of chondrogenesis within the tendon body at 6 weeks (**Figure 4f**) and abundant GAG expression at 3 months (**Figure 4m**), while this was not observed in the case of repair augmented with CS-PRP (**Figures 4 i & q**). Repaired tendons consisted mainly of disorganized, hypercellular and vascularized tissues (**Figures 3 & 4**). The one exception was in the case of repair augmented with CS-PRP at 3 months in the acute model, which was mostly organized in bundles and had a portion of repair tissue that was structurally similar to normal tendon (**Figure 4q-t**). Polarized light microscopy images better highlight the tendon structural organization, confirming the beneficial effect of tendon repair augmented with CS-PRP in the acute model at 3 months (**Figure 4t**).

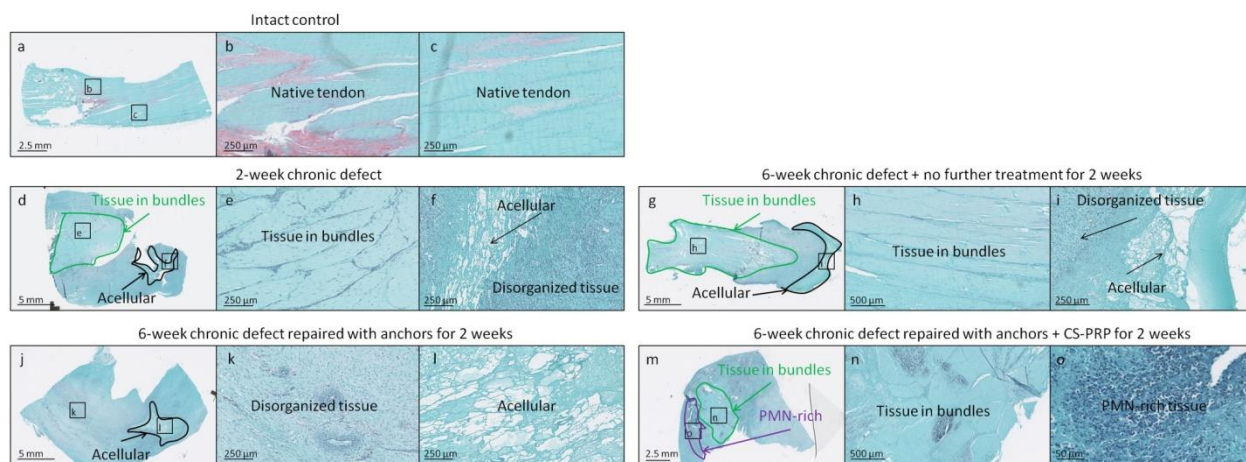


Figure 7-3. Safranin O/Fast Green stained paraffin sections of the ISP tendons in the chronic repair model. Intact control tendons were organized in bundles, as expected (a to c). Bundle organization was still apparent in areas of untreated tendons at chronic stage, while other areas were disorganized, hypercellular and vascularized or hypocellular (d to i). The tendon of the shoulder treated for 2 weeks with suture anchors was mostly disorganized, hypercellular and vascularized, with a small hypocellular area (j to l). The tendon of the shoulder treated with suture anchors + CS-PRP was mostly disorganized, hypercellular and vascularized, with a small area organized in bundles and another area rich in polymorphonuclear cells (m to o)

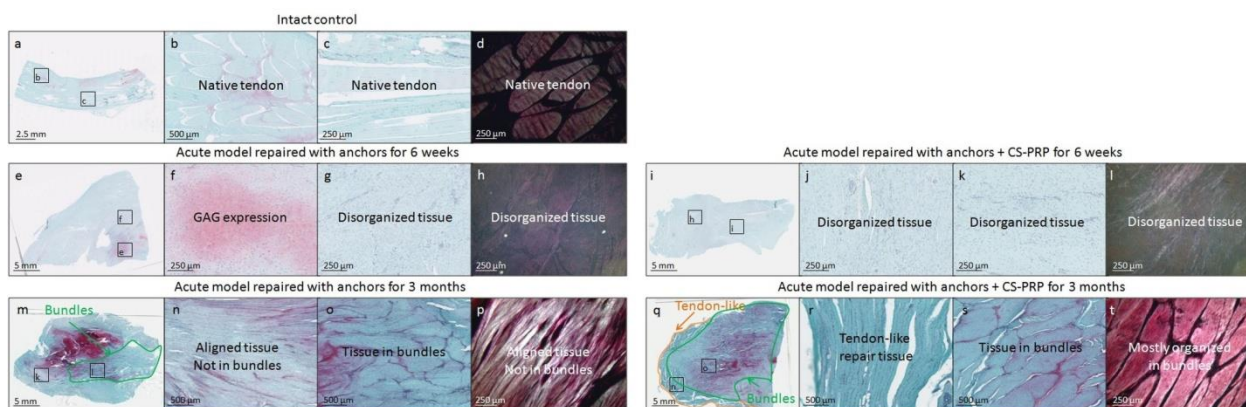


Figure 7-4. Safranin O/Fast Green-stained paraffin sections and polarized light microscopy (d, h, l, p & t) images of the ISP tendons in the acute repair model. Intact control tendons were organized in bundles, as expected (a to d). At 6 weeks post-surgery, the tendons were mostly



composed of a disorganized and vascular fibrous repair tissue in both groups (e to l). Chondrogenesis and GAG expression were apparent in the anchors only group at 6 weeks (e&f). At 3 months post-surgery, the tendon in the anchors only group contained aligned tissue, expressed high levels of GAG, and had a small area organized in bundles (m to p). In contrast, the tendon in the anchors + CS-PRP group was mostly organized in bundles with a smaller area of tendon-like repair tissue (m to t).

### **7.3.3 CS-PRP implants increased bone remodeling at the ISP tendon-bone junction**

Histologically, none of the repaired insertions had reformed the structure of the native enthesis. In the normal enthesis, the different zones were easily identified and no scar tissue was present above the bone front (**Figure 5a-c & Figure 6a-c**). The tidemark was still recognizable in the 2-week capped chronic defects (**Figure 5d**), but not in any other group (**Figures 5 & 6**). In all cases, even in untreated chronic defects (**Figure 5 d & g**), scar tissue was growing superior to the enthesis and integration of the scar tissue with the underlying bone was achieved through bone remodeling and ingrowth at the junction of the scar tissue with the original bone front (**Figures 5 & 6**). Augmentation with CS-PRP increased bone remodeling at the tendon-bone junction in both the chronic repair model (**Figure 5m-o**) and the acute repair model (**Figure 6m-o**).

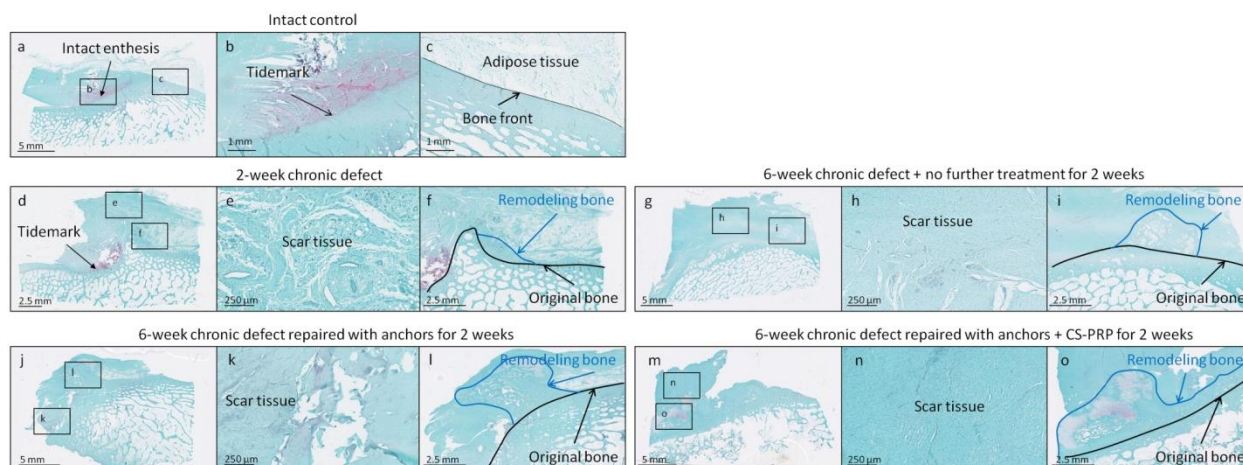


Figure 7-5. Safranin O/Fast Green stained paraffin sections of the ISP tendon entheses in the chronic repair model. Intact controls had normal entheses consisting of 1) unmineralized fibrocartilage, 2) tidemark, 3) mineralized fibrocartilage and 4) bone, as expected (a to c). The tidemark was still recognizable 2 weeks after defect creation (d), but not at longer time points or after repair (g, j & m). Scar tissue was growing above the entheses in the untreated chronic defects (d&g), suggesting that some spontaneous repair can occur even without any treatment in this model. Integration of the scar tissue with the underlying bone was achieved through bone remodeling and ingrowth into the scar tissue (f, i, l & o). Treatment with anchors + CS-PRP increased the area of remodeling bone (compare o to l).

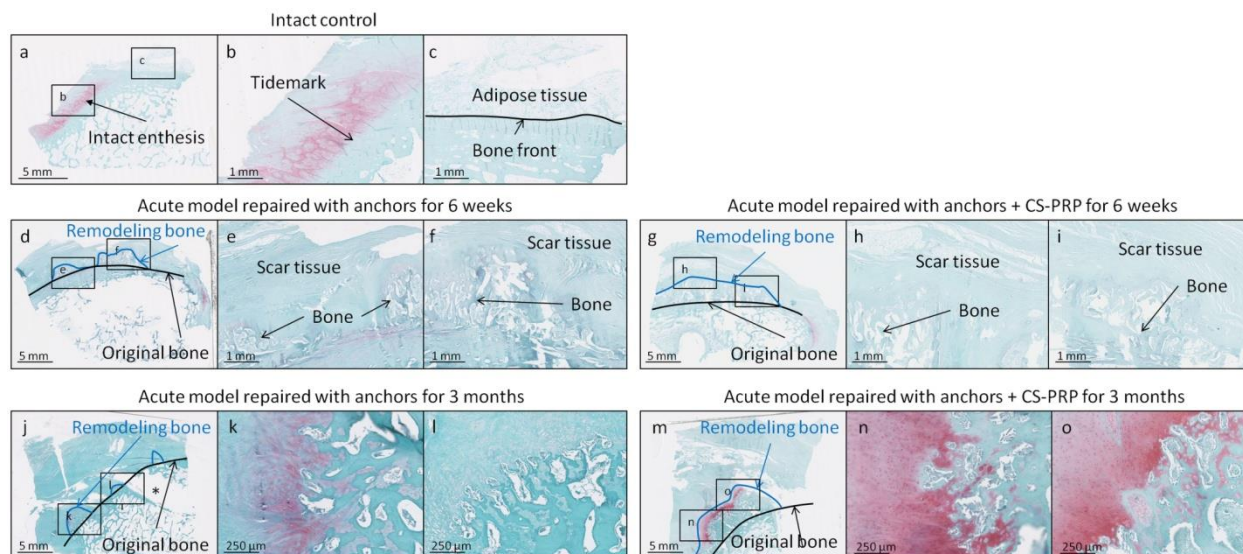


Figure 7-6. Safranin O/Fast Green stained paraffin sections of the ISP tendon entheses in the acute repair model. Intact controls had normal entheses consisting of 1) unmineralized fibrocartilage, 2) tidemark, 3) mineralized fibrocartilage and 4) bone, as expected (a to c). Scar tissue was growing superior to the entheses from 6 weeks (d to i) to 3 months (j to o) post-surgery. Integration of the scar tissue with the underlying bone was achieved through bone remodeling and ingrowth into the scar tissue (d to o). This was more apparent in the anchors + CS-PRP group (compare g&m to d&j). The site of anchor insertion was apparent in some sections (\* in panel j).

### **7.3.4 CS-PRP implants did not induce any treatment-specific deleterious effects in the shoulder joint**

In both the chronic and acute repair models, the humeral head was macroscopically free of defects, while small synovial fossae, defined as nonarticulating depressions, were apparent at the center of almost all of the glenoid surfaces. Almost all humeral heads, including intact controls, showed signs of GAG depletion (**Figure 7a, c, e, g & i**). Several glenoids, including intact controls, exhibited GAG depletion as well as other structural abnormalities including, hypercellularity, cell cloning and fissures (**Figure 7k-m**). Muscle histology showed increased fatty infiltration in chronic defects as early as 2 weeks after defect creation, which was not reversed by repair (**Figure 8 b & c**). Similarly, fatty infiltration was also induced by surgical detachment and immediate reattachment in the acute repair model (**Figure 8 d & e**). Histology of the synovial membranes showed that different forms of normal synovium can be found in sheep shoulders including the adipose form of synovium and the fibrous form of synovium (**Figure 9**). There was mild synovitis and increased cell infiltration in the chronic model treated with anchors + CS-PRP for 2 weeks (**Figure 9c**), but not in any other sample

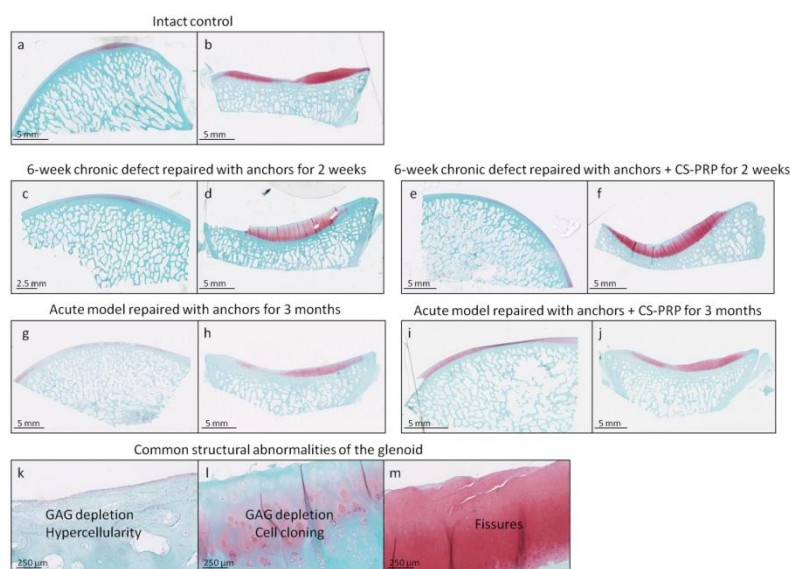


Figure 7-7. Safranin O/Fast Green stained sections of humeral head and glenoid articular surfaces from intact controls (a&b), from the chronic defect model (c to f) and from the acute defect model (g to j). The humeral articular surfaces were all structurally normal but showed signs of GAG depletion (a, c, e, g & i). Mild structural abnormalities were observed at the center of some glenoid articular surfaces, including GAG depletion, hypercellularity, cell cloning and fissures (k to m). These were apparent in all treatment groups as well as the intact controls.

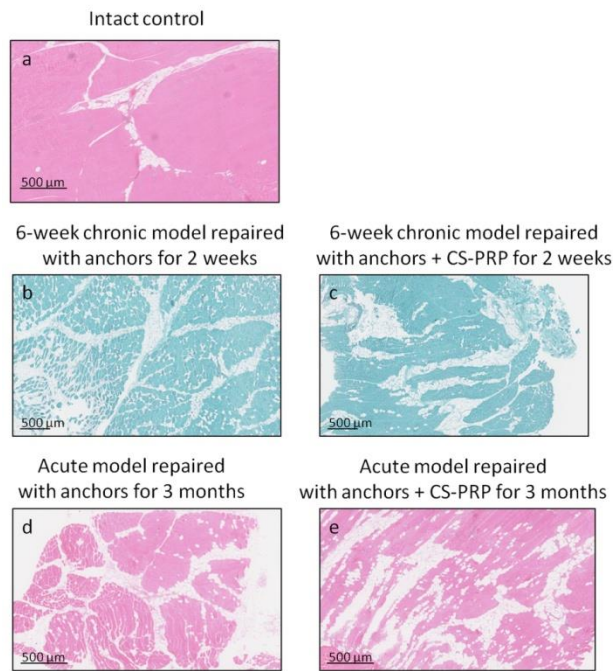


Figure 7-8. Hematoxylin and Eosin (a, d & e) and Safranin O/Fast Green (b & c) stained paraffin sections of muscle biopsies from intact control (a), from the chronic defect model (b & c) and from the acute defect model (d & f). Fatty infiltration was not prevented by any treatment

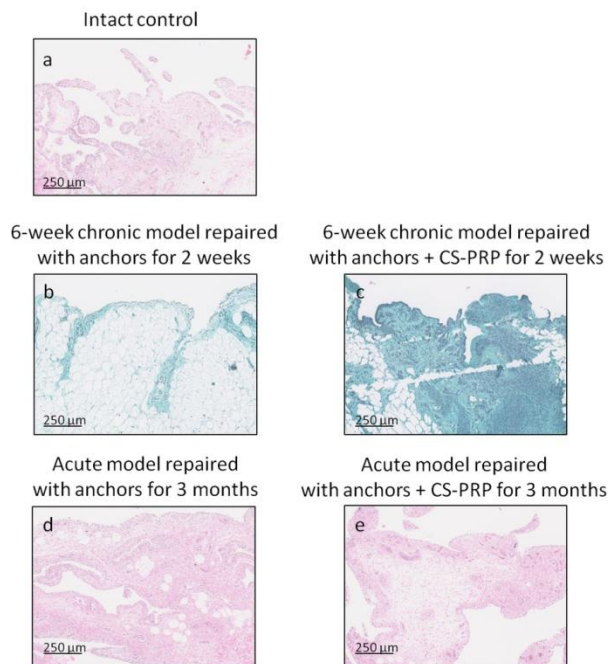


Figure 7-9. Hematoxylin and Eosin (a, d & e) and Safranin O/Fast Green (b & c) stained paraffin sections of synovial biopsies from intact control (a), from the chronic defect model (b & c) and from the acute defect model (d & f). There was mild synovitis and increased cell infiltration in the chronic model treated with anchors + CS-PRP for 2 weeks (c).

## 7.4 DISCUSSION

The purpose of the current study was to determine whether CS-PRP implants can improve rotator cuff repair in chronic and acute repair models in the sheep. Large animal models, like sheep, have infraspinatus tendons that are similar in size to the human supraspinatus<sup>34</sup>, making them amenable to using repair techniques commonly employed in humans<sup>6, 35</sup>. Although these are very preliminary pilot studies, our starting hypothesis was supported in that treatment augmented with CS-PRP implants led to improved tendon structural appearance, increased bone remodeling and ingrowth at the tendon-bone junction.

One important finding reported here, were the difficulties we faced during implementation of the chronic repair model. We found that capping the ISP tendons for 6 weeks with 5-cm e tubes likely prevented proper nutrient diffusion and led to cell death and severe tendon degeneration, which rendered some tendons irreparable. Although degeneration was not as marked when the tendons were capped for 2 weeks with 5-mm silicone length, reattachment at the footprint would have been difficult to achieve since the tendon-muscle unit had significantly retracted. Therefore, this chronic model would constitute a model of tissue formation in a gap, and not a “true” tendon repair model. Capping with silicone has been used by other research groups studying chronic rotator cuff repair in sheep, but the surgery usually involves osteotomy,

leaving a small bone chip attached to the ISP tendon, with the silicone covering the bone chip and not the tendon itself<sup>15,36</sup>. Other groups have used a Preclude™ sheet to wrap the ISP tendon and allow the tears to develop to chronic stage<sup>37-38</sup>. Preclude is a dura substitute composed of Gore-Tex, with pores of <1µm in size, which would still allow nutrient diffusion to the tendons, and most likely would have been a better choice than silicone in the current study. We found that abundant scar tissues bridged the gap between the capped tendon and the tuberosity after 2 weeks and 6 weeks, which supports the notion that the healing response is robust and spontaneous in sheep even in these well-established chronic models<sup>15,36</sup>. As of now, we consider the acute repair model to be more consistent and easily reproducible.

Even though this study presented some challenges, some interesting findings are worth further discussion. Polymorphonuclear (PMN) cells were observed in the tendon repair tissue of the shoulder treated with CS-PRP augmentation for 2 weeks, which is not unexpected at this time point, since CS-PRP implants were previously shown to induce PMN recruitment for at least 2 weeks in a rabbit transosseous rotator cuff repair model<sup>33</sup>. PMN were no longer visible at 6 weeks, which suggests that CS-PRP implants were fully degraded by then, which is consistent with previous sheep studies using similar doses of the CS-PRP implants, albeit in the knee joint for meniscus repair<sup>30-31</sup>. Similarly to what was previously seen in the transosseous rotator cuff repair model in the rabbit, the tendon treated with repair alone (non-augmented) showed chondrogenesis and GAG expression within the tendon body at 6 weeks, while the tendon repair augmented with CS-PRP did not. The significance of chondrogenesis occurring within the tendon repair tissue is still unclear, but we hypothesize that this may be the first step in heterotopic ossification, a well known complication of tendon injury, which we previously found was

inhibited by treatment with CS-PRP implants in the transosseous rabbit model <sup>33</sup>. GAG deposition is also frequently observed in cases of tendonosis <sup>39-40</sup>. The anchors + CS-PRP repair technique resulted in better tendon structural outcome than anchors only at 3 months only, with no apparent improvement at 6 weeks, possibly through a modulation of timing of the healing sequence or through increased repair tissue remodeling.

During development, tendon-bone integration occurs through establishment of an embryonic tendon-bone attachment unit, which matures into the fibrocartilaginous insertion, known as the enthesis <sup>41-42</sup>. Maturation of the enthesis appears to follow pathways similar to the growth plate development <sup>41</sup>. The insertion site matures through mineralization of fibrocartilage matrix under the influence of chondrocyte-like cells, with associated remodeling through osteoclasts and osteoblasts, creating the interface between tendon and the tuberosity <sup>41</sup>. Following repair however, the tendon-bone insertion site usually heals through a fibrovascular scar tissue formation, lacking any sort of reestablishment of the four zones of the native enthesis <sup>43</sup>. Rotator cuff healing occurs in overlapping phases similar to those observed in the case of wound healing, namely the inflammatory phase, the matrix production phase and the remodeling phase <sup>44</sup>. In the chronic and acute models used here, the integration of the tendon repair tissue occurred through bone remodeling and ingrowth at the junction between the tendon and the underlying bone, and the native structure of the enthesis was not re-established. Bone remodeling appears to be a mechanism that enables the repair to become mechanically stronger. It has previously been suggested that strong healing between tendon and the tuberosity, with reformation of a new enthesis, requires bone ingrowth into scar tissue and outer tendon <sup>45</sup>. Other authors have suggested that the formation of a callus appears to be essential for remodeling the tendon-bone



boundary after injury<sup>46</sup>. In that respect, it is significant that bone remodeling was greater in the case of the insertion sites treated with anchors + CS-PRP compared to suture anchors only, although it is impossible to draw solid conclusions on the basis of such a small number of samples. Of note, CS-PRP implants have previously been shown to increase bone remodeling over standard treatment in the context of rotator cuff and cartilage repair in small rabbit models, leading to better integration of repair tissues<sup>32-33</sup>.

There were no treatment-specific deleterious effects in the shoulder joint, suggesting that CS-PRP implants have high safety. Structural abnormalities were visible in most glenoids, suggesting that greater stresses are applied on that surface compared to the humeral head in the sheep model. Fatty infiltration of the ISP muscle was induced in both chronic and acute models, and no treatment could reverse that effect. A longer follow-up time may be required to see treatment-specific protective effects. Mild transient synovitis was present in the shoulder treated with CS-PRP at 2 weeks, and this was resolved at the later 6 weeks and 3-month time points, once the biomaterial was degraded.

There were several limitations to this study. The main limitation is the small number of animals used, although we feel that these numbers were reasonable for pilot feasibility studies. Obviously, a larger number of animals would be required to draw firm conclusions, and the results reported here should be viewed with caution. Moreover, different repair techniques were used for the chronic group, making it harder to compare treatments. Furthermore, although the sheep is a commonly used model of rotator cuff repair, it is not identical to human. In contrast to humans, the sheep infraspinatus tendon is not intraarticular, although a bursa exists underneath the tendon. The sheep forelimb is also weight-bearing, has no clavicle, a less-developed

acromion, and no coracoacromial arch<sup>47</sup>. Most importantly, robust scar tissue formation occurs between tendon stump and the bone in the sheep, not analogous to humans, where gaping is a common recurrent problem. Inability to control post-operative weight-bearing is another limitation. Finally, assessment was purely qualitative and, although improved histological appearance would be expected to translate into superior performance, no other type of measurement was performed

## **7.5 CONCLUSIONS**

In summary, developing techniques to augment of rotator cuff repair remains clinically relevant. The technical challenges associated with the chronic repair model in the sheep make the acute model preferable for future studies. Despite their limitations, these two very preliminary pilot studies provide the first evidence that CS-PRP implants improve the healing response in large animal models of rotator cuff repair, partly through increased bone remodeling at the tendon repair tissue and underlying bone interface. Future work will involve a larger number of animals and a longer duration of follow-up, with the long-term objective of translating this technology to the clinic.

### **AUTHOR INFORMATION**

#### **Corresponding Author**

\*Prof Michael D. Buschmann, Biomedical Engineering Institute and Chemical Engineering Department, Polytechnique Montreal, PO Box 6079 Succ Centre-Ville, Montreal, Quebec, Canada, H3C 3A7, Fax: 514 340 2980 Tel: 514 340 4711 ext. 4931, E-mail: michael.buschmann@polymtl.ca.

### **Author Contributions**

The manuscript was written through contributions of all authors. All authors have given approval to the final version of the manuscript. All authors contributed equally.

### **Conflict of Interest Disclosure**

AC, MBH and MDB hold shares, MDB is a Director of, and MS and SR are clinical advisors of Ortho Regenerative Technologies Inc.

### **Funding Sources**

We acknowledge the funding sources (Canadian Institutes of Health Research, Canada Foundation for Innovation, Groupe de Recherche en Sciences et Technologies Biomédicales, Natural Sciences and Engineering Research Council of Canada, Ortho Regenerative Technologies Inc.).

### **ACKNOWLEDGMENT**

We acknowledge the technical contributions of Geneviève Picard.

#### ABBREVIATIONS

CS, Chitosan; PRP, Platelet-rich plasma; ISP, Infraspinatus; GAG, Glycosaminoglycans; PMN, Polymorphonuclear.

#### REFERENCES

1. Lehman, C.; Cuomo, F.; Kummer, F. J.; Zuckerman, J. D., The incidence of full thickness rotator cuff tears in a large cadaveric population. *Bull Hosp Jt Dis* **1995**, *54* (1), 30-1.
2. Lippi, G.; Longo, U. G.; Maffulli, N., Genetics and sports. *Br Med Bul* **2010**, *93*, 27-47.  
DOI: 10.1093/bmb/ldp007.
3. Goutallier, D.; Postel, J. M.; Bernageau, J.; Lavau, L.; Voisin, M. C., Fatty muscle degeneration in cuff ruptures. Pre- and postoperative evaluation by CT scan. *Clin Orthop Relat Res* **1994**, (304), 78-83.
4. Thomazeau, H.; Boukobza, E.; Morcet, N.; Chaperon, J.; Langlais, F., Prediction of rotator cuff repair results by magnetic resonance imaging. *Clin Orthop Relat Res* **1997**, (344), 275-83.
5. Patte, D., Classification of rotator cuff lesions. *Clin Orthop Relat Res* **1990**, (254), 81-6.

6. Derwin, K. A.; Baker, A. R.; Codsì, M. J.; Iannotti, J. P., Assessment of the canine model of rotator cuff injury and repair. *J Shoulder Elbow Surg* **2007**, *16* (5), 140S-148S. DOI: 10.1016/j.ise.2007.04.002.
7. Laron, D.; Samagh, S. P.; Liu, X.; Kim, H. T.; Feeley, B. T., Muscle degeneration in rotator cuff tears. *J Shoulder Elbow Surg* **2012**, *21* (2), 164-174. DOI: 10.1016/j.jse.2011.09.027.
8. Cole, B. J.; ElAttrache, N. S.; Anbari, A., Arthroscopic rotator cuff repairs: An anatomic and biomechanical rationale for different suture-anchor repair configurations. *Arthroscopy* **2007**, *23* (6), 662-669. DOI: 10.1016/j.arthro.2007.02.018.
9. Di Giacomo, G., Pouliart, N, Costantini, C., De Vita, A., *Atlas of Functional Shoulder Anatomy*. Springer: Rome, Italy, 2008.
10. Denard, P. J.; Burkhart, S. S., The Evolution of Suture Anchors in Arthroscopic Rotator Cuff Repair. *Arthroscopy* **2013**, *29* (9), 1589-1595. DOI: 10.1016/j.arthro.2013.05.011.
11. Harryman, D. T., 2nd; Mack, L. A.; Wang, K. Y.; Jackins, S. E.; Richardson, M. L.; Matsen, F. A., 3rd, Repairs of the rotator cuff. Correlation of functional results with integrity of the cuff. *J Bone Joint Surg-Am* **1991**, *73* (7), 982-9.
12. Galatz, L. M.; Ball, C. M.; Teefey, S. A.; Middleton, W. D.; Yamaguchi, K., The outcome and repair integrity of completely arthroscopically repaired large and massive rotator cuff tears. *J Bone Joint Surg-Am* **2004**, *86A* (2), 219-224.
13. Yamaguchi, K.; Tetro, A. M.; Blam, O.; Evanoff, B. A.; Teefey, S. A.; Middleton, W. D., Natural history of asymptomatic rotator cuff tears: A longitudinal analysis of asymptomatic tears

detected sonographically. *J Shoulder Elbow Surg* **2001**, *10* (3), 199-203. DOI: 10.1067/mse.2001.113086.

14. Iannotti, J. P.; Williams, G. R.; Patel, N. J., Advances in the surgical treatment of disorders of the shoulder. *Surg Ann* **1994**, *26*, 227-250.

15. Meyer, D. C.; Hoppeler, H.; von Rechenberg, B.; Gerber, C., A pathomechanical concept explains muscle loss and fatty muscular changes following surgical tendon release. *J Orthop Res* **2004**, *22* (5), 1004-1007. DOI: 10.1016/j.orthres.2004.02.009.

16. Bartolozzi, A.; Andreychik, D.; Ahmad, S., Determinants of outcome in the treatment of rotator cuff disease. *Clin Orthop Relat Res* **1994**, (308), 90-7.

17. Riley, G. P.; Harrall, R. L.; Constant, C. R.; Chard, M. D.; Cawston, T. E.; Hazleman, B. L., Tendon degeneration and chronic shoulder pain: changes in the collagen composition of the human rotator cuff tendons in rotator cuff tendinitis. *Annals Rheum Dis* **1994**, *53* (6), 359-66.

18. Goutallier, D.; Postel, J. M.; Gleyze, P.; Leguilloux, P.; Van Driessche, S., Influence of cuff muscle fatty degeneration on anatomic and functional outcomes after simple suture of full-thickness tears. *J Shoulder Elbow Surg* **2003**, *12* (6), 550-4. DOI: 10.1016/s1058274603002118.

19. Shimokado, K.; Raines, E. W.; Madtes, D. K.; Barrett, T. B.; Benditt, E. P.; Ross, R., A significant part of macrophage-derived growth factor consists of at least two forms of PDGF. *Cell* **1985**, *43* (1), 277-86.

20. Barber, F. A.; Hrnack, S. A.; Snyder, S. J.; Hapa, O., Rotator Cuff Repair Healing Influenced by Platelet-Rich Plasma Construct Augmentation: A Novel Molecular Mechanism Reply. *Arthroscopy* **2011**, *27* (11), 1456-1457. DOI: .

21. Deprés-Tremblay, G.; Chevrier, A.; Snow, M.; Hurtig, M. B.; Rodeo, S.; Buschmann, M. D., Rotator cuff repair: a review of surgical techniques, animal models, and new technologies under development. *J Shoulder Elbow Surg* **2016**, *25* (12), 2078-2085. DOI: 10.1016/j.jse.2016.06.009.
22. Gulotta, L. V.; Rodeo, S. A., Growth factors for rotator cuff repair. *Clin Sports Med* **2009**, *28* (1), 13-23. DOI: 10.1016/j.csm.2008.09.002.
23. Vavken, P.; Sadoghi, P.; Palmer, M.; Rosso, C.; Mueller, A. M.; Szoelloesy, G.; Valderrabano, V., Platelet-Rich Plasma Reduces Retear Rates After Arthroscopic Repair of Small- and Medium-Sized Rotator Cuff Tears but Is Not Cost-Effective. *Am J Sports Med* **2015**, *43* (12), 3071-6 DOI: 10.1177/0363546515572777.
24. Li, X.; Xu, C.-P.; Hou, Y.-L.; Song, J.-Q.; Cui, Z.; Yu, B., Are Platelet Concentrates an Ideal Biomaterial for Arthroscopic Rotator Cuff Repair? A Meta-analysis of Randomized Controlled Trials. *Arthroscopy* **2014**, *30* (11), 1483-1490. DOI: 10.1016/j.arthro.2014.03.020.
25. Zhao, J.-G.; Zhao, L.; Jiang, Y.-X.; Wang, Z.-L.; Wang, J.; Zhang, P., Platelet-Rich Plasma in Arthroscopic Rotator Cuff Repair: A Meta-analysis of Randomized Controlled Trials. *Arthroscopy* **2015**, *31* (1), 125-135. DOI: 10.1016/j.arthro.2014.08.008.
26. Warth, R. J.; Dornan, G. J.; James, E. W.; Horan, M. P.; Millett, P. J., Clinical and Structural Outcomes After Arthroscopic Repair of Full-Thickness Rotator Cuff Tears With and Without Platelet-Rich Product Supplementation: A Meta-analysis and Meta-regression. *Arthroscopy* **2015**, *31* (2), 306-320. DOI: 10.1016/j.arthro.2014.09.007.

27. Chahal, J.; Van Thiel, G. S.; Mall, N.; Heard, W.; Bach, B. R.; Cole, B. J.; Nicholson, G. P.; Verma, N. N.; Whelan, D. B.; Romeo, A. A., The Role of Platelet-Rich Plasma in Arthroscopic Rotator Cuff Repair: A Systematic Review With Quantitative Synthesis. *Arthroscopy* **2012**, *28* (11), 1718-1727. DOI: 10.1016/j.arthro.2012.03.007.
28. Chevrier, A.; Darras, V.; Picard, G.; Nelea, M.; Veilleux, D.; Lavertu, M.; Hoemann, C. D.; Buschmann, M. D., Injectable chitosan-platelet-rich plasma (PRP) implants to promote tissue regeneration: In vitro properties, in vivo residence, degradation, cell recruitment and vascularization. *J Tiss Eng Reg Med* **2017**, *In Press*. DOI: 10.1002/term.2403.
29. Deprés-Tremblay, G.; Chevrier, A.; Tran-Khanh, N.; Nelea, M.; Buschmann, M. D., Chitosan-platelet-rich plasma implants for tissue repair - in vitro and in vivo characteristics. In *World Biomaterials Congress*, Montreal, QC, Canada, 2016.
30. Chevrier, A.; Deprés-Tremblay, G.; Hurtig, M. B.; Buschmann, M. D. Chitosan-platelet-rich plasma implants can be injected into meniscus defects to improve repair, In *Transactions Orthopaedic Research Society*, Orlando, FL, USA, March 5th-8th; Orlando, FL, USA, 2016.
31. Ghazi zadeh, L.; Chevrier, A.; Hurtig, M. B.; Farr, J.; Rodeo, S.; Hoemann, C. D.; Buschmann, M. D. Freeze-dried chitosan-PRP injectable surgical implants for meniscus repair: results from pilot ovine studies, In *Transactions Orthopaedic Research Society*, San Diego, CA, USA, ; San Diego, CA, USA, 2017.
32. Dwivedi, G.; Chevrier, A.; Hoemann, C. D.; Buschmann, M. D., Freeze dried chitosan/platelet-rich-plasma implants improve marrow stimulated cartilage repair in rabbit



chronic defect model In *Transactions Orthopaedic Research Society*, San Diego, CA, USA, 2017.

33. Deprés-Tremblay, G.; Chevrier, A.; Buschmann, M. D. Freeze-dried chitosan-PRP in a rabbit model of rotator cuff repair, In *Transactions Orthopaedic Research Society*, San Diego, CA, USA, San Diego, CA, USA, 2017.

34. Edelstein, L.; Thomas, S. J.; Soslowsky, L. J., Rotator Cuff Tears: What have we learned from animal models? *J Musculosk Neuron Int* **2011**, *11* (2), 150-162.

35. Schlegel, T. F.; Hawkins, R. J.; Lewis, C. W.; Turner, A. S., An in vivo comparison of the modified Mason-Allen suture technique versus an inclined horizontal mattress suture technique with regard to tendon-to-bone healing: a biomechanical and histologic study in sheep. *J Shoulder Elbow Surg* **2007**, *16* (1), 115-21. DOI: 10.1016/j.jse.2006.05.002.

36. Gerber, C.; Meyer, D. C.; Schneeberger, A. G.; Hoppeler, H.; Von Rechenberg, B., Effect of tendon release and delayed repair on the structure of the muscles of the rotator cuff: An experimental study in sheep. *J Bone Joint Surg-Am* **2004**, *86A* (9), 1973-1982.

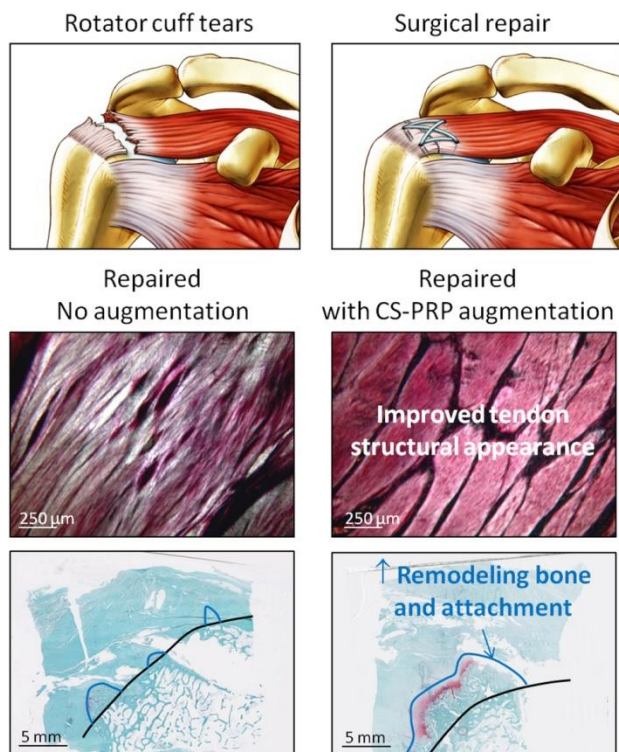
37. Uggem, C.; Dines, J.; McGarry, M.; Grande, D.; Lee, T.; Limpisvasti, O., The effect of recombinant human platelet-derived growth factor BB-coated sutures on rotator cuff healing in a sheep model. *Arthroscopy* **2010**, *26* (11), 1456-62. DOI: 10.1016/j.arthro.2010.02.025.

38. Coleman, S. H.; Fealy, S.; Ehteshami, J. R.; MacGillivray, J. D.; Altchek, D. W.; Warren, R. F.; Turner, A. S., Chronic rotator cuff injury and repair model in sheep. *J Bone Joint Surg-Am* **2003**, *85A* (12), 2391-2402.

39. DeGiorgi, S.; Saracino, M.; Castagna, A., Degenerative disease in rotator cuff tears: what are the biochemical and histological changes? *Joints* **2014**, *2* (1), 26-8.
40. Chard, M. D.; Cawston, T. E.; Riley, G. P.; Gresham, G. A.; Hazleman, B. L., Rotator cuff degeneration and lateral epicondylitis: a comparative histological study. *Ann Rheum Dis* **1994**, *53* (1), 30-4.
41. Thomopoulos, S.; Genin, G. M.; Galatz, L. M., The development and morphogenesis of the tendon-to-bone insertion - What development can teach us about healing. *J Musculosk Neuron Int* **2010**, *10* (1), 35-45.
42. Zelzer, E.; Blitz, E.; Killian, M. L.; Thomopoulos, S., Tendon-to-bone attachment: from development to maturity. *Birth defects research. Part C* **2014**, *102* (1), 101-12. DOI: 10.1002/bdrc.21056.
43. Apostolakos, J.; Durant, T. J.; Dwyer, C. R.; Russell, R. P.; Weinreb, J. H.; Alaei, F.; Beitzel, K.; McCarthy, M. B.; Cote, M. P.; Mazzocca, A. D., The enthesis: a review of the tendon-to-bone insertion. *Muscles Ligaments Tendons J* **2014**, *4* (3), 333-42.
44. Galatz, L. M., Soft Tissue to Bone Healing in Rotator Cuff Repair. In *Structural Interfaces and Attachments in Biology*, Thomopoulos, S.; Birman, V.; Genin, G. M., Eds. Springer Science+Business Media: New York, NY, USA, 2013.
45. Sanchez Marquez, J. M.; Martínez Díez, J. M.; Barco, R.; Antuña, S., Functional results after arthroscopic repair of massive rotator cuff tears: Influence of the application platelet-rich plasma combined with fibrin. *Rev Esp Cir Orthop Traumatol* **2011**, *55*, 282-287.

46. Newsham-West, R.; Nicholson, H.; Walton, M.; Milburn, P., Long-term morphology of a healing bone-tendon interface: a histological observation in the sheep model. *J Anat* **2007**, *210* (3), 318-27. DOI: 10.1111/j.1469-7580.2007.00699.x.
47. Turner, A. S., Experiences with sheep surgery: Strengths and as an animal model for shoulder shortcomings. *J Shoulder Elbow Surg* **2007**, *16* (5), 158S-163S. DOI: 10.1016/j.jse.2007.03.002.

#### TABLE OF CONTENTS GRAPHIC



## CHAPTER 8      GENERAL DISCUSSION

Rotator cuff injuries are extremely common and often require surgical repair to restore the tendon to its original footprint. Chronic rotator cuff tears are associated with structural changes such as fatty accumulation, loss of muscle volume, retraction, which all result in muscle remodeling, subtraction of sarcomeres and profound muscle weakness (Williams and Rockwood 1996). Finding the right animal model is challenging but critically important to improve our understanding of the cellular and molecular pathways involved in rotator cuff pathology. However, it is important to mention that none of the animals have anatomy comparable to humans. Open versus mini-open or arthroscopy does not seem to have a significant impact on clinical outcomes. The latest generation techniques involve the use of different configuration of sutures, which seem to increase the rate of tendon healing but this has not been translated into improved clinical and functional outcomes. ECM patches have shown some promising findings in some animal studies, but not in randomized clinical trials. Scaffolds and cells are becoming more popular in tissue engineering as structural supports and as cellular delivery aid but further clinical studies are still needed. Growth factors have been shown to improve healing but there is still no study on rotator cuff repair using growth factors in humans. One strategy would require using the ideal combination of growth factors and scaffold together to complement each other. PRP use in orthopedics is still controversial and under investigation for now, with limited data on its effectiveness. Present research on the use of growth factors, BMPs, gene therapy, stem-cell augmentation for tendon healing, and rotator cuff tear repair, is underway (Isaac, Gharaibeh et al. 2012, Jo, Shin et al. 2013). None of these strategies are perfectly suited for rotator cuff tear repair. In summary, several repair strategies are available but further clinical trials are needed to find the optimal treatment for rotator cuff repair. PRP growth factors are important in tissue repair, regeneration and signalling molecules in biological environment (Lee, Silva et al. 2011), by increasing endothelial, epithelial, epidermal regeneration, collagen, soft tissue healing, hemostatic reponse to injury, and decreases dermal scarring (Mohammadi, Mehrtash et al. 2016). Unfortunately, these released platelets diffuse very quickly and don't last long, hence decreasing their efficacy (Busilacchi, Gigante et al. 2013). On the other hand, chitosan can stimulate platelet activation in PRP (Zucker and Nachmias 1985, Kroll, Hellums et al. 1996, Li, Delaney et al.

2010, Brown, Narayanan et al. 2013) (Hattori and Ishihara 2016) and therefore increase PRP treatment efficacy (Oktay, Demiralp et al. 2010, Busilacchi, Gigante et al. 2013, Kutlu, Aydin et al. 2013). This was expected to have positive effects on rotator cuff tear repair.

Based on our data, CS-PRP implants coat various clot components and inhibited clot retraction and platelet aggregation *in vitro*. In cell suspension, CS was shown to induce platelet activation and granule secretion. This platelet activation was then translated to a greater sustained release of PDGF-AB and EGF in CS-PRP hybrids. Moreover, our *in vivo* data showed that CS-PRP reside for at least 6 weeks subcutaneously in rabbits and induce cell recruitment compared to PRP treatment alone. Under static or low shear stress conditions, platelet aggregation is mainly mediated by the interactions of GPIIb/IIIa on platelet surface with fibrinogen (Jackson 2007). Stimulation of platelets with agonists induces cytoskeletal rearrangement, shape change, protein synthesis, granule secretion and increases the affinity of the GPIIb-IIIa platelet receptor for fibrinogen. Platelet aggregation results from binding of multiple platelets to the same fibrinogen molecule (Jurk and Kehrel 2005). Clot retraction, mediated by the platelet actin and myosin contractile system then follows, as long as platelet stimulation, comprising shape change and primary aggregation, are maintained (Cohen, Gerrard et al. 1982, Cohen 1985). In the absence or non-functioning GPIIb/IIIa, clot retraction does not occur. Our Confocal, SEM and TEM images data provided support that chitosan physically coats platelets and other components of the blood clot to inhibit platelet aggregation, which is needed for clot retraction. In CS-PRP hybrids, chitosan physically interferes with the ability of platelets to adhere to each other as well as the fibrin network and exert mechanical forces.

In addition, chitosan (DDA > 90% and 50 kDa) was previously shown to be a platelet agonist and stimulate platelet activation and GPIIb/IIIa expression *in vitro* (Chahla, Dean et al. 2016). In another study, stimulation of platelet suspensions with chitosan (DDA 84%) induced p-selectin and GPIIb/IIIa expression, in a process that was shown to be modulated by plasma and extracellular matrix proteins (Lord, Cheng et al. 2011). Consistent with these previously published data, we found that chitosan induces platelet activation and granule secretion in cell suspensions, even more so than ADP, a known platelet agonist. Interestingly, incubation of cell suspension with trehalose along with chitosan slightly decreased expression of Pac-1 and p

selectin compared to incubation with chitosan alone. This is consistent with published reports that lyoprotectants impede haemostatic mechanisms (Bakaltcheva and Reid 2003, Luostarinen, Niiya et al. 2011).

In the case of physical adsorption of growth factors to chitosan, release is believed to be controlled by electrostatic interactions that exist between growth factors and chitosan (Yao, Li et al. 2012). The isoelectric point of PDGF is 9.8 (Antoniades, Scher et al. 1979) and, under physiological conditions, we expected ionic repulsion between positively charged PDGF-AB and cationic chitosan to result in burst release. Meanwhile, EGF, which has an isoelectric point of 4.6 (Taylor, Mitchell et al. 1972) would be expected to bind to chitosan under physiological conditions and be released in a more sustained manner. In contrast to this, we found that CS-PRP hybrid clots sustained and increased release of both PDGF-AB and EGF for 1 week *in vitro*, which suggests that additional factors are controlling their release in this system.

One important observation was that cumulative levels of PDGF-AB and EGF released in the culture medium were higher in the case of CS-PRP clots compared to PRP clots. These results were not completely unexpected. Kutlu et al (Kutlu, Aydin et al. 2013) previously prepared CS-PRP scaffolds by either adding PRP to a chitosan gel before freeze-drying or by delivering PRP to a lyophilized chitosan sponge. Sustained release of PDGF-BB was achieved in the first group, similarly to what we observed here, while a sharp burst release was observed in the second group. Interestingly, both of their CS-PRP scaffolds secreted higher cumulative levels of PDGF-BB when compared to unactivated PRP or PRP activated with collagen type-I, similarly to what was found here for PDGF-AB. Hattori et al (Hattori and Ishihara 2016) showed that platelets in whole blood are activated when mixed with solutions of chitosan with different DDA and  $M_w$ . Of particular relevance to our study, the amount of PDGF-AB released was the highest when chitosans of DDA 75-85% and  $M_w$  50-190 kDa were used in conjunction with calcium chloride than when calcium chloride was used by itself. Shen et al (Shen, Chou et al. 2006) showed that stimulation with chitosan of DDA > 90% and 450 kDa induced release of PDGF-AB and EGF from PRP for up to 60 minutes. Shimojo et al (Shimojo, Perez et al. 2015) prepared lyophilized scaffolds containing different concentrations of chitosan (DDA 83% and  $M_w$  400 kDa), loaded the scaffolds with PRP activated with autologous serum and calcium chloride and showed that

PDGF-AB cumulative release was higher from the scaffolds compared to activated PRP alone, provided that the scaffolds be lyophilized at low temperatures. In a subsequent study, Shimojo et al (Shimojo, Perez et al. 2016) showed that stabilizing the chitosan scaffolds by treating them with NaOH prior to loading them with PRP was another way to increase cumulative PDGF-AB release from scaffolds lyophilized at -20°C.

With regard to growth factor release, it is important to consider the contribution of each cell type present in the PRP preparation. Platelets are the main contributors to growth factor release from PRP and positive correlations were previously found between platelet doses and the amount of released growth factors including PDGF-AB, TGF- $\beta$ 1, VEGF and EGF (Weibrich, Kleis et al. 2012, Magalon, Bausset et al. 2014). While it appears that the inclusion of leukocytes in PRP increases the content of some pro-inflammatory cytokines (Sundman, Cole et al. 2011, Anitua, Zalduendo et al. 2014, Cavallo, Filardo et al. 2014, Pochini, Antonioli et al. 2016), the effect of leukocytes on growth factor content and release is still not fully understood. Previous studies found that leukocyte-rich PRP contained higher concentrations of growth factors compared to leukocyte-poor PRP, but that may be due to the fact that systems that include the buffy coat layer are usually more efficient at capturing platelets (Leitner, Gruber et al. 2006, Castillo, Pouliot et al. 2011, Cavallo, Filardo et al. 2014, Masuki, Okudera et al. 2016, Parrish, Roides et al. 2016, Fitzpatrick, Bulsara et al. 2017). However, positive correlations and close associations were also found between PRP leukocyte counts and levels of PDGF-AB, VEGF and EGF (Weibrich, Kleis et al. 2012, Magalon, Bausset et al. 2014), which suggests that leukocytes contribute to the release of growth factors from PRP. Here, we found increased cumulative PDGF-AB and EGF release from CS-PRP clots compared to PRP clots. One possible reason for this is that chitosan used in conjunction with calcium chloride stimulates platelet activation and granule secretion more than calcium chloride by itself. Another possibility would be that leukocytes, especially monocytes, present in CS-PRP hybrids are secreting higher amounts of growth factors than in PRP without chitosan. While it has been reported that M0 and polarized M2a macrophages secrete PDGF-BB (Spiller, Anfang et al. 2014, Spiller, Nassiri et al. 2015), and that biodegradable chitosan particles (DDA 81.5% and  $M_n$  132 kDa) enhance release of PDGF-BB from M0 and M2a macrophages (Fong, Ariganello et al. 2015), we believe that the main

contributors to growth factor release in the CS-PRP hybrid system are platelets and not monocytes, for the following reasons: 1) Monocytes typically require specific stimulatory signals to become macrophages, 2) There is a low number of monocytes present in each CS-PRP clot, compared to the number of platelets (on average ~ 2500X more platelets than monocytes); 3) In light of previous reports on the amount of growth factors released by M0 and M2a macrophages, it seems unlikely that such a limited number of monocytes could secrete the amount of PDGF-AB and EGF that was measured here in the culture medium.

In a subcutaneous implantation model in the mouse, porous chitosan scaffolds were found to elicit neutrophil migration into the implantation area along with angiogenic activity, as was shown here as well (VandeVord, Matthew et al. 2002). It is of interest to mention that the site of implantation along with implant volume influences biodegradability. We have previously shown that CS-PRP implants are degraded within 3 weeks in meniscus tears in the sheep (Ghazi zadeh, Chevrier et al. 2017), and between 2-8 weeks in rotator cuff tears (Deprés-Tremblay, Chevrier et al. 2017) and cartilage lesions in the rabbit (Dwivedi, Chevrier et al. 2017) compared to more than 6 weeks in the current study.

In conclusion, Chitosan physically coats platelets, blood cells and fibrin strands in CS-PRP hybrid clots, thus inhibiting platelet aggregation, which is required for clot retraction. Platelets are activated, granules secreted and higher levels of PDGF-AB and EGF are released from CS-PRP hybrid clots compared to PRP clots *in vitro*. Finally, CS-PRP implants reside for at least 6 weeks post-implantation subcutaneously and induce cell recruitment and granulation tissue synthesis, confirming a longer residency and higher bioactivity compared to PRP *in vivo*.

CS-PRP hybrids were then tested in a rabbit transosseous surgical repair model, which demonstrated an adherence to SSP tendon and a residence within the bony trough and lateral tunnels for at least a day. In addition, CS-PRP implants induced bone remodeling at the greater tuberosity and a better SSP attachment. One important finding in our rabbit model was the inhibition that CS-PRP had on heterotopic bone formation within soft tissue, which seemed to act like a protective or inhibiting agent. CS-PRP implants in a transosseous repair model in rabbit induced PMN recruitment at early time points post-surgery. Implant degradation and associated



inflammatory reactions were still ongoing in 3 out of 9 treated shoulders at 2 months. Results showed that CS-PRP would improve rotator cuff repair, since treatment improved SSP tendon attachment through increased bone remodeling. At 1 day post-surgery, CS-PRP implants were resident inside the bony trough and lateral tunnels and also adhered to tendon surfaces, probably due to the mucoadhesive properties of chitosan (Benjamin, Kumai et al. 2002). Similarly to CS-GP/blood implants (Chevrier, Hoemann et al. 2007), CS-PRP implants stimulated the innate immune response and induced recruitment of PMN cells, which contributed to implant degradation. It is well known that chitosans with higher degrees of deacetylation (DDA) and molar mass ( $M_n$ ) will have lower degradation rates, but the site of implantation will also have a significant impact on the implants' degradation rate. Unexpectedly, small areas of neutrophil-rich granulation tissue surrounding apoptotic/necrotic tissues were visible in 3 CS-PRP treated shoulders at 2 months, which suggests that implant degradation was not complete in these animals, as residual apoptotic/necrotic granulation tissues were previously shown to correlate with resident chitosan oligomer particles in a rabbit cartilage repair model (Lafantaisie-Favreau, Guzman-Morales et al. 2013). A leukocyte-rich PRP was used to prepare the implants in the current study, which would be expected to have an impact on the cytokine cocktail that is released upon activation. Previous *in vitro* studies have suggested that matrix metalloproteinases (MMP) and cytokines released from leukocyte-rich PRP could have deleterious effects on tendon healing (McCarrel and Fortier 2009, Pandey and Jaap Willems 2015). However, MMPs are believed to be essential for tissue remodeling during rotator cuff tear repair *in vivo* (Fabis, Kordek et al. 1998, Gulotta and Rodeo 2009) and clinical data regarding using leukocyte-rich versus leukocyte-poor PRP for rotator cuff repair is still inconclusive.

The suppression of SSP tendon heterotopic ossification (HO) by CS-PRP treatment was an unexpected finding in this study. HO is an abnormal formation of mature, lamellar bone in soft tissues where bone normally doesn't exist (Barile, Bruno et al. 2017). HO is a well-known complication following surgical procedures or traumatic injuries (Stein, Patel et al. 2003, Apostolakos, Durant et al. 2014). Osteoinductive factors are released as a consequence of soft tissue trauma thus inducing formation of heterotopic bone (VandeVord, Matthew et al. 2002, Fotiadou, Vlychou et al. 2008, Deprés-Tremblay, Chevrier et al. 2017). The pathogenesis is

unclear, but it may involve inappropriate differentiation of pluripotent mesenchymal stem cells (MSCs) into bone forming cells under growth factor influence (Naqvi, Jadaan et al. 2009). HO occurs through endochondral ossification (Barile, Bruno et al. 2017), the first step of which is differentiation of MSCs into chondrocytes, an event we observed here in the shoulder treated with suturing only at 7 days, but not in the shoulder treated with CS-PRP. Interestingly, CS-GP/blood implants were also previously shown to modulate the timing and spatial development of endochondral ossification in a rabbit cartilage repair model (Chevrier, Hoemann et al. 2011), although the mechanisms by which this occurs still remain unclear.

The bone surrounding the bony trough is a probable source of repair cells in this model, as are bursa or synovial-derived cells (Uthoff, Sano et al. 2000). The tendon stump appeared to contribute little to healing, and was integrated within the new repair tissue at 2 months. Improving tendon-bone healing is a common clinical challenge in rotator cuff repair (Lee, Lee et al. 2016). Development of bone-tendon junction occurs through endochondral ossification (Lin, Cardenas et al. 2004, Hamada, Katoh et al. 2006, Rees, Wilson et al. 2006), while tendon-bone repair appears to depend upon bone ingrowth into fibrovascular interface tissue. Surgical reattachment of rotator cuff tear with current repair techniques leads to a more abrupt interface and a disorganized scar tissue that is mechanically a lot weaker than a native interface (Thomopoulos, Hattersley et al. 2002, Tutwiler, Litvinov et al. 2016), and augmentation techniques still need to be developed to overcome this limitation. As reported previously (Uthoff, Sano et al. 2000), enthesis regeneration was not achieved in the transosseous repair model used here, however, partial restoration of the calcified interface was more common with CS-PRP treatment. Growth factors synthesized and secreted by cells involved in tissue repair, such as platelets, inflammatory cells, fibroblasts, epithelial cells, and vascular endothelial cells (Kobayashi, Itoi et al. 2006), all regulate tendon-bone repair, and it is likely that treatment with CS-PRP modulates such signals. Gap formation is thought to be associated with impaired rotator cuff healing (Gwinner, Gerhardt et al. 2016), preventing enthesis reformation (Trudel, Ramachandran et al. 2012a). CS-PRP treatment promoted attachment of the SSP tendon, possibly through an increase in bone remodeling at the greater tuberosity. Previous cartilage repair studies in the rabbit also showed that both CS-GP/blood implants and CS-PRP implants promote bone

remodeling and tissue integration (Chevrier, Hoemann et al. 2007, Hoemann, Sun et al. 2007, Chen, Sun et al. 2011, Dwivedi, Chevrier et al. 2016). The bony trough was incompletely healed in some rabbits, consistent with previously published data showing that complete recovery of the bony trough only occurs after 12 weeks post-surgery in this model (Uhthoff, Seki et al. 2002).

No treatment-specific adverse events occurred during the study, which suggests high safety. Surgical detachment and immediate reattachment of the SSP tendon was sufficient to cause fatty infiltration of the SSP muscle but did not induce degeneration of the humeral head and glenoid articular surfaces. CS-PRP implants in conjunction with transosseous suturing improved the attachment of the SSP tendon to the humeral head over suturing alone. These results provide evidence that CS-PRP implants are safe and effective in improving rotator cuff tear repair in a small animal model, and that this could potentially be translated to a clinical setting.

Subsequently, CS-PRP hybrids were tested in a sheep rotator cuff tear model. Our data showed that CS-PRP induced PMNs recruitment at 3 weeks and a better ISP tendon structural organization at 3 months. We also found that bone remodeling was significantly increased in CS-PRP treated shoulders. Moreover, no treatment-specific deleterious effects were seen. Large animal models, like sheep, have infraspinatus tendons that are similar in size to the human supraspinatus (Edelstein, Thomas et al. 2011), making them suitable for using repair techniques commonly employed in humans (Derwin, Baker et al. 2007, Schlegel, Hawkins et al. 2007), as was done here in this study with suture anchors. One important finding reported here, are the difficulties we faced during implementation of the chronic repair model. We found that capping the ISP tendons for 6 weeks with 5-cm e tubes likely prevented proper nutrient diffusion and led to cell death and severe tendon degeneration, which rendered some tendons unrepairable. Although degeneration was not as marked when the tendons were capped for 2 weeks with 5-mm silicone length, reattachment at the footprint would have been difficult to achieve since the tendon-muscle unit had significantly retracted. Capping with silicone has been used by other research groups studying chronic rotator cuff repair in sheep, but the surgery usually involves osteotomy, leaving a small bone chip attached to the ISP tendon, with the silicone covering the bone chip and not the tendon itself (Gerber, Meyer et al. 2004, Meyer, Hoppeler et al. 2004).

Other groups have used a Preclude sheet to wrap the ISP tendon and allow the tears to develop to a chronic stage (Coleman, Fealy et al. 2003, Uggen, Dines et al. 2010). Preclude is a dura substitute composed of Gore-Tex, with pores of  $<1\mu\text{m}$  in size, which would still allow nutrient diffusion to the tendons, and most likely would have been a better choice than silicone in the current study. We found that abundant scar tissues were bridging the gap between the capped tendon and the tuberosity after 2 and 6 weeks, which supports the notion that the healing response is robust and spontaneous in sheep even in these chronic models (Gerber, Meyer et al. 2004, Meyer, Hoppeler et al. 2004). As of now, we consider the acute repair model to be more consistent and easily reproducible.

Polymorphonuclear (PMN) cells were observed in the tendon repair tissue of the shoulder treated with anchors + CS-PRP for 2 weeks, which is not unexpected at this time point, since CS-PRP implants were previously shown to induce PMN recruitment for at least 2 weeks in a rabbit transosseous rotator cuff repair model (Wrana, Attisano et al. 1994). PMN recruitment was abrogated by 6 weeks, which suggests that CS-PRP implants were fully degraded by then, which is consistent with previous sheep studies using similar doses of the CS-PRP implants, albeit in the knee joint for meniscus repair (Laiho, Weis et al. 1990, Chevrier, Deprés-Tremblay et al. 2016). Similarly to what was previously seen in the transosseous rotator cuff repair model in the rabbit, the tendon treated with anchors only showed chondrogenesis and GAG expression within the tendon body at 6 weeks, while the tendon treated with anchors + CS-PRP did not. The significance of chondrogenesis occurring within the tendon repair tissue is still unclear, but we hypothesized that this may be the first step in heterotopic ossification, a well known complication of tendon injury, which we previously found was inhibited by treatment with CS-PRP implants in the transosseous rabbit model. Unexpectedly, the anchors + CS-PRP repair technique resulted in better tendon structural outcome than anchors only at 3 months, possibly through a modulation of timing of the healing sequence or through increased repair tissue remodeling.

During development, tendon-bone integration occurs through establishment of an embryonic tendon-bone attachment unit, which matures into the fibrocartilaginous insertion, known as the enthesis (Thomopoulos, Genin et al. 2010, Zelzer, Blitz et al. 2014). Maturation of the enthesis appears to follow pathways similar to the growth plate development (Thomopoulos,

Genin et al. 2010). The insertion site matures through mineralization of chondrocyte-like cells, with associated remodeling through osteoclasts and osteoblasts, creating the interface between tendon and tuberosity (Thomopoulos, Genin et al. 2010). Following repair however, tendon-bone insertion usually heals through a fibrovascular scar tissue formation, lacking any sort of reestablishment of the four zones of the native enthesis (Apostolakos, Durant et al. 2014). Rotator cuff healing occurs in overlapping phases similar to those observed in the case of wound healing, namely the inflammatory phase, the matrix production phase and the remodeling phase (Galatz 2013). In the chronic and acute models used here, the integration of the tendon repair tissue occurred through bone remodeling and ingrowth at the junction between the tendon and the underlying bone, and the native structure of the enthesis was not re-established. Bone remodeling appears to be a mechanism that enables the repair to become mechanically stronger. It has previously been suggested that strong healing between tendon and the tuberosity, with reformation of a new enthesis, necessitates bone ingrowth into scar tissue and outer tendon (Sanchez Marquez, Martínez Díez et al. 2011). Other authors have suggested that the formation of a callus appears to be essential for remodeling the tendon-bone boundary after injury (Newsham-West, Nicholson et al. 2007). In that respect, it is significant that bone remodeling and GAG expression were greater in the case of the insertion sites treated with anchors + CS-PRP compared to suture anchors only, although it is impossible to draw solid conclusions on the basis of such a small number of samples. Of note, CS-PRP implants have previously been shown to increase bone remodeling over standard treatment in the context of rotator cuff and cartilage repair in small rabbit models, leading to better integration of repair tissues (Wrana, Attisano et al. 1994, Angeline and Rodeo 2012).

There were no treatment-specific deleterious effects in the shoulder joint, suggesting that CS-PRP implants have high safety. Structural abnormalities were visible in most glenoids, suggesting that greater stresses are applied on that surface compared to the humeral head in the sheep model. Fatty infiltration of the ISP muscle was induced in both chronic and acute models, and no treatment could reverse that effect. Mild transient synovitis was present in the shoulder treated with CS-PRP at 2 weeks, and this was resolved at the later 6 weeks and 3 months time points, once the biomaterial was degraded.

In summary, developing techniques to augment of rotator cuff repair remains clinically relevant. The technical challenges associated with the chronic repair model in sheep make the acute model more preferable for future studies. These studies provide the first evidence that CS-PRP implants improve the healing response in animal models of rotator cuff repair, partly through increased bone remodeling at the tendon repair tissue and underlying bone interface.

## CHAPTER 9 CONCLUSION AND RECOMMENDATIONS

Surgical reattachment of rotator cuff tears with current repair techniques leads to a more disorganized scar tissue that is mechanically a lot weaker than a native interface, increasing the risk for failure. Over a third of the surgeries result in unsuccessful outcomes such as persistent pain and disabilities, regardless of repair technique used. Several new repair strategies are available but further clinical trials are needed to find the optimal treatment for rotator cuff repair. The best rotator cuff tear surgical treatment is currently a topic of debate, since current repair strategies do not regenerate the native enthesis. A biological strategy improving patient's intrinsic healing potential is hence needed. The thesis presented here was carried out with an objective to improve current surgical procedures in rotator cuff tear repair by injection of chitosan-PRP implants. These implants were tested in rabbit and sheep models of rotator cuff repair. Furthermore, cellular and molecular mechanisms of action of chitosan-PRP implants were elucidated, focusing on clot retraction mechanisms, platelet activation and growth factor secretion, the induction of cellular recruitment, vascularization, and biodegradability of the implants.

Our data provided support that chitosan physically coats platelets and other components of the blood clot to inhibit platelet aggregation, needed for clot retraction. Chitosan physically interferes with the ability of platelets to adhere to each other as well as the fibrin network and exert mechanical forces. Chitosan also induced platelet activation and granule secretion in cell suspensions, even more so than ADP, a known platelet agonist. Interestingly, incubation of cell suspension with trehalose along with chitosan slightly decreased expression of Pac-1 and p selectin compared to incubation with chitosan alone. One important observation was that cumulative levels of PDGF-AB and EGF released in the culture medium were higher in the case of CS-PRP clots compared to PRP clots. Platelets are activated, granules secreted and higher levels of PDGF-AB and EGF are released from CS-PRP hybrid clots compared to PRP clots *in vitro*. Finally, CS-PRP implant was still visible after 6 weeks post-implantation subcutaneously and induced cell recruitment and granulation tissue synthesis, confirming a longer residency and

higher bioactivity compared to PRP *in vivo*. It is of interest to mention that the site of implantation along with implant volume influences biodegradability.



CS-PRP implants induced PMN recruitment at early time points post-surgery in a transosseous repair model of the SSP tendon in the rabbit. At 1 day post-surgery, CS-PRP implants were resident inside the bony trough, the lateral tunnels and also adhered to the tendon surfaces, probably due to the mucoadhesive properties of chitosan. Small areas of neutrophil-rich granulation tissue surrounding apoptotic/necrotic tissues were visible in few shoulders at 2 months, suggesting that implant degradation was not complete in these animals. CS-PRP treatment suppressed SSP tendon heterotopic ossification; an event we observed in the shoulder treated with suturing only, but not in the shoulder treated with CS-PRP. Although the bony trough was incompletely healed in some rabbits, CS-PRP treatment promoted attachment of the SSP tendon, possibly through an increase in bone remodeling at the greater tuberosity. Surgical detachment and immediate reattachment of the SSP tendon was sufficient to cause fatty infiltration of the SSP muscle. CS-PRP implants in conjunction with transosseous suturing improved attachment of the SSP tendon to the humeral head compared to suturing alone. These results provide evidence that CS-PRP implants are safe and effective in improving rotator cuff tear repair in a small animal model, and that this could potentially be translated to a clinical setting.

One important finding reported here, are the difficulties we faced during implementation of the chronic sheep repair model. We found that capping the ISP tendons for 6 weeks with 5-cm silicone tubes likely prevented proper nutrient diffusion and led to cell death and severe tendon degeneration, which rendered some tendons unrepairable. Although degeneration was not as marked when the tendons were capped for 2 weeks with 5-mm silicone length, reattachment at the original footprint would have been difficult to achieve since the tendon-muscle unit had significantly retracted. Abundant scar tissues were bridging the gap between the capped tendon and the tuberosity after 2 and 6 weeks, supporting the notion that the healing response is robust and spontaneous in sheep even in chronic models. As of now, we consider the acute repair model to be more consistent and easily reproducible.

Polymorphonuclear (PMN) cells were observed in the tendon repair tissue of the shoulder treated with anchors + CS-PRP for 2 weeks, but abrogated by 6 weeks, which suggests that CS-PRP implants were fully degraded by then. The tendon treated with anchors only showed chondrogenesis and GAG expression within the tendon body at 6 weeks, while the tendon treated with anchors + CS-PRP did not. The anchors + CS-PRP repair technique resulted in better tendon

structural outcome than anchors only at 3 months, possibly through a modulation of timing of the healing sequence or through increased repair tissue remodeling. Bone remodeling was greater in the case of the insertion sites treated with anchors + CS-PRP compared to suture anchors only, although it is impossible to draw solid conclusions on the basis of such a small number of samples. Structural abnormalities were visible in most glenoids, suggesting that greater stresses are applied on that surface compared to the humeral head in the sheep model. Fatty infiltration of the ISP muscle was induced in both chronic and acute models, and no treatment could reverse that effect. Mild transient synovitis was present in the shoulder treated with CS-PRP at 2 weeks, and this was resolved at the later 6 weeks and 3 months time points, once the biomaterial was degraded.

In summary, there were no treatment-specific deleterious effects in the shoulder joint, suggesting that CS-PRP implants have high safety and developing techniques to augment of rotator cuff repair remains clinically relevant. The technical challenges associated with the chronic repair model in sheep make the acute model more preferable for future studies. These studies provide the first evidence that CS-PRP implants improve the healing response in large animal models of rotator cuff repair, partly through increased bone remodeling at the tendon repair tissue and underlying bone interface.

Although beyond the scope of this research, following recommendations are worth considering for the future:

1. *Mechanical testing of the SSP repair tendon.* Mechanical strength, such as load-to-failure and tensile strength are important parameters in determining the quality of repair tissue and should be used in future studies.
2. *Additional time points for the repair model.* We chose different time points according to our understanding from the current existing literature. Although our time points were relevant, additional time points must be studied in order to evaluate the long-term repair outcome, as well as the mechanisms of action of the implants. A long term study will

likely improve the quality and volume of the repair tissue, as well as a better enthesis reformation, since enthesis reformation takes a long time.

3. *PRP alone group.* The study presented in this research compared the effect of treatments augmented with CS-PRP compared to sutures or suture anchors alone. A group augmented with PRP was unfortunately absent. We did not use PRP augmentation as a treatment since it is well established in the current literature that PRP does not improve rotator cuff tear repair. However, it will be imperative to conduct a study with a control group receiving treatment with PRP augmentation, in order to distinguish between the effects arising from chitosan and from PRP.
4. *A different chronic model in a large animal.* CS-PRP augmentation must be retested in a large chronic animal model in order to evaluate the role of CS-PRP on chronic tears with fatty infiltration and tendon and muscle retraction. However, the use of a different chronic model is required; transecting the tendons then capping the tendon ends with Gore-Tex or Preclude sheets in order to avoid spontaneous reattachment while still diffusing nutrients appears to be more appropriate than capping with a silicone tube.
5. *Additional animals for larger animal models.* More animals must be tested with CS-PRP in a larger animal model, to evaluate fully its effect on rotator cuff tears. Statistical analysis requires a larger number of animals to obtain robust results.

To summarize our studies, augmentation of rotator cuff repair by CS-PRP implants induced superior healing in small and large rotator cuff tear repair models. Histological assessment showed improvements in CS-PRP treated shoulders, as indicated by better structural outcome, which seemed to be a result of a modulation of timing of the healing sequence, as well as better macroscopic and microscopic attachment scores. CS-PRP implants increased bone remodeling at

the enthesis, compared to sutures or suture anchors only, which contributed to improving tendon attachment. CS-PRP implants were also able to protect against heterotopic bone formation in soft tissue far from the enthesis zone. Finally, our results also provided evidence that CS-PRP implants are safe. Hence, due to their increased bioactivity, CS-PRP hybrid implants show a significant potential to be used to augment rotator cuff tear repair. We believe that we have made a significant contribution to the orthopaedic field of rotator cuff tear repair, by improving current standard-of-care surgical repair techniques, and that this technology could potentially be translated to a clinical setting in the future.

## BIBLIOGRAPHY

- (2005). Platelet function : assessment, diagnosis, and treatment Totowa, NJ, USA, Humana Press.
- Adams, J. E., M. E. Zobitz, J. S. Reach, K. N. An and S. P. Steinmann (2006). "Rotator Cuff Repair Using an Acellular Dermal Matrix Graft: An In Vivo Study in a Canine Model." Arthroscopy **22**(7): 700-709.
- Ahmad, Z., F. Henson, J. Wardale, A. Noorani, G. Tytherleigh-Strong and N. Rushton (2013). "Review article: Regenerative techniques for repair of rotator cuff tears." Journal of Orthopaedic Surgery **21**(2): 226-231.
- Akiyama, H. (2008). "Control of chondrogenesis by the transcription factor Sox9." Mod Rheumatol **18**(3): 213-219.
- Amiel, D., S. L. Woo, F. L. Harwood and W. H. Akeson (1982). "The effect of immobilization on collagen turnover in connective tissue: a biochemical-biomechanical correlation." Acta Orthop Scand **53**(3): 325-332.
- Andia, I., M. Sanchez and N. Maffulli (2010). "Tendon healing and platelet-rich plasma therapies." Expert Opin Biol Ther **10**(10): 1415-1426.
- Angeline, M. E. and S. A. Rodeo (2012). "Biologics in the management of rotator cuff surgery." Clin Sports Med **31**(4): 645-663.
- Anitua, E., M. M. Zalduendo, R. Prado, M. H. Alkhraisat and G. Orive (2014). "Morphogen and proinflammatory cytokine release kinetics from PRGF-Endoret fibrin scaffolds: Evaluation of the effect of leukocyte inclusion." J Biomed Mater Res A.
- Antoniades, H. N., C. D. Scher and C. D. Stiles (1979). "Purification of human platelet-derived growth factor." Proc Natl Acad Sci U S A **76**(4): 1809-1813.
- Antuna, S., R. Barco, J. M. Martinez Diez and J. M. Sanchez Marquez (2013). "Platelet-rich fibrin in arthroscopic repair of massive rotator cuff tears : A prospective randomized pilot clinical trial." Acta Orthop Belg **79**(1): 25-30.
- Aoki, M., H. Oguma, S. Fukushima, S. Ishii, S. Ohtani and G. Murakami (2001). "Fibrous connection to bone after immediate repair of the canine infraspinatus: the most effective bony surface for tendon attachment." J Shoulder Elbow Surg **10**(2): 123-128.
- Apostolakos, J., T. J. Durant, C. R. Dwyer, R. P. Russell, J. H. Weinreb, F. Alaei, K. Beitzel, M. B. McCarthy, M. P. Cote and A. D. Mazzocca (2014). "The enthesis: a review of the tendon-to-bone insertion." Muscles Ligaments Tendons J **4**(3): 333-342.
- Apreleva, M., M. Ozbaydar, P. G. Fitzgibbons and J. J. Warner (2002). "Rotator cuff tears: the effect of the reconstruction method on three-dimensional repair site area." Arthroscopy **18**(5): 519-526.
- (2005). Platelet function : assessment, diagnosis, and treatment Totowa, NJ, USA, Humana Press.
- Abrahamsson, S. O., R. H. Gelberman, D. Amiel, P. Winterton and F. Harwood (1995). "Autogenous flexor tendon grafts: fibroblast activity and matrix remodeling in dogs." J Orthop Res **13**(1): 58-66.
- Abrahamsson, S. O., G. Lundborg and L. S. Lohmander (1989). "Tendon healing in vivo. An experimental model." Scand J Plast Reconstr Surg Hand Surg **23**(3): 199-205.
- Adams, J. E., M. E. Zobitz, J. S. Reach, K. N. An and S. P. Steinmann (2006). "Rotator Cuff Repair Using an Acellular Dermal Matrix Graft: An In Vivo Study in a Canine Model." Arthroscopy **22**(7): 700-709.

- Agnihotri, S. A., V. D. Kulkarni, A. R. Kulkarni and T. M. Aminabhavi (2006). "Degradation of chitosan and chemically modified chitosan by viscosity measurements." Journal of Applied Polymer Science **102**(4): 3255-3258.
- Agrawal, P., G. J. Strijkers and K. Nicolay (2010). "Chitosan-based systems for molecular imaging." Adv Drug Deliv Rev **62**(1): 42-58.
- Ahmad, Z., F. Henson, J. Wardale, A. Noorani, G. Tytherleigh-Strong and N. Rushton (2013). "Review article: Regenerative techniques for repair of rotator cuff tears." Journal of Orthopaedic Surgery **21**(2): 226-231.
- Ahmad, Z., D. Howard, R. A. Brooks, J. Wardale, F. M. Henson, A. Getgood and N. Rushton (2012). "The role of platelet rich plasma in musculoskeletal science." JRSM short reports **3**(6): 40-40.
- Ahmadi, F., Z. Oveisi, S. M. Samani and Z. Amoozgar (2015). "Chitosan based hydrogels: characteristics and pharmaceutical applications." Res Pharm Sci **10**(1): 1-16.
- Akiyama, H. (2008). "Control of chondrogenesis by the transcription factor Sox9." Mod Rheumatol **18**(3): 213-219.
- Alfonso, C., O. M. Nuero, F. Santamaria and F. Reyes (1995). "Purification of a heat-stable chitin deacetylase from *Aspergillus nidulans* and its role in cell wall degradation." Curr Microbiol **30**(1): 49-54.
- Amiel, D., F. L. Harwood, R. H. Gelberman, C. R. Chu, J. G. Seiler, 3rd and S. Abrahamsson (1995). "Autogenous intrasynovial and extrasynovial tendon grafts: an experimental study of pro alpha 1(I) collagen mRNA expression in dogs." J Orthop Res **13**(3): 459-463.
- Amiel, D., S. L. Woo, F. L. Harwood and W. H. Akeson (1982). "The effect of immobilization on collagen turnover in connective tissue: a biochemical-biomechanical correlation." Acta Orthop Scand **53**(3): 325-332.
- Andia, I., M. Sanchez and N. Maffulli (2010). "Tendon healing and platelet-rich plasma therapies." Expert Opin Biol Ther **10**(10): 1415-1426.
- Angeline, M. E. and S. A. Rodeo (2012). "Biologics in the management of rotator cuff surgery." Clin Sports Med **31**(4): 645-663.
- Anitua, E., M. M. Zalduendo, R. Prado, M. H. Alkhraisat and G. Orive (2014). "Morphogen and proinflammatory cytokine release kinetics from PRGF-Endoret fibrin scaffolds: Evaluation of the effect of leukocyte inclusion." J Biomed Mater Res A.
- Antoniades, H. N., C. D. Scher and C. D. Stiles (1979). "Purification of human platelet-derived growth factor." Proc Natl Acad Sci U S A **76**(4): 1809-1813.
- Antuna, S., R. Barco, J. M. Martinez Diez and J. M. Sanchez Marquez (2013). "Platelet-rich fibrin in arthroscopic repair of massive rotator cuff tears : A prospective randomized pilot clinical trial." Acta Orthop Belg **79**(1): 25-30.
- Aoki, M., H. Oguma, S. Fukushima, S. Ishii, S. Ohtani and G. Murakami (2001). "Fibrous connection to bone after immediate repair of the canine infraspinatus: the most effective bony surface for tendon attachment." J Shoulder Elbow Surg **10**(2): 123-128.
- Apostolakos, J., T. J. Durant, C. R. Dwyer, R. P. Russell, J. H. Weinreb, F. Alaei, K. Beitzel, M. B. McCarthy, M. P. Cote and A. D. Mazzocca (2014). "The enthesis: a review of the tendon-to-bone insertion." Muscles Ligaments Tendons J **4**(3): 333-342.

- Apreleva, M., M. Ozbaydar, P. G. Fitzgibbons and J. J. Warner (2002). "Rotator cuff tears: the effect of the reconstruction method on three-dimensional repair site area." Arthroscopy **18**(5): 519-526.
- Araki, Y. and E. Ito (1974). "A pathway of chitosan formation in *Mucor rouxii*: enzymatic deacetylation of chitin." Biochem Biophys Res Commun **56**(3): 669-675.
- Ark, J. W., R. H. Gelberman, S. O. Abrahamsson, J. G. Seiler, 3rd and D. Amiel (1994). "Cellular survival and proliferation in autogenous flexor tendon grafts." J Hand Surg Am **19**(2): 249-258.
- Arnoczky, S. P., T. Tian, M. Lavagnino, K. Gardner, P. Schuler and P. Morse (2002). "Activation of stress-activated protein kinases (SAPK) in tendon cells following cyclic strain: the effects of strain frequency, strain magnitude, and cytosolic calcium." J Orthop Res **20**(5): 947-952.
- Asou, Y., A. Nifuji, K. Tsuji, K. Shinomiya, E. N. Olson, P. Koopman and M. Noda (2002). "Coordinated expression of scleraxis and Sox9 genes during embryonic development of tendons and cartilage." J Orthop Res **20**(4): 827-833.
- Athanasίου, K. A., A. R. Shah, R. J. Hernandez and R. G. LeBaron (2001). "Basic science of articular cartilage repair." Clin Sports Med **20**(2): 223-247.
- Aurora, A., J. McCarron, J. P. Iannotti and K. Derwin (2007). "Commercially available extracellular matrix materials for rotator cuff repairs: state of the art and future trends." J Shoulder Elbow Surg **16**(5 Suppl): S171-178.
- Awad, H. A., G. P. Boivin, M. R. Dressler, F. N. Smith, R. G. Young and D. L. Butler (2003). "Repair of patellar tendon injuries using a cell-collagen composite." J Orthop Res **21**(3): 420-431.
- Aydin, N., B. Kocaoglu and O. Guven (2010). "Single-row versus double-row arthroscopic rotator cuff repair in small- to medium-sized tears." Journal of Shoulder and Elbow Surgery **19**(5): 722-725.
- Azab, A. K., V. Doviner, B. Orkin, J. Kleinstern, M. Srebnik, A. Nissan and A. Rubinstein (2007). "Biocompatibility evaluation of crosslinked chitosan hydrogels after subcutaneous and intraperitoneal implantation in the rat." J Biomed Mater Res A **83**(2): 414-422.
- Azad, A. K., N. Sermsintham, S. Chandkrachang and W. F. Stevens (2004). "Chitosan membrane as a wound-healing dressing: characterization and clinical application." J Biomed Mater Res B Appl Biomater **69**(2): 216-222.
- Badhe, S. P., T. M. Lawrence, F. D. Smith and P. G. Lunn (2008). "An assessment of porcine dermal xenograft as an augmentation graft in the treatment of extensive rotator cuff tears." J Shoulder Elbow Surg **17**(1 Suppl): 35s-39s.
- Bakaltcheva, I. and T. Reid (2003). "Effects of blood product storage protectants on blood coagulation." Transfusion Medicine Reviews **17**(4): 263-271.
- Baleani, M., C. Ohman, L. Guandalini, R. Rotini, G. Glavaresi, F. Traina and M. Viceconti (2006). "Comparative study of different tendon grasping techniques for arthroscopic repair of the rotator cuff." Clinical Biomechanics **21**(8): 799-803.
- Barber, F. A., J. P. Burns, A. Deutsch, M. R. Labbe and R. B. Litchfield (2012). "A prospective, randomized evaluation of acellular human dermal matrix augmentation for arthroscopic rotator cuff repair." Arthroscopy **28**(1): 8-15.
- Barber, F. A., M. A. Herbert and M. H. Boothby (2008). "Ultimate tensile failure loads of a human dermal allograft rotator cuff augmentation." Arthroscopy **24**(1): 20-24.

- Barber, F. A., S. A. Hrnack, S. J. Snyder and O. Hapa (2011). "Rotator cuff repair healing influenced by platelet-rich plasma construct augmentation." *Arthroscopy* **27**(8): 1029-1035.
- Barber, F. A., S. A. Hrnack, S. J. Snyder and O. Hapa (2011). "Rotator Cuff Repair Healing Influenced by Platelet-Rich Plasma Construct Augmentation: A Novel Molecular Mechanism Reply." *Arthroscopy* **27**(11): 1456-1457.
- Barile, A., F. Bruno, S. Mariani, F. Arrigoni, A. Reginelli, M. De Filippo, M. Zappia, A. Splendiani, E. Di Cesare and C. Masciocchi (2017). "What can be seen after rotator cuff repair: a brief review of diagnostic imaging findings." *Musculoskelet Surg* **101**(Suppl 1): 3-14.
- Barroso, T., R. Viveiros, T. Casimiro and A. Aguiar-Ricardo (2014). "Development of dual-responsive chitosan–collagen scaffolds for pulsatile release of bioactive molecules." *The Journal of Supercritical Fluids* **94**: 102-112.
- Bartnicki-Garcia, S., J. Persson and H. Chanzy (1994). "An electron microscope and electron diffraction study of the effect of calcofluor and congo red on the biosynthesis of chitin in vitro." *Arch Biochem Biophys* **310**(1): 6-15.
- Baskar, D. and T. S. Sampath Kumar (2009). "Effect of deacetylation time on the preparation, properties and swelling behavior of chitosan films." *Carbohydrate Polymers* **78**(4): 767-772.
- Basmajian, J. V. and F. J. Bazant (1959). "Factors preventing downward dislocation of the adducted shoulder joint. An electromyographic and morphological study." *J Bone Joint Surg Am* **41-a**: 1182-1186.
- Baums, M. H., B. Schminke, A. Posmyk, N. Miosge, H. M. Klinger and S. Lakemeier (2015). "Effect of single- and double-row rotator cuff repair at the tendon-to-bone interface: preliminary results using an in vivo sheep model." *Arch Orthop Trauma Surg* **135**(1): 111-118.
- Baums, M. H., G. Spahn, G. H. Buchhorn, W. Schultz, L. Hofmann and H.-M. Klinger (2012). "Biomechanical and Magnetic Resonance Imaging Evaluation of a Single- and Double-Row Rotator Cuff Repair in an In Vivo Sheep Model." *Arthroscopy* **28**(6): 769-777.
- Beck, J., D. Evans, P. M. Tonino, S. Yong and J. J. Callaci (2012). "The biomechanical and histologic effects of platelet-rich plasma on rat rotator cuff repairs." *Am J Sports Med* **40**(9): 2037-2044.
- Bedi, A., A. J. Fox, D. Kovacevic, X. H. Deng, R. F. Warren and S. A. Rodeo (2010). "Doxycycline-mediated inhibition of matrix metalloproteinases improves healing after rotator cuff repair." *Am J Sports Med* **38**(2): 308-317.
- Bedi, A., D. Kovacevic, C. Hettrich, L. V. Gulotta, J. R. Ehteshami, R. F. Warren and S. A. Rodeo (2010). "The effect of matrix metalloproteinase inhibition on tendon-to-bone healing in a rotator cuff repair model." *J Shoulder Elbow Surg* **19**(3): 384-391.
- Beitzel, K., M. B. McCarthy, M. P. Cote, T. J. Durant, D. M. Chowaniec, O. Solovyova, R. P. Russell, R. A. Arciero and A. D. Mazzocca (2013). "Comparison of mesenchymal stem cells (osteoprogenitors) harvested from proximal humerus and distal femur during arthroscopic surgery." *Arthroscopy* **29**(2): 301-308.
- Benazzo, F., G. Zanon and N. Maffulli (2000). "An Operative Approach to Achilles Tendinopathy." *Sports Medicine and Arthroscopy Review* **8**(1): 96-101.
- Benjamin, M., T. Kumai, S. Milz, B. M. Boszczyk, A. A. Boszczyk and J. R. Ralphs (2002). "The skeletal attachment of tendons--tendon "entheses"." *Comp Biochem Physiol A Mol Integr Physiol* **133**(4): 931-945.



- Benjamin, M. and D. McGonagle (2009). "Entheses: tendon and ligament attachment sites." Scand J Med Sci Sports **19**(4): 520-527.
- Benjamin, M. and J. R. Ralphs (1997). "Tendons and ligaments--an overview." Histol Histopathol **12**(4): 1135-1144.
- Benjamin, M. and J. R. Ralphs (1998). "Fibrocartilage in tendons and ligaments--an adaptation to compressive load." J Anat **193** ( Pt 4): 481-494.
- Benjamin, M. and J. R. Ralphs (2001). "Entheses--the bony attachments of tendons and ligaments." Ital J Anat Embryol **106**(2 Suppl 1): 151-157.
- Benjamin, M., H. Toumi, J. R. Ralphs, G. Bydder, T. M. Best and S. Milz (2006). "Where tendons and ligaments meet bone: attachment sites ('enthese') in relation to exercise and/or mechanical load." J Anat **208**(4): 471-490.
- Bergeson, A. G., R. Z. Tashjian, P. E. Greis, J. Crim, G. J. Stoddard and R. T. Burks (2012). "Effects of platelet-rich fibrin matrix on repair integrity of at-risk rotator cuff tears." Am J Sports Med **40**(2): 286-293.
- Best, T. M. and W. E. Garrett (1994). "Basic science of soft tissue: muscle and tendon." Orthopaedic sports medicine.
- Bestwick, C. S. and N. Maffulli (2000). "Reactive Oxygen Species and Tendon Problems: Review and Hypothesis." Sports Medicine and Arthroscopy Review **8**(1): 6-16.
- Birch, H. L., G. A. Rutter and A. E. Goodship (1997). "Oxidative energy metabolism in equine tendon cells." Res Vet Sci **62**(2): 93-97.
- Birk, D. E. and R. Mayne (1997). "Localization of collagen types I, III and V during tendon development. Changes in collagen types I and III are correlated with changes in fibril diameter." Eur J Cell Biol **72**(4): 352-361.
- Bishop, J., S. Klepps, I. K. Lo, J. Bird, J. N. Gladstone and E. L. Flatow (2006). "Cuff integrity after arthroscopic versus open rotator cuff repair: a prospective study." J Shoulder Elbow Surg **15**(3): 290-299.
- Bishop, J., S. Klepps, I. K. Lo, J. Bird, J. N. Gladstone and E. L. Flatow (2006). "Cuff integrity after arthroscopic versus open rotator cuff repair: A prospective study." Journal of Shoulder and Elbow Surgery **15**(3): 290-299.
- Blackwell, J., Parker, K., & Rudall, K (1965). "Chitin in pogonophore tubes." Journal of the Marine Biological Association of the United Kingdom **45**(3): 659-661.
- Blitz, E., S. Viukov, A. Sharir, Y. Shwartz, J. L. Galloway, B. A. Pryce, R. L. Johnson, C. J. Tabin, R. Schweitzer and E. Zelzer (2009). "Bone ridge patterning during musculoskeletal assembly is mediated through SCX regulation of Bmp4 at the tendon-skeleton junction." Dev Cell **17**(6): 861-873.
- Boileau, P., N. Brassart, D. J. Watkinson, M. Carles, A. M. Hatzidakis and S. G. Krishnan (2005). "Arthroscopic repair of full-thickness tears of the supraspinatus: Does the tendon really heal?" Journal of Bone and Joint Surgery-American Volume **87A**(6): 1229-1240.
- Bond, J. L., R. M. Dopirak, J. Higgins, J. Burns and S. J. Snyder (2008). "Arthroscopic replacement of massive, irreparable rotator cuff tears using a GraftJacket allograft: technique and preliminary results." Arthroscopy **24**(4): 403-409.e401.
- Borges, O., G. Borchard, A. de Sousa, H. E. Junginger and A. Cordeiro-da-Silva (2007). "Induction of lymphocytes activated marker CD69 following exposure to chitosan and alginate biopolymers." Int J Pharm **337**(1-2): 254-264.

- Boyer, M. I., J. T. Watson, J. Lou, P. R. Manske, R. H. Gelberman and S. R. Cai (2001). "Quantitative variation in vascular endothelial growth factor mRNA expression during early flexor tendon healing: an investigation in a canine model." J Orthop Res **19**(5): 869-872.
- Bray, R. C., J. A. Smith, M. K. Eng, C. A. Leonard, C. A. Sutherland and P. T. Salo (2001). "Vascular response of the meniscus to injury: effects of immobilization." Journal of Orthopaedic Research **19**(3): 384-390.
- Brent, A. E., R. Schweitzer and C. J. Tabin (2003). "A somitic compartment of tendon progenitors." Cell **113**(2): 235-248.
- Brew, K. and H. Nagase (2010). "The tissue inhibitors of metalloproteinases (TIMPs): an ancient family with structural and functional diversity." Biochim Biophys Acta **1803**(1): 55-71.
- Brown, G. T., P. Narayanan, W. Li, R. L. Silverstein and T. M. McIntyre (2013). "Lipopolysaccharide stimulates platelets through an IL-1beta autocrine loop." J Immunol **191**(10): 5196-5203.
- Buchmann, S., G. H. Sandmann, L. Walz, H. Hoppe, K. Beitzel, G. Wexel, W. Tian, G. Winter and A. B. Imhoff (2013). "Refixation of the supraspinatus tendon in a rat model--influence of continuous growth factor application on tendon structure." J Orthop Res **31**(2): 300-305.
- Bunker, D. L., V. Ilie, V. Ilie and S. Nicklin (2014). "Tendon to bone healing and its implications for surgery." Muscles Ligaments Tendons J **4**(3): 343-350.
- Bunker, D. L., V. Ilie and S. Nicklin (2014). "Tendon to bone healing and its implications for surgery." Muscles Ligaments Tendons J **4**(3): 343-350.
- Burkhead WZ, S. S., Krishnan SG (2007). "Use of graft jacket as an augmentation for massive rotator cuff tears." Semin Arthroplasty(18): 11-18.
- Busilacchi, A., A. Gigante, M. Mattioli-Belmonte and e. al. (2013). "Chitosan stabilizes platelet growth factors and modulates stem cell differentiation toward tissue regeneration." Carbohydrate Polymers **98** (1): 665-676
- Busilacchi, A., A. Gigante, M. Mattioli-Belmonte, S. Manzotti and R. A. Muzzarelli (2013). "Chitosan stabilizes platelet growth factors and modulates stem cell differentiation toward tissue regeneration." Carbohydr Polym **98**(1): 665-676.
- Cabitza, P., G. Banfi, A. Ersen, M. Demirhan, A. C. Atalar, M. Kapicioglu and G. Baysal (2014). "Platelet-rich plasma for enhancing surgical rotator cuff repair: evaluation and comparison of two application methods in a rat model." Biomed Res Int **134**(3): 405-411.
- Carbonel, I., A. Antonio Martinez, A. Calvo, J. Ripalda and A. Herrera (2012). "Single-row versus double-row arthroscopic repair in the treatment of rotator cuff tears: a prospective randomized clinical study." International Orthopaedics **36**(9): 1877-1883.
- Carr, A. J. and S. H. Norris (1989). "The blood supply of the calcaneal tendon." J Bone Joint Surg Br **71**(1): 100-101.
- Castillo, T. N., M. A. Pouliot, H. J. Kim and J. L. Drago (2011). "Comparison of Growth Factor and Platelet Concentration From Commercial Platelet-Rich Plasma Separation Systems." American Journal of Sports Medicine **39**(2): 266-271.
- Castricini, R., U. G. Longo, M. De Benedetto, N. Panfoli, P. Pirani, R. Zini, N. Maffulli and V. Denaro (2011). "Platelet-Rich Plasma Augmentation for Arthroscopic Rotator Cuff Repair A Randomized Controlled Trial." American Journal of Sports Medicine **39**(2): 258-265.

- Castricini, R., U. G. Longo, M. De Benedetto, N. Panfoli, P. Pirani, R. Zini, N. Maffulli and V. Denaro (2011). "Platelet-rich plasma augmentation for arthroscopic rotator cuff repair: a randomized controlled trial." Am J Sports Med **39**(2): 258-265.
- Cavallo, C., G. Filardo, E. Mariani, E. Kon, M. Marcacci, M. T. Pereira Ruiz, A. Facchini and B. Grigolo (2014). "Comparison of platelet-rich plasma formulations for cartilage healing: an in vitro study." J Bone Joint Surg Am **96**(5): 423-429.
- Chahal, J., N. Mall, P. B. MacDonald, G. Van Thiel, B. J. Cole, A. A. Romeo and N. N. Verma (2012). "The role of subacromial decompression in patients undergoing arthroscopic repair of full-thickness tears of the rotator cuff: a systematic review and meta-analysis." Arthroscopy **28**(5): 720-727.
- Chahla, J., C. S. Dean, G. Moatshe, J. J. Mitchell, T. R. Cram, C. Yacuzzi and R. F. LaPrade (2016). "Meniscal Ramp Lesions: Anatomy, Incidence, Diagnosis, and Treatment." Orthop J Sports Med **4**(7): 2325967116657815.
- Chang, C. H., C. H. Chen, C. Y. Su, H. T. Liu and C. M. Yu (2009). "Rotator cuff repair with periosteum for enhancing tendon-bone healing: a biomechanical and histological study in rabbits." Knee Surg Sports Traumatol Arthrosc **17**(12): 1447-1453.
- Chang, K. L. B., G. Tsai, J. Lee and W.-R. Fu (1997). "Heterogeneous N-deacetylation of chitin in alkaline solution." Carbohydrate Research **303**(3): 327-332.
- Chang, S. J., S. M. Kuo, C.-W. Lan, I. Manousakas and P. H. Tsai (2009). "EVALUATION OF CHITOSAN/CaSO<sub>4</sub>/PLATELET-RICH PLASMA MICROSPHERE COMPOSITES AS ALVEOLUS OSTEOGENESIS MATERIAL." Biomedical Engineering: Applications, Basis and Communications **21**(02): 115-122.
- Charousset, C., A. Zaoui, L. Bellaïche and M. Piterman (2014). "Does Autologous Leukocyte-Platelet-Rich Plasma Improve Tendon Healing in Arthroscopic Repair of Large or Massive Rotator Cuff Tears?" Arthroscopy **30**(4): 428-435.
- Chen, G., J. Sun, V. Lascau-Coman, A. Chevrier, C. Marchand and C. D. Hoemann (2011). "Acute Osteoclast Activity following Subchondral Drilling Is Promoted by Chitosan and Associated with Improved Cartilage Repair Tissue Integration." Cartilage **2**(2): 173-185.
- Chen, M., W. Xu, Q. Dong, Q. Huang, Z. Xie and Y. Mao (2013). "Outcomes of Single-Row Versus Double-Row Arthroscopic Rotator Cuff Repair: A Systematic Review and Meta-Analysis of Current Evidence." Arthroscopy **29**(8): 1437-1449.
- Chenite, A., C. Chaput, D. Wang, C. Combes, M. D. Buschmann, C. D. Hoemann, J. C. Leroux, B. L. Atkinson, F. Binette and A. Selmani (2000). "Novel injectable neutral solutions of chitosan form biodegradable gels in situ." Biomaterials **21**(21): 2155-2161.
- Cheon, S. J., J. H. Kim, H. C. Gwak, C. W. Kim, J. K. Kim and J. H. Park (2017). "Comparison of histologic healing and biomechanical characteristics between repair techniques for a delaminated rotator cuff tear in rabbits." J Shoulder Elbow Surg **26**(5): 838-845.
- Chevrier, A., V. Darras, G. Picard, M. Nelea, D. Veilleux, M. Lavertu, C. D. Hoemann and M. D. Buschmann (2017). "Injectable chitosan-platelet-rich plasma (PRP) implants to promote tissue regeneration: In vitro properties, in vivo residence, degradation, cell recruitment and vascularization." J Tissue Eng Regen Med **In Press**.
- Chevrier, A., G. Déprés-Tremblay, M. B. Hurtig and M. D. Buschmann (2016). Chitosan-platelet-rich plasma implants can be injected into meniscus defects to improve repair. Transactions Orthopaedic Research Society, Orlando, FL, USA.

- Chevrier, A., G. Deprés-Tremblay, M. Nelea, M. B. Hurtig and M. D. Buschmann (2015). "Chitosan-platelet-rich plasma implants have in situ tissue building capacity and can be injected into meniscus defects to improve repair." Transactions International Cartilage Repair Society Chicago, USA.
- Chevrier, A., C. D. Hoemann, J. Sun and M. D. Buschmann (2007). "Chitosan-glycerol phosphate/blood implants increase cell recruitment, transient vascularization and subchondral bone remodeling in drilled cartilage defects." Osteoarthritis and Cartilage **15**(3): 316-327.
- Chevrier, A., C. D. Hoemann, J. Sun and M. D. Buschmann (2007). "Chitosan-glycerol phosphate/blood implants increase cell recruitment, transient vascularization and subchondral bone remodeling in drilled cartilage defects." Osteoarthritis and Cartilage **15**(3): 316-327.
- Chevrier, A., C. D. Hoemann, J. Sun and M. D. Buschmann (2011). "Temporal and spatial modulation of chondrogenic foci in subchondral microdrill holes by chitosan-glycerol phosphate/blood implants." Osteoarthritis and cartilage / OARS, Osteoarthritis Research Society **19**: 136-144.
- Cho, M. H., K. S. Kim, H. H. Ahn, M. S. Kim, S. H. Kim, G. Khang, B. Lee and H. B. Lee (2008). "Chitosan gel as an in situ-forming scaffold for rat bone marrow mesenchymal stem cells in vivo." Tissue Eng Part A **14**(6): 1099-1108.
- Cho, Y. W., J. Jang, C. R. Park and S. W. Ko (2000). "Preparation and solubility in acid and water of partially deacetylated chitins." Biomacromolecules **1**(4): 609-614.
- Chou, T. C., E. Fu, C. J. Wu and J. H. Yeh (2003). "Chitosan enhances platelet adhesion and aggregation." Biochem Biophys Res Commun **302**(3): 480-483.
- Chung, S. W., S. H. Kim and J. H. Oh (2014). "Animal Experiments Using Rotator Cuff." Clinics in Shoulder & Elbow **17**(2): 84-90.
- Chung, S. W., B. W. Song, Y. H. Kim, K. U. Park and J. H. Oh (2013). "Effect of platelet-rich plasma and porcine dermal collagen graft augmentation for rotator cuff healing in a rabbit model." Am J Sports Med **41**(12): 2909-2918.
- Cilli, F., M. Khan, F. Fu and J. H. Wang (2004). "Prostaglandin E2 affects proliferation and collagen synthesis by human patellar tendon fibroblasts." Clin J Sport Med **14**(4): 232-236.
- Clark, J. M. and D. T. Harryman, 2nd (1992). "Tendons, ligaments, and capsule of the rotator cuff. Gross and microscopic anatomy." J Bone Joint Surg Am **74**(5): 713-725.
- Clement, N. D., Y. X. Nie and J. M. McBirnie (2012). "Management of degenerative rotator cuff tears: a review and treatment strategy." Sports Med Arthrosc Rehabil Ther Technol **4**(1): 48-48.
- Cohen, I. (1985). The mechanism of clot retraction. Platelet membrane glycoproteins. New York, NY, USA, Springer US: 299-323.
- Cohen, I., J. M. Gerrard and J. G. White (1982). "Ultrastructure of clots during isometric contraction." J Cell Biol **93**(3): 775-787.
- Cole, B. J., N. S. ElAttrache and A. Anbari (2007). "Arthroscopic rotator cuff repairs: An anatomic and biomechanical rationale for different suture-anchor repair configurations." Arthroscopy **23**(6): 662-669.
- Coleman, S. H., S. Fealy, J. R. Ehteshami, J. D. MacGillivray, D. W. Altchek, R. F. Warren and A. S. Turner (2003). "Chronic rotator cuff injury and repair model in sheep." J Bone Joint Surg Am **85-a**(12): 2391-2402.

- Coleman, S. H., S. Fealy, J. R. Ehteshami, J. D. MacGillivray, D. W. Altchek, R. F. Warren and A. S. Turner (2003). "Chronic rotator cuff injury and repair model in sheep." Journal of Bone and Joint Surgery-American Volume **85A**(12): 2391-2402.
- Costic RS, B. P., Smolinski PJ, Gilbertson LG, Rodosky MW (2006). "Arthroscopic double row anchor repair of full thickness rotator cuff tear: Footprint restoration and biomechanical properties." Presented at the Annual Meeting of the Orthopaedic Research Society, Chicago, IL.
- Cserjesi, P., D. Brown, K. L. Ligon, G. E. Lyons, N. G. Copeland, D. J. Gilbert, N. A. Jenkins and E. N. Olson (1995). "Scleraxis: a basic helix-loop-helix protein that prefigures skeletal formation during mouse embryogenesis." Development **121**(4): 1099-1110.
- Dai, T., M. Tanaka, Y. Y. Huang and M. R. Hamblin (2011). "Chitosan preparations for wounds and burns: antimicrobial and wound-healing effects." Expert Rev Anti Infect Ther **9**(7): 857-879.
- Dash, M., F. Chiellini, R. M. Ottenbrite and E. Chiellini (2011). "Chitosan—A versatile semi-synthetic polymer in biomedical applications." Progress in Polymer Science **36**(8): 981-1014.
- De Aguiar, G., L. A. Chait, D. Schultz, S. Bleloch, A. Theron, C. N. Snijman and V. Ching (2009). "Chemoprotection of flexor tendon repairs using botulinum toxin." Plast Reconstr Surg **124**(1): 201-209.
- Del Buono, A., F. Oliva, U. G. Longo, S. A. Rodeo, J. Orchard, V. Denaro and N. Maffulli (2012). "Metalloproteases and rotator cuff disease." J Shoulder Elbow Surg **21**(2): 200-208.
- Denard, P. J. and S. S. Burkhart (2013). "The Evolution of Suture Anchors in Arthroscopic Rotator Cuff Repair." Arthroscopy **29**(9): 1589-1595.
- Denard, P. J., A. Z. Jiwani, A. Laedermann and S. S. Burkhart (2012). "Long-Term Outcome of Arthroscopic Massive Rotator Cuff Repair: The Importance of Double-Row Fixation." Arthroscopy **28**(7): 909-915.
- Deprés-Tremblay, G., A. Chevrier and M. D. Buschmann (2017). Freeze-dried chitosan-PRP in a rabbit model of rotator cuff repair. Transactions Orthopaedic Research Society, San Diego, CA, USA.
- Deprés-Tremblay, G., A. Chevrier, N. Tran-Khanh, M. Nelea and M. D. Buschmann (2017). "Chitosan inhibits platelet-mediated clot retraction, increases platelet-derived growth factor release, and increases residence time and bioactivity of platelet-rich plasma in vivo." Biomedical Materials **Submitted**.
- Derwin, K. A., S. F. Badylak, S. P. Steinmann and J. P. Iannotti (2010). "Extracellular matrix scaffold devices for rotator cuff repair." Journal of Shoulder and Elbow Surgery **19**(3): 467-476.
- Derwin, K. A., A. R. Baker, M. J. Codsì and J. P. Iannotti (2007). "Assessment of the canine model of rotator cuff injury and repair." Journal of Shoulder and Elbow Surgery **16**(5): 140S-148S.
- Derwin, K. A., A. R. Baker, J. P. Iannotti and J. A. McCarron (2010). "Preclinical Models for Translating Regenerative Medicine Therapies for Rotator Cuff Repair." Tissue Engineering Part B-Reviews **16**(1): 21-30.
- Di Giacomo, G., Pouliart, N, Costantini, C., De Vita, A. (2008). Atlas of Functional Shoulder Anatomy. Rome, Italy, Springer.
- Dines, J. S., L. Weber, P. Razzano, R. Prajapati, M. Timmer, S. Bowman, L. Bonasser, D. M. Dines and D. P. Grande (2007). "The effect of growth differentiation factor-5-coated sutures on tendon repair in a rat model." J Shoulder Elbow Surg **16**(5 Suppl): S215-221.

- Docheva, D., S. A. Muller, M. Majewski and C. H. Evans (2015). "Biologics for tendon repair." Adv Drug Deliv Rev **84**: 222-239.
- Dohan Ehrenfest, D. M., L. Rasmusson and T. Albrektsson (2009). "Classification of platelet concentrates: from pure platelet-rich plasma (P-PRP) to leucocyte- and platelet-rich fibrin (L-PRF)." Trends Biotechnol **27**(3): 158-167.
- Dolkart, O., O. Chechik, Y. Zarfati, T. Brosh, F. Alhajjra and E. Maman (2014). "A single dose of platelet-rich plasma improves the organization and strength of a surgically repaired rotator cuff tendon in rats." Arch Orthop Trauma Surg **134**(9): 1271-1277.
- Doschak, M. R. and R. F. Zernicke (2005). "Structure, function and adaptation of bone-tendon and bone-ligament complexes." J Musculoskelet Neuronal Interact **5**(1): 35-40.
- Dwivedi, G., A. Chevrier, C. D. Hoemann and M. D. Buschmann (2016). Freeze dried chitosan/platelet-rich-plasma implants improve marrow stimulated cartilage repair in rabbit chronic defect model International Cartilage Repair Society. Sorrento, Italy.
- Dwivedi, G., A. Chevrier, C. D. Hoemann and M. D. Buschmann (2017). Freeze dried chitosan/platelet-rich-plasma implants improve marrow stimulated cartilage repair in rabbit chronic defect model Transactions Orthopaedic Research Society. San Diego, CA, USA.
- Edelstein, L., S. J. Thomas and L. J. Soslowsky (2011). "Rotator Cuff Tears: What have we learned from animal models?" Journal of Musculoskeletal & Neuronal Interactions **11**(2): 150-162.
- Eide, K. B., A. L. Norberg, E. B. Heggset, A. R. Lindbom, K. M. Varum, V. G. Eijsink and M. Sorlie (2012). "Human chitotriosidase-catalyzed hydrolysis of chitosan." Biochemistry **51**(1): 487-495.
- Ellera Gomes, J. L., R. C. da Silva, L. M. Silla, M. R. Abreu and R. Pellanda (2012). "Conventional rotator cuff repair complemented by the aid of mononuclear autologous stem cells." Knee Surg Sports Traumatol Arthrosc **20**(2): 373-377.
- Ersen, A., M. Demirhan, A. C. Atalar, M. Kapicioglu and G. Baysal (2014). "Platelet-rich plasma for enhancing surgical rotator cuff repair: evaluation and comparison of two application methods in a rat model." Arch Orthop Trauma Surg **134**(3): 405-411.
- Fabis, J., M. Danilewicz, J. T. Zwierzchowski and K. Niedzielski (2016). "Atrophy of type I and II muscle fibers is reversible in the case of grade >2 fatty degeneration of the supraspinatus muscle: an experimental study in rabbits." J Shoulder Elbow Surg **25**(3): 487-492.
- Fabis, J., P. Kordek, A. Bogucki, M. Synder and H. Kolczynska (1998). "Function of the rabbit supraspinatus muscle after detachment of its tendon from the greater tubercle - Observations up to 6 months." Acta Orthopaedica Scandinavica **69**(6): 570-574.
- Feeley, B. T., R. A. Gallo and E. V. Craig (2009). "Cuff tear arthropathy: Current trends in diagnosis and surgical management." Journal of Shoulder and Elbow Surgery **18**(3): 484-494.
- Fei, W. and W. Guo (2015). "A biomechanical and histological comparison of the suture bridge and conventional double-row techniques of the repair of full-thickness rotator cuff tears in a rabbit model." Bmc Musculoskeletal Disorders **16**.
- Fitzpatrick, J., M. K. Bulsara, P. R. McCrory, M. D. Richardson and M. H. Zheng (2017). "Analysis of Platelet-Rich Plasma Extraction. Variations in Platelet and Blood Components Between 4 Common Commercial Kits." The Orthopaedic Journal of Sports Medicine **5**(1): 2325967116675272

- Flury, M., D. Rickenbacher, H. K. Schwyzer, C. Jung, M. M. Schneider, K. Stahnke, J. Goldhahn and L. Audige (2016). "Does Pure Platelet-Rich Plasma Affect Postoperative Clinical Outcomes After Arthroscopic Rotator Cuff Repair? A Randomized Controlled Trial." Am J Sports Med **44**(8): 2136-2146.
- Fong, D., M. B. Ariganello, J. Girard-Lauziere and C. D. Hoemann (2015). "Biodegradable chitosan microparticles induce delayed STAT-1 activation and lead to distinct cytokine responses in differentially polarized human macrophages in vitro." Acta Biomater **12**: 183-194.
- Fotiadou, A. N., M. Vlychou, P. Papadopoulos, D. S. Karataglis, P. Palladas and I. V. Fezoulidis (2008). "Ultrasonography of symptomatic rotator cuff tears compared with MR imaging and surgery." Eur J Radiol **68**(1): 174-179.
- Friel, N. A., A. G. McNickle, M. J. DeFranco, F. Wang, E. F. Shewman, N. N. Verma, B. J. Cole, B. R. Bach, Jr., S. Chubinskaya, S. M. Kramer and V. M. Wang (2015). "Effect of highly purified capsaicin on articular cartilage and rotator cuff tendon healing: An in vivo rabbit study." J Orthop Res **33**(12): 1854-1860.
- Friel, N. A., V. M. Wang, M. A. Slabaugh, F. Wang, S. Chubinskaya and B. J. Cole (2013). "Rotator cuff healing after continuous subacromial bupivacaine infusion: an in vivo rabbit study." J Shoulder Elbow Surg **22**(4): 489-499.
- Fujioka, H., R. Thakur, G. J. Wang, K. Mizuno, G. Balian and S. R. Hurwitz (1998). "Comparison of surgically attached and non-attached repair of the rat Achilles tendon-bone interface. Cellular organization and type X collagen expression." Connect Tissue Res **37**(3-4): 205-218.
- Funakoshi, T., T. Majima, N. Iwasaki, N. Suenaga, N. Sawaguchi, K. Shimode, A. Minami, K. Harada and S. Nishimura (2005). "Application of tissue engineering techniques for rotator cuff regeneration using a chitosan-based hyaluronan hybrid fiber scaffold." Am J Sports Med **33**(8): 1193-1201.
- Funakoshi, T., T. Majima, N. Iwasaki, S. Yamane, T. Masuko, A. Minami, K. Harada, H. Tamura, S. Tokura and S. I. Nishimura (2005). "Novel chitosan-based hyaluronan hybrid polymer fibers as a scaffold in ligament tissue engineering." Journal of Biomedical Materials Research Part A **74A**(3): 338-346.
- Funakoshi, T., T. Majima, N. Suenaga, N. Iwasaki, S. Yamane and A. Minami (2006). "Rotator cuff regeneration using chitin fabric as an acellular matrix." Journal of Shoulder and Elbow Surgery **15**(1): 112-118.
- Galatz, L., S. Rothermich, K. Vanderploeg, B. Petersen, L. Sandell and S. Thomopoulos (2007). "Development of the supraspinatus tendon-to-bone insertion: localized expression of extracellular matrix and growth factor genes." J Orthop Res **25**(12): 1621-1628.
- Galatz, L. M. (2013). Soft Tissue to Bone Healing in Rotator Cuff Repair. Structural Interfaces and Attachments in Biology. S. Thomopoulos, V. Birman and G. M. Genin. New York, NY, USA, Springer Science+Business Media.
- Galatz, L. M., C. M. Ball, S. A. Teefey, W. D. Middleton and K. Yamaguchi (2004). "The outcome and repair integrity of completely arthroscopically repaired large and massive rotator cuff tears." J Bone Joint Surg Am **86-a**(2): 219-224.
- Galatz, L. M., C. M. Ball, S. A. Teefey, W. D. Middleton and K. Yamaguchi (2004). "The outcome and repair integrity of completely arthroscopically repaired large and massive rotator cuff tears." Journal of Bone and Joint Surgery-American Volume **86A**(2): 219-224.

- Galatz, L. M., N. Charlton, R. Das, H. M. Kim, N. Havlioglu and S. Thomopoulos (2009). "Complete removal of load is detrimental to rotator cuff healing." J Shoulder Elbow Surg **18**(5): 669-675.
- Galatz, L. M., L. Gerstenfeld, E. Heber-Katz and S. A. Rodeo (2015). "Tendon regeneration and scar formation: The concept of scarless healing." J Orthop Res **33**(6): 823-831.
- Galatz, L. M., S. Y. Rothermich, M. Zaegel, M. J. Silva, N. Havlioglu and S. Thomopoulos (2005). "Delayed repair of tendon to bone injuries leads to decreased biomechanical properties and bone loss." J Orthop Res **23**(6): 1441-1447.
- Galatz, L. M., L. J. Sandell, S. Y. Rothermich, R. Das, A. Mastny, N. Havlioglu, M. J. Silva and S. Thomopoulos (2006). "Characteristics of the rat supraspinatus tendon during tendon-to-bone healing after acute injury." J Orthop Res **24**(3): 541-550.
- Gao, J., K. Messner, J. R. Ralphs and M. Benjamin (1996). "An immunohistochemical study of enthesis development in the medial collateral ligament of the rat knee joint." Anat Embryol (Berl) **194**(4): 399-406.
- Gao, X. D., T. Katsumoto and K. Onodera (1995). "Purification and characterization of chitin deacetylase from *Absidia coerulea*." J Biochem **117**(2): 257-263.
- Gartsman, G. M. (1997). "Massive, irreparable tears of the rotator cuff. Results of operative debridement and subacromial decompression." J Bone Joint Surg Am **79**(5): 715-721.
- Gartsman, G. M., G. Drake, T. B. Edwards, H. A. Elkousy, S. M. Hammerman, D. P. O'Connor and C. M. Press (2013). "Ultrasound evaluation of arthroscopic full-thickness supraspinatus rotator cuff repair: single-row versus double-row suture bridge (transosseous equivalent) fixation. Results of a prospective, randomized study." Journal of Shoulder and Elbow Surgery **22**(11): 1480-1487.
- Gelberman, R. H., C. R. Chu, C. S. Williams, J. G. Seiler, 3rd and D. Amiel (1992). "Angiogenesis in healing autogenous flexor-tendon grafts." J Bone Joint Surg Am **74**(8): 1207-1216.
- Genin, G. M., A. Kent, V. Birman, B. Wopenka, J. D. Pasteris, P. J. Marquez and S. Thomopoulos (2009). "Functional grading of mineral and collagen in the attachment of tendon to bone." Biophys J **97**(4): 976-985.
- Gerber, C., B. Fuchs and J. Hodler (2000). "The results of repair of massive tears of the rotator cuff." J Bone Joint Surg Am **82**(4): 505-515.
- Gerber, C., D. C. Meyer, M. Flueck, M. C. Benn, B. von Rechenberg and K. Wieser (2015). "Anabolic Steroids Reduce Muscle Degeneration Associated With Rotator Cuff Tendon Release in Sheep." American Journal of Sports Medicine **43**(10): 2393-2400.
- Gerber, C., D. C. Meyer, E. Frey, B. von Rechenberg, H. Hoppeler, R. Frigg, B. Jost and M. A. Zumstein (2009). "Neer Award 2007: Reversion of structural muscle changes caused by chronic rotator cuff tears using continuous musculotendinous traction. An experimental study in sheep." Journal of Shoulder and Elbow Surgery **18**(2): 163-171.
- Gerber, C., D. C. Meyer, A. G. Schneeberger, H. Hoppeler and B. von Rechenberg (2004). "Effect of tendon release and delayed repair on the structure of the muscles of the rotator cuff: an experimental study in sheep." J Bone Joint Surg Am **86-a**(9): 1973-1982.
- Gerber, C., D. C. Meyer, A. G. Schneeberger, H. Hoppeler and B. Von Rechenberg (2004). "Effect of tendon release and delayed repair on the structure of the muscles of the rotator cuff: An



- experimental study in sheep." Journal of Bone and Joint Surgery-American Volume **86A**(9): 1973-1982.
- Gerber, C., A. G. Schneeberger, S. M. Perren and R. W. Nyffeler (1999). "Experimental rotator cuff repair - A preliminary study." Journal of Bone and Joint Surgery-American Volume **81A**(9): 1281-1290.
- Gerentes, P., L. Vachoud, J. Doury and A. Domard (2002). "Study of a chitin-based gel as injectable material in periodontal surgery." Biomaterials **23**(5): 1295-1302.
- Ghazi zadeh, L., A. Chevrier, M. B. Hurtig, J. Farr, S. Rodeo, C. D. Hoemann and M. D. Buschmann (2017). Freeze-dried chitosan-PRP injectable surgical implants for meniscus repair: results from pilot ovine studies. Transactions Orthopaedic Reserach Society, San Diego, CA, USA.
- Gilotra, M., T. Nguyen, M. Christian, D. Davis, R. F. Henn, 3rd and S. A. Hasan (2015). "Botulinum toxin is detrimental to repair of a chronic rotator cuff tear in a rabbit model." J Orthop Res **33**(8): 1152-1157.
- Gomoll, A. H., J. N. Katz, J. J. Warner and P. J. Millett (2004). "Rotator cuff disorders: recognition and management among patients with shoulder pain." Arthritis Rheum **50**(12): 3751-3761.
- Goodship, A. E., H. L. Birch and A. M. Wilson (1994). "The pathobiology and repair of tendon and ligament injury." Vet Clin North Am Equine Pract **10**(2): 323-349.
- Grasso, A., G. Milano, M. Salvatore, G. Falcone, L. Deriu and C. Fabbriciani (2009). "Single-Row Versus Double-Row Arthroscopic Rotator Cuff Repair: A Prospective Randomized Clinical Study." Arthroscopy **25**(1): 4-12.
- Grimberg, J. and J. Kany (2014). "Latissimus dorsi tendon transfer for irreparable postero-superior cuff tears: current concepts, indications, and recent advances." Curr Rev Musculoskelet Med **7**(1): 22-32.
- Groth, G. N. (2004). "Pyramid of progressive force exercises to the injured flexor tendon." J Hand Ther **17**(1): 31-42.
- Grumet, R. C., S. Hadley, M. V. Diltz, T. Q. Lee and R. Gupta (2009). "Development of a new model for rotator cuff pathology: the rabbit subscapularis muscle." Acta Orthopaedica **80**(1): 97-103.
- Guilak, F., H. A. Awad, B. Fermor, H. A. Leddy and J. M. Gimple (2004). "Adipose-derived adult stem cells for cartilage tissue engineering." Biorheology **41**(3-4): 389-399.
- Gulotta, L. V., D. Kovacevic, J. R. Ehteshami, E. Dagher, J. D. Packer and S. A. Rodeo (2009). "Application of bone marrow-derived mesenchymal stem cells in a rotator cuff repair model." Am J Sports Med **37**(11): 2126-2133.
- Gulotta, L. V., D. Kovacevic, S. Montgomery, J. R. Ehteshami, J. D. Packer and S. A. Rodeo (2010). "Stem cells genetically modified with the developmental gene MT1-MMP improve regeneration of the supraspinatus tendon-to-bone insertion site." Am J Sports Med **38**(7): 1429-1437.
- Gulotta, L. V., D. Kovacevic, J. D. Packer, X. H. Deng and S. A. Rodeo (2011). "Bone marrow-derived mesenchymal stem cells transduced with scleraxis improve rotator cuff healing in a rat model." Am J Sports Med **39**(6): 1282-1289.

- Gulotta, L. V., D. Kovacevic, J. D. Packer, J. R. Ehteshami and S. A. Rodeo (2011). "Adenoviral-mediated gene transfer of human bone morphogenetic protein-13 does not improve rotator cuff healing in a rat model." Am J Sports Med **39**(1): 180-187.
- Gulotta, L. V. and S. A. Rodeo (2009). "Growth factors for rotator cuff repair." Clin Sports Med **28**(1): 13-23.
- Gumina, S., V. Campagna, G. Ferrazza, G. Giannicola, F. Fratalocchi, A. Milani and F. Postacchini (2012). "Use of platelet-leukocyte membrane in arthroscopic repair of large rotator cuff tears: a prospective randomized study." J Bone Joint Surg Am **94**(15): 1345-1352.
- Gupta, R. and T. Q. Lee (2007). "Contributions of the different rabbit models to our understanding of rotator cuff pathology." Journal of Shoulder and Elbow Surgery **16**(5): 149S-157S.
- Guzman-Morales, J., C. H. Lafantaisie-Favreau, G. Chen and C. D. Hoemann (2014). "Subchondral chitosan/blood implant-guided bone plate resorption and woven bone repair is coupled to hyaline cartilage regeneration from microdrill holes in aged rabbit knees." Osteoarthritis and Cartilage **22**(2): 323-333.
- Gwinner, C., C. Gerhardt, H. Haneveld and M. Scheibel (2016). "Two-staged application of PRP in arthroscopic rotator cuff repair: a matched-pair analysis." Arch Orthop Trauma Surg **136**(8): 1165-1171.
- Hajji, S., I. Younes, O. Ghorbel-Bellaaj, R. Hajji, M. Rinaudo, M. Nasri and K. Jellouli (2014). "Structural differences between chitin and chitosan extracted from three different marine sources." Int J Biol Macromol **65**: 298-306.
- Halim, A. S., L. C. Keong, I. Zainol and A. H. A. Rashid (2012). Biocompatibility and Biodegradation of Chitosan and Derivatives. Chitosan-Based Systems for Biopharmaceuticals, John Wiley & Sons, Ltd: 57-73.
- Hamada, Y., S. Katoh, N. Hibino, H. Kosaka, D. Hamada and N. Yasui (2006). "Effects of monofilament nylon coated with basic fibroblast growth factor on endogenous intrasynovial flexor tendon healing." J Hand Surg Am **31**(4): 530-540.
- Hannafin, J. A., S. P. Arnoczky, A. Hoonjan and P. A. Torzilli (1995). "Effect of stress deprivation and cyclic tensile loading on the material and morphologic properties of canine flexor digitorum profundus tendon: an in vitro study." J Orthop Res **13**(6): 907-914.
- Hapa, O., H. Cakici, A. Kukner, H. Aygun, N. Sarkalan and G. Baysal (2012). "Effect of platelet-rich plasma on tendon-to-bone healing after rotator cuff repair in rats: an in vivo experimental study." Acta Orthop Traumatol Turc **46**(4): 301-307.
- Harada, Y., Y. Mifune, A. Inui, R. Sakata, T. Muto, F. Takase, Y. Ueda, T. Kataoka, T. Kokubu, R. Kuroda and M. Kurosaka (2016). "Rotator cuff repair using cell sheets derived from human rotator cuff in a rat model." J Orthop Res.
- Hashimoto, Y., G. Yoshida, H. Toyoda and K. Takaoka (2007). "Generation of tendon-to-bone interface "entheses" with use of recombinant BMP-2 in a rabbit model." J Orthop Res **25**(11): 1415-1424.
- Hastings, C. L., H. M. Kelly, M. J. Murphy, F. P. Barry, F. J. O'Brien and G. P. Duffy (2012). "Development of a thermoresponsive chitosan gel combined with human mesenchymal stem cells and desferrioxamine as a multimodal pro-angiogenic therapeutic for the treatment of critical limb ischaemia." Journal of Controlled Release **161**(1): 73-80.

- Hattori, H. and M. Ishihara (2016). "Feasibility of improving platelet-rich plasma therapy by using chitosan with high platelet activation ability." Experimental and Therapeutic Medicine DOI: 10.3892/etm.2017.4041.
- Hee, C. K., J. S. Dines, D. M. Dines, C. M. Roden, L. A. Wisner-Lynch, A. S. Turner, K. C. McGilvray, A. S. Lyons, C. M. Puttlitz and B. G. Santoni (2011). "Augmentation of a rotator cuff suture repair using rhPDGF-BB and a type I bovine collagen matrix in an ovine model." Am J Sports Med 39(8): 1630-1639.
- HELBERT, W. and J. SUGIYAMA (1998). "High-resolution electron microscopy on cellulose II and  $\alpha$ -chitin single crystals." Cellulose 5(2): 113-122.
- Heldin, C. H. and B. Westermark (1999). "Mechanism of action and in vivo role of platelet-derived growth factor." Physiol Rev 79(4): 1283-1316.
- Hernigou, P., C. H. Flouzat Lachaniette, J. Delambre, S. Zilber, P. Duffiet, N. Chevallier and H. Rouard (2014). "Biologic augmentation of rotator cuff repair with mesenchymal stem cells during arthroscopy improves healing and prevents further tears: a case-controlled study." Int Orthop 38(9): 1811-1818.
- Hettrich, C. M., B. S. Beamer, A. Bedi, K. Deland, X. H. Deng, L. Ying, J. Lane and S. A. Rodeo (2012). "The effect of rhPTH on the healing of tendon to bone in a rat model." J Orthop Res 30(5): 769-774.
- Hirano, S., H. Tsuchida and N. Nagao (1989). "N-acetylation in chitosan and the rate of its enzymic hydrolysis." Biomaterials 10(8): 574-576.
- Hirooka, A., M. Yoneda, S. Wakaitani, Y. Isaka, K. Hayashida, S. Fukushima and K. Okamura (2002). "Augmentation with a Gore-Tex patch for repair of large rotator cuff tears that cannot be sutured." J Orthop Sci 7(4): 451-456.
- Hoemann, C. D., G. P. Chen, C. Marchand, N. Tran-Khanh, M. Thibault, A. Chevrier, J. Sun, M. S. Shive, M. J. G. Fernandes, P. E. Poubelle, M. Centola and H. El-Gabalawy (2010). "Scaffold-Guided Subchondral Bone Repair Implication of Neutrophils and Alternatively Activated Arginase-1+Macrophages." American Journal of Sports Medicine 38(9): 1845-1856.
- Hoemann, C. D. and D. Fong (2017). 3 - Immunological responses to chitosan for biomedical applications. Chitosan Based Biomaterials Volume 1, Woodhead Publishing: 45-79.
- Hoemann, C. D., M. Hurtig, E. Rossomacha, J. Sun, A. Chevrier, M. Shive and M. Buschmann (2005). "Chitosan-glycerol phosphate/blood implants improve hyaline cartilage repair in ovine microfracture defects." Journal of Bone and Joint Surgery-American Volume 87A(12): 2671-2686.
- Hoemann, C. D., M. Hurtig, E. Rossomacha, J. Sun, A. Chevrier, M. S. Shive and M. D. Buschmann (2005). "Chitosan-glycerol phosphate/blood implants improve hyaline cartilage repair in ovine microfracture defects." Journal of Bone and Joint Surgery-American Volume 87A(12): 2671-2686.
- Hoemann, C. D., M. Hurtig, E. Rossomacha, J. Sun, A. Chevrier, M. S. Shive and M. D. Buschmann (2005). "Chitosan-glycerol phosphate/blood implants improve hyaline cartilage repair in ovine microfracture defects." J Bone Joint Surg Am 87(12): 2671-2686.
- Hoemann, C. D., J. Sun, M. D. McKee, A. Chevrier, E. Rossomacha, G. E. Rivard, M. Hurtig and M. D. Buschmann (2007). "Chitosan-glycerol phosphate/blood implants elicit hyaline cartilage repair integrated with porous subchondral bone in microdrilled rabbit defects." Osteoarthritis and Cartilage 15(1): 78-89.

- Hoemann, C. D., J. Sun, M. D. McKee, A. Chevrier, E. Rossomacha, G. E. Rivard, M. Hurtig and M. D. Buschmann (2007). "Chitosan–glycerol phosphate/blood implants elicit hyaline cartilage repair integrated with porous subchondral bone in microdrilled rabbit defects." *Osteoarthritis and Cartilage* **15**(1): 78-89.
- Holland, T. A., J. K. Tessmar, Y. Tabata and A. G. Mikos (2004). "Transforming growth factor-beta 1 release from oligo(poly(ethylene glycol) fumarate) hydrogels in conditions that model the cartilage wound healing environment." *J Control Release* **94**(1): 101-114.
- Holtby, R., M. Christakis, E. Maman, J. C. MacDermid, T. Dwyer, G. S. Athwal, K. Faber, J. Theodoropoulos, L. J. Woodhouse and H. Razmjou (2016). "Impact of Platelet-Rich Plasma on Arthroscopic Repair of Small- to Medium-Sized Rotator Cuff Tears: A Randomized Controlled Trial." *Orthop J Sports Med* **4**(9): 2325967116665595.
- Howard, M. B., N. A. Ekborg, R. M. Weiner and S. W. Hutcheson (2003). "Detection and characterization of chitinases and other chitin-modifying enzymes." *J Ind Microbiol Biotechnol* **30**(11): 627-635.
- Howling, G. I., P. W. Dettmar, P. A. Goddard, F. C. Hampson, M. Dornish and E. J. Wood (2001). "The effect of chitin and chitosan on the proliferation of human skin fibroblasts and keratinocytes in vitro." *Biomaterials* **22**(22): 2959-2966.
- Huang, J. S., Y. H. Wang, T. Y. Ling, S. S. Chuang, F. E. Johnson and S. S. Huang (2002). "Synthetic TGF-beta antagonist accelerates wound healing and reduces scarring." *Faseb j* **16**(10): 1269-1270.
- Huang, W., U. I. Chung, H. M. Kronenberg and B. de Crombrughe (2001). "The chondrogenic transcription factor Sox9 is a target of signaling by the parathyroid hormone-related peptide in the growth plate of endochondral bones." *Proc Natl Acad Sci U S A* **98**(1): 160-165.
- Huegel, J., D. H. Kim, J. M. Cirone, A. M. Pardes, T. R. Morris, C. A. Nuss, R. L. Mauck, L. J. Soslowsky and A. F. Kuntz (2016). "Autologous tendon-derived cell-seeded nanofibrous scaffolds improve rotator cuff repair in an age-dependent fashion." *J Orthop Res*.
- Hynes, R. O. (1999). "Cell adhesion: old and new questions." *Trends Cell Biol* **9**(12): M33-37.
- Iannotti, J. P., M. J. Codsì, Y. W. Kwon, K. Derwin, J. Ciccone and J. J. Brems (2006). "Porcine small intestine submucosa augmentation of surgical repair of chronic two-tendon rotator cuff tears. A randomized, controlled trial." *J Bone Joint Surg Am* **88**(6): 1238-1244.
- Ibrahim, H. M. and E. M. R. E. Zairy (2015). Chitosan as a Biomaterial — Structure, Properties, and Electrospun Nanofibers. *Concepts, Compounds and the Alternatives of Antibacterials*. V. Bobbarala. Rijeka, InTech: Ch. 04.
- Ide, J., K. Kikukawa, J. Hirose, K. Iyama, H. Sakamoto, T. Fujimoto and H. Mizuta (2009). "The effect of a local application of fibroblast growth factor-2 on tendon-to-bone remodeling in rats with acute injury and repair of the supraspinatus tendon." *J Shoulder Elbow Surg* **18**(3): 391-398.
- Ide, J., K. Kikukawa, J. Hirose, K. Iyama, H. Sakamoto and H. Mizuta (2009). "The effects of fibroblast growth factor-2 on rotator cuff reconstruction with acellular dermal matrix grafts." *Arthroscopy* **25**(6): 608-616.
- Inui, A., T. Kokubu, Y. Mifune, R. Sakata, H. Nishimoto, K. Nishida, T. Akisue, R. Kuroda, M. Satake, H. Kaneko and H. Fujioka (2012). "Regeneration of rotator cuff tear using electrospun poly(d,l-Lactide-Co-Glycolide) scaffolds in a rabbit model." *Arthroscopy* **28**(12): 1790-1799.

- Isaac, C., B. Gharaibeh, M. Witt, V. J. Wright and J. Huard (2012). "Biologic approaches to enhance rotator cuff healing after injury." Journal of Shoulder and Elbow Surgery **21**(2): 181-190.
- Itoigawa, Y., O. Suzuki, H. Sano, T. Anada, T. Handa, T. Hatta, Y. Kuwahara, A. Takahashi, Y. Ezoe, K. Kaneko and E. Itoi (2015). "The role of an octacalcium phosphate in the re-formation of infraspinatus tendon insertion." J Shoulder Elbow Surg **24**(7): e175-184.
- Jackson, S. P. (2007). "The growing complexity of platelet aggregation." Blood **109**(12): 5087-5095.
- Jarry, C., C. Chaput, A. Chenite, M. A. Renaud, M. Buschmann and J. C. Leroux (2001). "Effects of steam sterilization on thermogelling chitosan-based gels." J Biomed Mater Res **58**(1): 127-135.
- Jayakumar, R., M. Prabakaran, P. T. S. Kumar, S. V. Nair and H. Tamura (2011c). "Biomaterials based on chitin and chitosan in wound dressing applications." Biotechnology Advances **29**(3): 322-337.
- Jayakumar, R., M. Prabakaran, S. V. Nair and H. Tamura (2010). "Novel chitin and chitosan nanofibers in biomedical applications." Biotechnology Advances **28**(1): 142-150.
- Jayakumar, R., R. L. Reis and J. F. Mano (2007). "Synthesis and Characterization of pH-Sensitive Thiol-Containing Chitosan Beads for Controlled Drug Delivery Applications." Drug Delivery **14**(1): 9-17.
- Ji, X., C. Bi, F. Wang and Q. Wang (2015). "Arthroscopic versus mini-open rotator cuff repair: an up-to-date meta-analysis of randomized controlled trials." Arthroscopy **31**(1): 118-124.
- Jo, C. H., J. E. Kim, K. S. Yoon, J. H. Lee, S. B. Kang, J. H. Lee, H. S. Han, S. H. Rhee and S. Shin (2011). "Does Platelet-Rich Plasma Accelerate Recovery After Rotator Cuff Repair? A Prospective Cohort Study." American Journal of Sports Medicine **39**(10): 2082-2090.
- Jo, C. H., J. S. Shin, Y. G. Lee, W. H. Shin, H. Kim, S. Y. Lee, K. S. Yoon and S. Shin (2013). "Platelet-Rich Plasma for Arthroscopic Repair of Large to Massive Rotator Cuff Tears A Randomized, Single-Blind, Parallel-Group Trial." American Journal of Sports Medicine **41**(10): 2240-2248.
- Jo, C. H., J. S. Shin, Y. G. Lee, W. H. Shin, H. Kim, S. Y. Lee, K. S. Yoon and S. Shin (2013). "Platelet-rich plasma for arthroscopic repair of large to massive rotator cuff tears: a randomized, single-blind, parallel-group trial." Am J Sports Med **41**(10): 2240-2248.
- Jo, C. H., J. S. Shin, W. H. Shin, S. Y. Lee, K. S. Yoon and S. Shin (2015). "Platelet-Rich Plasma for Arthroscopic Repair of Medium to Large Rotator Cuff Tears: A Randomized Controlled Trial." The American journal of sports medicine **43**(9): 2102--2110.
- Jurk, K. and B. E. Kehrel (2005). "Platelets: physiology and biochemistry." Semin Thromb Hemost **31**(4): 381-392.
- Kang, L., R. F. Henn, R. Z. Tashjian and A. Green (2007). "Early outcome of arthroscopic rotator cuff repair: a matched comparison with mini-open rotator cuff repair." Arthroscopy **23**(6): 573-582, 582.e571-572.
- Kannus, P. and L. Jozsa (1991). "Histopathological changes preceding spontaneous rupture of a tendon. A controlled study of 891 patients." J Bone Joint Surg Am **73**(10): 1507-1525.
- Kasten, P., C. Keil, T. Grieser, P. Raiss, N. Streich and M. Loew (2011). "Prospective randomised comparison of arthroscopic versus mini-open rotator cuff repair of the supraspinatus tendon." International Orthopaedics **35**(11): 1663-1670.

- Katzel, E. B., M. Wolenski, A. E. Loielle, P. Basile, L. M. Flick, H. N. Langstein, M. J. Hilton, H. A. Awad, W. C. Hammert and R. J. O'Keefe (2011). "Impact of Smad3 loss of function on scarring and adhesion formation during tendon healing." J Orthop Res **29**(5): 684-693.
- Kean, T. and M. Thanou (2011). Chapter 10 Chitin and Chitosan: Sources, Production and Medical Applications. Renewable Resources for Functional Polymers and Biomaterials: Polysaccharides, Proteins and Polyesters, The Royal Society of Chemistry: 292-318.
- Kern, S., H. Eichler, J. Stoeve, H. Kluter and K. Bieback (2006). "Comparative analysis of mesenchymal stem cells from bone marrow, umbilical cord blood, or adipose tissue." Stem Cells **24**(5): 1294-1301.
- Kida, Y., T. Morihara, K. Matsuda, Y. Kajikawa, H. Tachiiri, Y. Iwata, K. Sawamura, A. Yoshida, Y. Oshima, T. Ikeda, H. Fujiwara, M. Kawata and T. Kubo (2013). "Bone marrow-derived cells from the footprint infiltrate into the repaired rotator cuff." J Shoulder Elbow Surg **22**(2): 197-205.
- Kim, D. H., N. S. Elattrache, J. E. Tibone, B. J. Jun, S. N. DeLaMora, R. S. Kvitne and T. Q. Lee (2006). "Biomechanical comparison of a single-row versus double-row suture anchor technique for rotator cuff repair." Am J Sports Med **34**(3): 407-414.
- Kim, H. M., L. M. Galatz, N. Patel, R. Das and S. Thomopoulos (2009). "Recovery potential after postnatal shoulder paralysis. An animal model of neonatal brachial plexus palsy." J Bone Joint Surg Am **91**(4): 879-891.
- Kim, I. Y., S. J. Seo, H. S. Moon, M. K. Yoo, I. Y. Park, B. C. Kim and C. S. Cho (2008). "Chitosan and its derivatives for tissue engineering applications." Biotechnol Adv **26**(1): 1-21.
- Kim, M. Y. and J. Lee (2011). "Chitosan fibrous 3D networks prepared by freeze drying." Carbohydrate Polymers **84**(4): 1329-1336.
- Kim, S. H., J. Kim, Y. E. Choi and H. R. Lee (2016). "Healing disturbance with suture bridge configuration repair in rabbit rotator cuff tear." J Shoulder Elbow Surg **25**(3): 478-486.
- Kim, S. J., D. H. Song, J. W. Park, S. Park and S. J. Kim (2017). "Effect of Bone Marrow Aspirate Concentrate-Platelet-Rich Plasma on Tendon-Derived Stem Cells and Rotator Cuff Tendon Tear." Cell Transplant **26**(5): 867-878.
- Kim, Y. S., H. J. Lee, J. H. Ok, J. S. Park and D. W. Kim (2013). "Survivorship of implanted bone marrow-derived mesenchymal stem cells in acute rotator cuff tear." J Shoulder Elbow Surg **22**(8): 1037-1045.
- Kirkendall, D. T. and W. E. Garrett (1997). "Function and biomechanics of tendons." Scand J Med Sci Sports **7**(2): 62-66.
- Klinger, H.-M., G. H. Buchhorn, G. Heidrich, E. Kahl and M. H. Baums (2008). "Biomechanical evaluation of rotator cuff repairs in a sheep model: Suture anchors using arthroscopic Mason-Allen stitches compared with transosseous sutures using traditional modified Mason-Allen stitches." Clinical Biomechanics **23**(3): 291-298.
- Knese, K. H. and H. Biermann (1958). "[Osteogenesis in tendon and ligament insertions in the area of the original chondral apophyses]." Z Zellforsch Mikrosk Anat **49**(2): 142-187.
- Kobayashi, M., E. Itoi, H. Minagawa, N. Miyakoshi, S. Takahashi, Y. Tuoheti, K. Okada and Y. Shimada (2006). "Expression of growth factors in the early phase of supraspinatus tendon healing in rabbits." J Shoulder Elbow Surg **15**(3): 371-377.

- Koh, K. H., K. C. Kang, T. K. Lim, M. S. Shon and J. C. Yoo (2011). "Prospective randomized clinical trial of single- versus double-row suture anchor repair in 2- to 4-cm rotator cuff tears: clinical and magnetic resonance imaging results." Arthroscopy **27**(4): 453-462.
- Koh, K. H., K. C. Kang, T. K. Lim, M. S. Shon and J. C. Yoo (2011). "Prospective Randomized Clinical Trial of Single-Versus Double-Row Suture Anchor Repair in 2-to 4-cm Rotator Cuff Tears: Clinical and Magnetic Resonance Imaging Results." Arthroscopy **27**(4): 453-462.
- Koike, Y., G. Trudel, D. Curran and H. K. Uthoff (2006). "Delay of supraspinatus repair by up to 12 weeks does not impair enthesis formation: a quantitative histologic study in rabbits." J Orthop Res **24**(2): 202-210.
- Koike, Y., G. Trudel and H. K. Uthoff (2005). "Formation of a new enthesis after attachment of the supraspinatus tendon: A quantitative histologic study in rabbits." J Orthop Res **23**(6): 1433-1440.
- Kojima, K., Y. Okamoto, K. Kojima, K. Miyatake, H. Fujise, Y. Shigemasa and S. Minami (2004). "Effects of chitin and chitosan on collagen synthesis in wound healing." J Vet Med Sci **66**(12): 1595-1598.
- Koob, T. J. and K. G. Vogel (1987). "Site-related variations in glycosaminoglycan content and swelling properties of bovine flexor tendon." J Orthop Res **5**(3): 414-424.
- Koping-Hoggard, M., K. M. Varum, M. Issa, S. Danielsen, B. E. Christensen, B. T. Stokke and P. Artursson (2004). "Improved chitosan-mediated gene delivery based on easily dissociated chitosan polyplexes of highly defined chitosan oligomers." Gene Ther **11**(19): 1441-1452.
- Kosaka, T., Y. Kaneko, Y. Nakada, M. Matsuura and S. Tanaka (1996). "Effect of Chitosan Implantation on Activation of Canine Macrophages and Polymorphonuclear Cells after Surgical Stress." Journal of Veterinary Medical Science **58**(10): 963-967.
- Kovacevic, D., A. J. Fox, A. Bedi, L. Ying, X. H. Deng, R. F. Warren and S. A. Rodeo (2011). "Calcium-phosphate matrix with or without TGF-beta3 improves tendon-bone healing after rotator cuff repair." Am J Sports Med **39**(4): 811-819.
- Kovacevic, D. and S. A. Rodeo (2008). "Biological augmentation of rotator cuff tendon repair." Clinical Orthopaedics and Related Research **466**(3): 622-633.
- Kramer, E. J., B. M. Bodendorfer, D. Laron, J. Wong, H. T. Kim, X. Liu and B. T. Feeley (2013). "Evaluation of cartilage degeneration in a rat model of rotator cuff tear arthropathy." Journal of Shoulder and Elbow Surgery **22**(12): 1702-1709.
- Kroll, M. H., J. D. Hellums, L. V. McIntire, A. I. Schafer and J. L. Moake (1996). "Platelets and shear stress." Blood **88**(5): 1525-1541.
- Krueger, C. A., J. C. Wenke, B. D. Masini and D. J. Stinner (2012). "Characteristics and impact of animal models used for sports medicine research." Orthopedics **35**(9): e1410-1415.
- Kumagai, J., K. Sarkar, H. K. Uthoff, Y. Okawara and A. Ooshima (1994). "Immunohistochemical distribution of type I, II and III collagens in the rabbit supraspinatus tendon insertion." J Anat **185** ( Pt 2): 279-284.
- Kumar, R. V. and N. Shubhashini (2013). "Platelet rich fibrin: a new paradigm in periodontal regeneration." Cell Tissue Bank **14**(3): 453-463.
- Kurita, K., T. Sannan and Y. Iwakura (1977). "Studies on chitin, 4. Evidence for formation of block and random copolymers of N-acetyl-D-glucosamine and D-glucosamine by hetero- and homogeneous hydrolyses." Die Makromolekulare Chemie **178**(12): 3197-3202.

- Kutlu, B., R. S. T. Aydin, A. C. Akman, M. Gumusderelioglu and R. M. Nohutcu (2013). "Platelet-rich plasma-loaded chitosan scaffolds: Preparation and growth factor release kinetics." Journal of Biomedical Materials Research Part B-Applied Biomaterials **101B**(1): 28-35.
- Kvist, M., T. Hurme, P. Kannus, T. Jarvinen, V. M. Maunu, L. Jozsa and M. Jarvinen (1995). "Vascular density at the myotendinous junction of the rat gastrocnemius muscle after immobilization and remobilization." Am J Sports Med **23**(3): 359-364.
- Lafantaisie-Favreau, C. H., J. Guzman-Morales, J. Sun, G. P. Chen, A. Harris, T. D. Smith, A. Carli, J. Henderson, W. D. Stanish and C. D. Hoemann (2013). "Subchondral pre-solidified chitosan/blood implants elicit reproducible early osteochondral wound-repair responses including neutrophil and stromal cell chemotaxis, bone resorption and repair, enhanced repair tissue integration and delayed matrix deposition." Bmc Musculoskeletal Disorders **14**(27): 1-16.
- Laiho, M., M. B. Weis and J. Massague (1990). "Concomitant loss of transforming growth factor (TGF)-beta receptor types I and II in TGF-beta-resistant cell mutants implicates both receptor types in signal transduction." J Biol Chem **265**(30): 18518-18524.
- Lake, S. P., K. S. Miller, D. M. Elliott and L. J. Soslowsky (2010). "Tensile properties and fiber alignment of human supraspinatus tendon in the transverse direction demonstrate inhomogeneity, nonlinearity, and regional isotropy." J Biomech **43**(4): 727-732.
- Langberg, H., D. Skovgaard, M. Karamouzis, J. Bulow and M. Kjaer (1999). "Metabolism and inflammatory mediators in the peritendinous space measured by microdialysis during intermittent isometric exercise in humans." J Physiol **515** ( Pt 3): 919-927.
- Lavertu, M., D. Filion and M. D. Buschmann (2008). "Heat-induced transfer of protons from chitosan to glycerol phosphate produces chitosan precipitation and gelation." Biomacromolecules **9**(2): 640-650.
- Leadbetter, W. B. (1992). "Cell-matrix response in tendon injury." Clin Sports Med **11**(3): 533-578.
- Lee, C. G., C. A. Da Silva, C. S. Dela Cruz, F. Ahangari, B. Ma, M. J. Kang, C. H. He, S. Takyar and J. A. Elias (2011). "Role of chitin and chitinase/chitinase-like proteins in inflammation, tissue remodeling, and injury." Annu Rev Physiol **73**: 479-501.
- Lee, K., E. A. Silva and D. J. Mooney (2011). "Growth factor delivery-based tissue engineering: general approaches and a review of recent developments." Journal of The Royal Society Interface **8**(55): 153-170.
- Lee, K. W., J. S. Lee, Y. S. Kim, Y. B. Shim, J. W. Jang and K. I. Lee (2016). "Effective healing of chronic rotator cuff injury using recombinant bone morphogenetic protein-2 coated dermal patch in vivo." J Biomed Mater Res B Appl Biomater.
- Lehman, C., F. Cuomo, F. J. Kummer and J. D. Zuckerman (1995). "The incidence of full thickness rotator cuff tears in a large cadaveric population." Bull Hosp Jt Dis **54**(1): 30-31.
- Leitner, G. C., R. Gruber, J. Neumuller, A. Wagner, P. Kloimstein, P. Hocker, G. F. Kormoczi and C. Buchta (2006). "Platelet content and growth factor release in platelet-rich plasma: a comparison of four different systems." Vox Sanguinis **91**(2): 135-139.
- Lendeckel, S., A. Jodicke, P. Christophis, K. Heidinger, J. Wolff, J. K. Fraser, M. H. Hedrick, L. Berthold and H. P. Howaldt (2004). "Autologous stem cells (adipose) and fibrin glue used to treat widespread traumatic calvarial defects: case report." J Craniomaxillofac Surg **32**(6): 370-373.



- Lewis, C. W., T. F. Schlegel, R. J. Hawkins, S. P. James and A. S. Turner (1999). "Comparison of tunnel suture and suture anchor methods as a function of time in a sheep model." *Biomed Sci Instrum* **35**: 403-408.
- Li, X., C.-P. Xu, Y.-L. Hou, J.-Q. Song, Z. Cui and B. Yu (2014). "Are Platelet Concentrates an Ideal Biomaterial for Arthroscopic Rotator Cuff Repair? A Meta-analysis of Randomized Controlled Trials." *Arthroscopy* **30**(11): 1483-1490.
- Li, Z., M. K. Delaney, K. A. O'Brien and X. Du (2010). "Signaling during platelet adhesion and activation." *Arterioscler Thromb Vasc Biol* **30**(12): 2341-2349.
- Liem, D., C. Bartl, S. Lichtenberg, P. Magosch and P. Habermeyer (2007). "Clinical outcome and tendon integrity of arthroscopic versus mini-open supraspinatus tendon repair: A magnetic resonance imaging-controlled matched-pair analysis." *Arthroscopy* **23**(5): 514-521.
- Lin, T. W., L. Cardenas and L. J. Soslowky (2004). "Biomechanics of tendon injury and repair." *J Biomech* **37**(6): 865-877.
- Liu, S. H., D. W. Hang, A. Gentili and G. A. Finerman (1996). "MRI and morphology of the insertion of the patellar tendon after graft harvesting." *J Bone Joint Surg Br* **78**(5): 823-826.
- Liu, S. H., V. Panossian, R. al-Shaikh, E. Tomin, E. Shepherd, G. A. Finerman and J. M. Lane (1997). "Morphology and matrix composition during early tendon to bone healing." *Clin Orthop Relat Res*(339): 253-260.
- Liu, X., G. Manzano, H. T. Kim and B. T. Feeley (2011). "A Rat Model of Massive Rotator Cuff Tears." *Journal of Orthopaedic Research* **29**(4): 588-595.
- Liu, Y., V. Birman, C. Chen, S. Thomopoulos and G. M. Genin (2011). "Mechanisms of Biomaterial Attachment at the Interface of Tendon to Bone." *J Eng Mater Technol* **133**(1).
- Longo, U. G., F. Forriol, S. Campi, N. Maffulli and V. Denaro (2011). "Animal Models for Translational Research on Shoulder Pathologies: From Bench to Bedside." *Sports Medicine and Arthroscopy Review* **19**(3): 184-193.
- Longo, U. G., F. Franceschi, L. Ruzzini, C. Rabitti, S. Morini, N. Maffulli and V. Denaro (2009). "Characteristics at haematoxylin and eosin staining of ruptures of the long head of the biceps tendon." *Br J Sports Med* **43**(8): 603-607.
- Longo, U. G., A. Lamberti, N. Maffulli and V. Denaro (2010). "Tendon augmentation grafts: a systematic review." *Br Med Bull* **94**: 165-188.
- Longo, U. G., A. Lamberti, S. Petrillo, N. Maffulli and V. Denaro (2012). "Scaffolds in tendon tissue engineering." *Stem Cells Int* **2012**: 517165.
- Lorbach, O. and M. Tompkins (2012). "Rotator cuff: biology and current arthroscopic techniques." *Knee Surg Sports Traumatol Arthrosc* **20**(6): 1003-1011.
- Lord, M. S., B. Cheng, S. J. McCarthy, M. Jung and J. M. Whitelock (2011). "The modulation of platelet adhesion and activation by chitosan through plasma and extracellular matrix proteins." *Biomaterials* **32**(28): 6655-6662.
- Lovric, V., M. Ledger, J. Goldberg, W. Harper, N. Bertollo, M. H. Pelletier, R. A. Oliver, Y. Yu and W. R. Walsh (2013). "The effects of Low-intensity Pulsed Ultrasound on tendon-bone healing in a transosseous-equivalent sheep rotator cuff model." *Knee Surgery Sports Traumatology Arthroscopy* **21**(2): 466-475.
- Lu, H. H. and S. Thomopoulos (2013). "Functional attachment of soft tissues to bone: development, healing, and tissue engineering." *Annu Rev Biomed Eng* **15**: 201-226.

- Lu, H. H., J. M. Vo, H. S. Chin, J. Lin, M. Cozin, R. Tsay, S. Eisig and R. Landesberg (2008). "Controlled delivery of platelet-rich plasma-derived growth factors for bone formation." J Biomed Mater Res A **86**(4): 1128-1136.
- Luan, T., X. Liu, J. T. Easley, B. Ravishankar, C. Puttlitz and B. T. Feeley (2015). "Muscle atrophy and fatty infiltration after an acute rotator cuff repair in a sheep model." Muscles, ligaments and tendons journal **5**(2): 106-112.
- Lui, P., P. Zhang, K. Chan and L. Qin (2010). "Biology and augmentation of tendon-bone insertion repair." J Orthop Surg Res **5**: 59.
- Luostarinen, T., T. Niiya, A. Schramko, P. Rosenberg and T. Niemi (2011). "Comparison of Hypertonic Saline and Mannitol on Whole Blood Coagulation In Vitro Assessed by Thromboelastometry." Neurocritical Care **14**(2): 238-243.
- Ma, J., K. Goble, M. Smietana, T. Kostrominova, L. Larkin and E. M. Arruda (2009). "Morphological and functional characteristics of three-dimensional engineered bone-ligament-bone constructs following implantation." J Biomech Eng **131**(10): 101017.
- Ma, J., J. Shen, B. P. Smith, A. Ritting, T. L. Smith and L. A. Koman (2007). "Bioprotection of tendon repair: adjunctive use of botulinum toxin A in Achilles tendon repair in the rat." J Bone Joint Surg Am **89**(10): 2241-2249.
- Ma, L., C. Gao, Z. Mao, J. Zhou, J. Shen, X. Hu and C. Han (2003). "Collagen/chitosan porous scaffolds with improved biostability for skin tissue engineering." Biomaterials **24**(26): 4833-4841.
- Ma, R., R. Chow, L. Choi and D. Diduch (2011). "Arthroscopic rotator cuff repair: suture anchor properties, modes of failure and technical considerations." Expert Review of Medical Devices **8**(3): 377-387.
- MacLaughlin, F. C., R. J. Mumper, J. Wang, J. M. Tagliaferri, I. Gill, M. Hinchcliffe and A. P. Rolland (1998). "Chitosan and depolymerized chitosan oligomers as condensing carriers for in vivo plasmid delivery." Journal of Controlled Release **56**(1-3): 259-272.
- Maffulli, N., K. M. Khan and G. Puddu (1998). "Overuse tendon conditions: time to change a confusing terminology." Arthroscopy **14**(8): 840-843.
- Magalon, J., O. Bausset, N. Serratrice, L. Giraudou, H. Aboudou, J. Veran, G. Magalon, F. Dignat-Georges and F. Sabatier (2014). "Characterization and comparison of 5 platelet-rich plasma preparations in a single-donor model." Arthroscopy **30**(5): 629-638.
- Magnusson, S. P., H. Langberg and M. Kjaer (2010). "The pathogenesis of tendinopathy: balancing the response to loading." Nat Rev Rheumatol **6**(5): 262-268.
- Majima, T., T. Irie, N. Sawaguchi, T. Funakoshi, N. Iwasaki, K. Harada, A. Minami and S. I. Nishimura (2007). "Chitosan-based hyaluronan hybrid polymer fibre scaffold for ligament and tendon tissue engineering." Proc Inst Mech Eng H **221**(5): 537-546.
- Malavolta, E. A., M. E. Conforto Gracitelli, A. A. Ferreira Neto, J. Henrique Assuncao, M. Bordalo-Rodrigues and O. P. de Camargo (2014). "Platelet-Rich Plasma in Rotator Cuff Repair A Prospective Randomized Study." American Journal of Sports Medicine **42**(10): 2446-2454.
- Mall, N. A., J. Chahal, W. M. Heard, B. R. Bach, Jr., C. A. Bush-Joseph, A. A. Romeo and N. N. Verma (2012). "Outcomes of Arthroscopic and Open Surgical Repair of Isolated Subscapularis Tendon Tears." Arthroscopy **28**(9): 1306-1314.

- Manning, C. N., H. M. Kim, S. Sakiyama-Elbert, L. M. Galatz, N. Havlioglu and S. Thomopoulos (2011). "Sustained delivery of transforming growth factor beta three enhances tendon-to-bone healing in a rat model." *J Orthop Res* **29**(7): 1099-1105.
- Manske, P. R. (2005). "History of flexor tendon repair." *Hand Clin* **21**(2): 123-127.
- Mao, S., X. Shuai, F. Unger, M. Simon, D. Bi and T. Kissel (2004). "The depolymerization of chitosan: effects on physicochemical and biological properties." *Int J Pharm* **281**(1-2): 45-54.
- Marchand, C., H. Chen, M. D. Buschmann and C. D. Hoemann (2011). "Standardized Three-Dimensional Volumes of Interest with Adapted Surfaces for More Precise Subchondral Bone Analyses by Micro-Computed Tomography." *Tissue Engineering Part C-Methods* **17**(4): 475-484.
- Marchand, C., G. E. Rivard, J. Sun and C. D. Hoemann (2009). "Solidification mechanisms of chitosan-glycerol phosphate/blood implant for articular cartilage repair." *Osteoarthritis and Cartilage* **17**(7): 953-960.
- Martins, E. A., Y. M. Michelacci, R. Y. Baccarin, B. Cogliati and L. C. Silva (2014). "Evaluation of chitosan-GP hydrogel biocompatibility in osteochondral defects: an experimental approach." *BMC Vet Res* **10**: 197.
- Mascarenhas, R., P. N. Chalmers, E. T. Sayegh, M. Bhandari, N. N. Verma, B. J. Cole and A. A. Romeo (2014). "Is Double-Row Rotator Cuff Repair Clinically Superior to Single-Row Rotator Cuff Repair: A Systematic Review of Overlapping Meta-analyses." *Arthroscopy* **30**(9): 1156-1165.
- Masaki, H., T. Okudera, T. Watanebe, M. Suzuki, K. Nishiyama, H. Okudera, K. Nakata, K. Uematsu, C. Y. Su and T. Kawase (2016). "Growth factor and pro-inflammatory cytokine contents in platelet-rich plasma (PRP), plasma rich in growth factors (PRGF), advanced platelet-rich fibrin (A-PRF), and concentrated growth factors (CGF)." **2**(1): 19.
- Mathewson, M. A., A. Kwan, C. M. Eng, R. L. Lieber and S. R. Ward (2014). "Comparison of rotator cuff muscle architecture between humans and other selected vertebrate species." *J Exp Biol* **217**(Pt 2): 261-273.
- Mathieu, C., A. Chevrier, V. Lascau-Coman, G. E. Rivard and C. D. Hoemann (2013). "Stereological analysis of subchondral angiogenesis induced by chitosan and coagulation factors in microdrilled articular cartilage defects." *Osteoarthritis and Cartilage* **21**: 849-859.
- Matsumoto, F., H. K. Uthoff, G. Trudel and J. F. Loehr (2002). "Delayed tendon reattachment does not reverse atrophy and fat accumulation of the supraspinatus--an experimental study in rabbits." *J Orthop Res* **20**(2): 357-363.
- Mazzocca, A. D., P. J. Millett, C. A. Guanche, S. A. Santangelo and R. A. Arciero (2005). "Arthroscopic single-row versus double-row suture anchor rotator cuff repair." *Am J Sports Med* **33**(12): 1861-1868.
- McCarrel, T. and L. Fortier (2009). "Temporal growth factor release from platelet-rich plasma, trehalose lyophilized platelets, and bone marrow aspirate and their effect on tendon and ligament gene expression." *J Orthop Res* **27**(8): 1033-1042.
- McElvany, M. D., E. McGoldrick, A. O. Gee, M. B. Neradilek and F. A. Matsen, 3rd (2015). "Rotator cuff repair: published evidence on factors associated with repair integrity and clinical outcome." *Am J Sports Med* **43**(2): 491-500.
- Melamed, E., B. G. Beutel and D. Robinson (2015). "Enhancement of acute tendon repair using chitosan matrix." *Am J Orthop (Belle Mead NJ)* **44**(5): 212-216.

- Metcalf MH, S. F., III, Kelluzrm B (2002). "Surgical technique for xenograft (SIS) augmentation of rotator-cuff repairs." Oper Tech Orthop(12): 204–208.
- Méhot, S., A. Changoor, N. Tran-Khanh, C. D. Hoemann, W. D. Stanish, A. Restrepo, M. S. Shive and M. D. Buschmann (2015). "Osteochondral Biopsy Analysis Demonstrates That BST-CarGel Treatment Improves Structural and Cellular Characteristics of Cartilage Repair Tissue Compared With Microfracture." Cartilage.
- Meyer, D. C., H. Hoppeler, B. von Rechenberg and C. Gerber (2004). "A pathomechanical concept explains muscle loss and fatty muscular changes following surgical tendon release." Journal of Orthopaedic Research **22**(5): 1004-1007.
- Meyer, D. C., G. Lajtai, B. von Rechenberg, C. W. Pfirrmann and C. Gerber (2006). "Tendon retracts more than muscle in experimental chronic tears of the rotator cuff." J Bone Joint Surg Br **88**(11): 1533-1538.
- Millett, P. J., R. J. Warth, G. J. Dornan, J. T. Lee and U. J. Spiegl (2014). "Clinical and structural outcomes after arthroscopic single-row versus double-row rotator cuff repair: a systematic review and meta-analysis of level I randomized clinical trials." Journal of Shoulder and Elbow Surgery **23**(4): 586-597.
- Moffat, K. L., W. H. Sun, P. E. Pena, N. O. Chahine, S. B. Doty, G. A. Ateshian, C. T. Hung and H. H. Lu (2008). "Characterization of the structure-function relationship at the ligament-to-bone interface." Proc Natl Acad Sci U S A **105**(23): 7947-7952.
- Moffat KL, Z. C., Greco A (2011). "In vitro and in vivo evaluation of a biphasic nanofiber scaffold for integrative rotator cuff repair." Trans Orthop Res Soc. **36**(482).
- Mohammadi, R., M. Mehrtash, M. Mehrtash, N. Hassani and A. Hassanpour (2016). "Effect of Platelet Rich Plasma Combined with Chitosan Biodegradable Film on Full-Thickness Wound Healing in Rat Model." Bull Emerg Trauma **4**(1): 29-37.
- Montgomery, S. R., F. A. Petrigliano and S. C. Gamradt (2011). "Biologic augmentation of rotator cuff repair." Curr Rev Musculoskelet Med **4**(4): 221-230.
- Montgomery, S. R., F. A. Petrigliano and S. C. Gamradt (2012). "Failed rotator cuff surgery, evaluation and decision making." Clin Sports Med **31**(4): 693-712.
- Mooren, R. E., E. J. Hendriks, J. J. van den Beucken, M. A. Merckx, G. J. Meijer, J. A. Jansen and P. J. Stoelinga (2010). "The effect of platelet-rich plasma in vitro on primary cells: rat osteoblast-like cells and human endothelial cells." Tissue Eng Part A **16**(10): 3159-3172.
- Mora, M. V., M. A. Iban, J. D. Heredia, R. B. Laakso, R. Cuellar and M. G. Arranz (2015). "Stem cell therapy in the management of shoulder rotator cuff disorders." World J Stem Cells **7**(4): 691-699.
- Morgenstern, E., A. Ruf and H. Patscheke (1990). "Ultrastructure of the interaction between human platelets and polymerizing fibrin within the first minutes of clot formation." Blood Coagul Fibrinolysis **1**(4-5): 543-546.
- Mosser, D. M. and J. P. Edwards (2008). "Exploring the full spectrum of macrophage activation." Nat Rev Immunol **8**(12): 958-969.
- Murchison, N. D., B. A. Price, D. A. Conner, D. R. Keene, E. N. Olson, C. J. Tabin and R. Schweitzer (2007). "Regulation of tendon differentiation by scleraxis distinguishes force-transmitting tendons from muscle-anchoring tendons." Development **134**(14): 2697-2708.

- Murray, D. H., E. N. Kubiak, L. M. Jazrawi, A. Araghi, F. Kummer, M. I. Loebenberg and J. D. Zuckerman (2007). "The effect of cartilage-derived morphogenetic protein 2 on initial healing of a rotator cuff defect in a rat model." *J Shoulder Elbow Surg* **16**(2): 251-254.
- Murray, I. R., R. F. LaPrade, V. Musahl, A. G. Geeslin, J. P. Zlotnicki, B. J. Mann and F. A. Petrigliano (2016). "Biologic Treatments for Sports Injuries II Think Tank-Current Concepts, Future Research, and Barriers to Advancement, Part 2: Rotator Cuff." *Orthop J Sports Med* **4**(3): 2325967116636586.
- Murray, P. J., J. E. Allen, S. K. Biswas, E. A. Fisher, D. W. Gilroy, S. Goerdt, S. Gordon, J. A. Hamilton, L. B. Ivashkiv, T. Lawrence, M. Locati, A. Mantovani, F. O. Martinez, J. L. Mege, D. M. Mosser, G. Natoli, J. P. Saeij, J. L. Schultze, K. A. Shirey, A. Sica, J. Suttles, I. Udalova, J. A. van Ginderachter, S. N. Vogel and T. A. Wynn (2014). "Macrophage activation and polarization: nomenclature and experimental guidelines." *Immunity* **41**(1): 14-20.
- Muzzarelli, R. A. (1997). "Human enzymatic activities related to the therapeutic administration of chitin derivatives." *Cell Mol Life Sci* **53**(2): 131-140.
- Muzzarelli, R. A., M. Mattioli-Belmonte, A. Pugnali and G. Biagini (1999). "Biochemistry, histology and clinical uses of chitins and chitosans in wound healing." *EXS* **87**: 251-264.
- Muzzarelli, R. A. A. (2009). "Chitins and chitosans for the repair of wounded skin, nerve, cartilage and bone." *Carbohydrate Polymers* **76**(2): 167-182.
- Namdari, S., P. Voleti, K. Baldwin, D. Glaser and G. R. Huffman (2012). "Latissimus dorsi tendon transfer for irreparable rotator cuff tears: a systematic review." *J Bone Joint Surg Am* **94**(10): 891-898.
- Naqvi, G. A., M. Jadaan and P. Harrington (2009). "Accuracy of ultrasonography and magnetic resonance imaging for detection of full thickness rotator cuff tears." *Int J Shoulder Surg* **3**(4): 94-97.
- Neer, C. S., E. V. Craig and H. Fukuda (1983). "Cuff-tear arthropathy." *J Bone Joint Surg Am* **65**(9): 1232-1244.
- Newsham-West, R., H. Nicholson, M. Walton and P. Milburn (2007). "Long-term morphology of a healing bone-tendon interface: a histological observation in the sheep model." *J Anat* **210**(3): 318-327.
- Nho, S. J., B. S. Brown, S. Lyman, R. S. Adler, D. W. Altchek and J. D. MacGillivray (2009). "Prospective analysis of arthroscopic rotator cuff repair: prognostic factors affecting clinical and ultrasound outcome." *J Shoulder Elbow Surg* **18**(1): 13-20.
- Nho, S. J., B. J. Cole, A. D. Mazzocca, J. M. Williams, A. A. Romeo, C. A. Bush-Joseph, B. R. Bach, Jr. and N. J. Hallab (2006). "Comparison of ultrasonic suture welding and traditional knot tying in a rabbit rotator cuff repair model." *J Shoulder Elbow Surg* **15**(5): 630-638.
- Nho, S. J., M. K. Shindle, S. L. Sherman, K. B. Freedman, S. Lyman and J. D. MacGillivray (2007). "Systematic review of arthroscopic rotator cuff repair and mini-open rotator cuff repair." *J Bone Joint Surg Am* **89 Suppl 3**: 127-136.
- Nho, S. J., M. A. Slabaugh, S. T. Seroyer, R. C. Grumet, J. B. Wilson, N. N. Verma, A. A. Romeo and B. R. Bach, Jr. (2009). "Does the Literature Support Double-Row Suture Anchor Fixation for Arthroscopic Rotator Cuff Repair? A Systematic Review Comparing Double-Row and Single-Row Suture Anchor Configuration." *Arthroscopy* **25**(11): 1319-1328.

- Nishimura, K., S. Nishimura, N. Nishi, S. Tokura and I. Azuma (1986). Immunological Activity of Chitin Derivatives. Chitin in Nature and Technology. R. Muzzarelli, C. Jeuniaux and G. W. Gooday. Boston, MA, Springer US: 477-483.
- No, H. K. and S. P. Meyers (1995). "Preparation and Characterization of Chitin and Chitosan—A Review." Journal of Aquatic Food Product Technology **4**(2): 27-52.
- O'Brien, M. (1992). "Functional anatomy and physiology of tendons." Clin Sports Med **11**(3): 505-520.
- Oak, N. R., J. P. Gumucio, M. D. Flood, A. L. Saripalli, M. E. Davis, J. A. Harning, E. B. Lynch, S. M. Roche, A. Bedi and C. L. Mendias (2014). "Inhibition of 5-LOX, COX-1, and COX-2 increases tendon healing and reduces muscle fibrosis and lipid accumulation after rotator cuff repair." Am J Sports Med **42**(12): 2860-2868.
- Oh, J. H., S. W. Chung, S. H. Kim, J. Y. Chung and J. Y. Kim (2014). "2013 Neer Award: Effect of the adipose-derived stem cell for the improvement of fatty degeneration and rotator cuff healing in rabbit model." J Shoulder Elbow Surg **23**(4): 445-455.
- Oh, J. H., W. Kim, K. U. Park and Y. H. Roh (2015). "Comparison of the Cellular Composition and Cytokine-Release Kinetics of Various Platelet-Rich Plasma Preparations." Am J Sports Med **43**(12): 3062-3070.
- Okamoto, Y., S. Minami, A. Matsushashi, H. Sashiwa, H. Saimoto, Y. Shigemasa, T. Tanigawa, Y. Tanaka and S. Tokura (1993). "Application of polymeric N-acetyl-D-glucosamine (chitin) to veterinary practice." J Vet Med Sci **55**(5): 743-747.
- Okamoto Y, M. S., Matsushashi A, Sashiwa H, Saimoto H, Shigemasa Y, (1992). "Application of chitin and chitosan in small animals." Advances in chitin and chitosan: 70-78.
- Oktay, E. O., B. Demiralp, B. Demiralp, S. Senel, A. Cevdet Akman, K. Eratalay and H. Akincibay (2010). "Effects of platelet-rich plasma and chitosan combination on bone regeneration in experimental rabbit cranial defects." J Oral Implantol **36**(3): 175-184.
- Omae, H., S. P. Steinmann, C. Zhao, M. E. Zobitz, P. Wongtriratanachai, J. W. Sperling and K. N. An (2012). "Biomechanical effect of rotator cuff augmentation with an acellular dermal matrix graft: a cadaver study." Clin Biomech (Bristol, Avon) **27**(8): 789-792.
- Otarodifard, K., R. Bruce Canham and L. M. Galatz "Biologic augmentation of rotator cuff repair." Seminars in Arthroplasty **25**(4): 220-225.
- Oxlund, H. (1986). "Relationships between the biomechanical properties, composition and molecular structure of connective tissues." Connect Tissue Res **15**(1-2): 65-72.
- Padulo, J., F. Oliva, A. Frizziero and N. Maffulli (2013). "Muscle, Ligaments and Tendons Journal. Basic principles and recommendations in clinical and field science research." Muscles Ligaments Tendons J **3**(4): 250-252.
- Padulo, J., F. Oliva, A. Frizziero and N. Maffulli (2016). "Muscles, Ligaments and Tendons Journal - Basic principles and recommendations in clinical and field Science Research: 2016 Update." Muscles Ligaments Tendons J **6**(1): 1-5.
- Pandey, V., A. Bandi, S. Madi, L. Agarwal, K. K. Acharya, S. Maddukuri, C. Sambhaji and W. J. Willems (2016). "Does application of moderately concentrated platelet-rich plasma improve clinical and structural outcome after arthroscopic repair of medium-sized to large rotator cuff tear? A randomized controlled trial." J Shoulder Elbow Surg **25**(8): 1312-1322.
- Pandey, V. and W. Jaap Willems (2015). "Rotator cuff tear: A detailed update." Asia-Pacific Journal of Sports Medicine, Arthroscopy, Rehabilitation and Technology **2**(1): 1-14.

- Park, M. C., E. R. Cadet, W. N. Levine, L. U. Bigliani and C. S. Ahmad (2005). "Tendon-to-bone pressure distributions at a repaired rotator cuff footprint using transosseous suture and suture anchor fixation techniques." Am J Sports Med **33**(8): 1154-1159.
- Parrish, W. R., B. Roides, J. Hwang, M. Mafilios, B. Story and S. Bhattacharyya (2016). "Normal platelet function in platelet concentrates requires non-platelet cells: a comparative in vitro evaluation of leucocyte-rich (type 1a) and leucocyte-poor (type 3b) platelet concentrates." BMJ Open Sport & Exercise Medicine **2**(1).
- Parsons, I. M. I., M. Apreleva, F. H. Fu and S. L. Y. Woo (2002). "The effect of rotator cuff tears on reaction forces at the glenohumeral joint." Journal of Orthopaedic Research **20**(3): 439.
- Patel, S., A. P. Gualtieri, H. H. Lu and W. N. Levine (2016). "Advances in biologic augmentation for rotator cuff repair." Ann N Y Acad Sci **1383**(1): 97-114.
- Patel, S., A. P. Gualtieri, H. H. Lu and W. N. Levine (2016). "Advances in biologic augmentation for rotator cuff repair." Ann N Y Acad Sci.
- Paxton, J. Z., K. Baar and L. M. Grover (2012). "Current Progress in Enthesis Repair: Strategies for Interfacial Tissue Engineering." Orthopedic Muscul Sys **S1**: 003.
- Peach, M. S., D. M. Ramos and R. James (2017). "Engineered stem cell niche matrices for rotator cuff tendon regenerative engineering." **12**(4): e0174789.
- Pencev, D. and G. R. Grotendorst (1988). "Human peripheral blood monocytes secrete a unique form of PDGF." Oncogene Res **3**(4): 333-342.
- Percot, A., C. Viton and A. Domard (2003). "Characterization of Shrimp Shell Deproteinization." Biomacromolecules **4**(5): 1380-1385.
- Periyah, M. H., A. S. Halim, N. S. Yaacob, A. Z. Saad, A. R. Hussein, A. H. Rashid and Z. Ujang (2014). "Glycoprotein IIb/IIIa and P2Y12 induction by oligochitosan accelerates platelet aggregation." Biomed Res Int **2014**: 653149.
- Perry, S. M., C. L. Getz and L. J. Soslowsky (2009). "Alterations in function after rotator cuff tears in an animal model." Journal of Shoulder and Elbow Surgery **18**(2): 296-304.
- Persson, J. E., A. Domard and H. Chanzy (1992). "Single crystals of alpha-chitin." Int J Biol Macromol **14**(4): 221-224.
- Peterson, D. R., K. L. Ohashi, H. M. Aberman, P. A. Piza, H. C. Crockett, J. I. Fernandez, P. J. Lund, K. A. Funk, M. L. Hawes, B. G. Parks and R.-H. Mattern (2015). "Evaluation of a collagen-coated, resorbable fiber scaffold loaded with a peptide basic fibroblast growth factor mimetic in a sheep model of rotator cuff repair." Journal of Shoulder and Elbow Surgery **24**(11): 1764-1773.
- Phillips, J. E., K. L. Burns, J. M. Le Doux, R. E. Guldberg and A. J. Garcia (2008). "Engineering graded tissue interfaces." Proc Natl Acad Sci U S A **105**(34): 12170-12175.
- Picavet, H. S. and J. S. Schouten (2003). "Musculoskeletal pain in the Netherlands: prevalences, consequences and risk groups, the DMC(3)-study." Pain **102**(1-2): 167-178.
- Picker, S. M. (2011). "In-vitro assessment of platelet function." Transfus Apher Sci **44**(3): 305-319.
- Pochini, A. C., E. Antonioli, D. Z. Bucci, L. R. Sardinha, C. V. Andreoli, M. Ferretti, B. Ejnisman, A. C. Goldberg and M. Cohen (2016). "Analysis of cytokine profile and growth factors in platelet-rich plasma obtained by open systems and commercial columns." Einstein (Sao Paulo) **14**(3): 391-397.

- Prabaharan, M. and J. F. Mano (2004). "Chitosan-Based Particles as Controlled Drug Delivery Systems." Drug Delivery **12**(1): 41-57.
- Praemer, A., S. Furner and D. P. Rice (1999). Musculoskeletal conditions in the United States.
- Prasathaporn, N., S. Kuptniratsaikul and K. Kongruekreatiyos (2011). "Single-row repair versus double-row repair of full-thickness rotator cuff tears." Arthroscopy **27**(7): 978-985.
- Provot, S. and E. Schipani (2005). "Molecular mechanisms of endochondral bone development." Biochem Biophys Res Commun **328**(3): 658-665.
- Quigley, R. J., A. Gupta, J. H. Oh, K. C. Chung, M. H. McGarry, R. Gupta, J. E. Tibone and T. Q. Lee (2013). "Biomechanical comparison of single-row, double-row, and transosseous-equivalent repair techniques after healing in an animal rotator cuff tear model." J Orthop Res **31**(8): 1254-1260.
- Randelli, P., P. Arrigoni, V. Ragone, A. Aliprandi and P. Cabitza (2011). "Platelet rich plasma in arthroscopic rotator cuff repair: a prospective RCT study, 2-year follow-up." Journal of Shoulder and Elbow Surgery **20**(4): 518-528.
- Randelli, P., F. Randelli, V. Ragone, A. Menon, R. D'Ambrosi, D. Cucchi, P. Cabitza and G. Banfi (2014). "Regenerative medicine in rotator cuff injuries." Biomed Res Int **2014**: 129515-129515.
- Rao, S. B. and C. P. Sharma (1997). "Use of chitosan as a biomaterial: Studies on its safety and hemostatic potential." Journal of Biomedical Materials Research **34**(1): 21-28.
- Rees, J. D., A. M. Wilson and R. L. Wolman (2006). "Current concepts in the management of tendon disorders." Rheumatology (Oxford) **45**(5): 508-521.
- Rickert, M., M. Jung, M. Adiyaman, W. Richter and H. G. Simank (2001). "A growth and differentiation factor-5 (GDF-5)-coated suture stimulates tendon healing in an Achilles tendon model in rats." Growth Factors **19**(2): 115-126.
- Riley, G. (2004). "The pathogenesis of tendinopathy. A molecular perspective." Rheumatology (Oxford) **43**(2): 131-142.
- Roberts, G. A. F. (1992). Chitin Chemistry, Macmillan.
- Robertson, T. A., M. A. Maley, M. D. Grounds and J. M. Papadimitriou (1993). "The role of macrophages in skeletal muscle regeneration with particular reference to chemotaxis." Exp Cell Res **207**(2): 321-331.
- Robinson, D., S. Pachornik, N. B. Shalom, S. Sagiv, E. Melamed and Z. Nevo (2010). The Use of a Chitosan-Based Hyaluronate Gel in Musculoskeletal Afflictions. Advanced Technologies for Enhancing Quality of Life (AT-EQUAL), 2010.
- Rodeo, S. A., D. Delos, R. J. Williams, R. S. Adler, A. Pearle and R. F. Warren (2012). "The effect of platelet-rich fibrin matrix on rotator cuff tendon healing: a prospective, randomized clinical study." Am J Sports Med **40**(6): 1234-1241.
- Rodeo, S. A., H. G. Potter, S. Kawamura, A. S. Turner, H. J. Kim and B. L. Atkinson (2007). "Biologic augmentation of rotator cuff tendon-healing with use of a mixture of osteoinductive growth factors." J Bone Joint Surg Am **89**(11): 2485-2497.
- Rodriguez-Vazquez, M., B. Vega-Ruiz, R. Ramos-Zuniga, D. A. Saldana-Koppel and L. F. Quinones-Olvera (2015). "Chitosan and Its Potential Use as a Scaffold for Tissue Engineering in Regenerative Medicine." Biomed Res Int **2015**: 821279.



- Ross, D., T. Maerz, M. Kurdziel, J. Hein, S. Doshi, A. Bedi, K. Anderson and K. Baker (2015). "The effect of granulocyte-colony stimulating factor on rotator cuff healing after injury and repair." Clin Orthop Relat Res **473**(5): 1655-1664.
- Rotini, R., A. Marinelli, E. Guerra, G. Bettelli, A. Castagna, M. Fini, E. Bondioli and M. Busacca (2011). "Human dermal matrix scaffold augmentation for large and massive rotator cuff repairs: preliminary clinical and MRI results at 1-year follow-up." Musculoskelet Surg **95 Suppl 1**: S13-23.
- Roughley, P., C. Hoemann, E. DesRosiers, F. Mwale, J. Antoniou and M. Alini (2006). "The potential of chitosan-based gels containing intervertebral disc cells for nucleus pulposus supplementation." Biomaterials **27**(3): 388-396.
- Rudall, K. M. (1969). "Chitin and its association with other molecules." Journal of Polymer Science Part C: Polymer Symposia **28**(1): 83-102.
- Rudall, K. M. and W. Kenchington (1973). "THE CHITIN SYSTEM." Biological Reviews **48**(4): 597-633.
- Rudzki, J. R., R. S. Adler, R. F. Warren, W. R. Kadrmaz, N. Verma, A. D. Pearle, S. Lyman and S. Fealy (2008). "Contrast-enhanced ultrasound characterization of the vascularity of the rotator cuff tendon: age- and activity-related changes in the intact asymptomatic rotator cuff." J Shoulder Elbow Surg **17**(1 Suppl): 96s-100s.
- Ruiz-Moneo, P., J. Molano-Munoz, E. Prieto and J. Algorta (2013). "Plasma Rich in Growth Factors in Arthroscopic Rotator Cuff Repair: A Randomized, Double-Blind, Controlled Clinical Trial." Arthroscopy **29**(1): 2-9.
- Saha, A. K. (1971). "Dynamic stability of the glenohumeral joint." Acta Orthop Scand **42**(6): 491-505.
- Sakamoto, J., J. Sugiyama, S. Kimura, T. Imai, T. Itoh, T. Watanabe and S. Kobayashi (2000). "Artificial Chitin Spherulites Composed of Single Crystalline Ribbons of  $\alpha$ -Chitin via Enzymatic Polymerization." Macromolecules **33**(11): 4155-4160.
- Salamanna, F., F. Veronesi, M. Maglio, E. Della Bella, M. Sartori and M. Fini (2015). "New and Emerging Strategies in Platelet-Rich Plasma Application in Musculoskeletal Regenerative Procedures: General Overview on Still Open Questions and Outlook." Biomed Res Int.
- Sanchez Marquez, J. M., J. M. Martínez Díez, R. Barco and S. Antuña (2011). "Functional results after arthroscopic repair of massive rotator cuff tears: Influence of the application platelet-rich plasma combined with fibrin." Rev Esp Cir Ortop Traumatol **55**: 282-287.
- Sannan, T., K. Kurita and Y. Iwakura (1976). "Studies on chitin, 2. Effect of deacetylation on solubility." Die Makromolekulare Chemie **177**(12): 3589-3600.
- Sano, H., J. Kumagai and T. Sawai (2002). "Experimental fascial autografting for the supraspinatus tendon defect: remodeling process of the grafted fascia and the insertion into bone." J Shoulder Elbow Surg **11**(2): 166-173.
- Sano, H., I. Wakabayashi and E. Itoi (2006). "Stress distribution in the supraspinatus tendon with partial-thickness tears: an analysis using two-dimensional finite element model." J Shoulder Elbow Surg **15**(1): 100-105.
- SASHIWA, #160, H., SAIMOTO, #160, H., SHIGEMASA, #160, Y., OGAWA, #160, R., TOKURA, #160 and S. (1991). Distribution of the acetamide group in partially deacetylated chitins. Kidlington, ROYAUME-UNI, Elsevier.

- Schlegel, T. F., R. J. Hawkins, C. W. Lewis, T. Motta and A. S. Turner (2006). "The effects of augmentation with Swine small intestine submucosa on tendon healing under tension: histologic and mechanical evaluations in sheep." Am J Sports Med **34**(2): 275-280.
- Schlegel, T. F., R. J. Hawkins, C. W. Lewis and A. S. Turner (2007). "An in vivo comparison of the modified Mason-Allen suture technique versus an inclined horizontal mattress suture technique with regard to tendon-to-bone healing: a biomechanical and histologic study in sheep." J Shoulder Elbow Surg **16**(1): 115-121.
- Schwartz, A. G., J. D. Pasteris, G. M. Genin, T. L. Daulton and S. Thomopoulos (2012). "Mineral distributions at the developing tendon enthesis." PLoS One **7**(11): e48630.
- Schweitzer, R., J. H. Chyung, L. C. Murtaugh, A. E. Brent, V. Rosen, E. N. Olson, A. Lassar and C. J. Tabin (2001). "Analysis of the tendon cell fate using Scleraxis, a specific marker for tendons and ligaments." Development **128**(19): 3855-3866.
- Sclamberg, S. G., J. E. Tibone, J. M. Itamura and S. Kasraeian (2004). "Six-month magnetic resonance imaging follow-up of large and massive rotator cuff repairs reinforced with porcine small intestinal submucosa." J Shoulder Elbow Surg **13**(5): 538-541.
- Scott, A., J. L. Cook, D. A. Hart, D. C. Walker, V. Duronio and K. M. Khan (2007). "Tenocyte responses to mechanical loading in vivo: a role for local insulin-like growth factor 1 signaling in early tendinosis in rats." Arthritis Rheum **56**(3): 871-881.
- Seeherman, H. J., J. M. Archambault, S. A. Rodeo, A. S. Turner, L. Zekas, D. D'Augusta, X. J. Li, E. Smith and J. M. Wozney (2008). "rhBMP-12 accelerates healing of rotator cuff repairs in a sheep model." J Bone Joint Surg Am **90**(10): 2206-2219.
- Seitz, A. L., P. W. McClure, S. Finucane, N. D. Boardman, 3rd and L. A. Michener (2011). "Mechanisms of rotator cuff tendinopathy: intrinsic, extrinsic, or both?" Clin Biomech (Bristol, Avon) **26**(1): 1-12.
- Selvanetti, A., M. Cipolla and G. Puddu "Overuse tendon injuries: Basic science and classification." Operative Techniques in Sports Medicine **5**(3): 110-117.
- Sharma, P. and N. Maffulli (2005). "Basic biology of tendon injury and healing." Surgeon **3**(5): 309-316.
- Sharma, P. and N. Maffulli (2005). "Tendon injury and tendinopathy: healing and repair." J Bone Joint Surg Am **87**(1): 187-202.
- Sharma, P. and N. Maffulli (2006). "Biology of tendon injury: healing, modeling and remodeling." J Musculoskelet Neuronal Interact **6**(2): 181-190.
- Shea, J. E., R. K. Hallows and R. D. Bloebaum (2002). "Experimental confirmation of the sheep model for studying the role of calcified fibrocartilage in hip fractures and tendon attachments." Anat Rec **266**(3): 177-183.
- Shen, E. C., T. C. Chou, C. H. Gau, H. P. Tu, Y. T. Chen and E. Fu (2006). "Releasing growth factors from activated human platelets after chitosan stimulation: a possible bio-material for platelet-rich plasma preparation." Clin. Oral. Impl. Res. **17**( ): 572-578.
- Shen, W., J. Chen, Z. Yin, X. Chen, H. Liu, B. C. Heng, W. Chen and H. W. Ouyang (2012). "Allogeneous tendon stem/progenitor cells in silk scaffold for functional shoulder repair." Cell Transplant **21**(5): 943-958.
- Sheth, U., N. Simunovic, G. Klein, F. Fu, T. A. Einhorn, E. Schemitsch, O. R. Ayeni and M. Bhandari (2012). "Efficacy of autologous platelet-rich plasma use for orthopaedic indications: a meta-analysis." J Bone Joint Surg Am **94**(4): 298-307.

- Shi, J., L. Wang, F. Zhang, H. Li, L. Lei, L. Liu and Y. Chen (2010). "Incorporating protein gradient into electrospun nanofibers as scaffolds for tissue engineering." ACS Appl Mater Interfaces **2**(4): 1025-1030.
- Shi, L. L. and T. B. Edwards (2012). "The role of acromioplasty for management of rotator cuff problems: where is the evidence?" Adv Orthop **2012**: 467571.
- Shigemasa, Y. and S. Minami (1996). "Applications of chitin and chitosan for biomaterials." Biotechnol Genet Eng Rev **13**: 383-420.
- Shimojo, A. A., A. G. Perez, S. E. Galdames, I. C. Brissac and M. H. Santana (2015). "Performance of PRP associated with porous chitosan as a composite scaffold for regenerative medicine." ScientificWorldJournal **2015**: 396131.
- Shimojo, A. A., A. G. Perez, S. E. Galdames, I. C. Brissac and M. H. Santana (2016). "Stabilization of porous chitosan improves the performance of its association with platelet-rich plasma as a composite scaffold." Mater Sci Eng C Mater Biol Appl **60**: 538-546.
- Shinoda, T., Y. Shibata, T. Izaki, T. Shitama and M. Naito (2009). "A comparative study of surgical invasion in arthroscopic and open rotator cuff repair." J Shoulder Elbow Surg **18**(4): 596-599.
- Shive, M. S., W. D. Stanish, R. G. McCormack, F. Forriol, N. Mohtadi, S. Pelet, J. Desnoyers, S. Méthot, K. Vehik and A. Restrepo (2015). "BST-CarGel® Treatment Maintains Cartilage Repair Superiority over Microfracture at 5 Years in a Multicenter Randomized Controlled Trial. ." Cartilage **6**(2): 62-72.
- Siskosky MJ, E. N., Chu E, Tibone JE, Lee TQ (2007). "Biomechanical evaluation of the "transosseous equivalent" rotator cuff repair technique using the PushLock for lateral fixation compared to the double-row technique. ." Presented at the Annual Meeting of the American Academy of Orthopaedic Surgeons, San Diego, CA.
- Sittinger, M., D. W. Hutmacher and M. V. Risbud (2004). "Current strategies for cell delivery in cartilage and bone regeneration." Curr Opin Biotechnol **15**(5): 411-418.
- Sivashankari, P. R. and M. Prabakaran (2016). "Prospects of chitosan-based scaffolds for growth factor release in tissue engineering." Int J Biol Macromol **93**(Pt B): 1382-1389.
- Smith, L., Y. Xia, L. M. Galatz, G. M. Genin and S. Thomopoulos (2012). "Tissue-engineering strategies for the tendon/ligament-to-bone insertion." Connect Tissue Res **53**(2): 95-105.
- Snyder, S. J., S. P. Arnoczky, J. L. Bond and R. Dopirak (2009). "Histologic evaluation of a biopsy specimen obtained 3 months after rotator cuff augmentation with GraftJacket Matrix." Arthroscopy **25**(3): 329-333.
- Soler, J. A., S. Gidwani and M. J. Curtis (2007). "Early complications from the use of porcine dermal collagen implants (Permacol) as bridging constructs in the repair of massive rotator cuff tears. A report of 4 cases." Acta Orthop Belg **73**(4): 432-436.
- Sonnabend, D. H. and A. A. Young (2009). "Comparative anatomy of the rotator cuff." J Bone Joint Surg Br **91**(12): 1632-1637.
- Soslowky, L. J., J. E. Carpenter, C. M. DeBano, I. Banerji and M. R. Moalli (1996). "Development and use of an animal model for investigations on rotator cuff disease." Journal of shoulder and elbow surgery / American Shoulder and Elbow Surgeons ... [et al.] **5**(5): 383-392.
- Spiller, K. L., R. R. Anfang, K. J. Spiller, J. Ng, K. R. Nakazawa, J. W. Daulton and G. Vunjak-Novakovic (2014). "The role of macrophage phenotype in vascularization of tissue engineering scaffolds." Biomaterials **35**(15): 4477-4488.

- Spiller, K. L., S. Nassiri, C. E. Witherel, R. R. Anfang, J. Ng, K. R. Nakazawa, T. Yu and G. Vunjak-Novakovic (2015). "Sequential delivery of immunomodulatory cytokines to facilitate the M1-to-M2 transition of macrophages and enhance vascularization of bone scaffolds." Biomaterials **37**: 194-207.
- Spiller, K. L., E. A. Wrona, S. Romero-Torres, I. Pallotta, P. L. Graney, C. E. Witherel, L. M. Panicker, R. A. Feldman, A. M. Urbanska, L. Santambrogio, G. Vunjak-Novakovic and D. O. Freytes (2016). "Differential gene expression in human, murine, and cell line-derived macrophages upon polarization." Exp Cell Res **347**(1): 1-13.
- St Pierre, P., E. J. Olson, J. J. Elliott, K. C. O'Hair, L. A. McKinney and J. Ryan (1995). "Tendon-healing to cortical bone compared with healing to a cancellous trough. A biomechanical and histological evaluation in goats." J Bone Joint Surg Am **77**(12): 1858-1866.
- Stanish, W. D., R. G. McCormack, F. Forriol, N. Mohtadi, S. Pelet, J. Desnoyers, A. Restrepo and M. S. Shive (2013). "Novel Scaffold-Based BST-CarGel Treatment Results in Superior Cartilage Repair Compared with Microfracture in a Randomized Controlled Trial." Journal of Bone and Joint Surgery-American Volume **95A**(18): 1640-1650.
- Stein, D. A., R. Patel, K. A. Egol, F. T. Kaplan, N. C. Tejwani and K. J. Koval (2003). "Prevention of heterotopic ossification at the elbow following trauma using radiation therapy." Bull Hosp Jt Dis **61**(3-4): 151-154.
- Stouffer, D. C., D. L. Butler and D. Hosny (1985). "The relationship between crimp pattern and mechanical response of human patellar tendon-bone units." J Biomech Eng **107**(2): 158-165.
- Su, W. R., J. E. Budoff and Z. P. Luo (2009). "The effect of coracoacromial ligament excision and acromioplasty on superior and anterosuperior glenohumeral stability." Arthroscopy **25**(1): 13-18.
- Sugg, K. B., J. Lubardic, J. P. Gumucio and C. L. Mendias (2014). "Changes in macrophage phenotype and induction of epithelial-to-mesenchymal transition genes following acute Achilles tenotomy and repair." J Orthop Res **32**(7): 944-951.
- Suh, J. K. and H. W. Matthew (2000). "Application of chitosan-based polysaccharide biomaterials in cartilage tissue engineering: a review." Biomaterials **21**(24): 2589-2598.
- Sun, L. P., S. Wang, Z. W. Zhang, X. Y. Wang and Q. Q. Zhang (2009). "Biological evaluation of collagen-chitosan scaffolds for dermis tissue engineering." Biomed Mater **4**(5): 055008.
- Sundara, R. G. A., M.; Gowri, N (1982). Natural deacetylation of chitin to chitosan in the abdominal cuticle of the physogastric queen of Macrotermes estherae. In Proceeding Second International Conference Chitin/Chitosan, Sapporo, Japan,, Tottori, Japan.
- Sundman, E. A., B. J. Cole and L. A. Fortier (2011). "Growth Factor and Catabolic Cytokine Concentrations Are Influenced by the Cellular Composition of Platelet-Rich Plasma." American Journal of Sports Medicine **39**(10): 2135-2140.
- Tang, E. S., M. Huang and L. Y. Lim (2003). "Ultrasonication of chitosan and chitosan nanoparticles." Int J Pharm **265**(1-2): 103-114.
- Taylor, J. M., W. M. Mitchell and S. Cohen (1972). "Epidermal growth factor. Physical and chemical properties." J Biol Chem **247**(18): 5928-5934.
- Theodoropoulos, J. (2011). "Platelet-rich fibrin matrix augmentation did not improve recovery and healing more than nonaugmented rotator cuff repair." J Bone Joint Surg Am **93**(22): 2125.
- Thes, A., P. Hardy and K. Bak (2015). "Decision-making in massive rotator cuff tear." Knee Surg Sports Traumatol Arthrosc **23**(2): 449-459.

- Thomopoulos, S., G. M. Genin and L. M. Galatz (2010). "The development and morphogenesis of the tendon-to-bone insertion - What development can teach us about healing." Journal of Musculoskeletal & Neuronal Interactions **10**(1): 35-45.
- Thomopoulos, S., G. Hattersley, V. Rosen, M. Mertens, L. Galatz, G. R. Williams and L. J. Soslowsky (2002). "The localized expression of extracellular matrix components in healing tendon insertion sites: an in situ hybridization study." J Orthop Res **20**(3): 454-463.
- Thomopoulos, S., W. C. Parks, D. B. Rifkin and K. A. Derwin (2015). "Mechanisms of tendon injury and repair." J Orthop Res **33**(6): 832-839.
- Thomopoulos, S., E. Zampiakis, R. Das, M. J. Silva and R. H. Gelberman (2008). "The effect of muscle loading on flexor tendon-to-bone healing in a canine model." J Orthop Res **26**(12): 1611-1617.
- Tokuyasu, K., M. Ohnishi-Kameyama and K. Hayashi (1996). "Purification and characterization of extracellular chitin deacetylase from *Colletotrichum lindemuthianum*." Biosci Biotechnol Biochem **60**(10): 1598-1603.
- Tommersaas, K., K. M. Varum, B. E. Christensen and O. Smidsrod (2001). "Preparation and characterisation of oligosaccharides produced by nitrous acid depolymerisation of chitosans." Carbohydr Res **333**(2): 137-144.
- Tornero-Esteban, P., J. A. Hoyas, E. Villafuertes, C. Rodriguez-Bobada, Y. Lopez-Gordillo, F. J. Rojo, G. V. Guinea, A. Paleczny, Y. Lopiz-Morales, L. Rodriguez-Rodriguez, F. Marco and B. Fernandez-Gutierrez (2015). "Efficacy of supraspinatus tendon repair using mesenchymal stem cells along with a collagen I scaffold." J Orthop Surg Res **10**: 124.
- Totani, L., A. Cumashi, A. Piccoli and R. Lorenzet (1998). "Polymorphonuclear leukocytes induce PDGF release from IL-1beta-treated endothelial cells: role of adhesion molecules and serine proteases." Arterioscler Thromb Vasc Biol **18**(10): 1534-1540.
- Trappey, G. J. and G. M. Gartsman (2011). "A systematic review of the clinical outcomes of single row versus double row rotator cuff repairs." Journal of Shoulder and Elbow Surgery **20**(2): S14-S19.
- Trent, E. A., L. Bailey, F. N. Mefleh, V. P. Raikar, E. Shanley, C. A. Thigpen, D. Dean and D. M. Kwartowitz (2013). Assessment and characterization of in situ rotator cuff biomechanics. Medical Imaging 2013: Biomedical Applications in Molecular, Structural, and Functional Imaging.
- Trudel, G., G. Melkus, G. O. Cron, H. Louati, A. Sheikh, P. E. Larson, M. Schweitzer, P. Lapner, H. K. Uhthoff and O. Laneuville (2017). "Imaging of the rabbit supraspinatus enthesis at 7 Tesla: a 4-week time course after repair surgery and effect of channeling." J Magn Reson Imaging.
- Trudel, G., N. Ramachandran, S. E. Ryan, K. Rakhra and H. K. Uhthoff (2010a). "Supraspinatus Tendon Repair into a Bony Trough in the Rabbit: Mechanical Restoration and Correlative Imaging." Journal of Orthopaedic Research **28**(6): 710-715.
- Trudel, G., N. Ramachandran, S. E. Ryan, K. Rakhra and H. K. Uhthoff (2012a). "Improved strength of early versus late supraspinatus tendon repair: a study in the rabbit." Journal of Shoulder and Elbow Surgery **21**(6): 828-834.
- Trudel, G., S. E. Ryan, K. Rakhra and H. K. Uhthoff (2010b). "Extra- and Intramuscular Fat Accumulation Early after Rabbit Supraspinatus Tendon Division: Depiction with CT." Radiology **255**(2): 434-441.

- Trudel, G., S. E. Ryan, K. Rakhra and H. K. Uthoff (2012b). "Muscle tissue atrophy, extramuscular and intramuscular fat accumulation, and fat gradient after delayed repair of the supraspinatus tendon: A comparative study in the rabbit." Journal of Orthopaedic Research **30**(5): 781-786.
- Tsigos, I. and V. Bouriotis (1995). "Purification and characterization of chitin deacetylase from *Colletotrichum lindemuthianum*." J Biol Chem **270**(44): 26286-26291.
- Tucker, J. J., J. A. Gordon, R. C. Zanes, A. Zuskov, J. D. Vinciguerra, R. D. Bloebaum and L. J. Soslowky (2017). "P2 porous titanium implants improve tendon healing in an acute rat supraspinatus repair model." J Shoulder Elbow Surg **26**(3): 529-535.
- Turner, A. S. (2007). "Experiences with sheep surgery: Strengths and as an animal model for shoulder shortcomings." Journal of Shoulder and Elbow Surgery **16**(5): 158S-163S.
- Tutwiler, V., R. I. Litvinov, A. P. Lozhkin, A. D. Peshkova, T. Lebedeva, F. I. Ataullakhanov, K. L. Spiller, D. B. Cines and J. W. Weisel (2016). "Kinetics and mechanics of clot contraction are governed by the molecular and cellular composition of the blood." Blood **127**(1): 149-159.
- Uchida, H., H. Tohyama, K. Nagashima, Y. Ohba, H. Matsumoto, Y. Toyama and K. Yasuda (2005). "Stress deprivation simultaneously induces over-expression of interleukin-1beta, tumor necrosis factor-alpha, and transforming growth factor-beta in fibroblasts and mechanical deterioration of the tissue in the patellar tendon." J Biomech **38**(4): 791-798.
- Ueno, H., T. Mori and T. Fujinaga (2001). "Topical formulations and wound healing applications of chitosan." Adv Drug Deliv Rev **52**(2): 105-115.
- Ueno, H., H. Yamada, I. Tanaka, N. Kaba, M. Matsuura, M. Okumura, T. Kadosawa and T. Fujinaga (1999). "Accelerating effects of chitosan for healing at early phase of experimental open wound in dogs." Biomaterials **20**(15): 1407-1414.
- Uggen, C., J. Dines, M. McGarry, D. Grande, T. Lee and O. Limpisvasti (2010). "The effect of recombinant human platelet-derived growth factor BB-coated sutures on rotator cuff healing in a sheep model." Arthroscopy **26**(11): 1456-1462.
- Uggen, J. C., J. Dines, C. W. Uggen, J. S. Mason, P. Razzano, D. Dines and D. A. Grande (2005). "Tendon gene therapy modulates the local repair environment in the shoulder." J Am Osteopath Assoc **105**(1): 20-21.
- Uthoff, H. K., E. Coletta and G. Trudel (2014). "Effect of timing of surgical SSP tendon repair on muscle alterations." J Orthop Res **32**(11): 1430-1435.
- Uthoff, H. K., E. Coletta and G. Trudel (2014). "Intramuscular fat accumulation and muscle atrophy in the absence of muscle retraction." Bone Joint Res **3**(4): 117-122.
- Uthoff, H. K., F. Matsumoto, G. Trudel and K. Himori (2003a). "Early reattachment does not reverse atrophy and fat accumulation of the supraspinatus--an experimental study in rabbits." J Orthop Res **21**(3): 386-392.
- Uthoff, H. K., H. Sano, G. Trudel and H. Ishii (2000). "Early reactions after reimplantation of the tendon of supraspinatus into bone. A study in rabbits." J Bone Joint Surg Br **82**(7): 1072-1076.
- Uthoff, H. K., M. Seki, D. S. Backman, G. Trudel, K. Himori and H. Sano (2002). "Tensile strength of the supraspinatus after reimplantation into a bony trough: an experimental study in rabbits." J Shoulder Elbow Surg **11**(5): 504-509.

- Uthoff, H. K., G. Trudel and K. Himori (2003). "Relevance of pathology and basic research to the surgeon treating rotator cuff disease." Journal of orthopaedic science : official journal of the Japanese Orthopaedic Association **8**(3): 449-456.
- Usami, Y., Y. Okamoto, S. Minami, A. Matsushashi, N. H. Kumazawa, S. Tanioka and Y. Shigemasa (1994). "Chitin and chitosan induce migration of bovine polymorphonuclear cells." J Vet Med Sci **56**(4): 761-762.
- Usami, Y., Y. Okamoto, S. Minami, A. Matsushashi, N. H. Kumazawa, S. Tanioka and Y. Shigemasa (1994). "Migration of canine neutrophils to chitin and chitosan." J Vet Med Sci **56**(6): 1215-1216.
- Usami, Y., Y. Okamoto, T. Takayama, Y. Shigemasa and S. Minami (1998). "Chitin and chitosan stimulate canine polymorphonuclear cells to release leukotriene B4 and prostaglandin E2." J Biomed Mater Res **42**(4): 517-522.
- van der Zwaal, P., B. J. W. Thomassen, M. J. Nieuwenhuijse, R. Lindenburg, J.-W. A. Swen and E. R. A. van Arkel (2013). "Clinical Outcome in All-Arthroscopic Versus Mini-Open Rotator Cuff Repair in Small to Medium-Sized Tears: A Randomized Controlled Trial in 100 Patients With 1-Year Follow-up." Arthroscopy **29**(2): 266-273.
- VandeVord, P. J., H. W. Matthew, S. P. DeSilva, L. Mayton, B. Wu and P. H. Wooley (2002). "Evaluation of the biocompatibility of a chitosan scaffold in mice." J Biomed Mater Res **59**(3): 585-590.
- VandeVord, P. J., H. W. T. Matthew, S. P. DeSilva, L. Mayton, B. Wu and P. H. Wooley (2002). "Evaluation of the biocompatibility of a chitosan scaffold in mice." J Biomed Mater Res **59**(3): 585-590.
- Varum, K. M., M. H. Ottoy and O. Smidsrod (2001). "Acid hydrolysis of chitosans." Carbohydrate Polymers **46**(1): 89-98.
- Verma, N. N., W. Dunn, R. S. Adler, F. A. Cordasco, A. Allen, J. MacGillivray, E. Craig, R. F. Warren and D. W. Altchek (2006). "All-arthroscopic versus mini-open rotator cuff repair: a retrospective review with minimum 2-year follow-up." Arthroscopy **22**(6): 587-594.
- Viidik, A. (1973). "Functional properties of collagenous tissues." Int Rev Connect Tissue Res **6**: 127-215.
- Vogel, K. G., J. D. Sandy, G. Pogany and J. R. Robbins (1994). "Aggrecan in bovine tendon." Matrix Biol **14**(2): 171-179.
- Wall, L. B., J. D. Keener and R. H. Brophy (2009). "Clinical Outcomes of Double-Row Versus Single-Row Rotator Cuff Repairs." Arthroscopy **25**(11): 1312-1318.
- Waltrip, R. L., N. Zheng, J. R. Dugas and J. R. Andrews (2003). "Rotator cuff repair. A biomechanical comparison of three techniques." Am J Sports Med **31**(4): 493-497.
- Wang, D., J. Mo, S. Pan, H. Chen and H. Zhen (2010). "Prevention of postoperative peritoneal adhesions by O-carboxymethyl chitosan in a rat cecal abrasion model." Clin Invest Med **33**(4): E254-260.
- Wang, J. H. (2006). "Mechanobiology of tendon." J Biomech **39**(9): 1563-1582.
- Wang, X., E. Wenk, X. Zhang, L. Meinel, G. Vunjak-Novakovic and D. L. Kaplan (2009). "Growth factor gradients via microsphere delivery in biopolymer scaffolds for osteochondral tissue engineering." J Control Release **134**(2): 81-90.

- Watkins, J. P., J. A. Auer, S. Gay and S. J. Morgan (1985). "Healing of surgically created defects in the equine superficial digital flexor tendon: collagen-type transformation and tissue morphologic reorganization." *Am J Vet Res* **46**(10): 2091-2096.
- Weber, S. C., J. I. Kauffman, C. Parise, S. J. Weber and S. D. Katz (2013). "Platelet-rich fibrin matrix in the management of arthroscopic repair of the rotator cuff: a prospective, randomized, double-blinded study." *Am J Sports Med* **41**(2): 263-270.
- Weibrich, G., W. K. Kleis, P. Streckbein, M. Moergel, W. E. Hitzler and G. Hafner (2012). "Comparison of point-of-care methods for preparation of platelet concentrate (platelet-rich plasma)." *Int J Oral Maxillofac Implants* **27**(4): 762-769.
- White, J. G. (2000). "Platelet secretion during clot retraction." *Platelets* **11**(6): 331-343.
- Wieser, K., M. Farshad, D. C. Meyer, P. Conze, B. von Rechenberg and C. Gerber (2015). "Tendon response to pharmaco-mechanical stimulation of the chronically retracted rotator cuff in sheep." *Knee Surgery Sports Traumatology Arthroscopy* **23**(2): 577-584.
- Williams, G. R., Jr. and C. A. Rockwood, Jr. (1996). "Hemiarthroplasty in rotator cuff-deficient shoulders." *J Shoulder Elbow Surg* **5**(5): 362-367.
- Williams, J. G. (1993). "Achilles tendon lesions in sport." *Sports Med* **16**(3): 216-220.
- Wong, M. W., L. Qin, K. M. Lee and K. S. Leung (2009). "Articular cartilage increases transition zone regeneration in bone-tendon junction healing." *Clin Orthop Relat Res* **467**(4): 1092-1100.
- Woo S, M. J., Butler D (1988). "Ligament, tendon, and joint capsule insertions to bone." *Park Ridge: Am Acad Orthop Surg*: 133-166.
- Wrana, J. L., L. Attisano, R. Wieser, F. Ventura and J. Massague (1994). "Mechanism of activation of the TGF-beta receptor." *Nature* **370**(6488): 341-347.
- Wu, Y., Y. Dong, S. Chen and Y. Li (2014). "Effect of platelet-rich plasma and bioactive glass powder for the improvement of rotator cuff tendon-to-bone healing in a rabbit model." *Int J Mol Sci* **15**(12): 21980-21991.
- Wurgler-Hauri, C. C., L. M. Dourte, T. C. Baradet, G. R. Williams and L. J. Soslowsky (2007). "Temporal expression of 8 growth factors in tendon-to-bone healing in a rat supraspinatus model." *J Shoulder Elbow Surg* **16**(5 Suppl): S198-203.
- Yamamoto, A., K. Takagishi, T. Osawa, T. Yanagawa, D. Nakajima, H. Shitara and T. Kobayashi (2010). "Prevalence and risk factors of a rotator cuff tear in the general population." *J Shoulder Elbow Surg* **19**(1): 116-120.
- Yamamoto, E., S. Tokura and K. Hayashi (2003). "Effects of cyclic stress on the mechanical properties of cultured collagen fascicles from the rabbit patellar tendon." *J Biomech Eng* **125**(6): 893-901.
- Yan, L.-P., Y.-J. Wang, L. Ren, G. Wu, S. G. Caridade, J.-B. Fan, L.-Y. Wang, P.-H. Ji, J. M. Oliveira, J. T. Oliveira, J. F. Mano and R. L. Reis (2010). "Genipin-cross-linked collagen/chitosan biomimetic scaffolds for articular cartilage tissue engineering applications." *Journal of Biomedical Materials Research Part A* **95A**(2): 465-475.
- Yanke, A. B. and S. Chubinskaya (2015). "The state of cartilage regeneration: current and future technologies." *Curr Rev Musculoskelet Med* **8**(1): 1-8.
- Yao, K., J. Li, F. Yao and Y. Yin (2012). *Chitosan-Based Hydrogels: Functions and Applications*. Boca Raton, FL, USA, Taylor and Francis Group LLC  
CRC Press.



- Yao, Q., Y. Yang, X. Pu, L. Yang, Z. Hou, Y. Dong and Q. Zhang (2012). "Preparation, Characterization and Osteoblastic Activity of Chitosan/Polycaprolactone/In Situ Hydroxyapatite Scaffolds." Journal of Biomaterials Science-Polymer Edition **23**(14): 1755-1770.
- Ying, Z. M., T. Lin and S. G. Yan (2014). "Arthroscopic single-row versus double-row technique for repairing rotator cuff tears: a systematic review and meta-analysis." Orthop Surg **6**(4): 300-312.
- Yokoya, S., Y. Mochizuki, Y. Nagata, M. Deie and M. Ochi (2008). "Tendon-bone insertion repair and regeneration using polyglycolic acid sheet in the rabbit rotator cuff injury model." Am J Sports Med **36**(7): 1298-1309.
- Yokoya, S., Y. Mochizuki, K. Natsu, H. Omae, Y. Nagata and M. Ochi (2012). "Rotator cuff regeneration using a bioabsorbable material with bone marrow-derived mesenchymal stem cells in a rabbit model." Am J Sports Med **40**(6): 1259-1268.
- Younes, I. and M. Rinaudo (2015). "Chitin and chitosan preparation from marine sources. Structure, properties and applications." Mar Drugs **13**(3): 1133-1174.
- Zelzer, E., E. Blitz, M. L. Killian and S. Thomopoulos (2014). "Tendon-to-bone attachment: from development to maturity." Birth Defects Res C Embryo Today **102**(1): 101-112.
- Zhang, Z., B. Gu, W. Zhu, L. Zhu and Q. Li (2014). "Arthroscopic versus mini-open rotator cuff repair: a prospective, randomized study with 24-month follow-up." European journal of orthopaedic surgery & traumatology : orthopedie traumatologie **24**(6): 845-850.
- Zhao, S., L. Peng, G. Xie, D. Li, J. Zhao and C. Ning (2014). "Effect of the Interposition of Calcium Phosphate Materials on Tendon-Bone Healing During Repair of Chronic Rotator Cuff Tear." Am J Sports Med **42**(8): 1920-1929.
- Zhao, S., X. Xie, G. Pan, P. Shen, J. Zhao and W. Cui (2015). "Healing improvement after rotator cuff repair using gelatin-grafted poly(L-lactide) electrospun fibrous membranes." J Surg Res **193**(1): 33-42.
- Zhao, S., J. Zhao, S. Dong, X. Huangfu, B. Li, H. Yang and W. Cui (2014). "Biological augmentation of rotator cuff repair using bFGF-loaded electrospun poly(lactide-co-glycolide) fibrous membranes." Int J Nanomedicine **9**: 2373-2385.
- Zhou, S. F., A. L. Estrera, C. C. Miller, 3rd, C. Ignacio, S. Panthayi, P. Loubser, D. L. Sagun, R. Sheinbaum and H. J. Safi (2013). "Analysis of autologous platelet-rich plasma during ascending and transverse aortic arch surgery." Ann Thorac Surg **95**(5): 1525-1530.
- Zucker, M. B. and V. T. Nachmias (1985). "Platelet activation." Arteriosclerosis **5**(1): 2-18.
- Zuk, P. A., M. Zhu, P. Ashjian, D. A. De Ugarte, J. I. Huang, H. Mizuno, Z. C. Alfonso, J. K. Fraser, P. Benhaim and M. H. Hedrick (2002). "Human adipose tissue is a source of multipotent stem cells." Mol Biol Cell **13**(12): 4279-4295.
- Zumstein, M. A., A. Rumian, V. Lesbats, M. Schaer and P. Boileau (2014). "Increased vascularization during early healing after biologic augmentation in repair of chronic rotator cuff tears using autologous leukocyte- and platelet-rich fibrin (L-PRF): a prospective randomized controlled pilot trial." Journal of Shoulder and Elbow Surgery **23**(1): 3-12.

## APPENDIX A – CLINICAL STUDIES COMPARING ARTHROSCOPIC VERSUS OPEN ROTATOR CUFF REPAIR

Table 9-1 Clinical studies comparing arthroscopic versus open rotator cuff repair.

Study	Design	Inclusion criteria	Surgical approach 1	Surgical approach 2	Sample size (% males)	Mean age (years)	FU rate (%)	Mean FU times (months)	Outcome measures	Definition of retear	Results
Severud et al 2002	Level III Retrospective	Surgically proven full-thickness rotator cuff tears	Bone anchors were the primary method of fixation in the all-arthroscopic group, averaging 1.5 a case	The majority of fixations were through bone tunnels in the mini-open group	64 (60.9) 35 shoulders in the all-arthroscopic group 29 in the mini-open group	60.8	100	44.6	UCLA score ASES score RofM	NA	Clinical scores improved in both groups  No effect of surgical approach on clinical scores  Significantly better range of motion for all-arthroscopic group at 6 weeks and 12 weeks but not at final FU
Kim et al 2003	Level III Retrospective	Patients with medium and large rotator cuff tears	All-arthroscopic repair	Mini-open salvage of technically unsuccessful arthroscopic repair	76 (62.8) 42 patients in the all-arthroscopic group 34 in the mini-open group	56.5	100	39	UCLA score ASES score VAS scale for shoulder function VAS scale for	NA	Clinical scores improved in both groups  No effect of surgical approach on

									pain		clinical scores  Lower shoulder scores and less predictable recovery of strength and function for patients with large tears
Sauerbrey et al 2005	Level III Retrospective	Patients who had undergone mini-open and all arthroscopic rotator cuff repairs	The edge of the rotator cuff was secured to the tuberosity using anchors with nonabsorbable simple Sutures in the all arthroscopic group	The rotator cuff was secured to the tuberosity using sutures through bone in all cases in the mini-open group	54 (59.3) 28 patients in the all-arthroscopic group 26 in the mini-open group	56.5	100	Mini-open, 33 Arthroscopy, 19	Modified ASES score VAS scale for pain	NA	Clinical scores improved in both groups  No effect surgical approach on clinical scores
Warner et al 2005	Level III Retrospective	Patients with full-thickness rotator cuff tears	Absorbable suture anchor loaded with absorbable suture in the all arthroscopic group	Transosseous tendon repair in the mini-open group	21 (61.9) 9 patients in the all-arthroscopic group 12 in the mini-open group	54	100	50	SST score Pain score Flexion External rotation Strength	NA	Clinical scores improved in both groups  No effect of surgical approach on clinical scores  All arthroscopic group showed a significant improvement

											in strength
Youm et al 2005	Level III Retrospective	Surgically confirmed and repaired rotator cuff tear by either an all-arthroscopic repair or mini-open repair with at least 2 years of follow-up	The tendon was secured to the tuberosity with suture anchors in the all arthroscopic group	Margin convergence sutures were used in combination with suture anchors in the mini-open group If the hold of the anchor was determined to be inadequate, bone tunnels were used instead	84 (NR) 42 patients in the all arthroscopic group 42 in the mini-open group	59	100	36.3	UCLA score ASES score	NA	Good or excellent clinical scores for both groups post-surgery  No effect of surgical approach on clinical scores
Ide et al 2005	Level III Retrospective	Patients who had undergone mini-open and all arthroscopic rotator cuff repairs	Repair with suture anchors and nonabsorbable sutures in the all arthroscopic group	The majority of fixations were performed using the suture anchor technique in the mini-open group The conventional bone tunnel technique was used in 3 patients	100 (80) 50 patients in the all-arthroscopic group 50 in the mini-open group	57	100	49	UCLA score JOA score	NA	Clinical scores improved in both groups  No effect of surgical approach on clinical scores  Scores in patients with a large-to-massive tear were significantly lower than those with a small-to-medium tear
Bishop et al 2006	Level III Prospective	Patients treated with open, mini-open and all arthroscopic	The tendon was repaired to the prepared greater tuberosity with	The rotator cuff was repaired to the prepared	72 (43.1) 40 patients in the all-arthroscopic	64	100	≥ 12	ASES score Constant score Forward	Any tendon filled with fluid on MRI images was	Clinical scores improved in

		rotator cuff repairs	suture anchors in the all arthroscopic group	greater tuberosity with sutures placed in a modified Mason-Allen fashion and passed through bone tunnels, reinforced with CuffLink Bone Tunnel Devices in the mini-open or open group	group 32 in the mini-open (n=8) or open (n=24) group				elevation External rotation Short Form 36 VAS scale for pain	considered a retear	both groups Significantly greater strength of elevation and external rotation in all arthroscopic group More retears for tears greater than 3 cm in all arthroscopic group
Verma et al 2006	Level III Retrospective	Patients that had undergone arthroscopic or mini-open rotator cuff repair, with a minimum of 2 years' follow up	No consistent data on anchor configuration (single or double row) or on suture configuration (simple, mattress, etc.) could be obtained for the all arthroscopic group	Tendon repair was then carried out with the use of anchors, bone tunnels, or a combination of both in the mini-open group	71 (63.3 ) 38 patients in the all-arthroscopic group 33 in the mini-open group	60	100	38.9	ASES score SST score L'Insalata Scoring Survey VAS scale for pain Strength Ultrasound	Failure of repair was defined as any full-thickness rotator cuff defect on ultrasound images	Clinical scores improved in both groups No effect surgical approach on clinical scores or failure rate
Liem et al 2007	Level III Retrospective	An isolated supraspinatus tear confirmed by clinical examination and magnetic resonance imaging (MRI) that resulted in persistent pain and reduced function of the patient's	A single row of 1 to 3 bioabsorbable suture anchors armed with 2 pairs of nonabsorbable  No. 2 sutures that were placed along the lateral part of the footprint. According to the shape of the tendon, additional side-to-side	The supraspinatus was repaired by use of 1 to 3 bioabsorbable suture anchors armed with 2 pairs of nonabsorbable No. 2 sutures  Side-to-side FiberWire	38 (88.9) 19 patients in the all-arthroscopic group 19 in the mini-open group	62	100	Mini-open, 17.6 Arthroscopy, 25	Constant score Early RofM at 6 weeks and 3 months MRI	Cuff integrity was evaluated with established criteria (Owens et al 1993)	Clinical scores improved in both groups No effect surgical approach on clinical scores or failure rate

		arm	sutures were used  The tendon was then repaired via a Mason-Allen technique modified for the arthroscopic technique	sutures were used if necessary  The tendon was sutured to the bone via the modified Mason-Allen technique with the combination of a U-shaped mattress suture and single suture on top of the mattress suture							
Kose et al 2008	Level III Retrospective	Patient had required rotator cuff repair and that the tear was also confirmed intraoperatively	Suture anchors were used for fixation and repair of the rotator cuff in the all arthroscopic group	Tendon repairs were performed using sutures passed through bone tunnels in the mini-open group	50 (22) 25 patients in the all-arthroscopic group  25 in the mini-open group	59	100	Mini-open, 31.2  Arthroscopy, 21.6	Constant-Murley score  UCLA score  RofM  External rotation  Forward flexion	NA	Clinical scores improved in both groups  No effect surgical approach on clinical scores
Colegate-Stone et al 2009	Level III Prospective	Patients who had undergone mini-open and all arthroscopic rotator cuff repairs	Bioabsorbable Bio-corkscrew anchors with a single row repair technique in the all arthroscopic group	Bioabsorbable Bio-corkscrew anchors with a single row repair technique in the mini-open group	123 (48.8) 92 patients in the all-arthroscopic group  31 in the mini-open group	60	100	Longest 24	DASH  OSS  Constant-Murley score	NA	Clinical scores improved in both groups  No effect surgical approach on clinical scores

Shinoda et al 2009	Level II Randomized controlled trial	Patients who had undergone mini-open and all arthroscopic rotator cuff repairs	The rotator cuff was secured to the footprint using 2 or 4 Fastin RC suture anchors in the all arthroscopic group	The rotator cuff was secured to the footprint using 2 or 4 Fastin RC suture anchors in the mini-open group	32 (71.9) 17 patients in the all-arthroscopic group 15 in the mini-open group	64	100	Median 34	Serum levels C-reactive protein Hemoglobin IL-6 UCLA score JOA score	NA	Clinical scores improved in both groups  No effect surgical approach on clinical scores  Increased IL-6 at 24h in the mini-open group
Kasten et al 2011	Level III Prospective randomized	Rupture of the supraspinatus tendon with retraction with a maximum to the apex of the humeral head and minor fatty degeneration and atrophy of the muscle	Double row repair with resorbable anchors in the all arthroscopic group	Transosseous repair with Mason-Allen stitches in the mini-open group	34 (61.8) 17 patients in the all-arthroscopic group 17 in the mini-open group	60	For pain Mini-open, 94 Arthroscopy, 82  For scores Mini-open, 94 Arthroscopy, 100	Longest 6	VAS scale for pain Constant-Murley score ASES score Abduction Forward flexion External rotation MRI	Post-operative integrity evaluated on MRI images according to a modified Sugaya	Clinical scores improved in both groups  No effect surgical approach on clinical scores or failure rate  Decreased pain in mini-open group from 4-8 weeks
Cho et al 2012	Level II Randomized controlled trial	Intraoperative confirmation of the presence of a supraspinatus tear smaller than 3 cm	The tear was adequately mobilized and repaired by attaching the supraspinatus to the prepared greater tuberosity using either the	The torn tendon was repaired using either the single-row (n=7) or double-row (n=23) repair technique with	60 ( 56.7) 30 patients in the all-arthroscopic group 30 in the mini-open group	56	100	Longest 6	VAS scale for pain Forward flexion External rotation	NA	No effect of surgical approach on functional scores  Decreased pain in all arthroscopic group at 1

			single-row (n=5) or double-row (n=25) repair technique with a suture anchor in the all arthroscopic group	a suture anchor in the mini-open group							and 2 days
van der Zwaal et al 2013	Level II Randomized controlled trial	Eligible patients were (1) younger than 70 years of age and (2) had a small to medium-sized full-thickness supraspinatus and/or infraspinatus tendon tear with stage <3 fatty muscle infiltration on based on magnetic resonance imaging (MRI) findings	A Suture Bridge repair construct was applied, using 2 to 4 anchors depending on the size of the tear, to secure the tendons in both groups with a 5.5-mm CorkScrew in the medial row and a knotless 3.5-mm Bio-Push-Lock anchor in the lateral row in the all arthroscopic group	A Suture Bridge repair construct was applied, using 2 to 4 anchors depending on the size of the tear, to secure the tendons in both groups with a 5.5-mm CorkScrew in the medial row and a knotless 3.5-mm Bio-Push-Lock anchor in the lateral row in the mini-open group	100 (60) 50 patients in the all-arthroscopic group 50 in the mini-open group	58	95	Longest 13	DASH Constant-Murley score VAS scale for pain VAS scale for impairment Forward flexion External rotation Ultrasonogram	Scored as intact or retear on ultrasonogram	Clinical scores improved in both groups No effect surgical approach on clinical scores or failure rate DASH score, VAS pain and impairment scores and active forward flexion were significantly more improved in the all arthroscopic group at 6 weeks
Zhang et al 2014	Level I Randomized controlled trial	Inclusion criteria included (1) a full- or partial-thickness tear measuring more than 1 cm in diameter; (2)	A single row of 1–3 bioabsorbable suture anchors armed with 2 pairs of nonabsorbable No. 2 sutures were placed along the lateral part of the	The supraspinatus was repaired by use of 1–3 bioabsorbable suture anchors armed with 2 pairs of	125 (50.9) 62 patients in the all-arthroscopic group 63 in the mini-open group	54	86.4	29.1	UCLA score ASES score MRI	Retear visible on MRI images	Clinical scores improved in both groups No effect surgical approach on



		patient's willingness to be randomized to a arthroscopic or mini-open repair; and (3) adequate circumstances for MRI examination	<p>footprint in the all arthroscopic group According to the shape of the tendon, additional side-to-side sutures were used</p> <p>The tendon was then repaired via a Mason-Allen technique modified for the arthroscopic technique</p>	<p>nonabsorbable No. 2 sutures in the mini-open group</p> <p>Side-to-side FiberWire</p> <p>sutures were used if necessary</p> <p>The tendon was sutured to the bone via the modified Mason-Allen technique with the combination of a U-shaped mattress suture and single suture on top of the mattress suture.</p>								clinical scores Retearing rate was significantly higher in all arthroscopy group
--	--	--	--	--	--	--	--	--	--	--	--	--

**APPENDIX B – CLINICAL STUDIES COMPARING DIFFERENT SUTURING TECHNIQUES.**

Table 9-2 Clinical studies comparing different suturing techniques.

Study	Design	Inclusion criteria	Surgical approach 1	Surgical approach 2	Concomitant procedures	Sample size (% males)	Mean age (yrs)	FU rate (%)	Mean FU time (mo)	Outcome measures	Definition of retear	Results
Sugaya et al 2005	Level III Retrospective cohort study	Full thickness rotator cuff tear confirmed during surgery and	SR repair One to three anchors depending on tear length	DR repair Two to five anchors depending on tear length	Bursectomy, subacromial decompression, debridement of greater tuberosity in all	80 (69) 39 repairs arthroscopic with SR 41 repairs	58	75.5	35	UCLA score ASES score MRI	Cuff integrity was determined through MRI	Clinical scores improved in both groups No effect of

		no major associated pathology			patients As required: Osteophyte removal Tendon mobilization procedure	arthroscopic with DR					and classified into 5 categories	surgical approach on clinical scores Improved structural outcome in DR group
Charousset et al 2007	Level II Non-randomized Prospective comparative study	No previous surgery on shoulder concerned, no sign of adhesive capsulitis or shoulder instability, complete SSP tears	SR repair First suture into cortical bone 2-4 anchors	DR repair 2-4 anchors panalock Place a cuff tack between 2 suture anchors close to cartilaginous rim to ensure cuff spread over burred surface	Bursectomy and coracoacromial ligament resection and acromioplasty before cuff reinsertion	66 (50) 35 repairs arthroscopic with SR 31 repairs arthroscopic with DR	59	76	28.7	Constant score CT arthrogram		Clinical outcomes improved for both groups Tendon rate healing was better with DR repair
Franceschi et al 2007	Level I Randomized controlled trial	RCT diagnosed on clinical grounds, no episodes of shoulder instability, no radiographic signs of fracture of the glenoid or greater or lesser tuberosity, MRI evidence of cuff tear, duration of symptoms of at least 3cm, inadequate response to	SR repair 1 row of suture anchors double-loaded just inside lateral aspect of footprint 1-2 anchors	DR repair 1 row of anchors in medial aspect of footprint & lateral row placed on lateral aspect 2-4 anchors	NA	60 (47) 30 repairs arthroscopic SR 30 repairs arthroscopic DR	62	86.7	24	UCLA score RoM Shoulder pain, strength MRI arthrography	NA	Clinical outcomes improved for both groups No difference in MRI DR repair superior construct in restoring anatomical footprint of RC but does not translate to superior clinical performance.

		nonoperated management & an unretracted & sufficiently mobile full-thickness RC lesion to allow a DR repair found at the time of surgery.										
Park et al 2008	Level II Cohort study	Patients undergoing SR or DR surgical repair for full-thickness RCT	SR repair small to medium tears 1-2 anchors Large to massive tears 3 anchors	DR repair small to medium tears 1-2 anchors were used at both the medial row & the lateral row  For large to massive tears 2-3 anchors were used at the medial row & 3-4 anchors were used at the lateral row	Complete bursectomy performed to create a flat acromial undersurface in all patients. Osteophytes in inferior part of acromioclavicular joints were removed if mobility of the tendon was insufficient for repair, release of the coracohumeral ligament & debridement of RC from the bursal & articular sides were performed.	78 (54) 40 repairs arthroscopic with SR 38 repairs arthroscopic with DR	56	10	25.1	ASES score Constant score Shoulder strength index	NA	Functional outcomes improved for both groups  Patients with large to massive tears ASES score & Constant score & Shoulder strength were all significantly higher in DR repairs
Grasso et al 2009	Level I Prospective randomized	Repairable full thickness tear of the SSP or posterior-superior rotator cuff	SR repair One to four anchors depending on tear length	DR repair Medial row: One to two anchors at the articular margin of the humeral head	Debridement of greater tuberosity and cuff edges in all patients	80 (47) 40 repairs arthroscopic with SR 40 repairs arthroscopic with DR	57	90	24	DASH score Work-DASH score Constant-Murley	NA	Clinical scores improved in both groups  No effect of surgical approach on

				Lateral row: One to three anchors depending on tear length						score		clinical scores and strength
										Strength assessment		
Burks et al 2009	Level I Randomized Prospective controlled trial	Full thickness tear as seen on MRI, ability of the patient to complete serial MRI examination, willingness to comply with standardized rotator cuff physical therapy program, willingness to be randomized to a SR or DR repair, tear pattern that was amenable to repair with either SR or DR fixation	SR repair  Anchors were placed along the lateral edge of the greater tuberosity within the footprint of the rotator cuff and spaced at 5- to 10-mm increments  Average 2.25 anchors	DR repair  Medial row: Established with a diamond pattern of double-loaded anchors Lateral row: Established in a fashion similar to what had been done for the SR  Average 3.2 anchors	Acromioplasty in 38 of 40 cases Buffing of outer cortex to induce bleeding As required: Distal clavicle resections Tenodesis Biceps tenotomy SLAP repair	40 (NR)  20 repairs arthroscopic with SR  20 repairs arthroscopic with DR	57	100	12	UCLA score  Constant score, WORC index  SANE ASES score  RofM  Internal rotation  External rotation  MRI	Presence of a full-thickness tear on MRI, defined as fluid signal and/or absence of visible tendon fibers extending across the entire tendon from inferior to superior	Clinical scores improved in both groups  No differences in MRI  No effect of surgical approach on clinical scores and rate of retear
Aydin et al 2010	Level II Randomized clinical trial	Full thickness tear as seen on MRI, willingness to comply with physical therapy program and tear pattern amenable to repair by SR or DR	SR repair  One to three anchors depending on tear length	DR repair  Medial row: One to two anchors at the articular margin of the humeral head  Lateral row: One to three anchors	Complete bursectomy and subacromial decompression in all patients  As required: Osteophyte removal	68 (NR)  34 repairs arthroscopic with SR  34 repairs arthroscopic with DR	58	100	36	Constant score	NA	Clinical scores improved in both groups  No effect of surgical approach on clinical scores

				depending on tear length								
Koh et al 2011	Level I Randomized Prospective controlled trial	Full thickness tear as seen on MRI or arthrography, symptoms lasting more than 6 months, 2-cm to 4-cm tear	SR repair Two anchors with simple stitches	DR repair Medial row: One anchor with mattress sutures Lateral row: Two anchors with simple stitches	Debridement of tear and decortications in all patients  As required: Bursectomy Acromioplasty Osteophyte removal	71 (28) 37 repairs arthroscopic with SR 34 repairs arthroscopic with DR	61	Clinical 187 MRI 66	32	ASES score Constant score UCLA score VAS scale for pain MRI	MRI scans classified as in Sugaya	Clinical scores improved in both groups  No effect of surgical approach on clinical scores and rate of re-tear
Mihata et al 2011	Level III Cohort study	Patients who retrospectively underwent arthroscopic RC repair with SR, DR or combination of DR & suture bridge techniques	SR repair Average of 1.7 anchors	DR repair Average of 3.5 anchors DR compression Repair Average of 3.8 anchors	Arthroscopic subacromial decompression performed to create a flat acromion surface  Spurs in the inferior of the acromioclavicular joint & at the distal end of the clavicle were removed	206 (49) 65 repairs arthroscopic with SR 23 repairs arthroscopic with DR 107 repairs arthroscopic with compression DR	61	95	38.5	MRI ASES score JOA score UCLA score RoM	Sugaya's classification	Large to massive tears re-tear rate in compression DR was significantly less  Clinical outcomes improved in 3 groups
Denard et al 2012	Level III Retrospective comparative study	Arthroscopic complete or partial repair of a massive rotator cuff tear and a minimum of 5 years of follow-up	SR repair A mean of 3.3 anchors were used for the superior rotator cuff (SSP and ISP) A mean of 1.6 anchors was used to repair a subscapularis tendon tear	DR repair A mean of 5 anchors were used for the superior rotator cuff (SSP and ISP only)	As required: Modified acromioplasty Distal clavicle excisions Biceps tenodeses or tenotomise Coracoplasty SLAP repair	115 (64) 62 repairs arthroscopic with SR 45 repairs arthroscopic with DR	62	100	99	UCLA score ASES score VAS score Forward flexion	NA	Clinical scores improved in both groups  Better UCLA, subjective shoulder value, satisfaction and return to activity scores in DR repair group
Lapner et	Level I	RC of any	SR repair	DR repair	NA	90 (71)	57	81	24	WORC	MRI	Clinical and

al 2012	Randomized controlled trial	size was considered for inclusion. Full-thickness tear classified as repairable if the tendon could be restored to its anatomical insertion when traction was applied without undue tension	Anchors were placed along the lateral edge of the footprint	Anchors were placed along the lateral edge of the footprint Medial anchors placed along the bone-cartilage junction at the medial aspect of the footprint		48 repairs arthroscopic with SR 42 repairs arthroscopic with DR				score Constant score ASES score MRI Shoulder strength		functional outcomes improved for both groups
Kim et al 2012	Level II Cohort study	Full thickness SSP and/or ISP tears with 1 to 4 cm of anterior to posterior dimension	SB repair Medial row: Two or three anchors lateral to the articular surface of the humeral head Lateral row: Two anchors inserted perpendicular to the cortical surface of the humerus distal to the footprint	DR repair Medial row: One or two anchors lateral to the articular surface of the humeral head Lateral row: Two or three anchors at the lateral margin of the greater tuberosity	NR	52 (58) 26 repairs arthroscopic with DR 26 repairs arthroscopic with SB	58	Clinical 1100 MRI or ultrasonography 96	Clinical 137 MRI or ultrasonography 34	UCLA score ASES score Constant score VAS score MRI or ultrasonography	A full-thickness retear was diagnosed if there was a focal defect in the rotator cuff into which the deltoid muscle could be compressed with a probe to separate the torn tendon ends or if the cuff retracted to such an extent that the torn ends could be distinctly visualize	Clinical scores improved in both groups No effect of surgical approach on clinical scores and rate of retear

											MRI scans classified as in Sugaya	
Ma et al 2012	Level II Randomized Prospective control trial	Full thickness tear measuring more than 1 cm in diameter  (Medium to massive tear), a tear pattern that was amenable to repair with either SR or DR fixation, patient's willingness to be randomized to a SR or DR repair, adequate circumstances for MRI examination	SR repair  Two to four anchors placed on the lateral edge of the greater tuberosity	DR repair  Medial row:  One to two anchors at the articular margin of the humeral head  Lateral row: Placed in a fashion similar to the SR repair technique	Bursectomy, acromioplasty, coracoacromial ligament release, debridement of greater tuberosity in all patients  As required:  Release of the coracohumeral ligament and detachment of the tendon from the bursal and articular sides	53 (55)  27 repairs arthroscopic with SR  26 repairs arthroscopic with DR	61	100	33	UCLA score  ASES score  Abduction  External rotation  Contrast MRI	Partial tear was diagnosed in the presence of contrast material filling a partial tendon defect without tendon gap  A full thickness tear was diagnosed in the presence of tendon gap and presence of extravasation of contrast material to the subacromial space	Clinical scores improved in both groups  No effect of surgical approach on clinical scores and rate of retear  Strength better in DR group for tears larger than 3cm
Carbonel et al 2012	Level I Randomized Prospective clinical study	Rotator cuff tear, clinically confirmed, in a sane patient with complete passive range of motion (ROM) with inability to perform	SR repair  Anchors placed along the lateral edge of the greater tuberosity within the footprint of	DR repair  Medial row: Anchors placed in the medial aspect of the footprint, just lateral to the articular	Complete bursectomy, subacromial decompression, debridement of tendon and greater tuberosity in all patients As required:	160 (43)  80 repairs arthroscopic with SR  80 repairs arthroscopic with DR	55	100	24	UCLA score  ASES score  Constant-Murley score  SSI	MRI images graded as full thickness tear, partial thickness tear and cuff	Clinical scores improved in both groups  Better UCLA score for DR repair group  Better UCLA,

		activities of daily living, full thickness tears bigger than 10 mm with MRI evidence, older than 18, informed consent	the rotator cuff	surface of the humeral head Lateral row: Anchors placed in the lateral aspect of the footprint, slightly proximal to the greater tuberosity	Osteophyte removal, release of the coracohumeral ligament, detachment of the rotator cuff from the bursal and articular sides					RofM MRI	integrity	ASES scores, RofM for DR repair group for tears > 30 mm  No effect of surgical approach on MRI results
Gartsman et al 2013	Level I Randomized controlled trial	Full thickness SSP tears repairable less than 25 mm in their anterior to posterior dimension	SR repair Two double-loaded suture anchors were placed laterally 8mm distal to greater tuberosity	SB repair Medial row: Two single-loaded suture anchors positioned just lateral to the humeral articular margin  Lateral row: Two anchors	Abrasion of the footprint in all patients  As required:  Tenodesis, tenotomy, subacromial decompression	90 (NR) 43 repairs arthroscopic with SR  47 repairs arthroscopic with SB	NR	92	10	Ultrasound	Rotator cuff could not be visualized because of complete avulsion and retraction under the acromion, when there was a focal defect in the rotator cuff or when the torn cuff was retracted a variable degree from the surgical repair site	Higher tendon healing rate in SB repair group
Ide et al 2015	Level III Retrospective cohort design	Patients undergoing arthroscopic SR or SB repair for a Full thickness	SR repair One to three anchors	SB repair Knotless double-row suture bridge repair	Acromioplasty in all patients As required: Tenodesis, coracoplasty	61 (77) 25 repairs arthroscopic with SR  36 repairs	63	100	SR repair 81 SB repair 34	UCLA score JOA score MRI	Full thickness RCT was diagnosed when a fluid-	Clinical scores improved in both groups  No effect of surgical



		RCT in the subscapularis combined with a tear in the SSP or tears in the SSP and ISP, availability of preoperative and postoperative MRI of the affected shoulder joint, a follow-up of more than 2 years				arthroscopic with SB					equivalent signal appeared or when the tendon could not be visualized in at least 1 section of a fluid-sensitive sequence	approach on clinical scores Abduction strength score better in SB repair group
--	--	---	--	--	--	----------------------	--	--	--	--	---	---

**APPENDIX C – ROTATOR CUFF RABBIT REPAIR MODELS**

Table 9-3 Rotator cuff rabbit repair models

Study	Acute/Chronic? Age/Weight?	Tear model	Repair procedure	Associated procedures/Post-operative immobilization	Time points/ Outcome measures	Results
Chang et al 2009	Acute model 36 skeletally mature New Zealand white rabbits (average weight between 2.5 and 3 kg)	Infraspinatus tendon shoulder joint was approached and the infraspinatus tendon was detached from its insertion on the greater tuberosity by performing a sharp dissection.	Two tunnels (1-mm in diameter) were created from the footprint to the proximal humeral metaphysis. A section of periosteum (2 9 5 mm) was obtained from anterior cortex of proximal tibia. The sutured tendon end was pulled and attached to the footprint by the suture through the tunnel. The harvested periosteum was fixed between tendon end and footprint.	The limbs were not immobilized postoperatively and the rabbits were Allowed to exercise as desired in their respective cages.	Radiography and Histological examination at 4, 8, and 12 weeks	Histological analysis of the tendon–bone interface revealed that the periosteum formed a fibrous layer over the interface between t-b.  12 weeks, a statistically significant increase in failure load was noted in the attachment strength of the limb treated with the

						periosteum.
Fabis Et al 2016	Chronic model Twelve adult male rabbits of mixed breed (weight, 3.8-4.6 kg)	The deltoid muscle was split and retracted, and  3 mm of the SSP tendon was resected and detached from the greater tubercle.	Twelve weeks after the procedure, the edges of SSP tendon were resected, and the tendon was reattached to the abraded groove between the humeral head and the greater tubercle using a modified Mason-Allen suture.  The suture was passed through the groove with the help of the needle and tied over the external cortex.	The shoulder was not immobilized postoperatively.  After 6 weeks, the animals were moved every second week from the standard cage to an open cage 4 times as large to allow more space for activity.	Histologic morphometry  8 weeks (n=2) 9 weeks (n=2)  24 weeks (n=10)	No statistically significant differences were found between controls and operated-on shoulders for type I and II muscle fibers.
Fei Et al 2015	64 NZW rabbits were randomly divided into 2 groups, the SB group and DR group.  Aged  12 to 13 months, with a mean body-weight of 2.8 kg  (Range: 2.5 to 3 kg)	The SSP tendon was identified and sharply divided over a 10 mm width, near its insertion at the greater tuberosity. The surface of the greater tuberosity was decorticated using a scalpel to promote healing.	<u>DR:</u>  The medial suture was sutured through the greater tuberosity_cancellous bone and the supraspinatus tendon at the medial part of the footprint. The second and third sutures were placed equidistant from the lateral part of the footprint in the coronal plane of the humerus head.  These sutures were then tied down using a simple suture Configuration  <u>Suture bridge:</u> Two sutures each were placed through the center of the anterior 1/3 zone and posterior 1/3 zone of the tendon and then through the greater tuberosity of the humeral head in the coronal direction. The other two sutures were oblique and crossed each other.	No restrictions were placed on animal movement.	Histology 2nd, 4th, or 8th week  Biomechanical comparison 8th week.	The load to failure of the SB group significantly higher than in the DR group. Histological evaluation showed that the collagen fibers of the SB group were more compact than those of the DR group at all times tested. At the 4th and 8th weeks, the collagen fibers and cartilage cells in the SB group were arranged in a column modality, but those in the DR group were distributed horizontally.
Friel Et al 2015	44 skeletally mature, male NZW rabbits  4 months old with a mean body mass of 4.1_0.1 kg	The left supraspinatus tendon was transected approximately 1mm medial to its insertion and repaired through two transosseous tunnels within the lateral aspect of the proximal humerus.	In accordance with the specific treatment group, using a syringe, 1ml of highly purified capsaicin aqueous solution was instilled into the joint, and the rotator cuff was subjected to gentle passive motion to facilitate distribution of the aqueous solution into both the rotator cuff tendon-bone insertion site, transosseous tunnels, as well as into the joint space. In the	Rabbits were housed in individual cages with no limitations on their motion.	Biomechanical and histological analysis  18-week	Biomechanical testing revealed no difference. Histologic features of both cartilage and repaired tendons showed minimal differences across groups.

	(Range, 3.6–4.4 kg)		right (sham treated) shoulder, the surgical approach to the rotator cuff was identical to that of the left shoulder.			
Funakoshi Et al 2006	Twenty-one mature Japanese white rabbits, weighing 3 kg	Both infraspinatus tendons were removed to create a defect of 10 mm in length and 10 mm in width. A trough was created in the cortical bone over the insertion of the infraspinatus tendon until cancellous bone was exposed.	In the right shoulder, the defect was covered with a 10X10–mm patch of nonwoven chitin fabric.  The distal end of the fabric was fixed into the bony trough, and the proximal stump of the fabric was sutured to the infraspinatus tendon via the same technique.  The defect of the contralateral (left) shoulder was left free as a control.	The animals were not immobilized and were allowed to move freely in their cages.	Histological and immunohistochemical at 2, 4, 8, and 12 weeks and biomechanically at 12 weeks.	The matrix increased cell numbers and improved collagen fiber alignment. The regenerated tissues were composed of type III collagen. The structural properties of the grafted shoulder were significantly greater than those of the control.
Gilotra Et al 2015	Chronic model  14 skeletally mature NZW rabbits average weight of 7 to 9 lbs.	The SSP tendon was detached from its insertion with a scalpel and then sutured using a 5-0 Prolene suture to a Penrose drain to prevent healing.	The second procedure was performed 12 weeks after. Penrose drain removed. A bony trough approximately 2 X2X5 mm was made at the medial aspect of the greater tuberosity. Three 1-mm drill holes were created from the lateral aspect of the greater tuberosity. The SSP tendon was repaired to its original insertion site with two horizontal mattress sutures with 2-0 nonabsorbable-braided sutures. The suture was then passed through the drill holes; Botox was injected into the SSP muscle 2 cm from the myotendinous junction.	Rabbit shoulders were not immobilized postoperatively.	Biomechanics, histology, and MRI  6 weeks	Botox-treated repairs were significantly weaker than control repairs. 80% of Botox-treated repairs and 40% of control repairs healed with some partial defect. Fatty infiltration of the SSP was present in all shoulders but was increased in the setting of Botox.
Inui Et al 2012	42 skeletally mature female Japanese white rabbits.  Mean age was 16.3 weeks (range, 15 to 18 weeks), and their mean weight was 3.1 kg  (Range, 2.7 to	A 3-cm incision was made in the right shoulder and the infraspinatus tendon was exposed. Rotator cuff defects were created by resecting the infraspinatus tendon (5-mm width and  5-mm length) from the greater tuberosity	Scaffolds were implanted into this defect. The proximal edge of the scaffold was sutured to the mid-substance of the tendon by No. 4-0 nylon mattress suture. Decortication was performed at the greater tuberosity and the distal edge of the scaffold was fixed to the bone by No. 4-0 nylon transosseous mattress suture.  In the contralateral shoulder, the ISP tendon was resected. Decortication was performed at the footprint of the humeral head, and the tendon was reattached to the humeral head without creating a defect by No. 4-0 nylon	The rabbits were allowed free cage movement.	Histologic analyses (4, 8, and 16 weeks)  Mechanical evaluations  (0, 4, 8, and 16 weeks)	At 8 weeks, the PLG scaffold had dissolved and bone formation was observed at the scaffold-bone interface. At 16 weeks, the scaffold-bone interface matured and expression of type II collagen was observed.  No difference in ultimate failure load and stiffness at 8 weeks.

	3.6 kg).		transosseous mattress suture as a control.			
Itoigawa Et al 2015	29 adult male Japanese white rabbits weighing 3.0 to 3.5 kg.	Both omovertebral and deltoid muscles were retracted to expose the ISP tendon. The ISP tendon was detached from the greater tuberosity. The medial tendinous stump retracted after creation of the defect.	With a dental burr, a trough, 10 mm long X2 mm wideX2mm deep,was prepared to mount the OCP/Gel composite on the greater tuberosity. Two small drill holes were made from the lateral aspect of the humerus into the bony trough. Either theOCP/Gel composite (OCPpgroup) or Gel alone was mounted onto the trough of the greater tuberosity. Then, the stump of the ISP tendon was inserted into the bony trough. Each suture end was passed through a drill hole and tied to the lateral aspect of the cortex.	The animals were not immobilized postoperatively.	All shoulders were harvested at 2 (n = 6), 4 (n = 6), and 8 (n = 7 or 8) weeks postoperatively for Histologic Macroscopic Immunohistochemistry observations	On immunohistochemical evaluation, both the bone and the fibers in the OCP group demonstrated that type I collagen was picked up, whereas the newly formed tendon fibers and Sharpey fibers revealed type III collagen.
Kang Et al 2013	12 adult male NZW rabbits, with an average age of 15 weeks and an average weight of 4.1kg.	The rabbits were randomly divided into 2 groups: group A, the nonpore bioabsorbable anchor group and control group, and group pA, the micropore bioabsorbable anchor group and experimental group.  A 5-cm incision was made parallel to the scapular spine and the SSP tendon. The release of the SSP tendon was performed with a sharp blade at the base of the tendon insertion area.	An anchor was inserted into the junction area of the articular cartilage, and the greater tuberosity of the humeral head and detached cuff were repaired using the single-row method	Antibiotics were used for 3 days after surgery, and the dressing of the surgical site was performed at 3-day intervals.	CT 4 and 8 weeks (BVF),  Biomechanical strength4 weeks	The mean BVF was higher in-group pA than in-group A.  The micropore anchor had higher pullout strength than the nonpore anchor. Biomechanical no Significant difference
Kim Et al 2016	Acute Model  36 mature NZW male rabbits (average age, 24 weeks old; weight, 3.5-4.0 kg)	The SSP tendon, posterior to the bicipital groove and anterior to the scapular spine, was identified. Insertion of the SSP at the greater tuberosity was sharply released using a scalpel. Decortication of the greater tuberosity was performed using a small burr.	The repair technique of PTR or SBCR was randomly chosen. Two bone tunnels were created parallel to the tendon for PTR, and crisscross transosseous tunnels were added for SBCR. Two transosseous simple stitches were made with two 3-0-nylon sutures for PTR, and 2 crisscross sutures were added for SBCR. The other repair type was then performed on the contralateral shoulder.	The limbs were not immobilized postoperatively.	Biomechanical evaluation  Histologic evaluation  1, 2, and 5 weeks postoperatively	Failure loads at 1 week and 5 weeks were not statistically different between groups, respectively, but were significantly lower in the SBCR group than in the PTR group  Markedly greater fibrinoid deposition was observed in the SBCR group than in the PTR group at 2 weeks.

Koike Et al 2005	89 mature NZW rabbits (male, average weight 3.2 kg)	The SSP tendon was transected 3 mm proximal to its insertion into the greater tuberosity at the level of the tendon proper.	Attached SSP: A 7 mm long, 2 mm wide and 2 mm deep trough was prepared in the cancellous bone of the greater tuberosity.  Three small holes were made from the lateral aspect of the humerus into the bony trough. Two sutures were placed in the SSP tendon, each being passed through one hole, then going through the tendon, exiting through another hole and tied to the lateral aspect of the humeral cortex. Not attached SSP: To prevent spontaneous adhesion to surrounding tissues [7], the SSP tendon was not attached but rather wrapped with a polyvinylidene fluoride membrane in 14 animals.	After surgery, the animals were not immobilized but kept in cages	Histology 2, 6, 8, 12 or 24 weeks.	In the attached group, chondrocytes appeared at 2 weeks and their number reached control levels by 6 weeks  The percentage of chondrocytes aligned in rows increased at 2 weeks to reach near normal values at 24 weeks. Area of metachromasia increased from at 24 weeks.  Neither chondrocytes nor metachromasia were observed in the non-attached tendons.
Koike Et al 2006	Acute versus chronic models  35 animals	The SSP tendon was transected at the tendon proper and the fibrocartilaginous enthesis resected. In 35 animals, the SSP tendon was inserted	The SSP tendon was wrapped with a polyvinylidene fluoride membrane after transection. The polyvinylidene fluoride membrane has pores of 5 mm in size that allowed some nutrition to diffuse to the end of the tendon but inhibited adhesion of the tendon to the surrounding soft tissue. The SSP tendon was inserted immediately, after 6 or 12 weeks into the bony trough of the greater tuberosity.	N/A	Histology 2, 8, or 12 weeks	Formation of a fibrocartilaginous enthesis depended on the elapsed time after repair and not on the duration between detachment and repair.
Lee Et al 2016	Chronic model  42 adult (5-month-old) male NZW rabbits (3.0 kg)	The SSP tendon was cut off from the right proximal humerus bone. The detached end of the tendon was placed in a silicone tube and fixed by suturing. The silicone tube-inserted tendon was relocated and sutured with a polygluconate DexonVR 5-0 suture from the outside to the inside.	Dermal patch implantation, the SSP repair by SR repair technique. After 4 weeks, the silicone tube was removed and two holes were made on the proximal humerus bone for patch insertion. The rabbits were assigned to groups: Normal; no patch, the cut SSP tendon was inserted into the hole without patch and fixed by suturing; dermal patch insertion, a dermal patch was inserted and fixed by suturing between tendon and bone; rhBMP-2-coated dermal-patch insertion, a dermal patch coated with rhBMP-2 was inserted and fixed by suturing.	Postoperatively, the animals were allowed free movement without use of any type of immobilization.	Bone mineral density, biomechanical strength, histological and histomorphometric analyses  4 and 8 weeks	Insertion of an rhBMP-2-coated acellular dermal patch not only significantly ameliorated new bone formation, it also improved biomechanical properties such as ultimate tensile strength.

Matsumoto Et al 2002	Chronic model 28 mature NZW rabbits (average body weight 3.3 kg, age between 24 and 27 months)	The SSP tendon was transected close to its insertion and any fibrocartilaginous tissue still attached to the greater tuberosity was removed. The proximal stump of the supraspinatus tendon was wrapped with a polyvinylidene fluoride membrane to prevent Spontaneous reattachment.	After 12 weeks the supraspinatus tendon was reattached to the greater tuberosity.  The polyvinylidene fluoride membrane was removed and a bony trough (2 r 2 x 5 mm3) made between articular cartilage of the humeral head and medial wall of the tuberosity. Three drill holes were then made with a 1 mm diameter drill bit from the lateral aspect of the greater tuberosity into the bony trough. Two horizontal mattress sutures with non-resorbable, monofilament 3-0 prolene were placed, each suture passing through one drill hole then through the tendon and exiting through the second drill hole. The sutures were tied over the lateral aspect of the cortex.	The shoulders were not immobilized postoperatively.	Volume of the supraspinatus and extramuscular fat Biochemical quantification of intramuscular fat Overall fat content Histomorphometric quantification of intramuscular fat 24 weeks	Accumulation of fat was increased in both groups when compared to controls. The muscle atrophy was significant. Neither atrophy nor fat accumulation was reversed by surgical reattachment of the supraspinatus tendon. On the contrary, the fat accumulation was higher in the reattached group
Oh Et al 2014	Chronic model 40 mature NZW male rabbits (average age, 24 weeks; weight, 3.5-4.0 kg) into 5 groups  ADSC repair group, saline repair group, ADSC-only group, saline-only group, and control group.	The chronic tear model was created in both rabbit shoulders by completely severing the SSC tendon and the torn tendon was wrapped with a 10-mm-long silicone Penrose drain with an 8-mm outer diameter.	After 6 weeks, removed the Penrose drain wrapped around the SSC tendon and reattached it to the lesser tuberosity by using 2 singleloaded 1.9-mm Mini Quick Anchor Plus. This was performed in the ADSC repair and saline repair groups. Both sutures were tied in a mattress fashion over the lateral aspect of the SSC tendon. In the ADSC repair and ADSC-only groups, injected ADSCs into SSC muscle. In the saline repair group, injected the same volume of Saline.	The rabbits were permitted usual cage activity without immobilization.	Electromyographic, Biomechanical, and Histologic evaluation  12 weeks	On electromyographic evaluation, the ADSC repair group exhibited a larger compound muscle action potential area than the saline repair group  Biomechanically, no significant difference.
Quigley et al 2013	Chronic model 21 NZW Rabbits weighing 3-4 kg	The tendon of the left shoulder was used as a sham control by exposing it and observing it to be free of any tendon pathology. The SSC tendon of the right shoulder was resected at its insertion, followed by wrapping in	Six weeks after tendon resection SR: two holes were punched and tapped in the middle of the footprint, one dorsally and the other ventrally. Two 1.3 mm Micro Quickanchor suture anchors were sunk into the holes orthogonally to the footprint surface. For DR: The first row of anchors was placed at the medial part of the footprint, one dorsally and one ventrally,	Rabbits were allowed ad-lib activity immediately after surgery	Cyclic loading and load to failure, biomechanical testing  12 weeks.	The TOE repair showed greater biomechanical characteristics than DR, which in turn were greater than SR.

		sterile penrose drain.	orthogonally to the footprint surface. A horizontal mattress suture configuration was used to tie these sutures down. The second row was placed at the lateral part of the footprint. For TOE repair the medial row of sutures was placed in the exact same manner as with the DR repair, except that after tying the horizontal mattress sutures the limbs were not cut. Two lateral suture anchors were then placed 5 mm to 1 cm distal to the lateral edge of the footprint in line with the anchors from the medial row. One suture limb from each of the medial row anchors was then tied to a suture limb from the lateral row.			
Sano et al 202	21 mature Japanese white rabbits.  Their mean age was 6.1 months (SD, 1.2 months), and their mean body weight was 3.3 kg	5-cm-long skin incision was made at the lateral aspect of the thigh to harvest a 2x2-cm strip of fascia. A tendinous defect was made close to the SSP insertion. The medial tendinous stump retracted after creation of the defect.	With a dental burr, a 10-mm-longX2-mm-wide trough was prepared in the cancellous bone of the greater tuberosity. Two small drill holes were made from the lateral aspect of the humerus into the bony trough. The fascia was sutured to the lateral stump of the SSP tendon. The other end of the fascia was inserted into the bony trough. Each suture end was passed through a drill hole and tied to the lateral aspect of the cortex.	The animals were not immobilized postoperatively.	<i>Histological and immunohistochemical evaluation</i>  1, 2, 3, 4, 6, and 8 weeks.	<i>The distribution of collagen types II and III represented a pattern similar to that of a normal SSP tendon insertion. In the grafted fascia, the cellular density showed a marked increase over time.</i>
Yokoya Et al 2008	30 adolescent Japanese white rabbits, weighing 3.0 to 3.4 kg.	A full-thickness defect of the rotator cuff was created by completely resecting a segment 10 mm in length and 5 mm in width at the insertion of the infraspinatus into bone.	A trough was created in the cortical bone over the insertion of the infraspinatus tendon, exposing the cancellous bone. In the left shoulders, the defects were covered using a PGA sheet. The distal end of the scaffold was fixed into the bony trough. The proximal end of the scaffold was sutured to the ISP tendon. In the right shoulders, the defects were covered with PLC sheet.	After surgery, the animals were not immobilized and were allowed to move freely in their cages.	Histology 4, 8, and 16 weeks, and mechanical evaluations 4 and 16 weeks	In mechanical examinations, the PGA group had higher values in the maximum failure load, tensile strength, and Young's modulus for the 4-week and 16-week periods.
Trudel Et al 2010a	40adult female NZW rabbits (3.1–3.3 kg)	The tendon was transected close to its insertion, and any tendinous/fibrocartilaginous tissue still attached to the greater tuberosity was removed.	A 2X2X5mm bony trough was made using a burr. Three 1-mm holes were drilled from the lateral aspect of the greater tuberosity. The first thread was passed first through the most proximal drill hole, then through the tendon in a modified MA fashion, and finally through the middle drill hole. The second thread was	The shoulders were not immobilized postoperatively.	CT and Biomechanical Testing 1, 2, and 6 weeks	Suture pullout was the most common mode of failure, whereas at 6 weeks, mid-substance tears predominated. Hypoattenuation on CT was associated with increased strength of the tendon–bone

			passed first through the middle drill hole, then through the tendon in a modified MA fashion, and then through the distal drill hole.			construct.
Trudel Et al 2012a	Chronic model 54 adult male NZW rabbits weighing 3.1 kg	The SSP tendon was transected close to its insertion. Sutured a polyvinylidene membrane over the proximal stump of the SSP to prevent spontaneous reattachment.	The tendons were repaired 1, 2, or 3 months after transaction we produced a bony trough (2X2X5 mm) at the medial wall of the greater tuberosity. Three 1-mm holes were drilled from the lateral aspect of the greater tuberosity into the bony trough. The first thread was passed through the most proximal drill hole and then through the tendon in a modified MA fashion, exiting through the middle drill hole; the second thread was passed through the middle drill hole and the tendon in a modified MA fashion, exiting through the distal drill hole.	We did not immobilize the shoulders postoperatively; the rabbits were housed in large cages with free access to water and food	CT and Biomechanical testing 3 months	The mean peak loads to failure 3 months after repair delayed by 1 month and delayed by 2 months were significantly greater than control values, there was no difference after a delay of 3 months.
Trudel Et al 2012b	Chronic model 36 NZW rabbits	The SSP was transected close to its insertion. The proximal stump of the tendon was wrapped with a polyvinylidene fluoride membrane to prevent spontaneous postoperative reattachment.	Repaired at 4, 8, or 12 weeks. The polyvinylidene membrane removed. A bony trough (2 mmX2 mmX5 mm) at the medial wall of the greater tuberosity was created. Three 1-mm holes were drilled from the lateral aspect of the greater tuberosity into the bony trough. The first thread was passed first through the most proximal drill hole, then through the tendon in a modified MA fashion, and finally through the middle drill hole. The second thread was passed first through the middle drill hole, then through the tendon in a modified MA fashion, and then through the distal drill hole.	The rabbits were housed in large cages and bore weight; they had free access to water and food.	SSP muscle, e-fat weights and volumes, muscle tissue and i-fat areas on histology, e-fat and attenuation values on CT between the experimental and control shoulders.12 weeks	SSP muscle tissue atrophy, e-fat and i-fat accumulation was present after tendon repair delayed by 4, 8, or 12 weeks (all $p < 0.05$ ). SSP muscles showed tissue atrophy, e-fat and i-fat accumulation after successful SSP tendon repairs delayed by 4, 8, or 12 weeks.
Uththoff Et al 2000	14 mature NZW rabbits: body- weight of 3.9 kg (3.6 to 4.2).	SSP tendon was then transected close to its insertion into the greater tuberosity.	Using a dental burr, a trough 7 mm long, 2 mm wide and 2 mm deep was made in the cancellous bone of the greater tuberosity. Three small drill holes were made from the lateral aspect of the humerus into the bony trough. Two horizontal mattress sutures with non-absorbable 3-0 prolene were placed, each suture passing through a drill hole then through	The animals were not immobilised after the operation	Histology 2 weeks	Cellularity of the underlying bone and the thickness of the subacromial bursa were significantly increased.  The cellularity of the stump of the tendon, however, was significantly decreased in the



			the tendon and exiting through the second hole.			operated shoulders.
Uthhoff Et al 2002	21 adult NZW rabbits (age, 24-27 months; mean body weight, 4.1 kg, range, 3.7-4.3 kg)	SSP tendon was transected medial to its insertion on the greater tuberosity at the level of the tendon proper.	A 7-mm-long, 2-mm-wide, 2-mm-deep trough was prepared in the cancellous bone of the greater tuberosity. Three drill holes on the lateral aspect of the humerus into the bony trough were used to tie the SSP tendon in the trough. Each suture passed through a drill hole, then through the tendon, and exited through the second hole.	Neither postoperative immobilization nor any restrictions in activity were used.	Tensile strength, Microscopically, 8 and 12 weeks	The mean peak loads of the operated tendons were significantly over than their controls. Histologically, at 8 weeks, the fibrocartilaginous entheses had partially reformed; Twelve weeks after reimplantation, 4 of 7 entheses had a normal histologic appearance.
Uthhoff Et al 2003a	Chronic model 17 mature NZW rabbits (average weight 3.0 kg)	The SSP tendon was transected close to its insertion. The proximal stump of the SSP tendon was wrapped with a polyvinylidene fluoride membrane to prevent spontaneous reattachment.	Reattachment after 6 weeks The polyvinylidene fluoride membrane was removed and a bony trough (2 x 2 x 5 mm) made between articular cartilage of the humeral head and medial wall of the tuberosity. Three drill holes were then made with a 1 mm in diameter drill bit from the lateral aspect of the greater tuberosity into the bony trough. Two horizontal mattress sutures were placed, each suture passing through one drill hole then twice through the tendon and exiting through the second drill hole. The sutures were tied over the lateral aspect of the cortex.	The shoulders were not immobilized postoperatively.	Muscle, extra- and intramuscular Fat in volume and cross-sectional area 6 and 12 weeks	Extra- and intramuscular fat in the reattachment group was greater than in both, the detachment group and control group.
Uthhoff Et al 2014a	30 adult female NZW rabbits (3.4 kg to 4.3 kg)	The SSP tendon was transected close to its insertion.	A 2 x 2 x 5 mm bony trough was made between the rim of the wall of the tuberosity and the articular cartilage using a burr. Three 1 mm holes were drilled from the lateral aspect of the greater tuberosity into the bony trough. The first thread was passed first through the most proximal drill hole, then through the tendon in a modified MA fashion and finally exited through the middle drill hole. The second thread was passed first through the middle drill hole, then passed through the tendon in a similar fashion to the first suture and brought through the distal drill hole. Both sutures were tied over the lateral aspect of the cortex.	The shoulder was not immobilised post-operatively.	Weight and volume of SSP muscles and quantified the cross-sectional area of intramuscular fat (i-fat) histologically 1, two and six weeks	There was significant loss of muscle weight and volume after one week and two weeks in the experimental group. I-fat continued to accumulate up to six weeks at all sites of the SSP muscle. More fat accumulated closer to the musculotendinous junction than at the mid-part after two and six weeks.

Uthoff Et al 2014b	30 female NZW rabbits,	After complete detachment of SSP tendon at the greater tuberosity, the tendon stump was enveloped with a polyvinylidene fluoride membrane to avoid spontaneous reattachment.	SSP tendon was repaired after 4 weeks or 8 weeks of detachment or after 12 weeks. In the second cohort, the polyvinylidene membrane was removed, a trough burred into the greater tuberosity and the tendon inserted into it.	All animals were allowed to roam freely in their cages.	SSP fossa volume, percentage of intramuscular at (i-fat), and muscle tissue volume (muscle belly volume minus i-fat), CT determination of e-fat and i-fat  12 weeks	Muscle belly and muscle tissue volumes did not increase after repair, but early repair prevented further volume losses, a fact not seen after 8 and 12 weeks delay of repair. No reversal of e-fat or of i-fat occurred. CT studies confirmed the fat results.
Trudel Et al 2017	112 adult female NZW rabbits (3.0 kg)	SSP tendon was transected at the humerus insertion Site and the tendon stump was wrapped in a polyvinylidene membrane stitched to the tendon to allow nutrition to diffuse but to prevent adhesion to surrounding tissue. At the first surgery (the channeling group) was performed at the footprint while the remaining were only subjected to tendon detachment (the no-channeling group). Channeling consisted of exposing the SSP insertion footprint, dividing it into four quadrants, and drilling a 1-mmdiameter hole at the center of each quadrant. The four holes were drilled to a depth of 10mm to ensure communication with the medullary canal. In the no-channeling group, the footprint of the SSP was left untouched.	The repair surgery was performed 1 week after tendon detachment and was identical for the no channeling and channeling groups. Used a curette to clear and microfracture the footprint for SSP tendon reattachment. The retracted SSP tendon was mobilized and Millipore was removed. A single 3 anchor was inserted lateral and distal to the footprint, and apposing the SSP tendon to the footprint using an inverted horizontal mattress suture completed the repair.	Nothing	Quantitative T2 mapping 0, 1, 2, 4 or 16 weeks	Tendon repair and postoperative duration both affected significantly the T2 values while channeling had no significant effect. For the time effect, the only pair with a statistical difference was the 0-week and 4-week for the channeling groups.

## APPENDIX D – ROTATOR CUFF SHEEP REPAIR MODELS

Table 9-4 Rotator cuff sheep repair models

Study	Acute/Chronic? Age/Weight?	Tear model	Repair procedure	Associated procedures/Post-operative immobilization	Time points/ Outcome measures	Results
Baums et al 2012	Acute model in 18 skeletally mature ewes (2-3 years; average weight 57 kg)	Unilateral, the infraspinatus tendon was detached sharply from its insertion on the proximal part of the humerus to create a full-thickness standardized tear.	Bioabsorbable suture anchors (Duet Suture Anchors; ConMed Linvatec, Largo, FL) coupled with braided, nonabsorbable polyester suture material (No. 2 Ethibond; Ethicon, Somerville, NJ) were used. In SR repair (n = 9), 1 row of 2 suture anchors, with arthroscopic Mason-Allen stitch technique. In DR repair (n = 9), 2 rows of suture 2 anchors running parallel to each other with arthroscopic Mason-Allen stitches in the lateral aspect of the tendon and mattress stitches medially.	Surface of the tuberosity was roughened with a curette to create a bleeding surface and remove any fibrocartilage. A soft protector, 10 cm in diameter, was affixed to the hoof of the operatively treated limb to try to reduce weight bearing and to simulate relief of the strains on the operated shoulder.  The animals were placed in a small pen for the first 6 weeks to limit their activities.	6 weeks (n = 3 per group), 12 weeks (n = 3 per group), and 26 weeks (n = 3 per group). 1.5T MRI of isolated shoulders and scoring according to Sugaya. Macroscopic evidence of foreign-body reaction to the anchors.  Biomechanical tensile testing.	No difference in MRI integrity. Mean load to failure was significantly higher in the DR compared with SR group at 6 and 12 weeks, but not at 26 weeks. DR group achieved a mean load to failure similar to that of a healthy infraspinatus tendon, whereas SR reached only 70% of the load of a healthy infraspinatus tendon.
Baums et al 2015	Acute model in 24 skeletally mature ewes (2-3 years; average weight 57 kg)	Unilateral, the infraspinatus tendon was identified and sharply removed from its insertion site on the proximal humerus, antero-inferior to the acromial aspect of the deltoid muscle, to mimic an acute tendon tear.	In the SR group, an arthroscopic Mason-Allen stitch configuration with two double-loaded bio-absorbable anchors was applied in a single row. In the DR group, the repair consisted of two rows of suture anchors running parallel to each other. Each row consisted of two 6.0 mm suture anchor systems (Duet_ Suture Anchor, Conmed Livatec, Largo, FL, USA). A combination of laterally applied arthroscopic Mason-Allen stitches was combined with mattress stitches medially. Tendons were fixed using braided, non-absorbable No. 2 polyester sutures (Ethibond, Ethicon, Somerville, NJ,	The surface of the tuberosity was roughened with a curette to generate bleeding and to remove fibrocartilage. Soft protectors 10 cm in diameter were affixed to the hooves of the treated limbs to reduce weight-bearing, as previously described. Animals were housed in small pens for the first 6 weeks to limit excessive movement.	1, 2, 3, 6, 12, and 26 weeks (n=2 per group). Histology. Immunohistochemistry for Col 1, Col 2, Col 3.	Collagen expression differed between SR and DR repair. Col 3 collagen was no longer visible 6 weeks postoperatively in the DR group, but remained detectable until 12 weeks in the SR group. Clusters of chondrocytes were detectable only in the DR group between weeks three and twelve, and the content of proteoglycans was higher in the DR group.

			USA).			Faster healing in DR group.
Coleman et al 2003	Acute and chronic models in 36 skeletally mature ewes (> 3.5 years; average weight 67 kg)	Unilateral, the infraspinatus tendon was detached sharply from its insertion on the proximal part of the humerus. For the chronic groups, the tendons were wrapped in a 5 cm X 3 cm sheet of Preclude (WL Gore and associates, Flagstaff, AZ), a porous membrane composed of Gore-Tex.	Twelve sheep underwent immediate repair of the tendon to bone with use of 2 sheep allograft bone-suture anchors with 2 No 2 Ethibond suture per anchor. The tendons were grasped in a modified Mason-Allen technique. The other sheep underwent delayed repair at 6 weeks (n=8) and at 18 weeks (n=16). For the 6-week delayed group, repair technique was the same as acute group. For the 18-week delayed group, repair was with a PLA patch (Smith and Nephew).	The surface of the tuberosity was roughened with use of a curet to create bleeding surface prior to anchor insertion. No post-operative immobilization for the acute group. Softballs were affixed to the hooves for 5 weeks in the chronic groups.	For acute group: 6 weeks (n=4), 12 weeks (n=4) and 20 weeks (n=4). For chronic 6-week delayed group: 12 weeks (n=4) and 20 weeks (n=4). For chronic 18-week delayed group: 12 weeks (n=8), 20 weeks (n=4), 36 weeks (n=4). In vivo muscle testing. Muscle lipid content. EM. Biomechanics. Histology.	There was retraction of the tendon in the delayed repair groups. Muscle force decreased initially in the delayed repair groups but increased following repair. Muscle lipid content increased initially in the delayed repair groups but decreased following repair. Module of elasticity increased initially in the delayed repair groups and decreased following repair only in the 6-week delayed group. There is probably a point-of-no-return after which tears become irreparable.
Farshad et al 2011	Chronic model in 12 ewes (Mean age 16 months; average weight 45 kg)	Unilateral, the infraspinatus tendon was released through an osteotomy of the greater tuberosity. During the 16 week period of retraction, the bone chip and distal part of the tendon of the musculotendinous unit were shielded against spontaneous healing (scar formation) by encasement within a silicone tube as previously described	Continuous traction of the tendon to the original tendon reinsertion site, and then 12 weeks of rehabilitation	Not described	34 weeks after tendon release MRI Histology	Retracted musculotendinous units have deteriorated tendons, characterized by increased collagen fiber crimp, and ultrastructural collagen fibril atrophy and disorganization. Continuous traction may arrest and partially restore degenerative changes in retracted tendon.
Gerber et al 1999	Acute and chronic models in 47 skeletally mature ewes (Mean age 5 years; average	Unilateral, the infraspinatus tendon was released at its insertion.	For chronic group, the sheep were kept in a hanging device, which kept them immobilized for 4-6 weeks prior to repair. For acute group, the infraspinatus tendon was shortened by 5-10 mm to simulate tendon retraction. Two modified Mason-Allen stiches or three simple stiches with Ethibond No 3 were placed into	The bone of the greater tuberosity was decorticated until cancellous bone was exposed. In early studies, no post-op immobilization. In later studies fixation of a ball	6 weeks, 3 months, 6 months. Histology. Biomechanics.	Transient localized tissue damage induced by the two suturing techniques. Modified Mason-Allen stitch is a more secure way of suturing the tendon. Rate of failure exceedingly high when no

	weight 60 kg)		the tendon end and passed through a bony trough created at the site of the original insertion and tied over the greater tuberosity. In the Mason-Allen group, the sutures were tied over absorbable poly lactide plates.	under the hoof of the sheep.		post-operative immobilization was used. The Mason-Allen technique with poly lactide plates gave superior repair.
Gerber et al 2004	Chronic model in 6 skeletally mature ewes (Mean age 3.6 years; average weight 51 kg)	Unilateral, the insertion of the infraspinatus tendon was released by osteotomy of the greater tuberosity leaving a 2 cm X 1.5 cm fragment of the greater tuberosity attached to the tendon. The end of the tendon was covered with a 5-cm long silicone rubber tube (Silicone Penrose drain tube 12-mm diameter), which was closed with a running suture at distal end.	At 40 weeks after tendon release, repair was carried out with a sensor device interposed between the tendon and the greater tuberosity (to allow measurement of tension in the muscle). Sensors were removed after ~2 weeks, sensor screw reinserted and tendon attached to these screws using Ethibond No 6 sutures.	None	75 weeks. CT Biopsies. Histology. EM.	Tendon release induced muscle atrophy, fatty infiltration, and histological changes in the muscle tissue. Structural changes worsened after the repair and then recovered but only partially. Repair should be performed before significant muscle retraction occurs.
Gerber et al 2009	Chronic model in 6 males and 6 females (Mean age 16 months; average weight 45 kg)	Unilateral, the infraspinatus tendons were released using a greater tuberosity osteotomy. A fragment of the greater tuberosity of 20 x 10 x 10 mm attached to the tendon. The distal part of the musculotendinous unit was encased in a silicone tube (Silicone Penrose drain tube, 12 mm diameter; Fortune Medical Instrument, Taipei, Taiwan) and allowed to retract for 4 months.	A device was mounted on the scapular spine and used to extend the infraspinatus musculotendinous unit transcutaneously by 1 mm per day for 4 weeks. Rotator cuff repair was performed as near as possible to the original insertion area of the greater tuberosity, using a 3.5-mm cortical bone screw and the previously placed 2 Fiberwire #5 sutures (Arthrex Medical, Naples, FL). As in a previous study, <sup>15</sup> the threads were augmented by 2 Fiberwire 2.5 threads (Arthrex, Naples, FL).	None. A ball was attached to the sheep's claw for 6 weeks postoperatively, followed by a full weight bearing rehabilitation protocol for another 12 weeks.	34 weeks (18 weeks after tensioner implantation and 12 weeks after tendon repair). CT. Biopsies. MRI. Histology. EM.	Elongation protocol technically difficult. Tendon release induced muscle atrophy and fatty infiltration. In the sheep where elongation worked, muscle atrophy decreased and fatty infiltration remained stable. There was no improvement in the group where elongation failed.
Gerber et al 2015	Chronic model in 18 ewes (Mean age 25 months; average weight 53 kg)	Unilateral, ISP tendon was released by an osteotomy of the greater tuberosity (20 x 10 x 10 mm). Piece wrapped in a silicone tube (Silicone Penrose drain tube, 12-mm diameter; Fortune Medical Instruments) and allowed to retract for 16 weeks.	The tendon–bone chip complex was released from adhesions to the surrounding structures, the silicone tube was removed. Reattaching the bone chip to its original site then performed rotator cuff repair, or as near as possible, with Fiberwire No. 2 sutures and a 3.5-mm self-tapping cortical bone screw.	Weekly injections of 150 mg (3 mL) of nandrolone decanoate into the gluteus maximus muscle for test test group. During the first 3 weeks of the rehabilitation period, animals were prevented from full weightbearing and stress to	6 weeks after cuff repair CT. MRI. Biopsies. Histology.	In a sheep model of rotator cuff tendon tear, further muscle atrophy can be prevented with the application of anabolic steroids starting immediately after tendon repair. In addition, fatty muscle infiltration can largely be

				the repaired tendon by attachment of a ball to the sheep's claws, and they were prevented from lying down by use of a loose suspension belt.		prevented if the steroids are applied immediately after tendon release.
Klinger et al 2008	Acute model in 18 skeletally mature ewes (2-3 years; average weight 57 kg) + 16 matched cadaveric controls	Unilateral, the infraspinatus tendon was sharply detached from its insertion on the proximal part of the humerus.	Sutures were braided, non-absorbable polyester Ethibond (Ethicon, Somerville, NJ, USA) suture size No. 2. In group 1, two transosseous sutures were passed through three bone tunnels and placed in the rotator cuff tendon 5 mm apart from the free margin of the tendon using a modified Mason-Allen technique. In-group 2, two bioabsorbable anchors (Duet Suture Anchor, Conmed Linvatec, Largo, FL, USA), double loaded, were used with the so-called arthroscopic Mason-Allen stitch configuration.	The surface of the tuberosity was roughened with use of a curet to create bleeding of the surface prior to tendon Refixation. 10 cm diameter softball was affixed to the hoof of the operatively treated limb to inhibit weight bearing. The animals were placed in a small pen for the first six weeks to limit activities. After six weeks, the ball was removed and the sheep were turned into a large pen.	6, 12, or 26 weeks (n=3 per treatment per time point). MRI. Biomechanics.	Imaging showed good cuff integrity in both groups and no evidence of foreign body reaction to the anchors. At time 0, there was a higher load-to-failure in the anchor group, but not at longer time points.
Kovacevic et al 2008	Group 1: Acute model in 72 skeletally mature ewes  Group 2: Acute model in 56 skeletally mature ewes	Unilateral, infraspinatus detachment.	Group 1: Repair of the infraspinatus tendon to the greater tuberosity using sutures through bone tunnels. The experimental animals (n = 24) received an osteoinductive bone protein extract (containing BMP-2-7, TGF-b1-3, FGF) at the tendon-bone interface using a type I collagen sponge carrier. The two control groups (n = 24 each) consisted of repairs treated with the collagen sponge carrier alone or no implant. Group 2: Double-row suture reattachment of the infraspinatus tendon to the proximal humerus. RhBMP-12 was tested using various delivery vehicles -hyaluronon paste, hyaluronon sponge, absorbable type I collagen sponge, and type I/III collagen sponge (n=8 per group), type I/III collagen sponge alone (n=10), the tendon repair with no implant (n=14).	None. No post-operative immobilization.	Group 1: 6 and 12 weeks. Group 2: 4 and 8 weeks. MRI. Plain radiographs. Histology.  Mechanical testing.  Ultrasound.	Group 1: A gap consistently formed between the end of the repaired tendon and bone, with reparative scar tissue and new bone spanning the gap. MRI showed the volume of newly formed bone and soft tissue in the tendon-bone gap was greater in the growth-factor-treated animals. The repairs treated with the osteoinductive growth factors had greater failure loads at 6 weeks and 12 weeks. Group 2: Ultrasound evaluation demonstrated a gap (10-18 mm) between the tendon and the bone in all repair groups at both time points, with no differences between groups. RhBMP-12- treated repairs

						had increased load-to-failure and stiffness compared to the sponge carrier alone or untreated repairs. Reestablishment of collagen fiber continuity between the bone and the fibrovascular interface scar tissue, with increased glycosaminoglycan content in the rhBMP-12-treated repairs.
Lewis et al 1999	Acute model in 38 skeletally mature ewes	Unilateral, using sharp dissection the infraspinatus tendon was detached from the greater tuberosity. The tendon was then split longitudinally for 2 cm into 2 strips.	The proximal strip was reattached with suture anchors, and the distal half was reattached using bone tunnel sutures. Bone tunnel method: A bony trough was created in the proximal humerus, three holes were created into the greater tuberosity to pass the sutures, the tendon was sutured into the trough using two Ethibon No 2 sutures in a modified Mason-Allen pattern. Anchor method: Two SDSorb suture anchors were used and sutures placed in the tendon using a horizontal mattress pattern.	None. No post-operative immobilization.	0, 3, 6, 9, 12 weeks (n=6 for day 0 and n=8 for other days).  Biomechanics on proximal and distal attachments done separately.	Most failures were at the tendon-bone interface. No difference in tensile force and stiffness between two repair techniques, except at time 0, where the bone tunnel technique had higher tensile force.
Liem et al 2015	Acute model in 18 ewes (40-50 kg)	Unilateral, the tendon was sharply detached from the greater tuberosity.	SR repair: The modified Mason-Allen sutures were performed with a single row of two Corkscrew suture anchors positioned at the lateral edge of the footprint, each armed with two strands of No. 2 FiberWire (Arthrex Inc., Naples, FL, USA), the first one passed through the tendon in a horizontal mattress pattern, the second one as a simple stitch on top of the horizontal mattress. SB repair: A medial row of two Corkscrew suture anchors at the medial edge of the footprint, armed with No. 2 FiberWire and a lateral row of two PushLock anchors (Arthrex Inc., Naples, FL, USA). The medial row sutures were tied before the suture limbs were affixed with the lateral row of PushLock anchors.	Light decortication of the humeral insertion. The animals were kept in a small pen of approximately 3 m <sup>2</sup> for one week to limit ambulation and protect the repair.	12 weeks. Doppler flowmetry. Macroscopic.	Tendon blood flow decreased after repair. No difference in restoration of blood flow and in failure rates at 12 weeks.
Lovric et al	Acute model in 8 skeletally	Unilateral, the infraspinatus tendon was sharply detached	The infraspinatus tendon was repaired with a transosseous-equivalent suture bridge construct	Cartilage at the footprint of the muscle insertion was	28 days.	Improved histological appearance, increased BMD

2013	mature wethers (18 months)	from its insertion into the greater tuberosity.	using medial row and lateral push-in suture anchors (Arthrex, Inc, Naples, Florida, USA). Low-intensity Pulsed Ultrasound treatment was done on 4 of the sheep.	burred to create a bleeding bone bed. No post-operative immobilization.	MicroCT. Histology. Immunohistochemistry for BMP-2, Smad4, VEGF and RUNX2.	at the tendon-bone interface, increased immuno of VEGF, Smad4 and Runx2 with Ultrasound.
Luan et al 2015	Acute model in 12 skeletally mature ewes.	Unilateral, the insertion of the infraspinatus tendon to the greater tuberosity of the humerus was sharply transected, and any remaining fibrocartilage at the insertion was removed.	Two 5.5 mm suture anchors were deployed into the dense bone of the medial footprint of the proximal humerus (one anchor cranially and one anchor caudally). The suture anchors were placed approximately 1 cm apart and 2 mm to 4 mm deep to the cortex. Sutures were passed from inferior to superior through the infraspinatus tendon and tied in simple mattress fashion on the superior surface of the tendon.	A hall air drill and burr were used to create a bed of bleeding bone at the footprint of the infraspinatus tendon. After suturing the tendon back to the footprint, the surgical site was lavaged with sterile saline. No post-operative immobilization.	6 months. Histology. Western blot. qRT-PCR.	Increased adipocytes, muscle fatty infiltration, and collagen deposition in rotator cuff muscles compared to contralateral. Also, increased expression of genes related to muscle atrophy, fatty infiltration and fibrosis.
Meyer et al 2004	Chronic model in 8 sheep (Mean age 3.75 years; average weight 48 kg)	Unilateral, the infraspinatus tendon was released by osteotomy of the greater tuberosity. The tendon end was encased using a closed silicone rubber tube of 5 cm length to prevent spontaneous healing.	Forty weeks after tendon release, the silicone sheath was removed and the retracted tendon was reconnected to the humeral head using three USP#3 sutures bridging the gap between tendon end and bone.	None. No post-operative immobilization.	35 weeks. Biopsies. MRI. Macroscopic. Histology. EM.	At necropsy, muscles had retracted, pennation angle had increased and fiber length had decreased compared to contralateral. Fat and fibrous tissue in the muscle was also increased.
Meyer et al 2006	Chronic model in 6 sheep (Mean age 3.75 years; average weight 48 kg)	Unilateral, the infraspinatus tendon was released by osteotomy of the greater tuberosity, leaving a bone chip approximately 1 cm long and 0.5 cm thick on the tendon. The tendon end was encased using a closed silicone rubber tube of 5 cm length to prevent spontaneous healing.	40 weeks after release, the retracted tendon was surgically repaired using two sutures under moderate tension.	None. No post-operative immobilization.	75 weeks. CT was performed under general anaesthesia at intervals of 0, 16, 40, 46, 52 and 75 weeks. MRI. Histology.	Tendon retracted after release and stayed partly retracted after repair. Muscle retracted less.



Peterson et al 2015	Acute model in 80 skeletally mature ewes (2-4 years; 50-80 kg)	Unilateral, the infraspinatus tendon was released completely from the humerus with a scalpel, beginning with the most distal portion of the tendon attachment.	The tendon was repaired to the footprint using 2 double-loaded 5- mm Poly Insite anchors (Tornier) placed in the humerus about 5 mm beyond the distal edge of the tendon footprint. The 4 sutures from these 2 anchors were used to secure the tendon to the humerus using 4 modified Mason-Allen stitches 1 cm from the distal edge of the infraspinatus tendon. The repairs in the treatment groups were reinforced with scaffolds containing 0, 1, 8, or 32 mg of F2A (a synthetic mimetic of bFGF). Two No. 2 ForceFiber sutures (Tornier) were embedded into the tendon 2 cm from the distal edge of the tendon using Mason-Allen stitches before reattachment of the tendon to the footprint in the same manner as the controls. These sutures were used to attach the proximal edge of the scaffold to the tendon. Two more No. 2 ForceFiber sutures were placed at the distal edge of the scaffold in a mattress stitch pattern and then tensioned to the humerus using two 3.5-mm Piton anchors (Tornier) so that the scaffold fit tightly against the infraspinatus with the limb in neutral abduction.	None. No post-operative immobilization.	8 and 26 weeks. Macroscopic. Histology (they refer to the Movin score, a validated scoring system for tendinopathy). MRI. Immunohistochemistry for F2A. Biomechanics.	Scaffold-repaired tendons were thicker than surgically repaired controls (at 8 weeks. There was more new bone formed at the tendon footprint in sheep treated with F2A.  The extent of delamination decreased to with increasing doses of F2A. More of the repair tissue at the footprint was tendon-like in the peptide-treated sheep.
Schlegel et al 2006	Acute model in 26 sheep	Unilateral, the tendon was sharply detached from the greater tuberosity of the humerus, and 5 mm of the distal tendon was resected before reattachment to simulate a rotator cuff repair being performed under tension.	A bone trough, 2.0 cm in length and 0.5 cm in depth, was prepared in the proximal humerus using an osteotome and burr. Four separate tunnels were created in the greater tuberosity using the Linvatec shoulder set (Linvatec Corp, Largo, Fla). The infraspinatus tendon was sutured into the trough using three No. 2 nonabsorbable sutures (Ethibond, Ethicon Inc, Somerville, NJ) in a modified Mason-Allen stitch. Each limb of the suture was passed through a separate osseous tunnel, with the 2 center tunnels being used twice. The sutures were tied over a cortical bridge. In the treatment group, a 10 to 20-mm patch of SIS was placed on the superficial aspect of the repaired tissue. The initial fixation of the patch was achieved by using a free No. 5 Mayo needle to pass the free ends of the 2 central limbs of the nonabsorbable suture used in the	Once the repair was completed, the surgical site was lavaged with sterile saline solution. The animals were placed in a small pen for the first 6 weeks to limit activities.	12 weeks. Histology. Biomechanics.	No difference in load-to-failure between groups. Increased stiffness in the augmented group. Insertion of the tendon to bone was through a fibrocartilaginous zone.

			transosseous repair of the infraspinatus tendon, eventually tying these ends over the patch. The implant was sutured to the surrounding tissues using simple 2-0 polydioxanone sutures.			
Rodeo et al 2007	Acute model in 72 skeletally mature ewes	Unilateral, the tendon was sharply detached from the greater tuberosity.	Four 2.0-mm drillholes were placed into the greater tuberosity for repair of the rotator cuff tendon to bone. These holes exited laterally over the proximal humeral cortex. Two number-5 Ethibond sutures (Ethicon, Somerville, New Jersey) were passed in a Mason-Allen configuration through the tendon, and each suture was brought through one of the four holes. The sutures were then tied over the lateral humeral cortex over a stainless-steel cortical bone augmentation plate (Synthes, Paoli, Pennsylvania). The experimental group consisted of twenty-four animals that received 1.0 mg of an osteoinductive bone protein extract (Growth Factor Mixture [GFM; Sulzer Biologics, Wheat Ridge, Colorado] described in detail below) on a Type-I collagen sponge carrier applied to the tendon-bone interface. Twenty-four animals received only the collagen sponge carrier with no growth factors and twenty-four animals underwent the tendon repair with no implant.	The greater tuberosity was then prepared for repair of the tendon by removing any remaining soft tissue and fibrocartilage. The greater tuberosity was lightly decorticated with use of a high-speed burr until punctate bleeding from the bone was noted. Decortication was done to a depth of only 1 mm; cortical bone still remained.	6 and 12 weeks Radiographs. MRI. Histology. Biomechanical testing.	A gap consistently formed between the end of the repaired tendon and bone in this model, with reparative scar tissue and new bone spanning the gap. This model tests the effects of growth factors on scar tissue formation in a gap between tendon and bone. The administration of osteoinductive growth factors resulted in greater formation of new bone, fibrocartilage, and soft tissue, with a concomitant increase in tendon attachment strength but less stiffness than repairs treated with the collagen sponge carrier alone.
Uggen et al 2010	Chronic model in 18 sheep	Unilateral, the infraspinatus tendon was detached sharply from its insertion on the proximal humerus. The tendon was wrapped in a 5 to 3-cm sheet of Preclude (Gore Medical, Flagstaff, AZ).	Two weeks after release, the tendon was repaired. For the single-row repair, 1 double-loaded, 5.5-mm metal corkscrew anchor (Arthrex) was placed proximally in the tendon footprint and 1 single-loaded 3.5-mm metal corkscrew anchor (Arthrex) was placed distally in the footprint. The tendon was unwrapped and mobilized by blunt dissection. The tendon was then repaired with uncoated No. 2 FiberWire (n = 9) or No. 2 FiberWire coated with rhPDGF-BB (n = 9). Repairs were performed with a "rip-stop" horizontal mattress stitch and medially placed simple stitch from the double-loaded anchor and a horizontal mattress stitch from the single-loaded anchor.	The surface of the tuberosity was roughened with a burr to create a bleeding bone surface before anchor insertion.	6 weeks. Histology (they used the Soslowsky scoring system). Biomechanics.	Improved tendon-to-bone healing in the rhPDGF-BB-augmented repairs. There was no significant difference in the ultimate load to failure between both groups.

Wieser et al 2015	Chronic model in 20 skeletally mature ewes (Average age 23 months; average weight 55 kg)	Unilateral, the right infraspinatus (ISP) tendon was released using an osteotomy of the greater tuberosity, immediately after initial biopsy of the ISP tendon. The biopsy site was marked with non-resorbable USP no. 4-0 monofilament suture, and the tendon-bone chip complex was wrapped in a silicone tube to prevent scarring and was allowed to retract for a total of 4 months.	A second biopsy of the tendon was performed next to the first biopsy site, which was again marked with a second suture. A device, allowing continuous lengthening (1 mm/day) of the musculotendinous unit by external manipulation of the lever arm, was then implanted on the scapular spine of all sheep. The tendon-bone chip complex was grasped with 2 USP No. 2 FiberWire sutures (Arthrex, Naples, Florida), which were connected to the traction device. After the relengthening period of 6 weeks (+ or - anabolic steroids/IGF), during which the sheep could ambulate freely, the traction device was removed and the rotator cuff was repaired by re-attaching the bone chip to its original site or as near to this site as possible with attachment of the remaining sutures to a 3.5-mm cortical bone screw with a washer.	None. For the first 6 weeks after this repair, a suspension belt and a ball, attached to the sheep's hooves, were used to prevent the sheep from stressing the repaired tendon. Subsequently, a full weight-bearing period of 8 weeks was allowed before killing.	14 weeks. Histology (they developed a new degeneration score for tendinous tissues (DSTT), based on established knowledge on histological changes associated with tendon degeneration).	Histological score improved after re-lengthening. Adding steroids or IGF had no further benefit on the histological score.
Zumstean et al 2012	Chronic model in 12 sheep (Mean age 16 months; average weight 45 kg)	Unilateral, the infraspinatus was released using an osteotomy of the greater tuberosity. Two Fibre wire No. 5 sutures (Arthrex, Naples, FL) were passed in a figure-of-eight configuration through tendon and bone. The sutures and the greater tuberosity were wrapped into a 5 cm long silicone rubber tube (Silicone Penrose drain tube, 12 mm, Fortune medical instrument corp. Taipei, Taiwan). The tube was closed with non-resorbable suture at its end to prevent spontaneous healing.	After a retraction and degeneration time of 40 weeks, the tensioner was implanted using the same approach. The tensioner pulled the tendon axially by a distance of 1 mm/day towards its original insertion. Subsequent to the elongation protocol, the tensioner was removed and the greater tuberosity was reattached as near as possible to its original insertion using 3.5 mm cortical bone screws and the previously prepared sutures. The fixation was augmented by two Fiber Wire No. 2 sutures (Arthrex, Naples, FL).	None. Rehabilitation included prevention from lying down by using a loose suspension net. To avoid full weight bearing, a ball was attached to the sheep's claw for six weeks postoperatively.	Radiographic assessment.	The tensioner proved to be capable of actively stretching the retracted and degenerated muscle back to the original length and to withstand the external forces acting on it.

## APPENDIX E- CLINICAL STUDIES COMPARING PRP STUDY IN ROTATOR CUFF REPAIR.

Table 9-5 Clinical studies comparing PRP study in Rotator cuff repair.

Study	Design	Inclusion criteria	Details of surgery	PRP fomulation	Sample size (% males)	Mean age (years)	FU rate (%)	Mean FU times (months)	Outcome measures	Definition of retear	Results
Sanchez Marquez et al 2011	Level II Prospective randomized	Evidence of a massive rotator cuff tear of at least 5 cm and including 2 tendons (SSP and ISP)	SR repair Average three suture anchors Removal of osteophytes in 3 patients	Vivostat PRF (Visostat A/S, Alleroed, Denmark) L-PRF	28 (28.6) 14 in PRP+ group 14 in PRP- group	65	100	12	Constant score VAS score for pain Retear rate-MRI	Frank re-tearing of the tendon with retraction of the cable on MRI	No effect on clinical scores No effect on re-tear rate
Barber et al 2011	Level III case-control study	1- or 2-tendon Full-thickness rotator cuff tear measuring 10-50 mm in width; stage 2 fatty infiltration or lower	SR repair 1 or 2 double-loaded suture anchors Abrasion of the bone at the attachment site	Cascade PRP fibrin matrix construct (Musculoskeletal Transplant Foundation) P-PRF Recalcified with CaCl <sub>2</sub>	40 (67.5) 20 in PRP+ group 20 in PRP- group	57	100	Clinical, 31 MRI, 4	ASES score Constant score Rowe score SANE score SST score Retear rate-MRI (Primary outcome)	Full-thickness rotator cuff defect	Less retears in PRP+ group No effect on clinical scores except higher Rowe score in PRP+ group
Randelli et al 2011	Level I Prospective randomized	Complete rotator cuff tear confirmed intraoperatively, agreed to wear a dedicated brace for 4 weeks, preoperative platelet count >150,00, minimum preop hemoglobin 11,0g/dl or +, no infectious disease, BMI >33	SR repair Acromioplasty	Autologous PRP (GPSII-Plasmax Biomet, Warsaw, IN, USA) L-PRP Mixed with autologous thrombin and recalcified with CaCl <sub>2</sub>	53 (40) 26 in PRP+ group 27 in PRP- group	60	85	Clinical 3,6,12,24 months. VAS 3,7,14,30 days MRI 12 months	SER score, VAS score, SST score, UCLA score, MRI	Lack of continuity of the tendon in 1 slice of the coronal plane.	VAS < in PRP+ group in 1 <sup>st</sup> month. No change 3,6,12 months. Clinical outcome better in PRP+ group at 3 months, no change between two groups at 6,12,24 months .

												Re-tear 9 in PRP+(40%), 12 in PRP-(52%). SER score high in PRP+ at 3,6,12,24 months.
Castricini et al 2011	Level I Randomized controlled clinical trial	Rotator cuff tear MRI evidence, isolated SSP tendon, failure of 6 months of nonoperative treatment, no shoulder instability, no sign of fracture of glenoid or greater or lesser tuberosity, full-thickness, associated injury of long head of biceps	DR repair	Cascade PRP fibrin matrix construct (Musculoskeletal Transplant Foundation) P-PRF Recalcified with CaCl <sub>2</sub>	88 (45) 43 in PRFM+ group 45 in PRFM- group	55	Clinical 100%  MRI 92%	Clinical constant score and MRI 16 months	Constant-Murley scoring system, MRI: thickness and size of footprint	Absence of visible tendon fiber extending across entire tendon from inferior to superior	No change in Cst score, no change of signal intensity, MRI reruptures 4 in PRFM-group (10.5%)  1 in PRFM+ group (2.5%)	
Jo et al 2011	Level II cohort study	Full-thickness rotator cuff tear treated by arthroscopy	Open technique SB repair  2 or 3 suture anchors with small or medium tears, 3 or 5 suture anchors with large or massive tears	Plateletpheresis system with leukoreduction set (COBE spectra LRS turbo, Colorado)  Mixed with 10% calcium gluconate	42 (36) 19 in PRP+ group 23 in PRP- group	60	100	Clinical 3, 6,12,16 months MRI 13 months	Clinical outcome: pain, ROM, strength, satisfaction, VAS  Functional scores: ASES score, UCLA score, DASH score, SST score, SPADI score	Sugaya's method: grade IV (minor discontinuity) & V (major discontinuity)	No difference between two groups in pain, ROM, strength, functional scores, satisfaction  Retears 26.7% PRP+  41.2% in PRP- group	
Rodeo et al 2012	Level II Randomized controlled clinical trial	Patients of 40 years old or >, who had failed nonoperative treatment for full-	Suture anchors SR or DR or SB repair technique	Cascade PRP fibrin matrix construct (Musculoskeletal	79 (56) 40 in PRFM+ group 39	58	85	6 and 12 weeks	Primary outcome: ultrasound and power Doppler at 6	Not assessed	No difference between the two groups  Higher failure	

		thickness rotator cuff tear		Transplant Foundation) P-PRF Recalcified with CaCl <sub>2</sub>	in PRFM-group				amd 12 weeks Secondary outcome: strength measurements, ASES and l'insalata shoulder score		rate in PRFM+ group with DR or TOE technique at 12 weeks
Bergeson et al 2011	Level III prospective cohort with historical control	High-risk tears included per algorithm score 3; minimum age, 50 yr; minimum tear size, 2 cm  Full-thickness tear	SR repair in majority Mean no. Of suture anchors 2.9	Cascade PRP fibrin matrix construct (Musculoskeletal Transplant Foundation) P-PRF Recalcified with CaCl <sub>2</sub>	37 (NR)  16 in PRP+ group  21 in PRP- group	65	Clinical and MRI, 97.3	Clinical, 12 for PRP+ group and 27 for PRP- group MRI, 12	ASES score Constant score SANE score UCLA score WORC score Retear rate-MRI	Full-thickness defect in repaired tendon in which no fibers were visualized spanning defect in any MRI plane	More retears in PRP+ group  No effect on clinical scores
Ruiz-Moneo et al 2013	Level I Randomized double-blind controlled clinical trial	Diagnosis of rotator cuff tears based on physical examination and imaging and agreement to cooperate with study procedures (follow-up for at least 1 year including arthro-MRI). Cases with tendon retraction and fatty atrophy were allowed.	DR repair  1 or 2 simple stitches depending on tear size  2-6 total suture anchors	PRGF System (B.T.I. Biotechnology Institute, Vitoria-Gasteiz, Spain) P-PRP Recalcified with CaCl <sub>2</sub>	63 (39.7)  32 in PRP+ group  31 in PRP- group	55	Clinical, 100 MRI, 95.2	Clinical and MRI, 12	UCLA score as modified by Burkhart  Healing rate assessed as in Charousset-MRI	Not assessed	No effect on healing rate  No effect on clinical scores
Weber et al 2013	Level I Randomized controlled clinical trial	Patients who required arthroscopic rotator cuff repair with or without additional arthroscopic procedures	SR repair  All patients had acromioplasty	Cascade PRP fibrin matrix construct (Musculoskeletal Transplant Foundation)	60 (60)  30 in PRP+ group  30 in PRP- group	62	Clinical, 100 MRI, 89	Clinical, 12 MRI, 3-5	ASES score SST score UCLA score FF ER	MRI images	No effect on clinical scores  No effect on re-tear rate  No effect on FF and ER

				P-PRF Recalcified with CaCl <sub>2</sub>							
Antuna et al 2013	Level II Prospective randomized	Patients with a diagnosis of a massive rotator cuff tear of the postero-superior rotator cuff (two tendons, larger than 5 cms) made by clinical examination and magnetic resonance imaging (MRI). Only patients with tears affecting the supraspinatus and infraspinatus tendons were included	Bioabsorbable suture anchors were used in every case  (Biocorkscrew, Arthrex, Naples, FL, USA) and in all cases the repair was considered complete	Vivostat PRF (Visostat A/S, Allerød, Denmark)  L-PRF	28 (21.4)  14 in PRP+ group  14 in PRP- group	65	100	Clinical, 12,24  MRI, 12	Constant score FF RofM  DASH score  VAS score for pain  Sugaya-MRI	MRI images	No effect on clinical scores  No effect on re-tear rate  No effect on FF and RofM
Jo et al 2013	Level I Randomized controlled clinical trial	Patients between 45 and 85 years of age, large to massive rotator cuff tear >30mm MRI evidence	Suture anchors 3-5 anchors	Plateletpheresis system with leukoreduction set (COBE spectra LRS turbo, Colorado)  Mixed with 10% calcium gluconate	48  24 in PRP+ group  24 in PRP- group	63	Clinical 100  MRI 79	MRI, CTA 9 months  Functional scores (clinical) 12m months	Primary outcome: MRI, CTA  Secondary outcomes: CSA, clinical (pain, ROM, strength, satisfaction, functional scores), VAS score, ASES score, ULCA score, DASH score, SST score, SPADI score	Sugaya's method: grade IV (minor discontinuity) & V (major discontinuity)	Retear rate lower in PRP+ group 4/20 (20%), versus PRP- group 10/18 (55.6%)  No difference in pain, ROM, strength, satisfaction, functional scores, CSA.
Malavolta et al 2014	Level I Randomized controlled	Complete SSP tears with MRI evidence without history of trauma and	SR + acromioplasty	99-CFE-apheresis set (Haemonics corp.) PRP	54 (31)  In PRP+ group 28	55	98	Clinical 3, 6,12,24 months	UCLA score, CST score, VAS score, MRI	Sugaya's method: grade IV (minor discontinuity) &	No change in clinical results, partial re-tear 4fold higher in

	clinical trial	retraction of less than 3cm.		mixed with autologous thrombin and recalcified with CaCl <sub>2</sub>	and in PRP-group 27			MRI 12 months		V (major discontinuity)	control group at 3 months and 2fold higher at 6 and 12 months compared to PRP+ group.  1 retear in control group only.
Zumstein et al 2014	Level I Randomized controlled clinical trial	Presence of a posterosuperior chronic full-thickness detachment that was limited to the supraspinatus and infraspinatus tendons with an intact insertion of the subscapularis, a double-row cuff repair performed solely with use of arthroscopic techniques, and age older than 55 years. Patients with rotator interval involvement or biceps disease were also included.	Suture bridge	Choukroun's PRF (PRF Process, Nice, France)  L-PRF	20 (59) 10 in L-PRP+ group  10 in L-PRP- group	64	100	Clinical and MRI, 3  Ultrasound, 1.5 and 3	SST score  Constant-Murley score  Retear rate and Suguya-MRI  Vascularity-ultrasound	When a fluid-equivalent signal or nonvisualization of the supraspinatus or infraspinatus tendon was found	No effect on clinical scores  No effect on re-tear rate  Increased vascularization in in PRP+ group
Jo et al 2015	Level I Randomized controlled clinical trial	Patients between 45 and 85 years of age with medium to large rotator cuff tear (anteroposterior size >10mm <50mm) MRI evidence	Suture bridge  3-5 anchors  1 or 2 anchors for medial row, 2 or 3 anchors for lateral row	Plateletpheresis system with leukoreduction set (COBE spectra LRS turbo; caridian BCT)	73 (23) 36 in PRP+ group and 37 in PRP- group	60	MRI 86  Clinical 100	Clinical and functional scores 3,6 and 12 months  MRI 9 months	Clinical outcome: pain, ROM, strength, satisfaction  Functional scores: ASES score, UCLA score, SST score, SPADI score, CSA	Sugaya's method: grade IV (minor discontinuity) & V (major discontinuity)	No change in functional scores  Retear rate PRP+ 1/33 3%  PRP- 6/30 20%



